The Effects of Turbulence on Organ Sound Quality and its Minimisation in Blowing Systems

Jude T.A. NGU
Division of Mechanical Engineering
School of Engineering
University of Huddersfield

April1995

The Effects of Turbulence on Organ Sound Quality and its Minimisation in Blowing Systems

Jude Thaddeus Anye NGU
B.Sc (Essex). M.Sc.(Lond) AMIEE. MIEEE

Thesis Submitted to the University of Huddersfield
in Partial Fulfilment of the Requirements for the degree of
Doctor of Philosophy

April 1995

Director of Studies
Prof. H. V. Rao. (School of Engineering.)

Supervisors
Mr. Keith Jarvis (School of Music and Humanities, University Organist)
Dr. Keith Sherwin (School of Engineering)

Advisers
Dr. Paul F. Arthur (Assistant Principal)
Prof. George Pratt (School of Music and Humanities)

The University of Huddersfield in Collaboration with:

Wood of Huddersfield,
Organ Builders, St. Andrews Rd, Huddersfield.
(Directors: Mr. Philip Wood and Mr. David Wood)

Dedication

To my parents;

Ambrose Ngang Ngu

&

Theresia Mbunue Ngu

I have always wanted my work to have the lightness and joy of springtime which never lets anyone suspects the labour it has cost.

Henri Matisse

The improvement of understanding is for two ends: first our own increase of knowledge; secondly to enable us to deliver that knowledge to others.

John Locke

It is not by discoveries only and the registration of them by learned societies that science is advanced. The true seat of science is not the volumes of transactions but in the living mind.

Anonymous

ACKNOWLEDGMENTS

This research project could not have been realised without the help and support of many people and institutions. It is only fair that I take this opportunity to express my gratitude to all of them.

My profound gratitude goes to the University of Huddersfield for providing me with a studentship to undertake this research. The directors of Wood of Huddersfield (industrial collaborators in this project), Philip Wood and David Wood provided me with a lot of assistance for which I am also deeply grateful. Thanks also to Mark Venning of Harrison & Harrison organ builders, Durham, for all his help.

I am delighted to have had my studies directed by Professor Vasu Rao (School of Engineering) and supervised by Keith Jarvis (School of Music and Humanities) and Dr. Keith Sherwin (School of Engineering). Their constructive criticism and guidance throughout this work has been immeasurable and extremely valuable. I would also like to thank Professor George Pratt who also provided useful advice and assistance during this project. I also owe some gratitude to Dr. Bill Weston, Deputy Dean, School of Engineering, who was immensely helpful through out this research.

My gratitude also goes to Dr. Paul Arthur, Assistant Principal, who provided us with a lot of support throughout this project.

The entire staff of the research office were very helpful. In particular, I wish to thank Mrs. Rosalind Watt, Assistant Registrar, Research and Validation for all her support. Ros, Muyaka (Thanks in my language, Mankon)! You have been very marvelous.

May I also thank the technicians in the School of Engineering for all their assistance; in particular, Peter Norman for all his help with the building and setting up of my test rigs, Graham Butler and Adam Isherwood for sorting out the SUN computers when the machines threatened to hold up my work. My gratitude also goes to Mark Bromwich, the Electro-Acoustic Studio Manager for all his help.

I would also like to express my gratitude to the security staff and caretakers of the engineering block and Z-block for putting up with my irregular working hours. You all have been magnificent.

Thanks also goes to my colleagues in the research students office (Z2/44): Steve Kendal, David Palmer, Michael Fish, Nihat Yildrim and Craig Edwards for the useful discussions we had. Those discussions helped my Electronic Engineering tuned mind come to terms with some of the complexities of Mechanical Engineering. I would also like to thank the secretaries in the School of Engineering, Mrs. Laurie Hampshire, Mrs. Jane Godfrey and Mrs. Jill Healey for all their help and for putting up with my incessant demands on their time.

Finally, I will like to thank my family and friends for their invaluable support throughout this research. My parents, Ambrose Ngang Ngu and Theresia Mbunue Ngu as well as Fru Ngu, Foleng Ngu, Atanga Ngu, Chewfung Ngu, Aghanwi Ngu, Manka Ngu, Mambo Nyamnjoh, Francis Nyamnjoh, Anye-Nkwenti Nyamnjoh, Miss Mum, Andrew Tembon, Mercy Tembon, N N Susungi, Mme P Susungi, Agbor Ntui, Donna Francis, Rahan Shaheen, Ade Angwafo III, Sule Nformi, Erica Charles, Saah Lamango and all others who for want of space have not been mentioned here.

I hope that in finishing this work, I have done all of you, who helped me in any way, very proud.

ABSTRACT

This research sets out to study the effects of turbulence on organ sound and examine ways of minimizing it in blowing systems.

The efficacy of application of statistical and spectral techniques for a quantitative analysis of the effects of turbulence on the organ sound has been established.

The sound generated for different inlet levels of turbulence intensity were analyzed. The inlet turbulence variation was achieved by mixing in different proportions, the wind generated by a centrifugal fan which has high levels of turbulence and turbulence attenuated wind. The latter was obtained by suppressing the levels of turbulence through flow stratification in narrow channels. Turbulence attenuation by flow stratification was used in this research as it could attenuate turbulence for very high Reynolds number ($> 10^5$) flows such as encountered in the study.

The effects of turbulence attenuation were evaluated aurally, in a qualitative manner and also analyzed quantitatively. The aural evaluation indicates that changes in the sound with changing levels of turbulence were perceivable. In addition, the lower the turbulence levels, the better the sound quality - the instrument (organ) is said to have a better "degree of articulation... and expressiveness." Spectral analysis of certain notes with and without turbulence attenuation showed changes to the spectral shape. Ripples in the spectra in the leading and trailing edges of the fundamental were much reduced. The spectra were smoother. The fundamental frequency shifted, on average by 0.3%, up or down, depending on the nicking condition of the pipe. In one note, $F^{\#}_{43}$, the fundamental had two peaks without any turbulence attenuation. One of the peaks vanished when turbulence attenuated wind was used.

A technique was developed for quantitatively evaluating the fundamental from the frequency spectra. The fundamentals were sampled, normalized and moments taken about the central frequency. The 3rd and 4th moments computed gave an indication of the changing skewness and "peakedness" of the note with turbulence. It was noted, from experiments conducted on a test rig, that the notes got more negatively skewed and peaks more with increasing turbulence attenuation. It was also noted that the notes underwent a non-monotonical increase in asymmetry with falling levels of turbulence. There were similar increments in the "peakedness" of the pipe fundamental amplitude with decreasing turbulence.

An electrical analogous circuit of the organ flue pipe for turbulence studies was developed. A circuit model with linear components was simulated and tested. It was found that most of the circuit component parameters were dependent on the geometric dimensions of the pipe, especially the pipe length. Calculations and a simulation of the circuit using HSPICE with parameters determined using the effective length of the pipe gave resonant frequencies much less than those obtained from acoustic experiments. The concept of an active length, L_a, which works out to be a third of the effective length, L_e, was introduced. Calculations and simulations using L_a, gave more accurate results. A hardware implementation of the circuit developed was also done in order to study the effects of turbulence.

The statistical analysis and electrical analysis studies undertaken in the current work may find application in the design of computer organs and other areas were turbulence in flow plays a significant role.

TABLE OF CONTENTS

List of Figures

List of Tables

List of Symbols

a	Pipe radius
a	Channel radius
A	Area
A	Amplitude
A1	Channel arm 1
A2	Channel arm 2
A_p	Data point
BPF	Band pass frequency
c	Speed of sound
C_{yx}	Covariance between signals y and x
C	Capacitance
D	Diameter
DD	Diode
E[]	Expectation of []
E(s)	Source Potential, emf, driving voltage
f	Frequency
f_c	Central frequency
f	Frequency
F	Frequency
G_{yy}	One sided auto-spectrum of Y(t)
I	Current
ID	Inner diameter
K	Bulk modulus
K'	Loss parameter
K^1	Loss parameter
L	Inductance
L	Length
L_ω	Honeycomb length
m	Mass
M	Inertance
M	Moment
M_k	K^{th} moment about ψ
M_{cs}	Moment coefficient of skewness
M_{ck}	Moment coefficient of kurtosis
^1M_k	K^{th} moment about the mean
N_b	Number of blades on an impeller
o/p	output

OD	Outer diameter
p	Pressure
P	Pressure
P1	Pipe 1
P2	Pipe 2
P3	Pipe 3
P4	Pipe 4
Q	Volume flow rate
Q	Quality factor
Qe	Charge
r	Radius
R	Resistance
Re	Reynolds number
RPM	Rotations per minute
R_{yx}	Cross correlation between Y(t) and X(t)
S	Cross sectional area
S_x	Sensor for X(t)
S_y	Sensor for Y(t)
S_{yy}	Autospecrtrum of Y(t)
S_{yx}	Cross power spectral density between Y(t) and X(t)
u'	turbulence intensity
U	Flow velocity
Up	Mean flow in honeycomb
V	Speed
V	Voltage
V1	Valve 1
V2	Valve 2
V3	Valve 3
X	Random variable
X'	Velocity
X(t)	Arbitrary signal
Y(t)	Arbitrary signal
Z	Impedance

Greek Alphabet

β	Blockage ratio
μ	Viscousity

μ	Moment
μ	Mean
ρ	Density
θ	Half angle of deviation
ψ	Some origin
Δf	Normalised frequency shift
ΔV	Volume displacement
Δp	Pressure drop
τ	Time delay
τ	Pulse width
∞	Infinity

Subscripts

a	Active
cp	Pipe capacitance
C	Capacitance
d	Downstream
e	Effective
eff	Effective
in	Input
j	Jet
Lp	Pipe inductance
L	Inductance
m	Pipe mouth
max	Maximum
min	Minimum
n	Normalised
n	Resonant mode
p	Pipe
T	Termination
u	Upstream
x	Signal X(t)
y	Signal Y(t)
100T	100% turbulence

CHAPTER ONE

INTRODUCTION

1.1 Introduction

The musical organ has been in existence for about 2000 years.[34] It would be expected that enough work would have been done to explain the acoustics, fluid dynamics and aero-acoustics of the instrument by now. This does not seem to be the case. There is still a lot of work to be done. In fact, "there are still many problems in understanding details of the mechanism by which the sound is produced!";[34] these "details" are not yet "well established"[16]. The amount of research being carried out around the world - Australia, Japan, Hungary, Germany, Holland, France and USA - seems to indicate that a lot of knowledge still has to be squeezed out from this domain not only to shed light on the behaviour of organ pipes and similar wind instruments but also the behaviour of other aero-acoustic mechanisms that are similar to those occurring in organ pipes.

Some research has also been done to throw more light on the musical acoustics of the organ pipe.[3 25 42 49] In Hungary, some studies were conducted to study the build up of sound in the organ.[3] Some researchers have also studied the evolution of the timbre with changing [1#]tessitura[25]. Others have conducted research to understand the interaction between the mouths of resonating pipes placed on the same soundboard.[49]

Several researchers have invested a lot of efforts to studying the jet stream from the flue and its interaction with the resonant modes of the pipe, see for example references 10, 29-36. Different aspects of this flow interaction have been studied.

Research work on the organ sound production has not been confined to studies on the pipe.

---

1. section of total compass of voiced part of organ in which most tones lie

There has been research undertaken to study the flow in the note channel[27] and wind trunks delivering wind into the organ.[39 59 77 94 96] These studies did not investigate the effects of turbulence on the pipe sound quality; they were mainly concerned with the effect of pressure pulsations on the pipe sound or reverberation of the bellows. [58]

Caddy and Pollard[9] and others[3 52 53 69] studied the transient sounds and their implications on the steady state resonance of the organ pipe but did not consider turbulence effects. In Spain, Agullo and Martrinez, [1 55 56] have studied the behaviour of pressure waves (not turbulence) within cones similar to the organ pipe foot, but did not look at their subsequent effects on any resonant column that could be attached to such "conical bores".

Studies have also been conducted on the voicing of organ pipes,[60] the end corrections and resonance frequencies of the pipe,[86] flow at the pipe exit during resonance,[20] the quality of the tones[28] as well as relation between pipe resonance and its sound spectra. [5]

Research was carried out on the fluid dynamics of organ pipes not to understand the aesthetics of its musical character, but to extend and apply that knowledge to other applications. Most of this work has been done in France, Holland and USA. Elder[23] has applied some of the findings from his investigations of organ pipe aero-acoustics to study jets generated in moving vehicles and flow noise in research conducted for the US Navy. In Holland and France, [8 20 26 52 72 73 76 93] considerable research has been conducted on the aero-acoustics of organ pipes and subsequently applied to the analysis of flow excited resonance in gas pipe lines. Studies have also been conducted in the UK[66 67] on the fluid dynamics of flow excited resonance in ducts using some of the arguments developed in the study of the aero-acoustics of organ pipes.

The main areas of the research on organs are concentrated around the soundboard, pipe jet drive mechanism and the interaction between the jet from the flue and the resonance

modes of the pipes. Very little effort has been invested in studying the wind delivery system of the organ. Studies on organ wind-delivery have mainly been discussion papers on the problems faced, mainly one of unsteady wind and insufficient pressure and an expression of the desire for smooth flowing wind.[59 94 96] Research on wind supply into organs has mainly looked at the pressure fluctuations in the wind.[39 77] Rooij[77] studied the effects of pressure waves in the wind system on pipe sound. Gueritey investigated the effects of pressure waves on the pipe sound when an organ is being played[39] and showed that there was a discernible shift in the frequency of the fundamental of a pipe. In the investigations carried out to study the effects of pressure waves in the wind-delivery on the pipe sound, it has to be borne in mind that pressure waves are deterministic quantities unlike turbulent fluctuations which are random.

Of all the previous research carried out on the organ, apart from Hirschberg who evaluated the effects of jet (from the pipe flue) turbulence on pipe tones in his paper on the fluid dynamics of speech, no other study was found to have been conducted to study the effects of turbulence from the wind-delivery system on the quality of organ sound. Hirschberg demonstrated that the jet turbulence produces low levels of broad band spectra which are modulated by the pipe modes.

1.2 Previous Work

When the St. Paul's organ[1] was built, in 1977, the organ blower was placed inside the organ case behind the console (keyboard). Although the fan was placed in an acoustic box, mechanical noise was audible throughout the building. Preliminary tests taken in 1981 suggested that much of the noise was impeller generated. In 1985 the blower was moved to an adjacent cellar. 40 ft (~12 m) of wooden trunking was constructed and installed leading from the blower to the organ. The resiting of the fan improved the sound of the

1. Details of the stop list, compass of notes on the organ console and the pipe scale of the St Paul's organ are given in appendix 1

instrument, reducing the shrillness of the instrument, and improving the tonal blend of the organ stops. An added benefit was the improvement in the touch of manual III (swell). The pallets in the soundboard, because of the proximity of the blower, were affected by turbulence and vibrations from the impeller - and this was transmitted through the action to the keyboard. This characteristic reinforced a basic organ building rule that fans should be placed as far away from the instrument as realistically possible, in order to allow the air flow from the fan to the pipes to be as smooth as possible.

Even after removing the fan, the problem of flutter, ripples and unsteady pitch still remained in the tonal characterisitics of the organ. In 1990 a fan regulator (air reservoir) was installed to steady the air flow. It was found to make no audible difference to the tonal quality of the instrument since when the air inlet to the reservoir was open (when the organ was played) turbulence passed straight to the organ itself.

In 1991 the 12 radial blades of the impeller were replaced by 24 backward facing blades (together with a new 3 phase ac motor). The impeller speed was unchanged. The wind output was increased by 50%. These changes gave some improvement but not a complete solution to the problem. The notes now affected by flutter and ripple were shifted upwards by an octave, suggesting that the sound of the pipes was affected by the quality of the wind.

What emerged from the foregoing previous work on the organ was that the complete solution to the problems emanating from the wind supply was not obvious. Working towards a complete solution to the problem therefore required that the turbulence situation in the organ wind system be studied.

1.3 An overview of the Organ and Organ Pipe

Figure 1.1 and 1.2 gives a block diagram of a typical organ pipe and organ respectively.

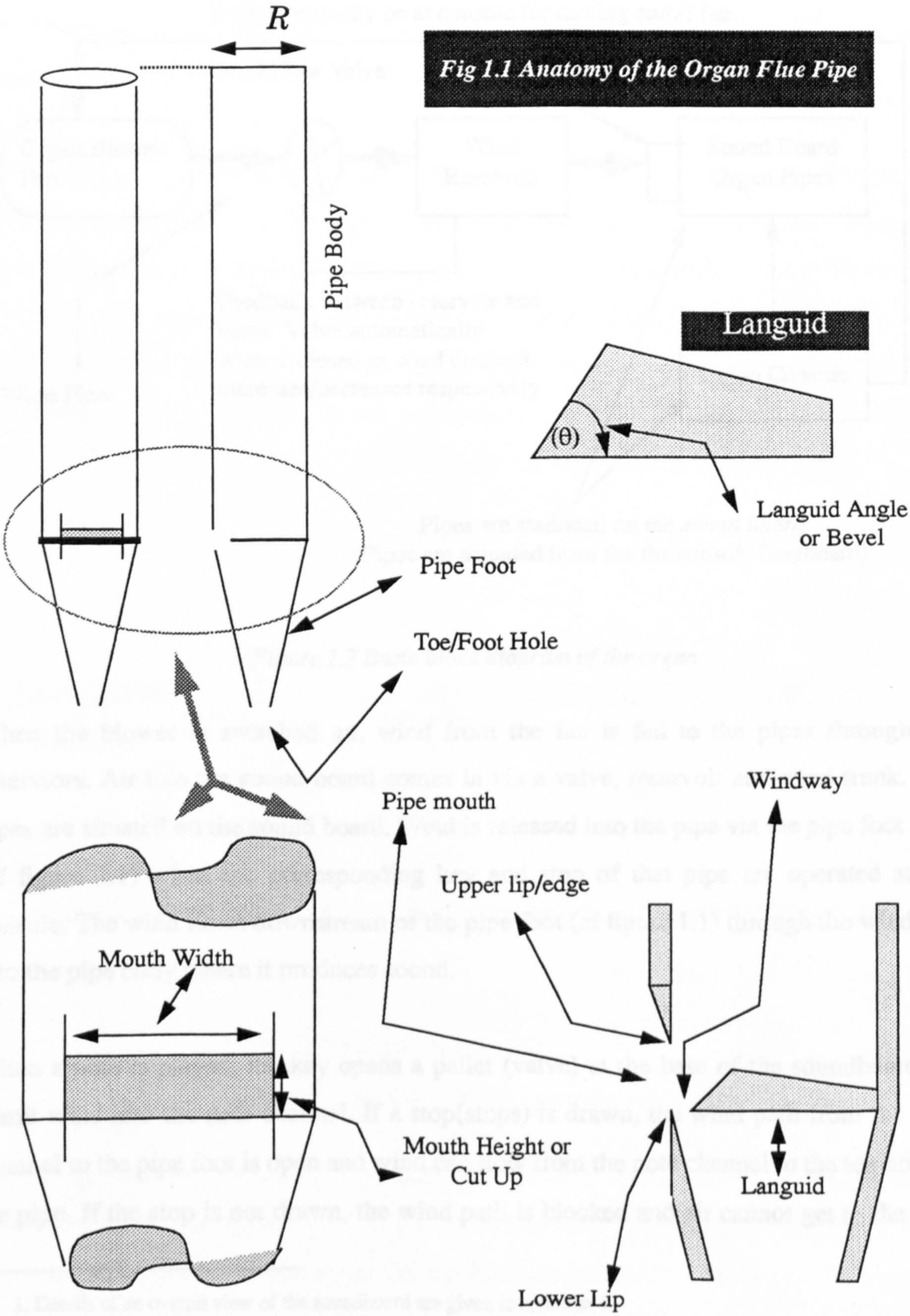

Fig 1.1 Anatomy of the Organ Flue Pipe

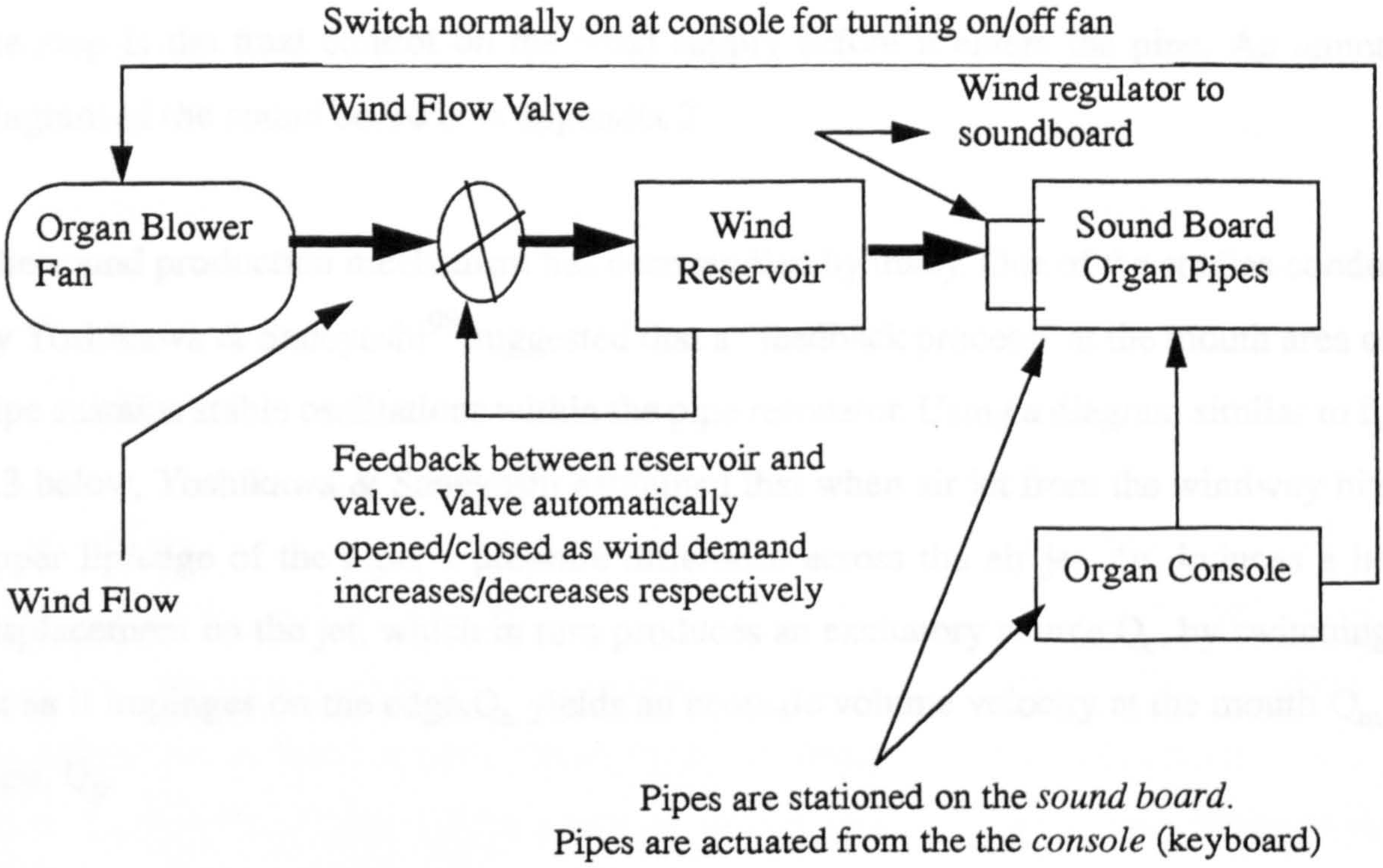

Figure 1.2 Basic block diagram of the organ

When the blower is switched on, wind from the fan is fed to the pipes through the reserviors. Air into the sound board comes in via a valve, reservoir and wind trunk. The pipes are situated on the sound board. Wind is released into the pipe via the pipe foot hole (cf figure 1.1) when the corresponding key and stop of that pipe are operated at the console. The wind flows downstream of the pipe foot (cf figure 1.1) through the windway into the pipe body where it produces sound.

When a note is played, the key opens a pallet (valve) at the base of the soundboard[1] to admit wind into the note channel. If a stop(stops) is drawn, the wind path from the note channel to the pipe foot is open and wind can flow from the note channel to the toe hole of the pipe. If the stop is not drawn, the wind path is blocked and air cannot get to the pipe

1. Details of an overall view of the soundboard are given in appendix 2

foot. This kind of sound board is the slider soundboard since the movement of a slide by the stop is the final control on the wind supply before it enters the pipe. An annotated diagram of the sound board is in appendix 2

The sound production mechanism has been studied by many. One of the studies conducted by Yoshikawa & Saneyoshi[98] suggested that a "feedback process" at the mouth area of the pipe sustains stable oscillations within the pipe resonator. Using a diagram similar to figure 1.3 below, Yoshikawa & Saneyoshi explained that when air jet from the windway hits the upper lip/edge of the pipe, a pressure difference across the air jet, Δp, induces a lateral displacement on the jet, which in turn produces an excitatory source Q_e, by switching the jet as it impinges on the edge.Q_e yields an acoustic volume velocity at the mouth Q_m and pipe, Q_p.

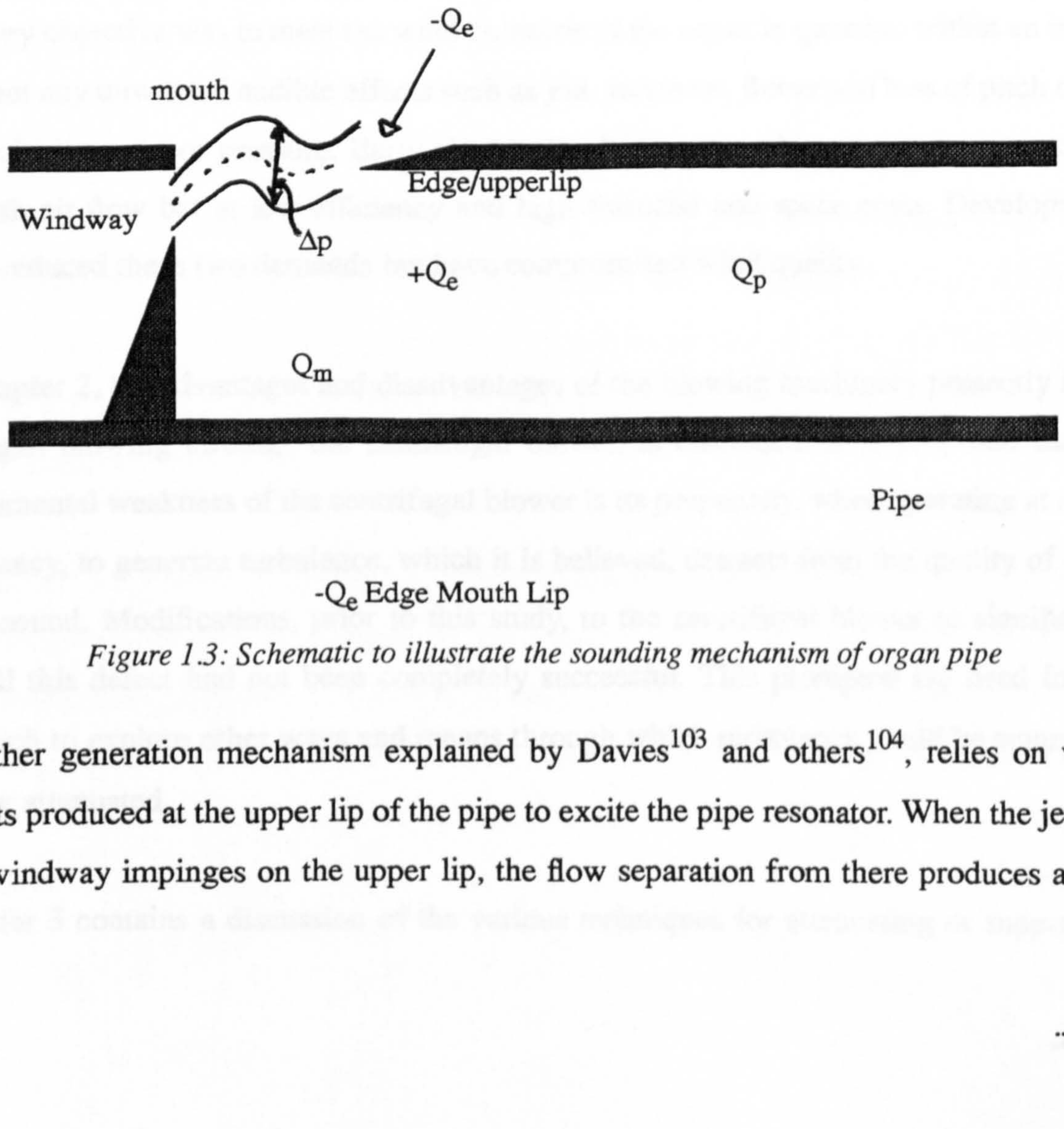

Figure 1.3: Schematic to illustrate the sounding mechanism of organ pipe

Another generation mechanism explained by Davies[103] and others[104], relies on vortex sheets produced at the upper lip of the pipe to excite the pipe resonator. When the jet from the windway impinges on the upper lip, the flow separation from there produces a shear

layer/vortex sheets that serve as an excitatory source for the pipe resonator. The sound in the resonantor interacts with the vortex sheet synchronising it to produce "an ordered train of vortices"[103] which in turn produce self sustained oscillations. It is possible that both mechanisms outlined above contribute to the sound excitation mechanism.

1.4 Thesis outline

A study of the historical evolution of organ blowing equipment was undertaken and a brief account is presented in chapter 2. Organ blowing machinery had evolved over the centuries from human operated bellows to today's centrifugal blowers. The evolution from one system to another has been driven by the inadequacies of the blowing machinery in use at the prevailing time. Which ever type of blower was in use at a particular time, the primary objective was to meet the wind demands of the organ in question within an instant without any unwanted audible effects such as jolt, jerkiness, flutter and loss of pitch due to inefficient supply or pressure. Early electrically driven organ blowing systems produced smooth air flow but at low efficiency and high financial and space costs. Developments have reduced these two demands but have compromised wind quality.

In chapter 2, the advantages and disadvantages of the blowing machinery presently in use in organ blowing circles, the centrifugal blower, is discussed. It is proposed that the fundamental weakness of the centrifugal blower is its propensity, when operating at a high efficiency, to generate turbulence, which it is believed, detracts from the quality of organ pipe sound. Modifications, prior to this study, to the centrifugal blower to significantly curtail this defect had not been completely successful. This prompted the need for this research to explore other ways and means through which turbulence could be suppressed and or attenuated.

Chapter 3 contains a discussion of the various techniques for attenuating or suppressing

turbulence. Methods of reverting turbulent flows to laminar or near-laminar flow and postponing the onset of turbulence are given. These techniques include; channel enlargement, channel spanwise axis rotation, helical wound wind trunks, curved flows and flow stratification. Most of these techniques work for flows with Reynolds numbers below 20,000. Flows in wind trunks supplying wind to organs generally have Reynolds numbers in excess of 50,000. The technique of flow stratification could handle flows with very large Reynolds numbers and will be used to attenuate turbulence.

An attenuator was designed and built to be used for St. Paul's organ blowing system. This was tested in the laboratory (University of Huddersfield) prior to installation. It will be shown, via spectral analysis, that the attenuator significantly attenuated the turbulence in the flow by up to 30dB. Differences in the organ pipe notes played with turbulent and turbulent attenuated wind will be demonstrated through qualitative and quantitative analysis.

The spectrum of pipe sounds recorded when played with the turbulent attenuator connected and disconnected are shown in chapter 4. An aural evaluation of the notes played with and without the turbulence attenuator is also discussed. Similar experiments were repeated in the laboratory using pipes on the windchest of a test rig. It is shown in chapter 5 that the improvements encountered in the St Paul's Hall organ were also realised in a laboratory environment.

In chapter 5 a model is developed (which supports experimental results) to provide a quantitative evaluation of changes in pipe note when played with wind of different turbulence flow conditions. The technique used is based on adaptation of the principles of statistical moments about some reference point. The skewness (deduced from the 3rd moments) and the peakedness or kurtosis (deduced from the 4th moment) will be evaluated. It was demonstrated through experimental results that the peakedness and

skewness change and that the frequency of the notes tend to shift with changes in flow conditions.

In research conducted elsewhere to study the dynamics and aero-acoustics of the organ pipe and note channel, the researchers have resorted to electrical circuit models of the pipe or section of the organ under study to assist with their analysis.[9 11 13 14] A linear equivalent circuit model of the organ pipe was developed for turbulence studies in chapter 6.

Chapter 7 discusses areas where further developments and research can be conducted as well as other applications of this research. Most of the studies on the organ pipe have been applied to understanding the aero-acoustics of fluid pipelines and other wind instruments. Some of the findings here could be applied to research in these sectors.

In the final chapter, chapter 8, the concluding remarks are presented.

CHAPTER TWO

A REVIEW OF ORGAN BLOWING MECHANISMS

Organ blowing machinery has had a colourful History. What ever their nature organ blowers had to provide wind pressures ranging from 350 Pa to over 5000 Pa^2, and maximum volumes required over a similar range. Today a typical new organ will beoperating at about 2000 Pa requiring wind flow in the region of 0.7 m^3/s.

The blowers used ranged from the human operated blowers, through hydraulic blowers and gas engines to centrifugal blowers. The ensuing sections discusses the principal types of blowers that have been in use so far.

2.1 Manual Blowers

These blowers involved the distension and compression of bellows by hand and/or foot,[24] [70] as per figures 2.1 and 2.2.

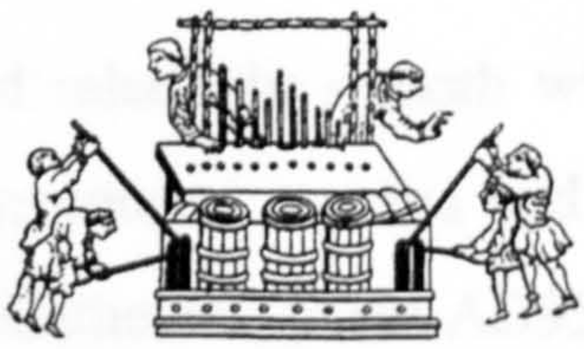

Figure 2.1 Sketch of four persons handblowing an organ. (Courtesy of Elvin[24])

Bellows that were, and are still, used in organs are similar to the lungs in operation, except that in lungs there are no valves and air comes in and goes out the same way. The similarity are more pronounced during distension. When the wall(s) is(are) distended, air is sucked in through a valve(s). On compression, the valve(s) is(are) closed and the air is forced out into the reservoir and downstream via the trunk(duct) into the wind chest or soundboard.[44] [70]

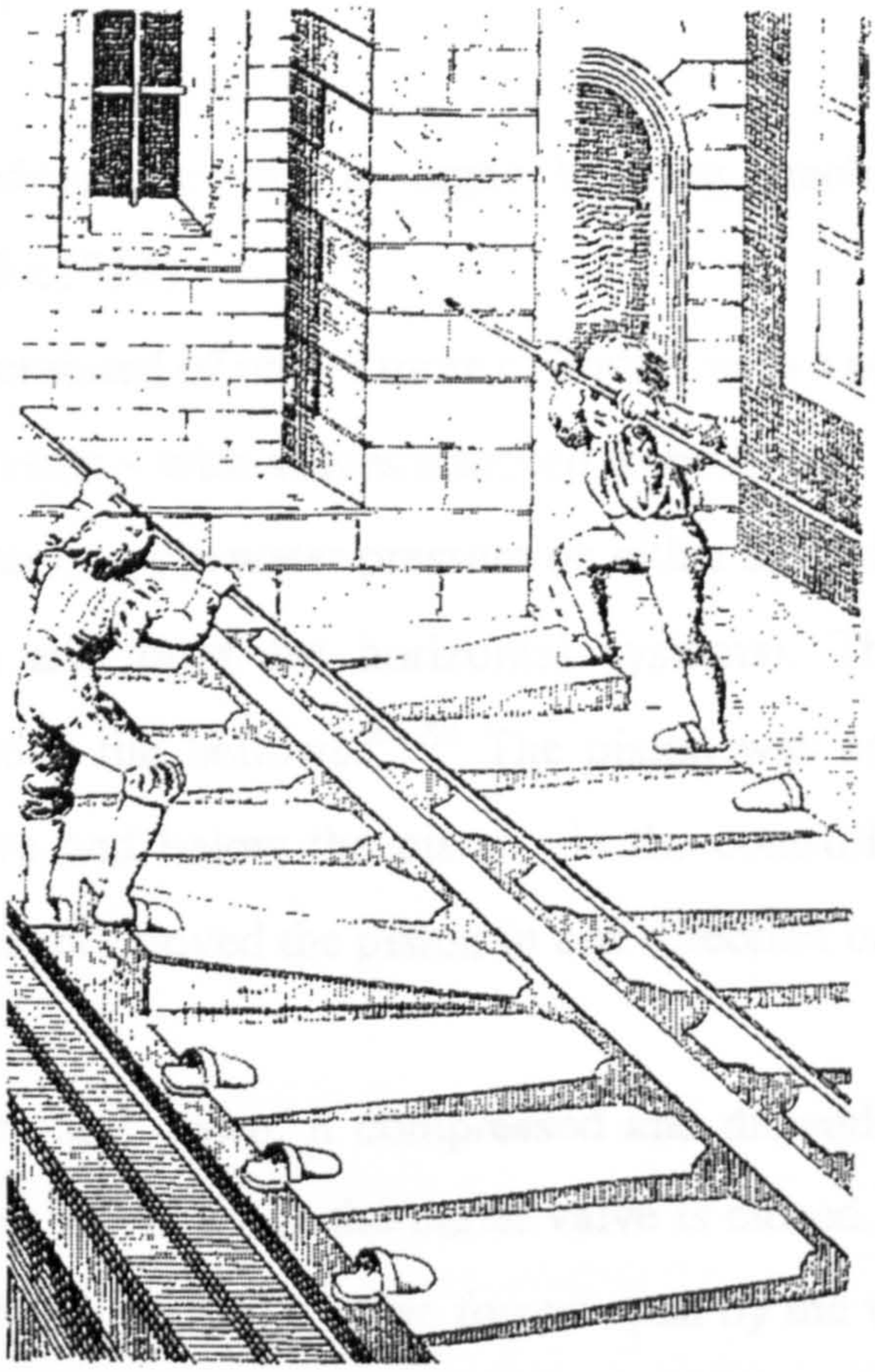

Fig 2.2, Two persons blowing an organ with their feet - Halberstadt Cathedral Organ - 16th Century -(Courtesy of Elvin [24])

Human operated blowers provided relatively smooth wind, however, large volume and high pressure demands required prolonged stamina and a sizeable human labour force. The first organ built in Winchester Cathedral, (circa AD951) had 400 pipes and 26 bellows that had to be operated by hands and feet of "... 70 strong men." [24 35]. Clearly the logistics of labour force requirements posed a fundamental restriction on the size of organ that could be built and upon its utilisation.

Few organs are manually blown nowadays. Of over a dozen organs visited as part of this work, one, Thurstonland Anglican Church, West Yorkshire, had a dual blowing system: a manual blower and a centrifugal fan.

2.2 Hydraulic Blower

The application of hydraulic power in organ blowing machinery dates back to the Victortian age.(ie c1850-c1914)

The hydraulic blower consisted of one or more cylinders with a piston inside each of them. The cylinders had two vents - with valves attached to both: one at the water inlet and the other at the outlet. By varying the water pressure on either side of the piston, it was moved up and down (or left and right for horizontal systems). The (reciprocating) piston compressed and distended the bellows.[24 88] The piston was actuated by the controlled injection of water above and below the piston via the controlling valves. The pressure differential across the piston moved the piston in one direction or the other.

As the piston moved up and down, it compressed and distended bellows - the bellows sucked air in via its inlet valve, while the outlet valve is closed. On the downward stroke the inlet valve is closed and the outlet valve forced open by the wind pressure, forcing the wind downstream into the wind reservoir and trunks into the soundboard. The system had provision for a leakage valve for situations where the air reservoir was full and further wind input was superfluous. [2 4 24]

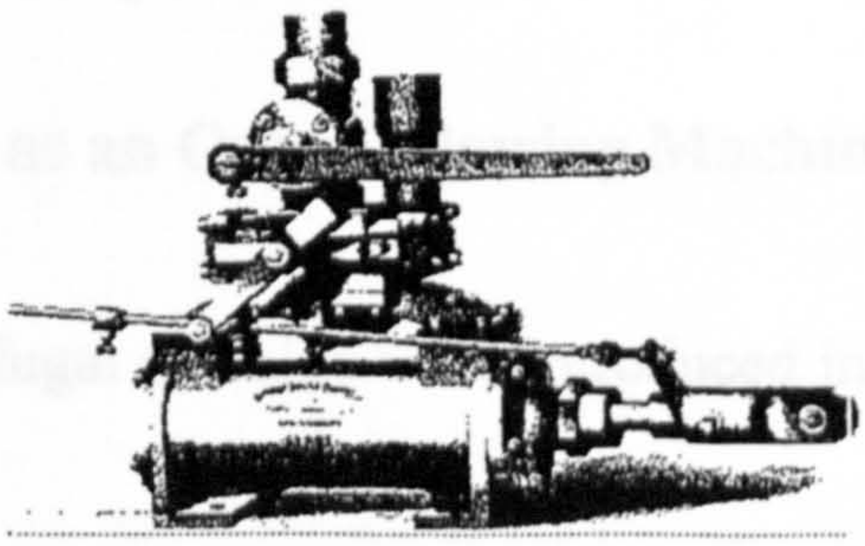

Figure 2.3 An example of a hydraulic machinery used for organ blowing (Courtesy of Elvin [24])

The principal advantage with hydraulic operated blowers, was their quiet operation, attributed to their slow speed (about 50 rpm).[24] The wind generated was not very turbulent relative to latter day ones.[70]

Water mains controlled hydraulic blowers had one major disadvantage: there were variation in the mains water pressure which could cause operational difficulties.
In fact the cost of maintenance turned out to be more than the cost of the equivalent centrifugal fan.[70]

2.3 The Gas Engine

After the hydraulic machines came gas engines. These were mainly in use during the late 19th and early 20th century.[88]
The combustion of a gas mixture in a cylinder, released Energy which in turn was used to drive a piston(s) that were attached to bellows via cranks. The compression and distension of the bellows supplied wind into the organ.
In some organs, the kinetic energy of steam was used. Around 1860 (and up to the 1920s) the organ in St. George's Hall, Liverpool used a steam engine of 1.9 kW - 2.5 hp (and later 6kW, i.e. 8 hp) to supply up to 5500 Pa (22 inH_20) of wind pressure.[24]
The gas engines were bulky, and had to be kept at long distances from the organ. Furthermore, the fumes and oil from the engine were inevitably sucked into the bellows with damaging and costly consequences.

2.4 The Centrifugal Fan as an Organ Blowing Machine

Early versions of the centrifugal machine were introduced in the organ blowing circle as Kinetic Blowers.

2.4.1 The Kinetic Blower

Basically this is a brand of multistage impeller centrifugal machine where all the stages are in the same casing, with each stage separated from the preceeding and/or proceeding stage by a plate with a circular orifice cut out at the centre of this plate to clear the main

shaft. Air compressed at the edge of the first set of impellers is channelled to the centre of the next set of impellers on the same shaft, as a consequence, progressively increasing the pressure of the wind. Where required, wind can be tapped off after any impeller stage.

Such blowers are still in use today. The blowers of the Anglican Liverpool and Durham Cathedral Organ and St. Peter's Parish Church, Huddersfield, are some of many examples. The Liverpool Anglican Cathedral organ is blown by three kinetic blowers: two operating at 1440 rpm at 13.5 KW (18 hp) and the other at 1400 rpm at 9.4KW (~12.5 hp). (These are rated values). Each occupy a space of about 3 m by 0.70 m by 0.8 m; delivering a sum volume of about over 3.33 m^3/s and an overall wind pressure of 5500 Pa. A comparable organ in St. George's Hall in Liverpool, uses two centrifugal blowers rated at 2.83 m^3/s flow rate, 12.5 KW and 0.233 m^3/s at 12 KW, both running at 1450 rpm. These machines have outer diameters of 1.5 m and 1 m diameters respectively; while both have a breadth of 0.25 m. These devices were large, noisy and expensive to run. They also require large and expensive reservoir system to support them. Advances were therefore sought that were small cheaper and less expensive to operate. The centrifugal blower offered gain in all these areas.

2.4.2 The Centrifugal Blower

The centrifugal fan is much smaller and more efficient than a kinetic blower, for a given wind demand specification.

Air sucked in via the inlet of the centrifugal blower is imparted kinetic energy by the moving blades of the impeller and the pressure rise is then achieved by diffuser action as the air flows in the casing (and diffuser where present). This is known as dynamic compression.[68]

Where a single stage fan can not meet the pressure requirements of a specific organ, several centrifugal blowers are used in cascade: the output of one feeding the input of the

next machine in the cascade. The final output or output tapped off at intermittent stages are then channelled off, via a reservoir, through appropriate trunking into the organ soundboard.

Between the blower and the reservoir, there usually is a regulator, regulating the volume flow rate into the reservoir according to demand. The valve used, undoubtedly introduces extra turbulence in the wind and is likely to influence the acoustics of the organ pipe.

2.4.3 Advantages of the Centrifugal and Kinetic Blowers

a They are very compact machines.

b They have no valves and hence fluctuations in pressure which may arise from valve motion are absent.

c Mechanical balance is easily achieved as the construction is mainly axi-symmetrical in structure, inherently resulting in less mechanical vibrations.

d Because direct motor drive of the centrifugal machine is possible, gear noise is avoided.

e These blowers require minimal maintenance.

2.4.4 The Disadvantages of the Centrifugal and Kinetic Blowers.

In spite of the several advantages of the centrifugal blower, they have disadvantages for organ blowing purposes.

Among the disadvantages are:-

a The process of raising wind in the centrifugal blower, is by dynamic compression; involving the conversion of a velocity head into a pressure head. This generally yields a temperature rise which tends to increase with decreasing efficiency;

b Centrifugal machines raise wind that has pressure fluctuations which are dependent on the rotational speed and impeller blade count of the machine. Guelich and

Bolleter[38] have studied and discussed the effects and mechanisms of pressure pulsations in other applications, wherein it is proposed that there are two principal types of pressure pulsations that matter:-

i those that have discrete frequency peaks, and

ii broadband pressure fluctuations (ie flow noise and turbulence).

Pressure pulsations with discrete frequency peaks are determined by the Blade Rate Frequency and the Blade Pass Frequency.[19 37 38]

c The flow path from the inlet to the outlet of the centrifugal machine involves a complicated and contorted geometry, which generates considerable turbulence and pressure fluctuations. It has to be mentioned that pressure fluctuations are different from turbulence: the former is not random and covers a wider range on the frequency spectrum. The finite number of blades and the eddy separation at the blade tips gives rise to pressure fluctuations.

Basically, the overall machine concept wherein rotating blades are enclosed within a confined space is inherently a turbulence generating situation. This further makes it difficult to design a low turbulent wind supply using a centrifugal machine;

d There is a conflict of requirements for smooth flow dynamics and for high pressure. The centrifugal machine is principally a low pressure rise machine; typically 250Pa to 5,000Pa in a single stage.

The pressure head, P, is generated by converting a velocity head, due to a bulk velocity of U, as given in the basic equation outlined below, assuming no viscous effects,.

$$P = \frac{(\rho U^2)}{2} \quad \text{.....2.1}$$

Because the air density, ρ, is low, a high velocity is required to realise a high pressure rise. A high velocity inherently produces more turbulence as this increases the Reynolds

Number, R_e; where

$$R_e = \frac{(\rho U D_e)}{\mu} \quad \text{.....2.2}$$

D_e = a characteristic length dimension, hydraulic (equivalent) diameter and

μ= viscosity of the fluid. [21]

Where: $D_e = \frac{4xDuctArea}{DuctPerimeter}$ 2.3

2.5 Surmounting the defects of the Centrifugal Machine

There are two possible ways of tackling the short comings of the centrifugal fan. The two approaches are:

a) minimising turbulence through design and/or

b) eliminating the turbulence down stream.

The first method is discussed in the ensuing section, while the later will be treated in more detail in chapter 3.

2.5.1 Modifications to the Impeller Blade Geometry

The different configurations (see figure 2.4) of the centrifugal machine impellers include:[82]

a forward facing impellers;

b backward facing impellers and

c paddle (radial) impellers.

The shape of the blade used in most applications depends on the pressure rise, flow rate and impeller diameter required.

In many organs, the centrifugal machine providing the required wind have radial blades. The modifications on the impeller geometry involed using backward facing blades with a

split impeller configuration.

Why use backward facing blades? This question will be answered with the aide of figure 2.4 overleaf. An examination of the pressure versus volume curves of the different blade geometries indicate that the backward facing blade provides the most stable operation. The pressure versus volume curve of the forward facing blade impeller (fig 2.4, II-a) shows some non-uniformity in the changes in pressure with increasing volume. There are operating pressures that have two and even three possible volumetric flow rates. Operating the fan at such pressures may result in instabilites that cause stalling. The Paddle/Radial bladed impeller configuration also has a non-uniform pressure versus volume curve (c.f. fig 2.4, III-a). As the volumetric flow rate increases, the pressure increases before falling. At certain operating pressures, there are two possible volumetric flow rates. Operating the radial bladed centrifugal fan at such pressures can result in stalling. Judging from the pressure versus volume curve of the backward bladed centrifugal fan (c.f. fig 2.4, I-a), it can be inferred that at any operating pressure, there is only one volumetric flow rate. This uniform pressure versus volume flow characteristic is what gives the backward facing bladed impeller fan its operational stabily and superior performance relative to the other blade configurations, they are also more efficient and give rise to less turbulence. It has to be said that efficiency is not necesarily an advantage. In chapter 4, section 4.3, this will be dealt with further further when a discussion on some experiments with a blower borrowed from Harrison & Harrison Organ Builders, Durham, is given.

Another modification of the blade geometry involves the use of a split impeller configuration. This is especially so for large pressure rise applications. The split blade geometry increases the radial depth of the blade which helps in reducing the boundary layer separation around the blades, thereby also reducing the formation of eddies that do induce turbulence. Plate 2.1 depicts a modified impeller geometry that is in use in the centrifugal machine in St. Paul's Hall, University of Huddersfield.[99]

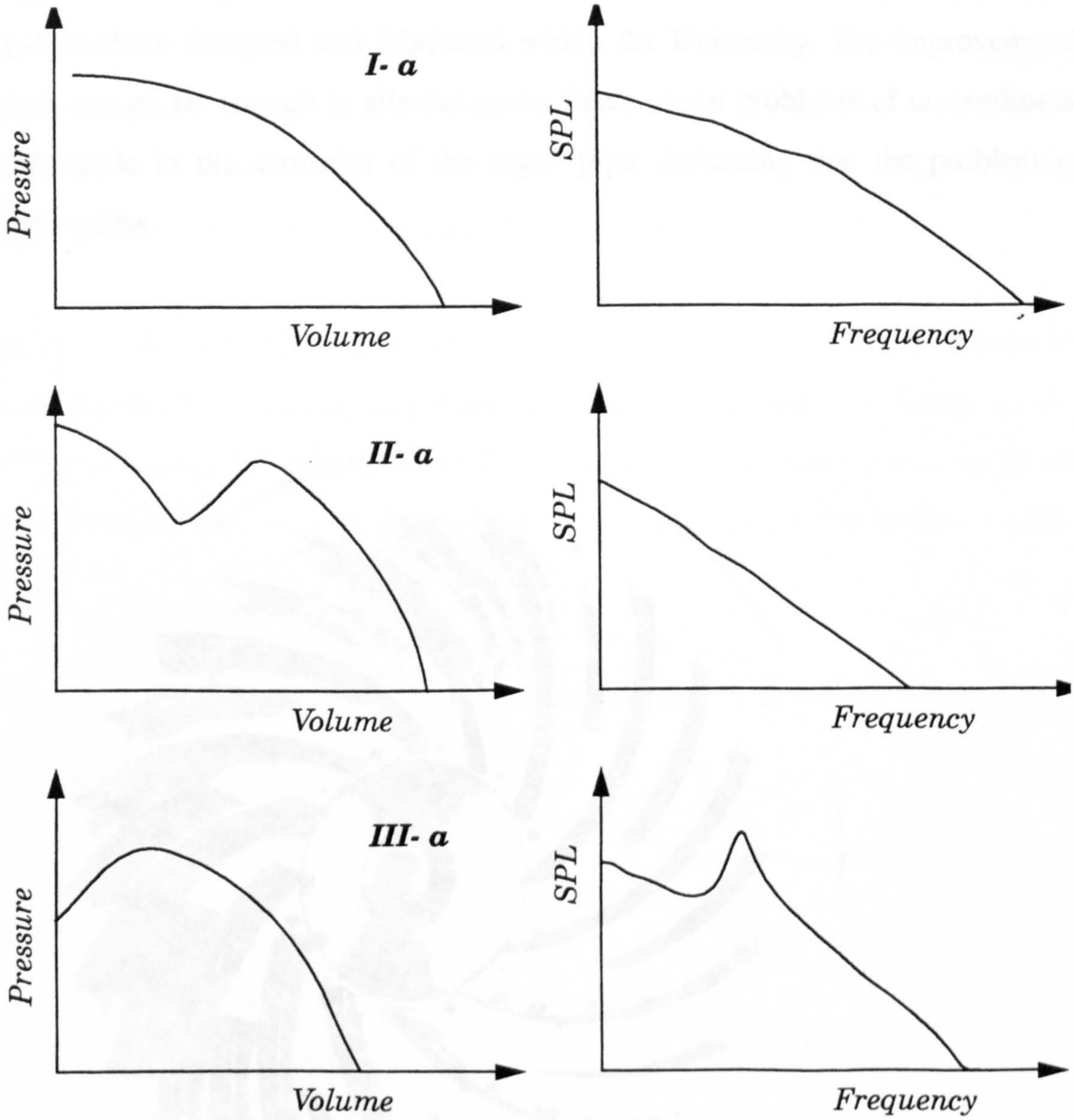

Fig. 2.4: Graphs Pairs I-a, II-a, III-a, are Static Pressure vs Volume and Sound Pressure Level vs Frequency for
I-b; Backward Facing Blades
II-b: Forward Facing Blades and
III-b Paddle (or Radial) Bladed Impellers, respectively

The aforementioned improvements of the blade geometry have been implemented in a centrifugal machine designed and fabricated within the University. The improvements achieved do not go far enough in alleviating the fundamental problems of unsteadiness, flutter and ripple in the acoustics of the organ pipe. Indicating that the problem of turbulence persists.

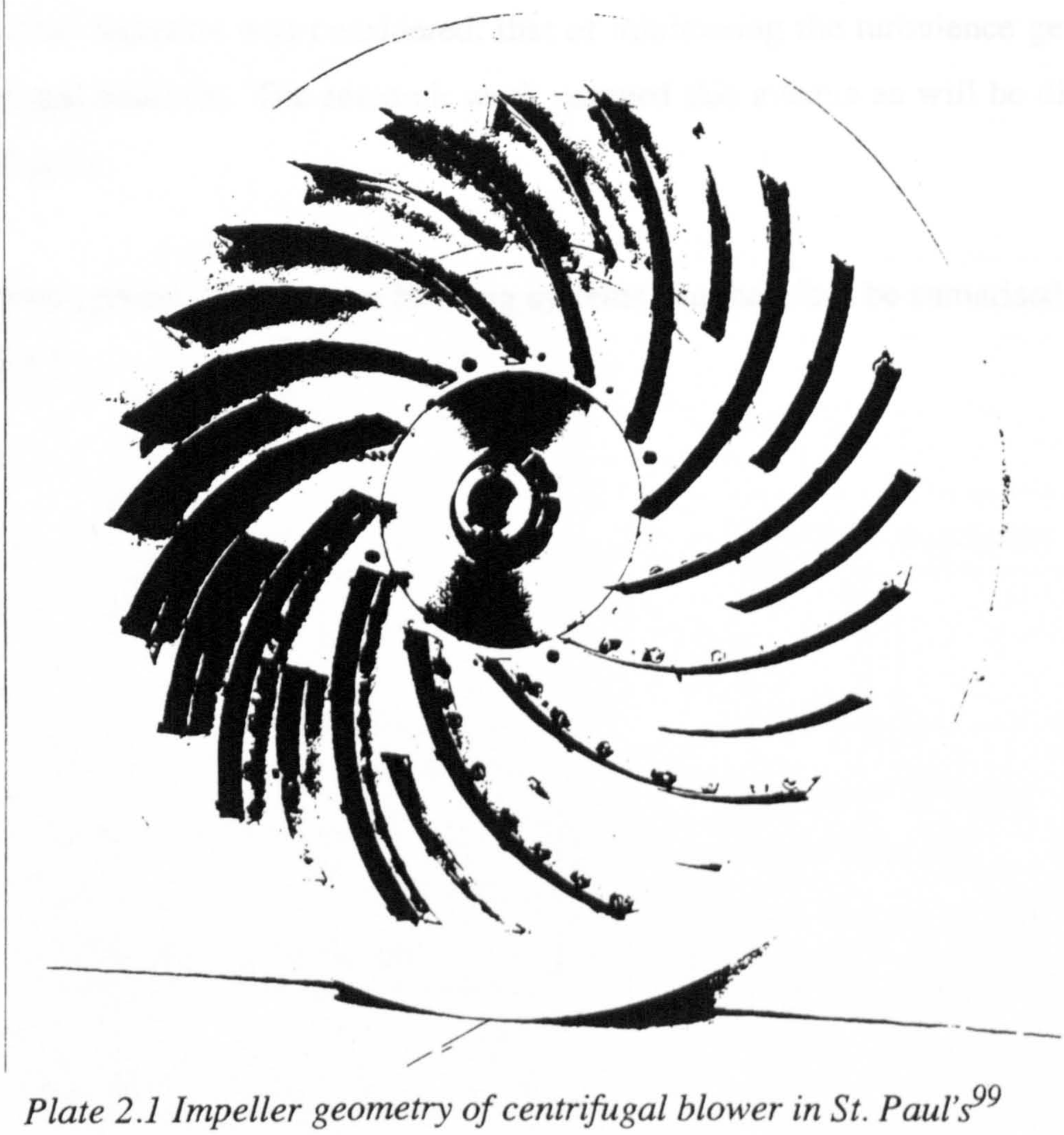

Plate 2.1 Impeller geometry of centrifugal blower in St. Paul's[99]

This impeller configuration shifted the turbulence problem upwards by one octave, i.e. doubling the frequency, on the organ in St. Paul's Hall, University of Huddersfield.[48] This is due to the doubling of the number of blades previously used from 12 to 24. It becomes

increasingly clear therefore that pursuing further improvements on the centrifugal machine for the application of interest in this research may only lead to a further marginal improvements. Some experiments carried out, indicate that the level of turbulence in the flow depends on the operating point on the *efficiency versus flow rate* curve of the Centrifugal Blower in use (will be discussed in chapter four).

An innovative solution to this problem was to consider designing a machine centred on new concepts apart from the centrifugal machine. Before that, another remedy for the turbulence situation was considered: that of minimizing the turbulence generated by the centrifugal machine. The research work pursued this avenue as will be discussed in the next chapter.

The development of the organ blowing systems can therefore be sumarised in the chart in figure 2.5.

Fig 2.5 Flow diagram of organ blowing machinery

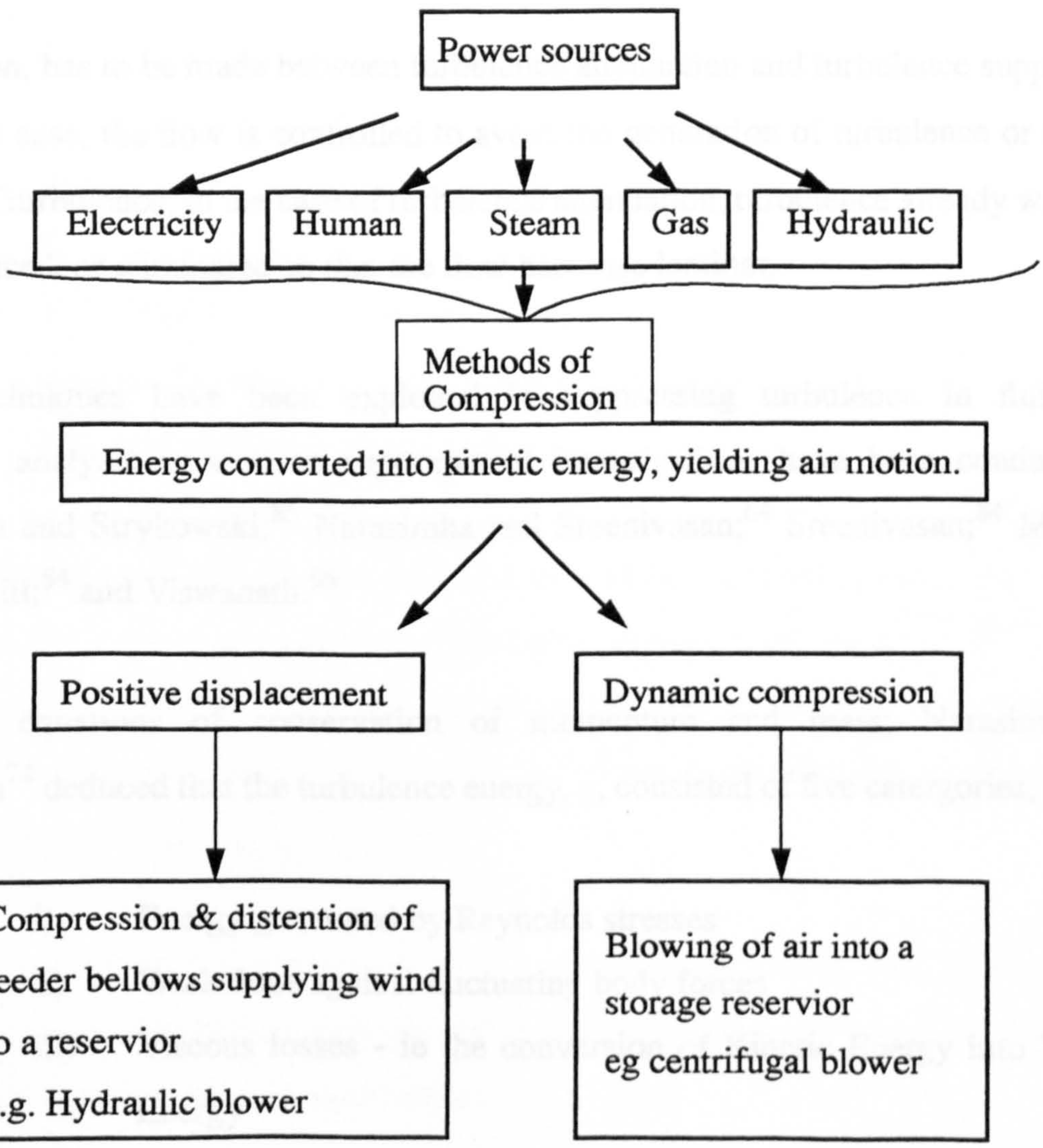

CHAPTER 3

TURBULENCE SUPRESSION AND ATTENUATION

3.1 Principles of Turbulence Attenuation and Suppression[1]

A distinction, has to be made between turbulence attenuation and turbulence suppression. In the latter case, the flow is controlled to avoid the generation of turbulence or to delay the onset of turbulence. In the case of turbulence attenuation, turbulence already within the flow is reduced, or eliminated so that the flow becomes laminar.

Several techniques have been exploited in suppressing turbulence in fluid flow. Theoretical analysis as well as experimental investigations have been conducted by Sreenivasan and Strykowski;[85] Narasimha and Sreenivasan;[64] Sreenivasan;[84] Manlapaz and Churchill;[54] and Viswanath.[95]

Using the equations of conservation of momentum and mass; Narasimha and Sreenivasan[74] deduced that the turbulence energy, q, consisted of five catergories, namely:

i) Energy generated by Reynolds stresses
ii) Work done against fluctuating body forces
iii) Viscous losses - ie the conversion of Kinetic Energy into Thermal Energy
iv) Viscous diffusion and
v) Diffusion due to pressure and turbulent fluctuations.

---

1. A theoretical overview of turbulence is outline in appendix 3 together with a discussion on method of analysing turbulence for the for the purposes of this work.

Techniques that contributed to minimise q, would result in relaminarization.

It turns out that the decorrelation of the principal velocities that directly contributed to the level of the Reynolds stresses contributed significantly in reducing turbulence.[64 84] This concept shall be treated in more detail in subsequent sections.

Parameters used to determine the onset of relaminarized flow were:

cessation of bursting,
change in the stress gradient at the wall,
fall in the skin friction,
fall in Reynolds numbers to below its critical value,
flow profile approaches the laminar velocity profile and
a drop in the heat transfer coefficient.[64 84]

Photographs of turbulent to laminar reversion in fluid flow as well as oscillograms of Hot Wire Anemometer traces were given to corroborate experimental findings.[84 85 95] Manlapaz and Churchill[54] on their part carried out detailed studies on skin friction and the *helical number* (the modified Deans number) to study relaminiarization in helically coiled channels of finite pitch.

The investigations of the researchers cited principally concluded that there are three methods of turbulent to laminar flow reversion, namely: dissipative reversion, Richardson type reversion and reversion by domination.

3.1.1 Dissipative Reversion.

In this process, molecular transport agents, e.g., friction, causes the loss of turbulence energy, demonstrated by the changes in the Reynolds number. Pipe flow experiments conducted by Narasimha and Sreenivasan,[64] concur that the weakened Reynolds stresses

indicated that the turbulence energy has been attenuated.

3.1.2 Richardson Type Reversion (Dissipation via Stabilized Stratified Flows)

Here turbulence is suppressed by a "stabilizing density gradient"[64] as proposed by Richardson circa 1920. This can be demonstrated by injecting a strand of dye in a water tank of uniform temperature. The dye is injected at the base and allowed to flow towards the ceiling. The flow is observed to be turbulent as it progresses downstream.

If the top of the tank is heated, such that the water nearer the ceiling becomes hotter and less dense relative to the base, the strand of dye flowing upwards towards the ceiling now has the perilous task of working against the density gradient: the turbulent energy of the dye is now converted into gravitational potential energy. This dissipation of turbulence energy yields reversion from turbulent to laminar flow. Viswanath[95] and Sreenivasan[85] took some pictures illustrating this phenomenom.

This phenomenom also occurs in the atmosphere when turbulent smoke reverts to laminar flat clouds as the smoke moves towards the stratosphere. The hot atmosphere nearer the sun and the cooler earth surface (cooled by convection currents) leaves a density gradient not conducive for sustaining turbulence flow - hence the turbulence suppression.

3.1.3 Reversion by Domination.

This occurs when a turbulent boundary layer is subjected to strong streamwise acceleration. Viswanath[95] have conducted experiments with supersonic flows to demonstrate this type of reversion. Narasimha and Sreenivasan[64] found evidence of decorrelation of the velocity components that determined Reynolds stresses. They also noted that there was a drastic fall in the skin friction. The foregoing corroborate the retransition into laminar flow. Here the observation of relaminarisation was principally in the boundary layer and not within the entire flow. This kind of reversion is found to be dominant in flow reversion that takes place in helically coiled ducts.[54 95]

3.2 Some Techniques used to realise reversion.

Some of the techniques used include: curved flows, spanwise axis rotation of the flow channel, helically wound ducts and channel enlargement.

3.2.1 Curved Flows

The diagram of figure 3.2 gives an illustration of the process involved.

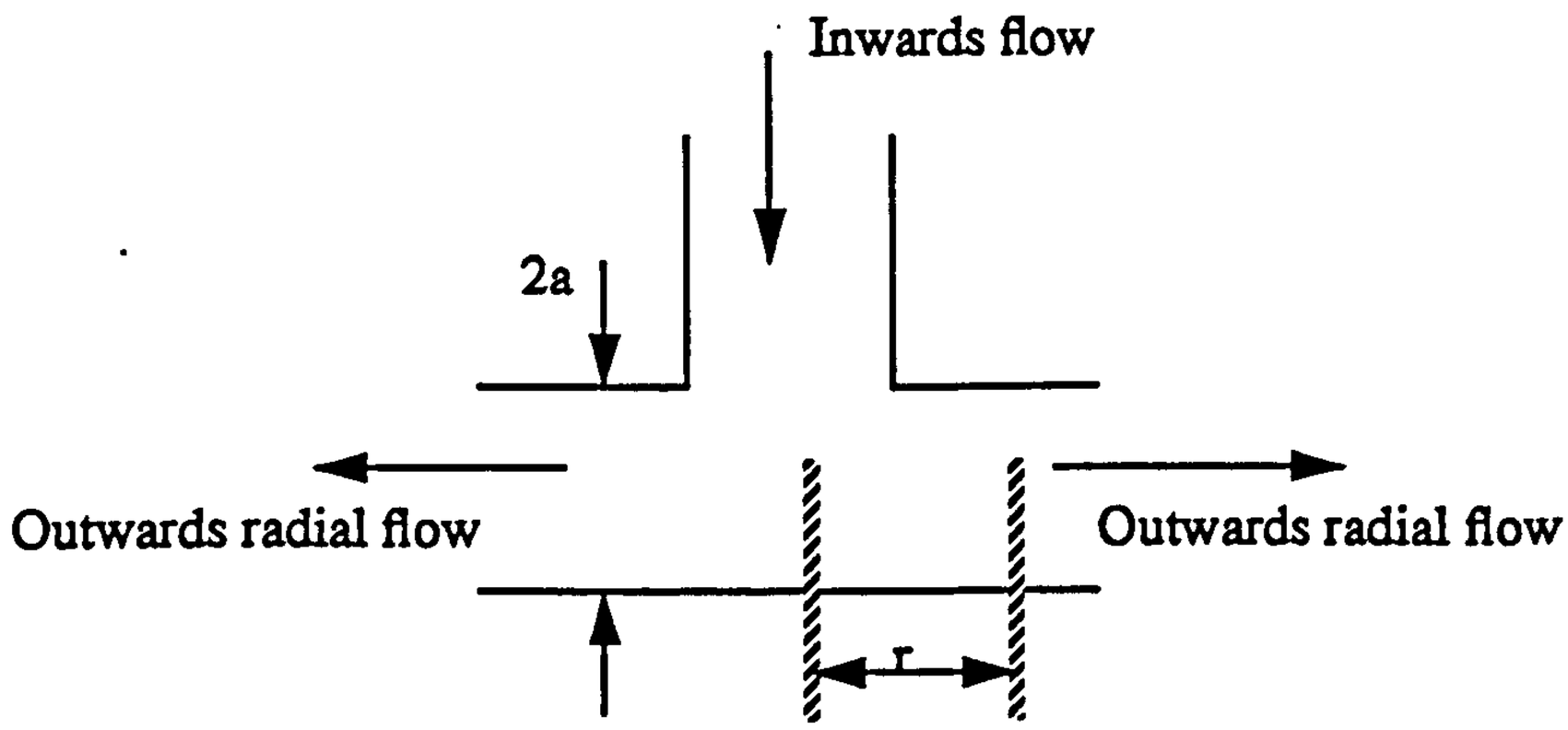

Fig 3.2 - Schematic diagram to demonstrate reversion by means of curved flows

The incoming flow at the centre is converted into outward radial Poiseuille Flow between the two parallel discs. It turns out that the $R_e(r)$ at a radius, r, from the centre of the feeder pipe is inversely proportional to, r, and directly proportional to, a, the pipe radius.[64]

3.2.2 Turbulence Attenuation via Spanwise Axis rotation of the Flow Channel

Flow visualisation techniques have been used to illustrate that turbulent flow reverted to near laminar flow especially near the walls.[64] The skin friction was found to have dropped significantly. Narasimha and Sreenivasan's[64] experiments were conducted with flows that have R_e not exceeding $2x10^4$.

3.2.3 Channel Enlargement

Laminarisation is realised by gradually enlarging the wind trunk from a smaller to larger (hydraulic) diameter (cf Fig. 3.3), while ensuring that the half angle of divergence, θ, is small enough to avoid flow separation.

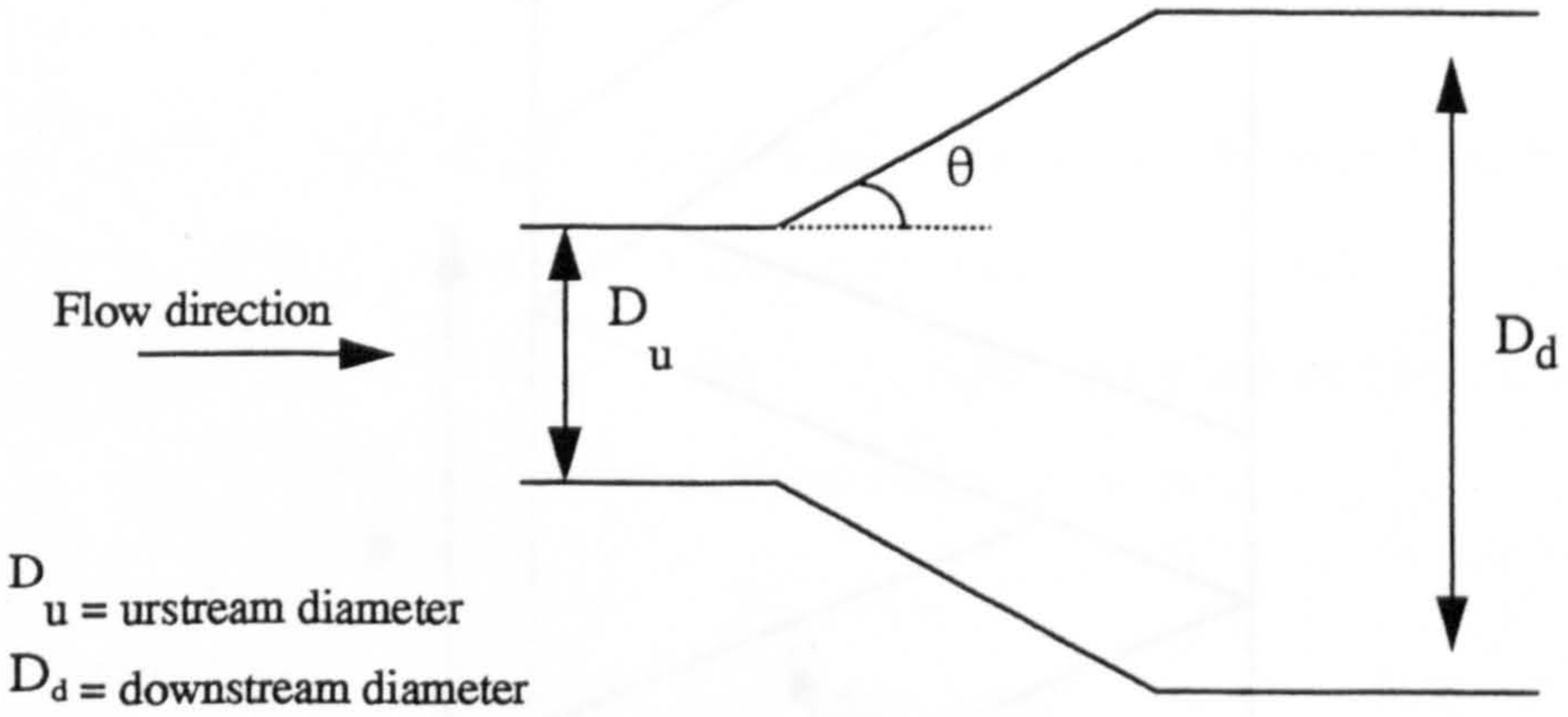

Fig 3.3 Reversion due to channelenglargement

Experimental results reported by other researchers and cited by Sreenivasan[84] illustrate an attenuation in turbulence by as much as 80%, for half angles of deviation, θ, of 1° and 3°. Channel enlargement is believed to be a typical example of dissipative reversion.[64]

The velocity profile was found to approach the Poiseuille solution[64] downstream after the enlargement. Add to that, a drop in skin friction. Narasimha and Sreenivasan,[64] further noted from experimental measurements that at 20a and 180a downstream, after the enlargement, the correlation coefficient of the two dimensional (x and y) velocity components fell from 0.36 to 0.13 (~70% attenuation) respectively. They thus concluded that a "decorrelation mechanism" was destroying the "coherent motions" and weakening the Reynolds stresses, with the net result that turbulence was being destroyed far more than it was being created.

3.2.4 Turbulence Reversion using Helically Coiled Pipes

By using helically coiled pipes as depicted in Fig 3.4 below, turbulent flow has been shown to revert to laminar flow.

Re-conversion to turbulent flow further downstream, occured, at much higher critical Reynolds numbers.[54 95 85 89]

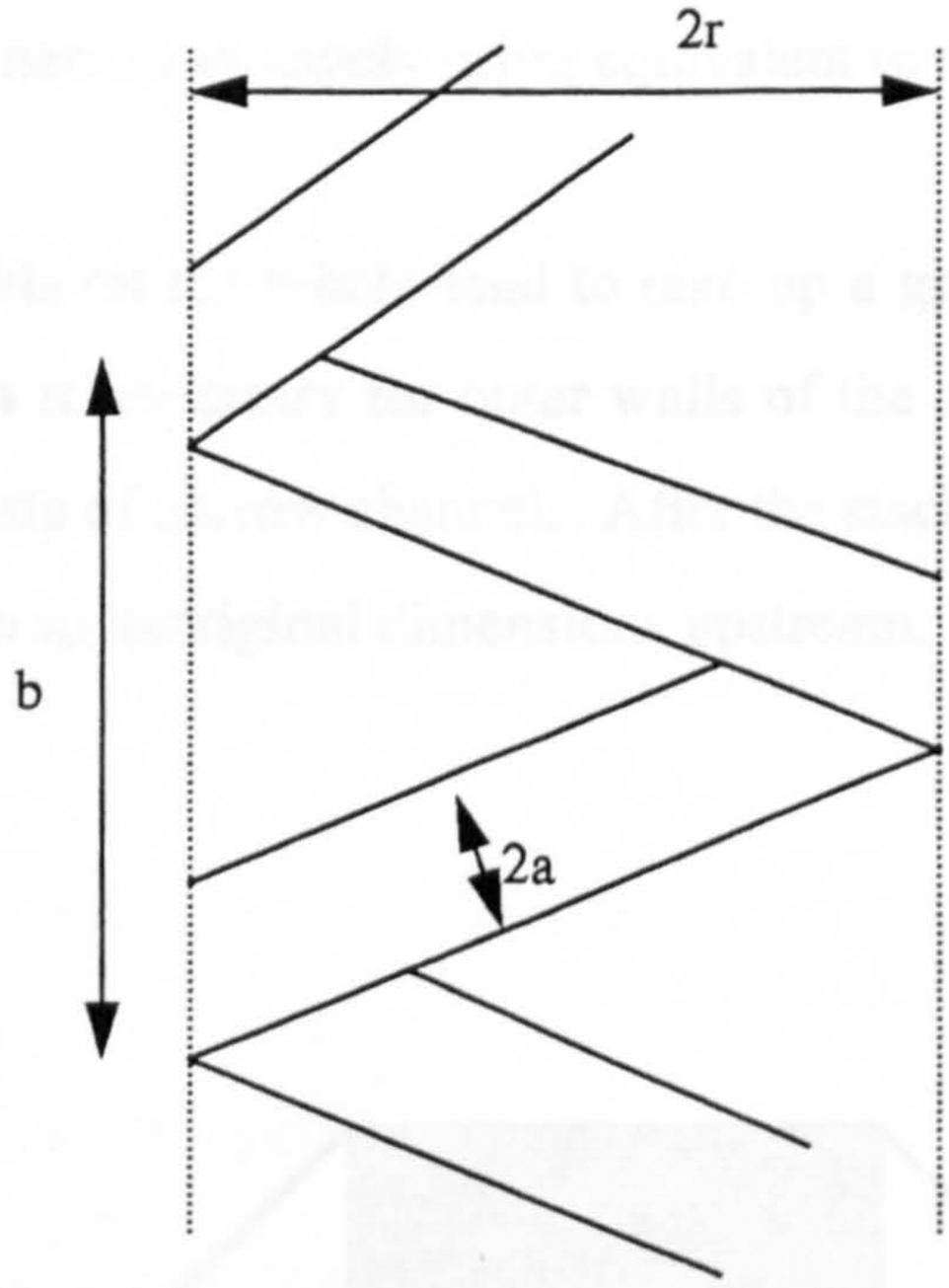

Fig 3.4 Turbulence reversion in flow through helically coiled pipes.

Viswanath,[95] conceded that though the reversion process in these types of flow have been known since the 1920s, there was still a lot of ambiguity surrounding it, however, they did postulate that it could be due to the Richardson effect - a change in density gradient between the inner and outer wall. It can be infered from experiments conducted by Manlapaz and Churchill,[54] and the arguments of Narasimha and Sreenivasan,[64] that a combination of the Richardson effect and suppression by domination are taking place in the flow. The faster flow in the outer wall dominates the turbulent fluctuations taking place in the inner wall.

3.2.5 Turbulence attenuation by flow stratification

If the fluid flowing upstream is conveyed from one large channel to several narrower ducts, with significantly smaller hydraulic diameters, the Reynolds number of the flow could be reduced significantly. The narrow ducts are stacked next to each other.

The total area of the narrow channels being equivalent to the area of the preceeding duct.

The narrower channels on the whole tend to take up a greater area because of their wall thickness: this makes it necessary for outer walls of the duct to be gradually enlarged to accommodate the strata of narrow channels. After the stack of narrow channels, the duct is again narrowed down to itsoriginal dimensions upstream.

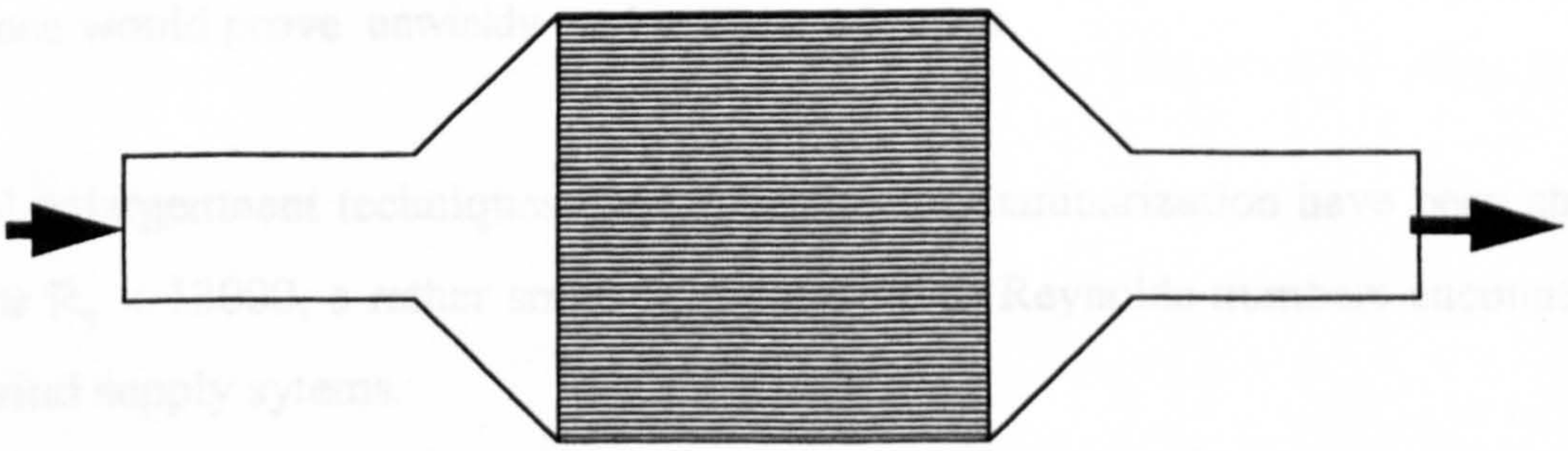

Fig. 3.5: Section of schematic for turbulence attenuation by stratified flow

The strata of narrow channels can be a stack of honeycombs or tiny polygonal ducts. The channels should be sufficiently long enough to attain steady flow conditions: i.e. the length should be atleast 20 times the hydraulic diameter of the narrow ducts.

So if the dimensions of the trunk went from say 20 mm by 20 mm in the main trunk to say

3 mm by 3 mm in the rectangular "honeycomb", there would be a change in hydraulic diameter from 20 to 3 respectively. The change in hydraulic diameter would yield a proportionate change in the Reynolds number.

If the narrower channels have a wall thickness of 500μm, say, then the main trunk would have to be enlarged to 625 mm^2 from 400 mm^2 to accommodate a strata of narrow channels with identical flow area.

3.2.6 Choice of turbulence attenuation or suppression technique

Where curved flows are used to realise reversion, reversion has been demonstrated for flows with Reynolds numbers (R_e) not exceeding 10^4. Much less than the turbulence conditions experiences in organ blowing situations, where R_e in excess of $5x10^4$ are encountered.

In organ blowing situations, the ducts have large hydraulic (equivalent) diameters and are, made of clay or wood in most cases. Spanwise axis rotation as a means of curbing turbulence would prove unwieldy and not cost effective.

Channel enlargemnent techniques used in realising relaminarization have been shown to work for $R_e < 13000$, a rather small R_e, compared to Reynolds numbers encountered in organ wind supply sytems.

The experiments conducted to study reversion in helically wound ducts process have been done with radius ratios: a/r, of less than 0.1. The technique was found to be valid for maximum upstream Reynolds numbers of less than 10^4. Further downstream if re-conversion (retransition) into turbulence flow occurred, it did so at a much higher critical Reynolds number of ~ 5200^{85}.

Typical organ wind trunks supplying church and hall organs with wind tend to have diameters in the neighbourhood of 200 mm or more. To achieve a radius ratio of less than

0.1, would require a coil radius, r, of greater than 2000 mm. There is hardly such large space to spare for trunking within organ systems. Besides their wind supply Reynolds number of upstream flow is in excess of 10^4.

Realising that many of the prevailing schemes for attenuating or suppressing turbulence are not suitable for organ applications, the technique of turbulence attenuation by flow stratification was adopted.

In determining whether turbulence had been attenuated to revert to laminar or near laminar flow conditions, the energy spectral density and the time domain oscillographs of the turbulence signal were measured, before and after the attenuation process, with a hot wire anemometer. The Reynolds number before and after attenuation was also evaluated.
The hot wire anemometer could only measure turbulent fluctuations in one dimension, meaning that we could not evaluate the correlation of the principal velocities in 2 or 3 dimensions. The instrumentation for measuring boundary layer bursting and skin friction were unaffordable or unavailable. Though other sophisticated measuring instrumentation could have been used, the hot wire anemometer was adequate for the application in hand.

CHAPTER FOUR

EFFECTS OF TURBULENCE ATTENUATION

4.1 The Turbulence Attenuator (Filter)

The turbulence attenuator was designed for the St Paul's Hall organ to reduce the Reynolds number of the flow without compromising the flow rate. The method that will be proposed also seeks to decrease the scale/intensity of turbulence by decreasing the space over which the "random motions" of turbulence can fluctuate and hence its fluctuation amplitude thereby realising reversion by dissipation.

The turbulence attenuator was made up of a stack of small rectangular "honeycomb" passages of length L_ω where L_ω is chosen such that a steady flow is obtained downstream of the stack length before the wind exits the attenuator.

The rectangular passages in use have an area of 8.22 mm^2. The leading edge of the duct into the entrance of the attenuator was gradually expanded to accommodate the increase in area due to the wall thickness of the narrower channels . The channel expansion decreases the flow speed and increases the pressure of the wind before it gets into the passages. This also helped to compensate for the very small, but extant, decrease in pressure (found to be less than 50 Pa; ie less than 0.2 inches H_20) that comes with the increased wind speed as the wind flows downstream into the passage. After the honeycomb, the duct is funnelled down to its original dimensions. The angle of the leading and trailing funnels were both less than 10° so as to minimize any flow separation, especially after the honeycomb (see fig. 4.0 below) Fig 4.0 depicts the attenuator (with an L_ω of 100 mm) designed for the St. Paul's Hall organ.

It is speculated that the flutter and ripple on sustained notes at certain stops on the organ are due to the turbulence in the wind flowing into the soundboard. Experiments carried out to investigate the influence of turbulent wind on the quality of organ sound will be described in chapter four. Ideally this should be done by taking measurements (recordings) of some pipe sounds at wind possessing different levels of turbulence flowing into the soundboard.

The first phase of this scheme involved introducing the turbulence attenuator outlined above in the path of the wind and qualitatively analyse whether any improvements in sound quality have occurred. This was done by comparing the spectrum of the sound of

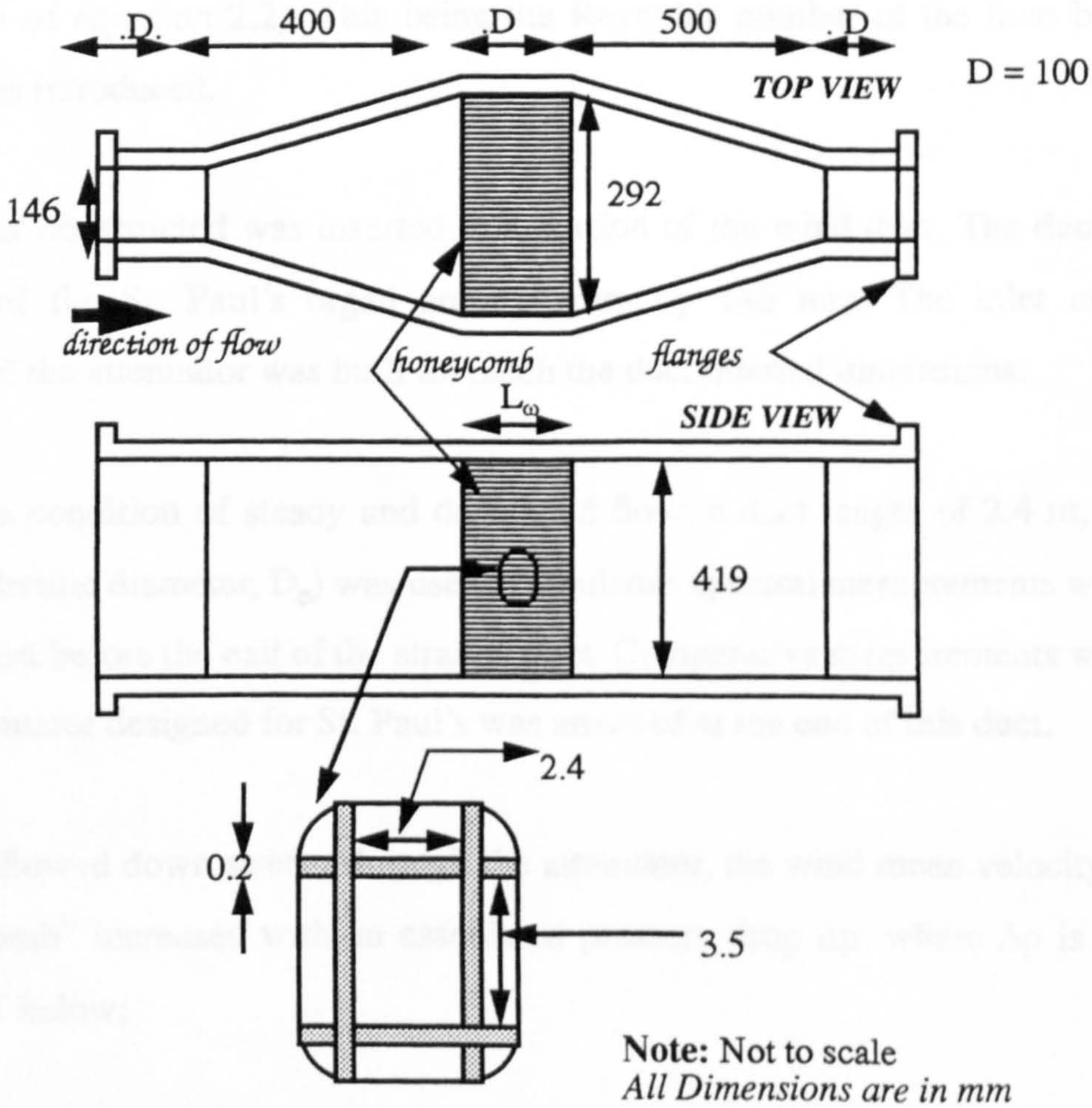

Fig. 4..0: Turbulence attenuator built for the St. Paul's Organ, Univ. of Huddersfield.

the organ pipe under investigation before and after the attenuator was installed.

4.2 Evaluation of the Turbulence Attenuator

Flow velocity and turbulence measurements were made on a test rig in the laboratory with wind supplied by a centrifugal blower that has a flow rate of 0.6 m^3/s (i.e. 1200 $ft.^3/min.$); driven by a Brook Crompton 1.5 KW, 3 phase motor. This is identical to the blower in use in St. Paul's with the exceptions that the blades were radial, and the finish inside of the casing was coarse.For the given duct dimensions, this meant a mean flow velocity of 9.258 m/s and a duct hydraulic (equivalent) diameter, D_e, of 216.5 mm. (The details of these calculations are given in appendix 4). Using 1.8×10^{-5} Ns/m^2 and 1.2 Kg/m^3 as the viscosity, μ, and density, ρ, of air respectively, an R_e of 133723 is obtained (calculated with the help of equation 2.2). This being the Reynolds number of the flow before the attenuator was introduced.

The attenuator constructed was inserted in a portion of the wind duct. The duct internal dimensions of the St. Paul's organ are 419 mm by 146 mm. The inlet and outlet dimensions of the attenuator was built to match the duct internal dimensions.

To satisfy the condition of steady and developed flow; a duct length of 2.4 m, (over 10 times the hydraulic diameter, D_e) was used. Turbulence spectral measurements were made of the wind just before the exit of the straight duct. Comparative measurements were taken after the attenuator designed for St. Paul's was attached at the end of this duct.

As the wind flowed down stream through the attenuator, the wind mean velocity through the "honeycomb" increased with an associated pressure drop Δp, where Δp is given by equation 3.11 below;

$$\Delta p = 4(\rho f L_\omega U_p)/2d_e \qquad 4.1$$

with $f = 16/R_e$ for laminar flow conditions

and $f = 0.079/(R_e)^{0.25}$ for turbulent flow[21] 4.2

where f = friction factor; and U_p = mean flow velocity in passage.

With the "honeycomb" dimensions of 2.4 mm by 3.5 mm, => d_e = 2.85 mm, yielding a Reynolds number, R_e of 1085.

R_e has decreased by a factor of more than 120; transforming the flow into the laminar flow regime.

The turbulence reduction is at the expense of a small pressure drop, calculated from equation 4.1 to be 40.62 N/m^2, (in organ builders language: 4.14 mmH_2O or 0.163 inH_2O). Using a TECquipment AF10 multitube manometer, a pressure drop of 0.4 mbar (≡ 40.53 N/m^2) was measured across the "honeycomb", in agreement with theoretical calculations.

4.2.1 Choice of Flow Measurement Equipment

Several measurement systems do exist with different forms of sensors for measuring turbulence motions. The HWA technique used is just one of several techniques that uses a probe operating on electrical principles.

The thermistor operates on similar principles to the HWA. However its poor sensitivity and unpopularity in measurements systems required for such application ruled it out.[41] Other electrical probes exploit *electrochemical and electric discharge* techniques which make them more suitable for liquid than gaseous applications.

Mechanically based probes include:- *the total head tube*, based on the hypodermic needle with a pressure transducer at one end. Unfortunately the needle behaves like a resonator usually requiring compensation for or annulment of these effects. The multiplicity of

coupled systems involved: acoustic, mechanical and electrical systems together with their low frequency response (typical bandwidth of 3KHz[41]), makes this approach a complicated and unsuitable choice for our measurements.

Other mechanical systems like the *static pressure tubes* amongst others could not be used because of their unnecessary complication relative to the application and/or low frequency response: usually less than 5 KHz.

Most contemporary flow measurement techniques do involve some form of flow visualisation, e.g. the Hydrogen bubble technique, *light refraction techniques*, others that take advantage of the *absorption and scattering of light* by the fluid etc. These techniques were not used because of their bulkiness, prohibitive costs and complexity relative to application in hand.

With the other schemes discounted, the HWA was resorted to. In Hot Wire Anemometry, there is the Constant Current and the Constant Temperature approach. Though the former is the simpler method, however, the wire time constant (impulse response) and hence frequency response, changes with change in operating point,[41 65] making the constant current approach undesirable. Add to that, there are very few manufacturers of the Constant Current Anemometer. The constant temperature HWA is much simpler to use. Furthermore, its sensitivity does not change significantly with the operating point of the device, hence its use in our measurements.

4.3 Fluid Dynamic Evaluation of the Turbulence Attenuator

4.3.1 Spectral measurement of turbulence

The turbulence spectrum of the wind from the duct attached upstream to the centrifugal machine was measured using a film type Hot Wire (HWA).

The turbulence spectrum was measured with a TSI 1210-20 HWA (from BIRAL UK Ltd., Bristol, TSI's UK representative) film probe placed in contra flow to the wind flowing downstream. The probe was connected to a TSI constant temperature anemometer bridge model 1750 and its output in turn fed into the B&K dual channel spectrum analyser (model 2034). When required, the data displayed on the screen of the analyser was plotted on a Hewlett-Packard HP 7475A plotter. Only data displayed on screen could be plotted. *The display scales of the spectrum analyser are not under operator control and hence it was not possible to plot/generate displays which readers will wish to compare to common scales. Hence when reading the plots from the spectrum analyser, attention should be paid on the scale as in some cases it varies.* The block diagram of figure 4.1 is a schematic of the experimental setup.

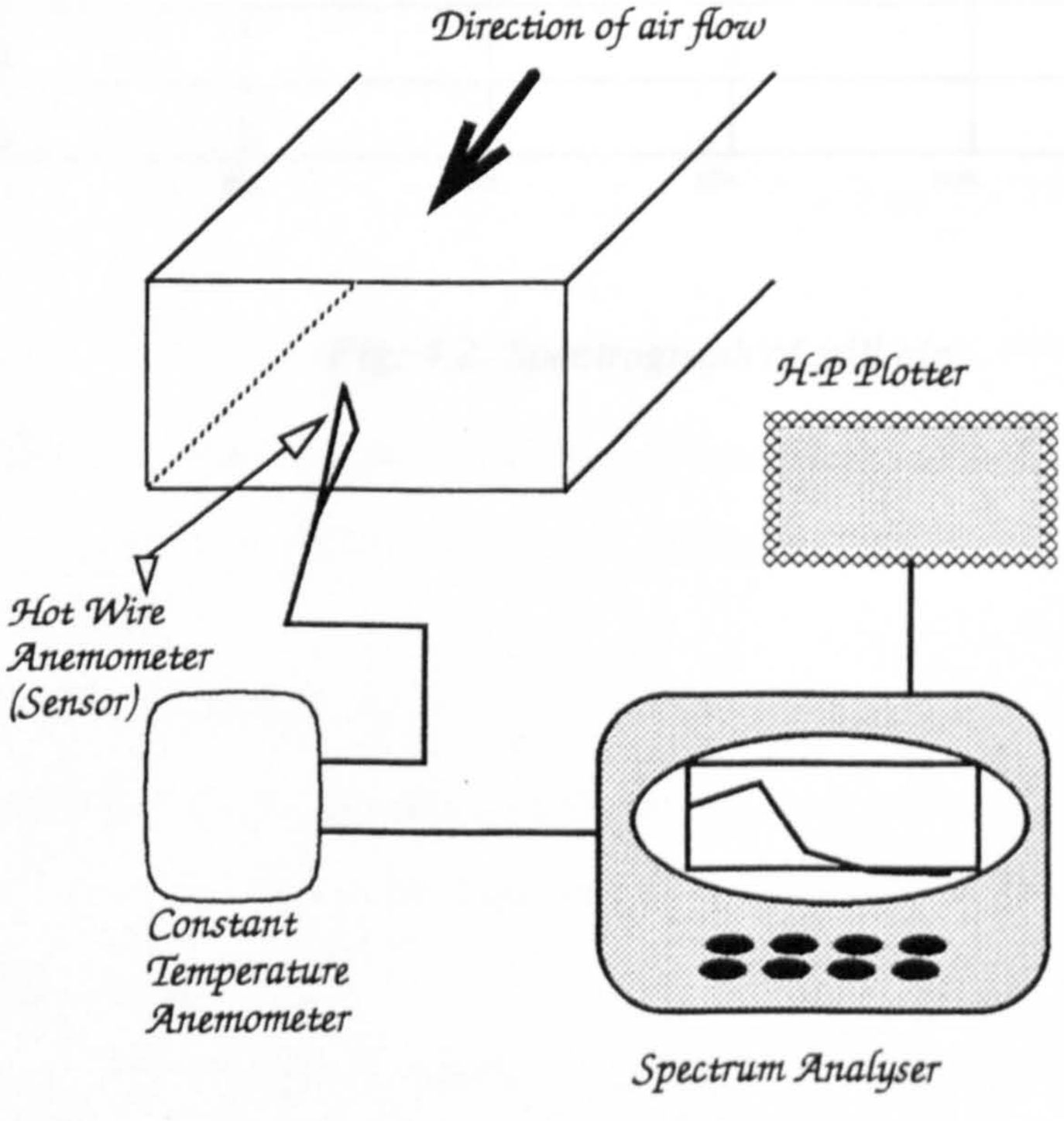

Fig. 4.1: Experimental Setup for the Evaluation of the Turbulence attenuator

Before these measurements were taken, the frequency response of the film sensor was

evaluated as prescribed by TSI (appendix 5) and found to have a bandwidth of 50 KHz; implying, the probe can track turbulence motions, fluctuating between 0 Hz and 50 KHz.[92]

The turbulence measurements were made with and without the attenuator connected. With the probe at the outlet of the duct, the spectrograph of the turbulence signal was evaluated. After the attenuator was installed, similar measurements were again made at the outlet of the attenuator. Prior to these measurements, the spectrograph of still air was measured.

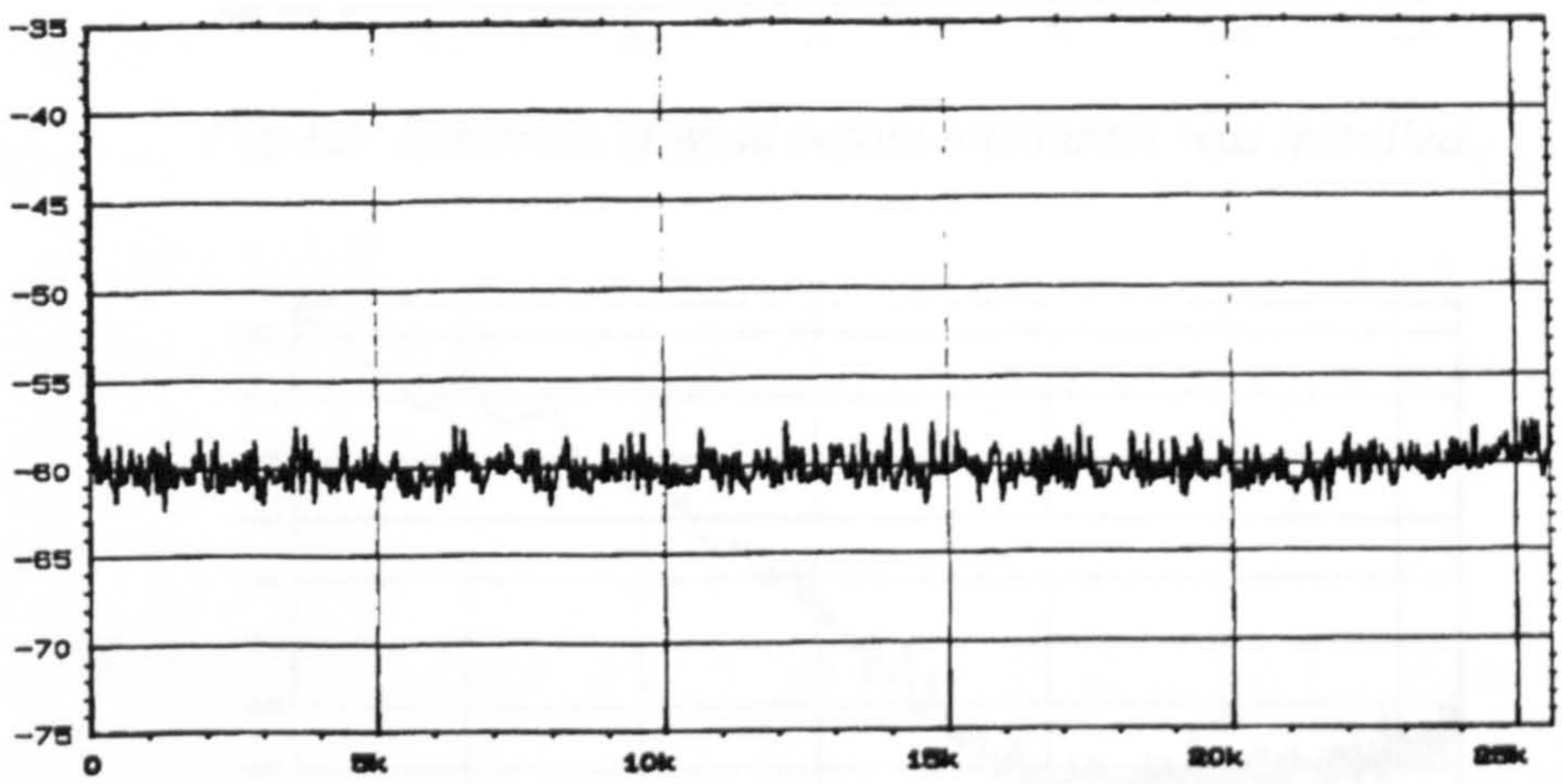

Fig: 4.2- Spectrograph of still air

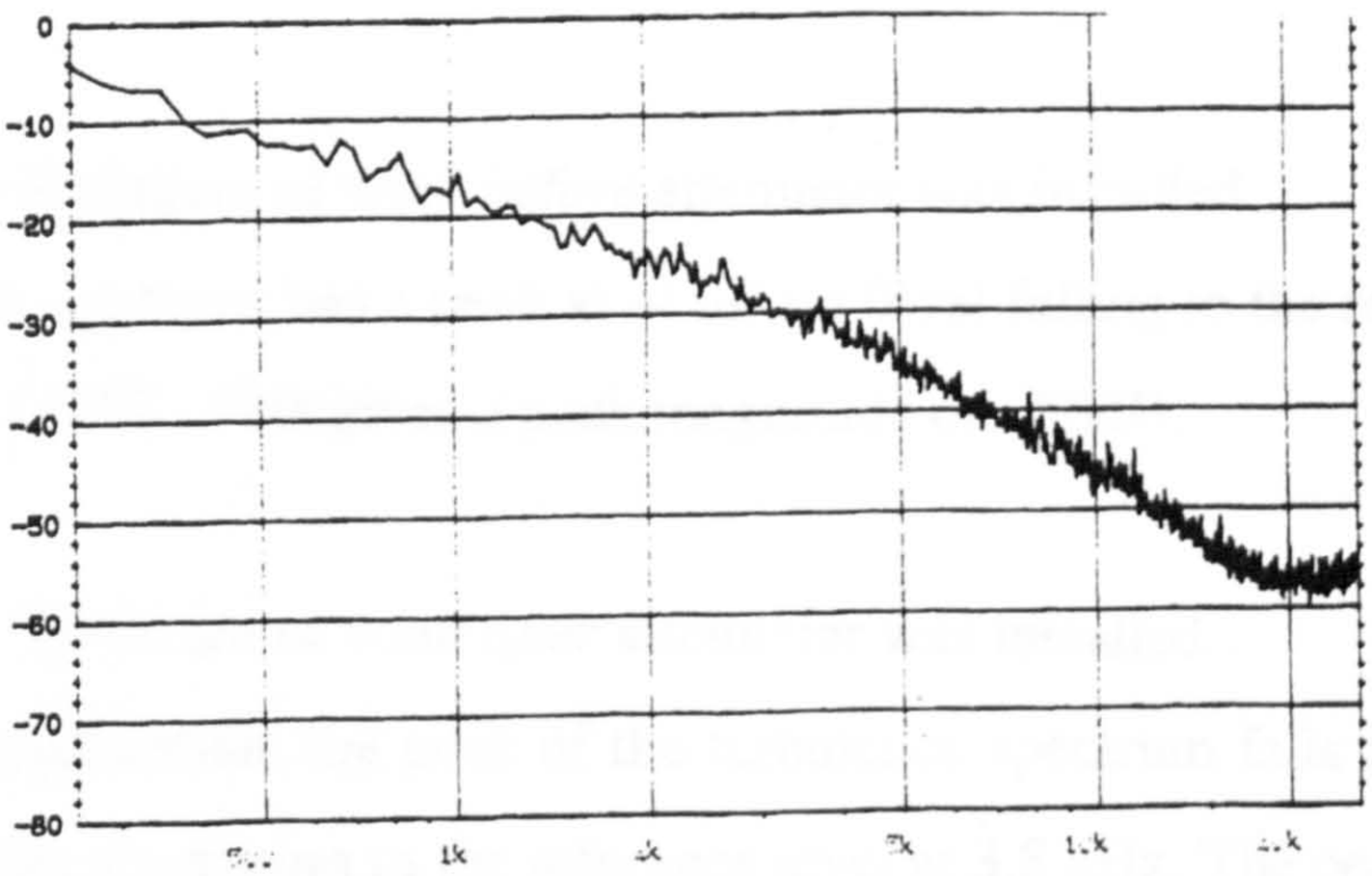

Fig 4.3- Spectrum of wind before attenuator was installed.

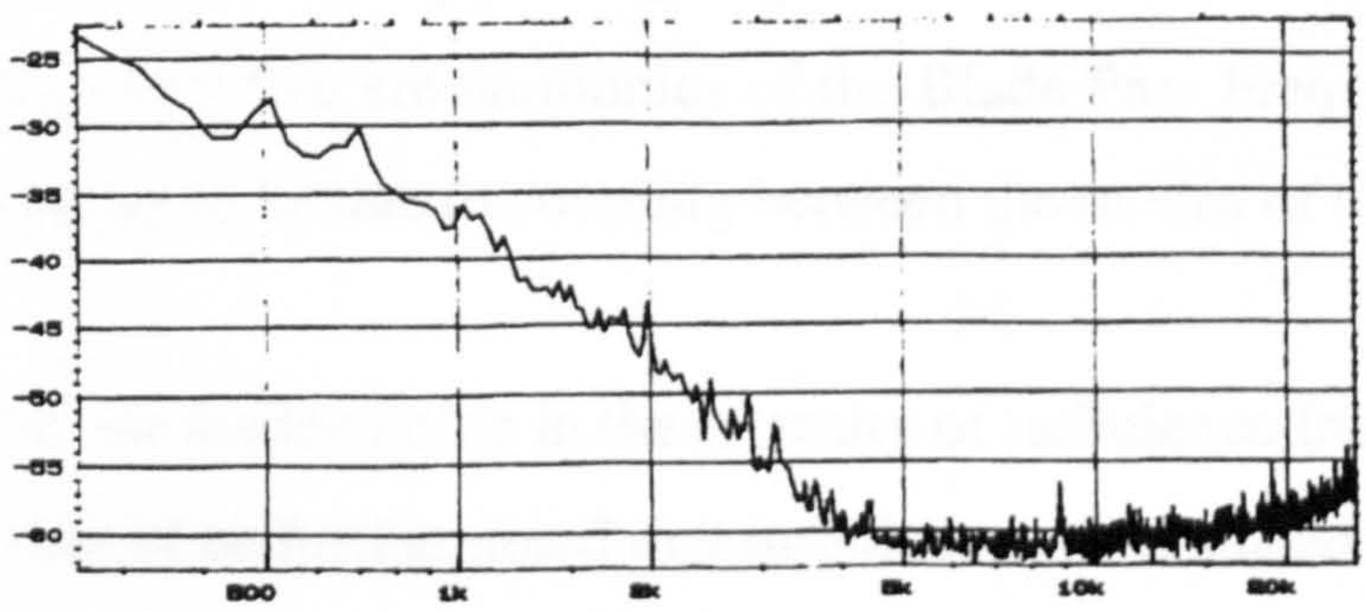

Fig 4.4- Spectrum of wind after attenuator was installed

Figures 4.2, 4.3, and 4.4 are plots of the spectrographs taken: a - still air; b - before attenuator installed and c- after attenuator installed.

Some comments on Figs 4.2 - 4.3[1]

Fig: 4.2- Spectrograph of still air.

This measurement was taken to be used as the reference level (a sort of ground level) for

---

1. A note on the scale of figures 4.2-4.4

The scale of the spectra are different. This unfortunate occurence was due to the limitations of the measuring equipment used. (B & K spectrum analyser) The area of screen available for viewing displayed data is limited. The range on the magnitude axis had to be adjusted to bring the data on display into view and so that it could be printed.

other turbulence measurements. The observed still air (reference) level is -60dB (fig 4.2)

- 4.3- Spectrum of wind *before* attenuator was installed.

Note here that thte spectrum has a peak at -4 dB (at 0Hz) falling to the reference (still air) levels of -60dBat 20kHz. This gives a peak magnitude of ~56dB.

- 4.4- Spectrum of wind *after* attenuator was installed .

After turbulence attenuation, the peak of the turbulence spectrum falls to -23 dB from (-4dB) at 0Hz, rapidly decreasing to the reference level at 3.8 kHz. The peak magnitude has dropped by almost 20dB from ~56dB to 37dB. In addition, after attenuation, some bumps became more prominent on the spectrum, at just over both 500Hz and 1000Hz plus another at 700Hz. The first two are harmonics of the Blade Pass Frequency (BPF), while the 700Hz bump is likely to be due to coupling between the modes of the BPF.

Figures 4.3 and 4.4 show a attenuation in the intensity of turbulence from a maximum of --4 dB to -23 dB. It should be further noted that turbulence is attenuated to still air levels at 3.8 KHz and beyond. 3.8 KHz could therefore be regarded as the ***cut off frequency*** of the attenuator. Figure 4.4 further illustrates an average attenuation of turbulence intensity of about 20 dB (a factor of 100) with a maximum attenuation of 30 dB (a factor of 1000) at 4 KHz. All measurements of turbulence were made while the spectrum analyser was programmed to a reference voltage level of 10mV.

It can be argued that the narrowness of the filter channel/passage contributed significantly in curtailing the intensity of turbulence. The boundary conditions changed as the flow went from a wide to a set of narrow channels. The change in boundary conditions caused a restriction in fluctuations and eddie generation. The fall in the Reynolds number meant an increase in the friction factor, and hence increased viscous losses.

This turbulence attenuation technique can be thought of as reversion by dissipation .[64 84 95]

From figure 4.3 it can be conjectured that the turbulent fluctuations are predominant at lower frequencies. Figure 4.3 depicts a cut off frequency before installation of 20 KHz when the attenuator was not installed.

4.3.2 Turbulence in the time domain

Figure 4.5 and 4.6[1] are snapshots of the time domain turbulence signals before and after the attenuator was installed respectively. Figure 4.7 is a more elaborate picture of figure 4.6 - the time domain turbulence signal after attenuation

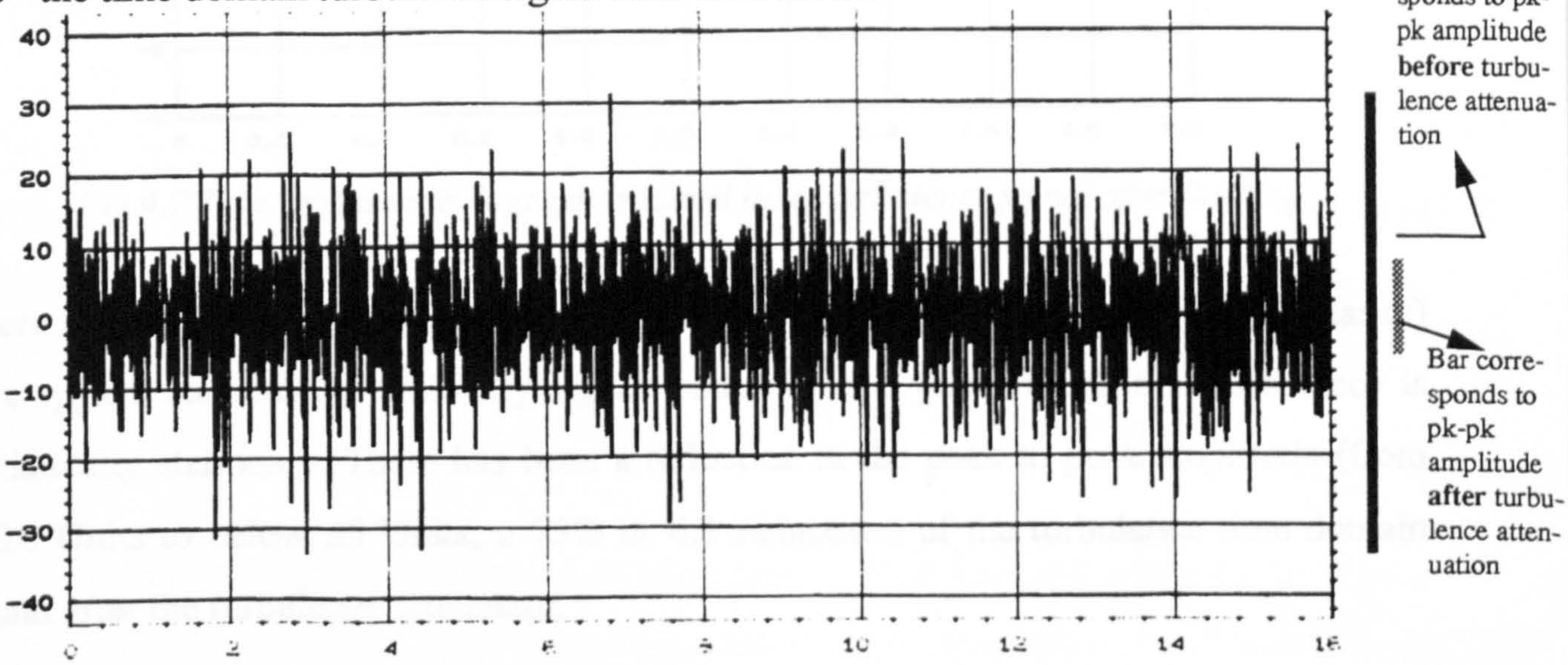

Fig 4.5 Time domain oscillograph of turbulence signal before filtering

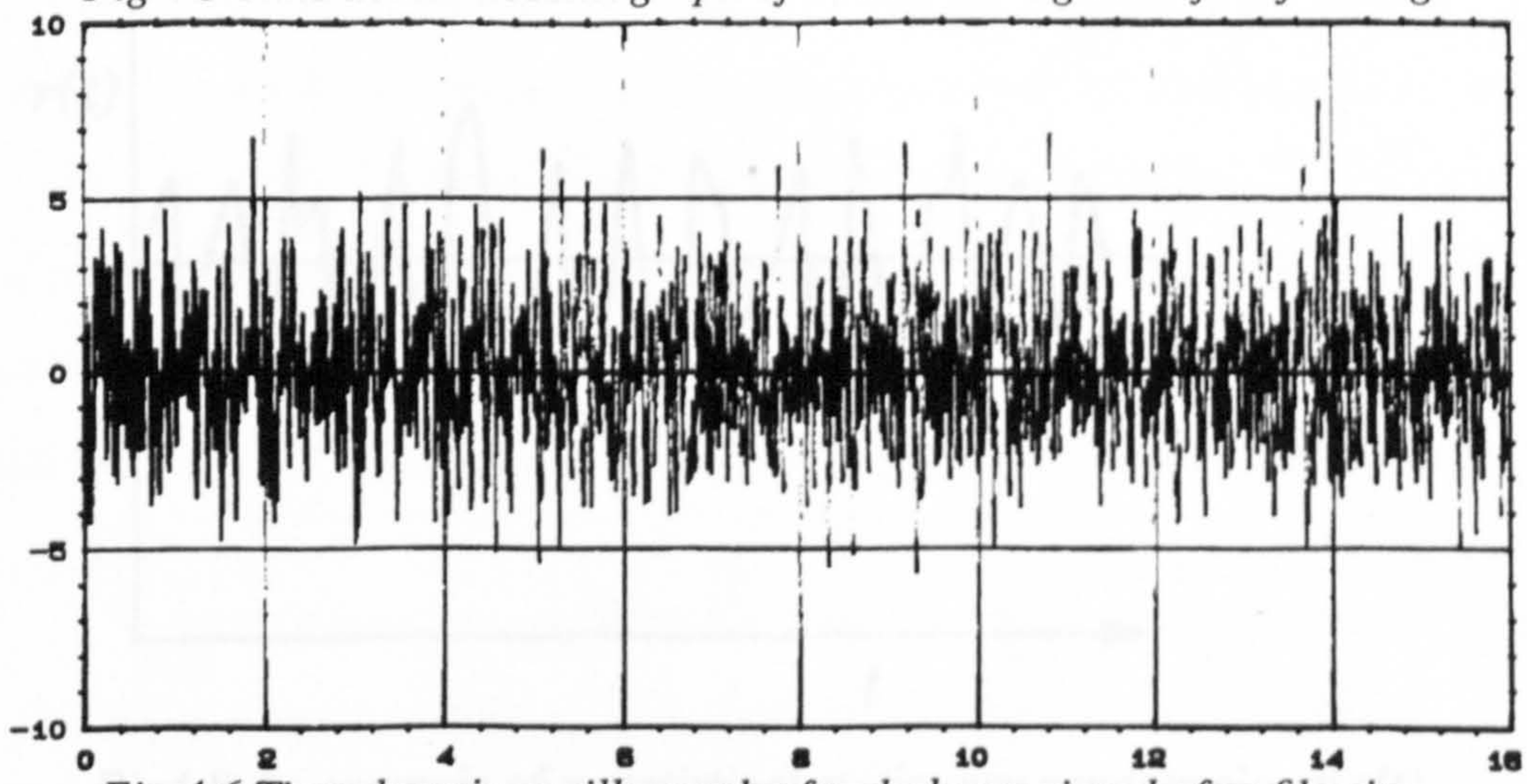

Fig 4.6 Time domain oscillograph of turbulence signal after filtering

---

1. The graphs of figures 4.5 & 4.6 are on different scales also. This adjustment was made so that the data captured on the spectrum analyser could be observed and printed.

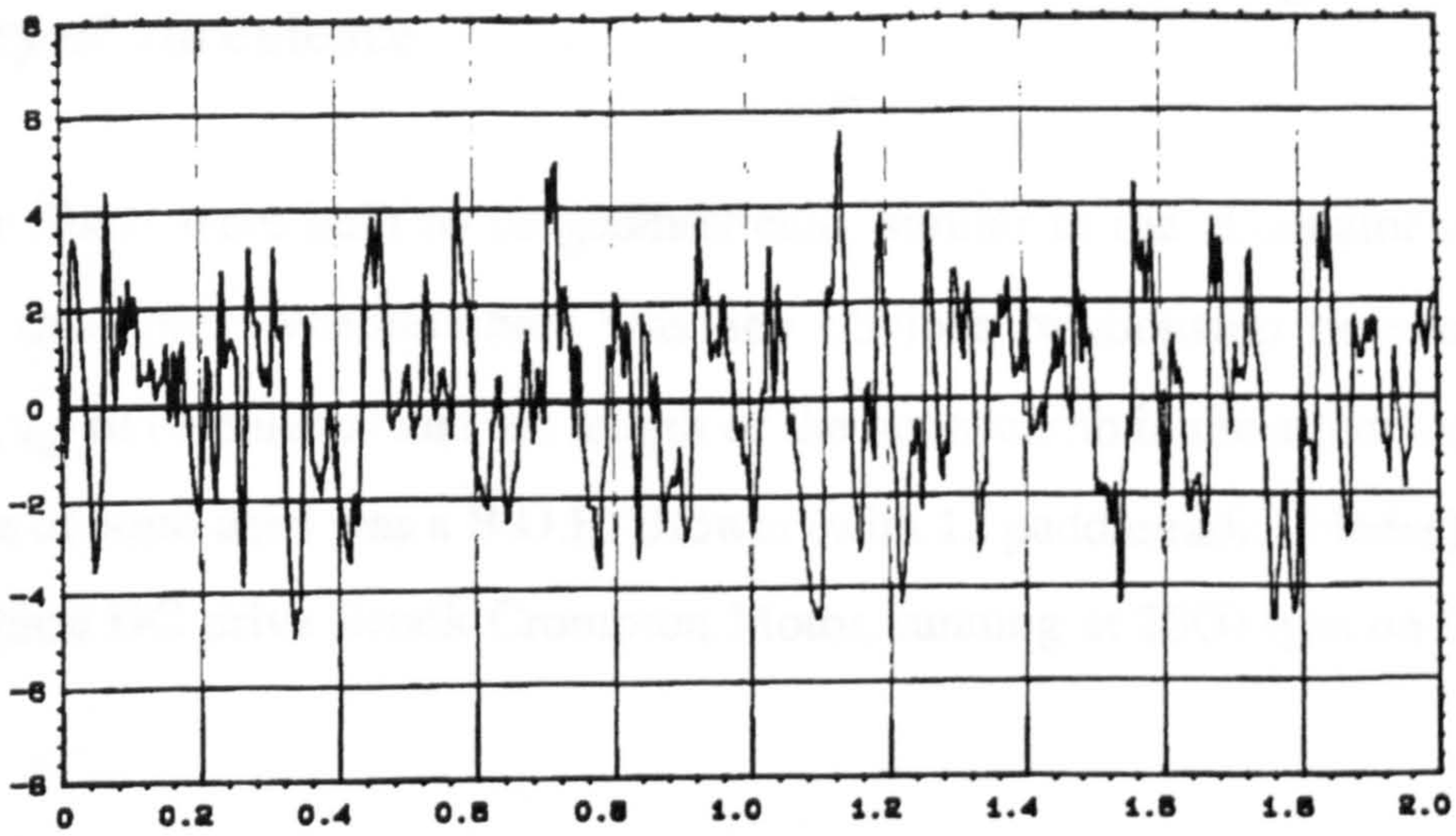

Fig 4.7 Time domain oscillograph (zoomed in) of turbulence signal after filtering

There is a similarity in figures 4.5, 4.6 and 4.7 to figure 3.1-i, (repeated below for clarity) of a typical statistically stationary signal: endorsing the presumption that turbulence is statistically stationary. There has been a reduction in the peak to peak amplitude (from ≈±20 Units to below ±5 Units; a 75% or 4:1 reduction) of the turbulence time domain signal after the turbulence attenuator.

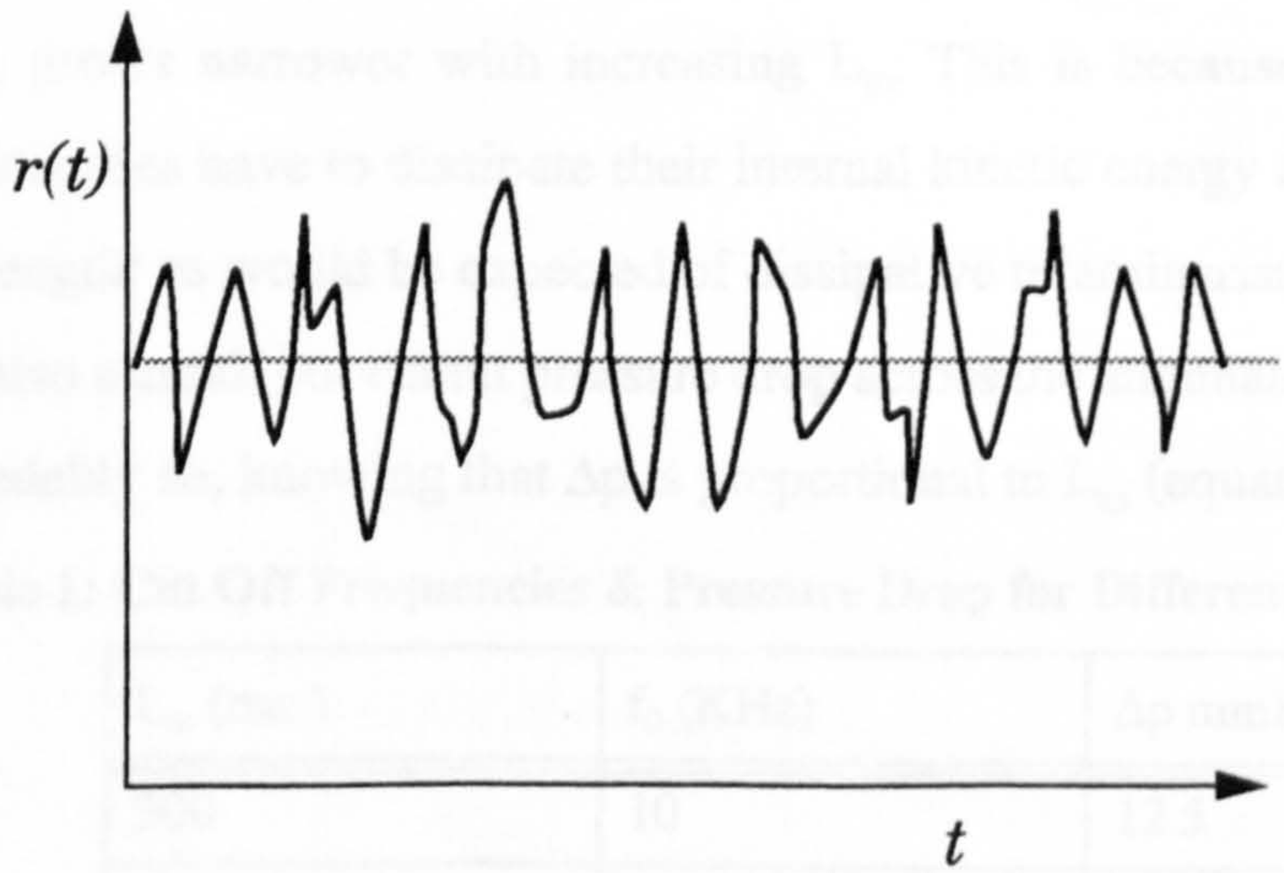

Fig4.8 An example of a statistical stationary random signal r(t)

The performance of the organ in St. Paul's Hall was evaluated before and after this device was installed will be given in section 4.4.

4.4 Relationship Between Attenuator Honeycomb Length L_ω and Cutoff Frequency of Turbulence

Four other filters were built to be geometrically similar to the attenuator installed in St. Paul's, to determine whether there was any obvious relationship between the cut off frequency, f_o, of turbulence and the length of the honeycomb in the attenuator, L_ω.

The source of wind used was a B.O.B. Blower (with 12 paddle/radial blades), propelled by a single phase DC drive Brook Crompton Motor, running at 2800 rpm on 0.54 kW (0.75 hp).

Attenuators with L_ω of 150 mm, 200 mm, 250 mm, and 300 mm, were built. The turbulence spectrum of the filtered and unfiltered wind were taken as earlier discussed and the cutoff frequencies and pressure drops measured. Results obtained are as in the Table I below. Details of their behaviour are as in Figures 4.10, 4.11 and 4.12 below.

The increase in pressure loss, Δp, with increasing L_ω is to be expected as Δp is directly proportional to L_ω, all the other parameters being equal. The turbulence bandwidth, as expected, grows narrower with increasing L_ω. This is because there is more time over which the eddies have to dissipate their internal kinetic energy as a result of the increased passage length: as would be expected of dissipative relaminarisation.[64 84 95]

There is also a small but extant pressure drop across the attenuator which increase with L_ω, understandably so, knowing that Δp is proportional to L_ω (equation 4.1)..

Table 1: Cut Off Frequencies & Pressure Drop for Different Attenuator Lengths

L_ω (mm)	f_0 (KHz)	Δp mmH_2O
300	10	12.5
250	12.5	11.7
200	14	10.5
150	19	8.7

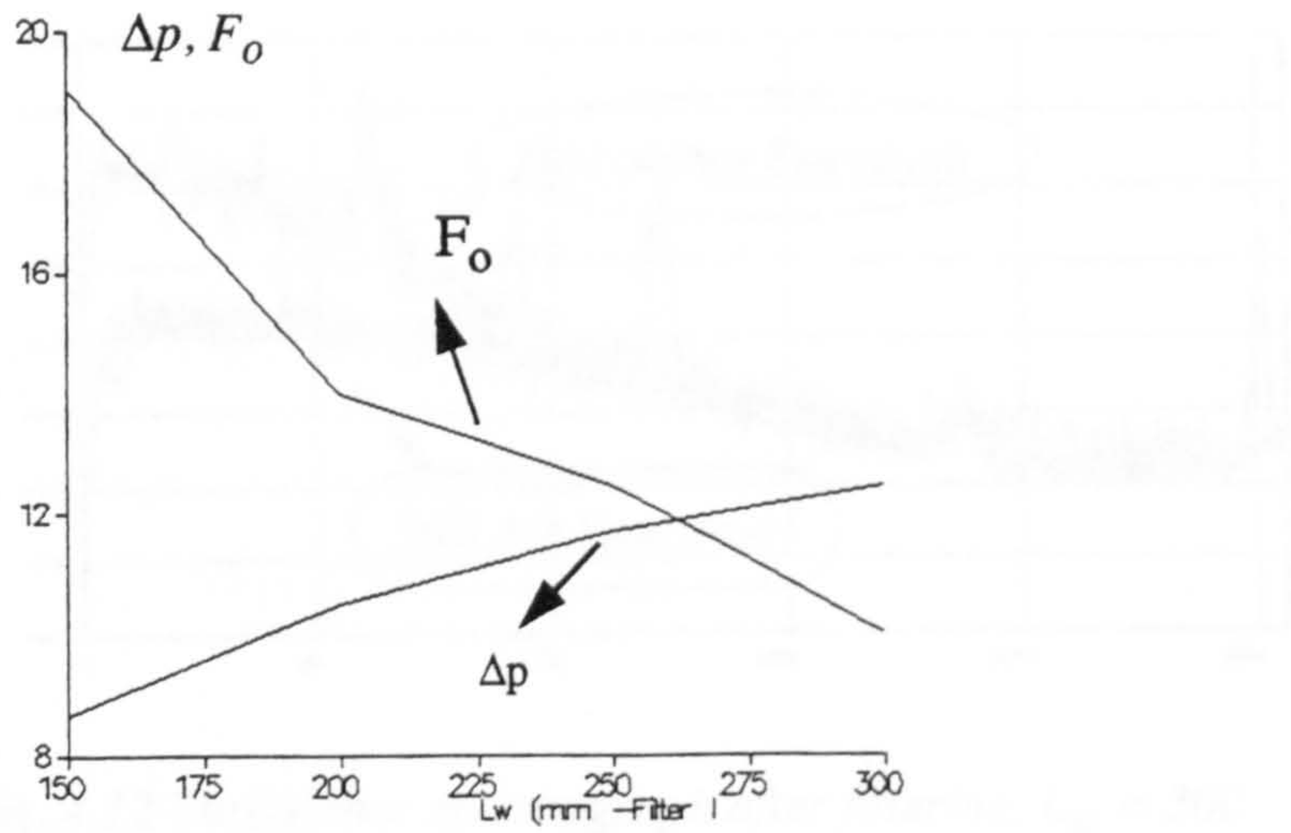

Fig 4.9 Changing cut-off freq. & pressure loss with filter length

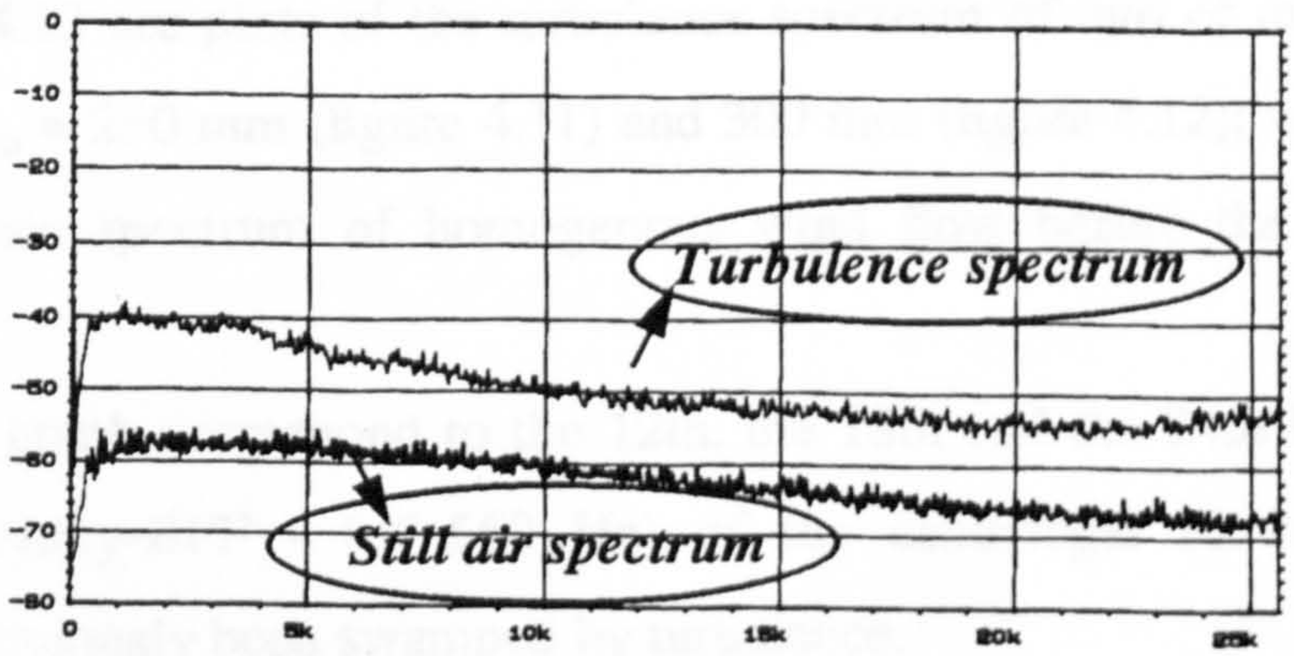

Fig. 4.10 Turbulence spectrograph before filtering

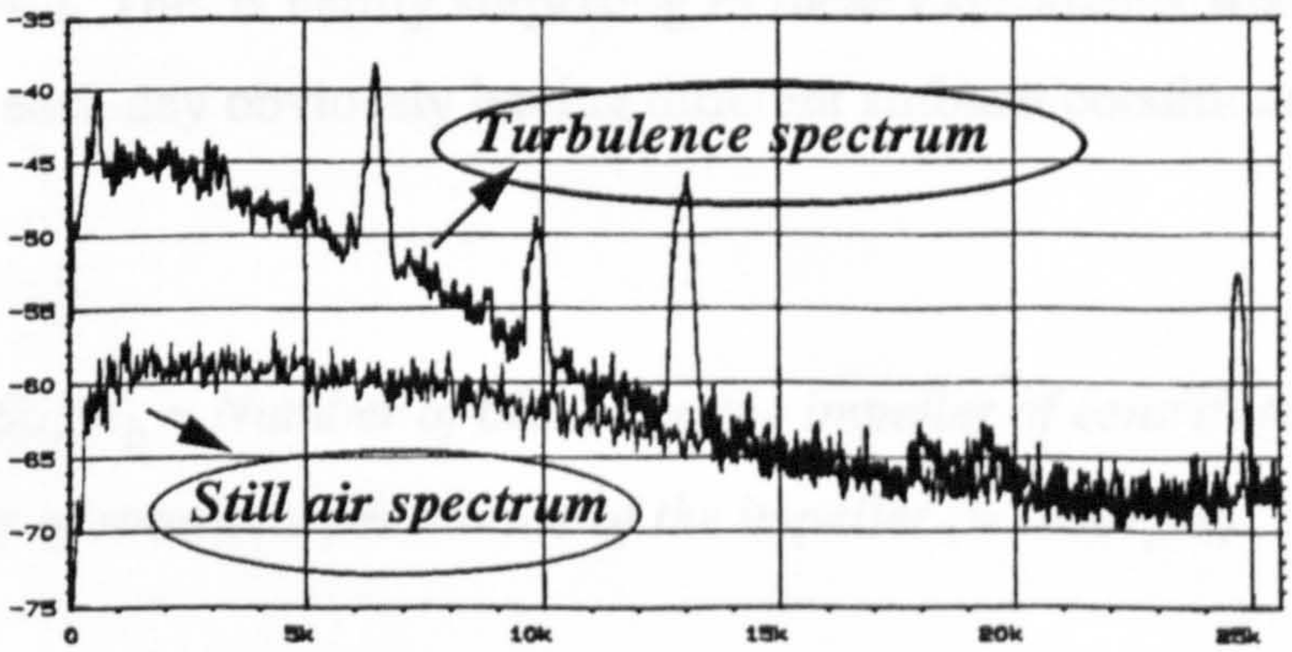

Fig. 4.11 Turbulence spectrograph after filtering, $L_\omega = 250$

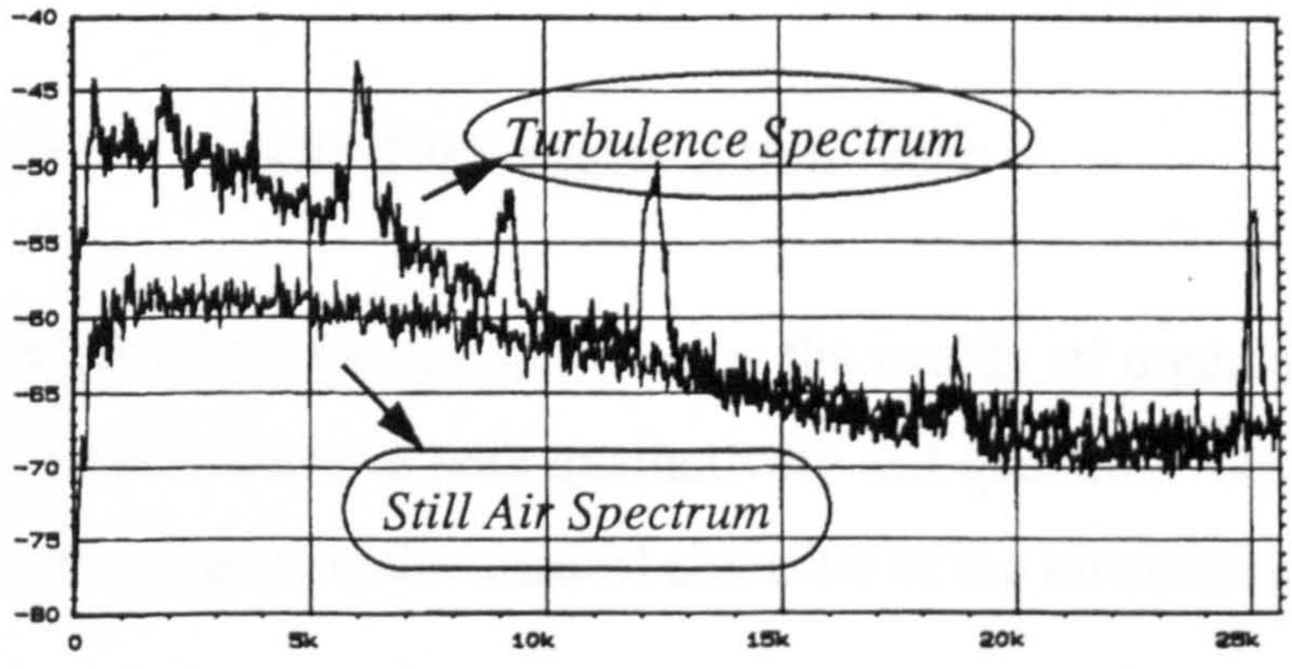

Fig. 4.12 Turbulence spectrograph after filtering, $L_\omega = 300$

Figures 4.11 and 4.12 are plots of the turbulence spectrum of two of the attenuators in table 1. Case of L_ω = 250 mm (figure 4.11) and 300 mm (figure 4.12); while figure 4.10 gives the turbulence spectrum of homogenous wind flow before the attenuator was installed.

The peaks on the graph correspond to the 12th, the 18th and the 24th harmonic of the Blade Pass Frequency-BPF - (of 560 Hz) of the centrifugal blower used. These frequencies had previously been swamped by turbulence.

The still air spectrum is the reference spectrum. It has a different level to that measured in figure 4.2. This is hardly surprising as these ex[eriments were conducted on separate days, with each day obviously having different ambient conditions.

Note

$BPF = (N_b \, xRPM)/60$; N_b = Number of blades on the impeller of centrifugal blower (=12) and RPM = Number of rotations per minute of the impeller (=2800rpm)

The filters were found to have an average wind speed of 22.5 m/s. The wind speed and pressure drop were measured using a hand held HWA model TA6000 and a Mark 4

manometer respectively, both by AIRFLOW Developments Ltd.

4.5 Acoustic Evaluation of the Turbulence Attenuator.

To appreciate the effects of the turbulence filter on the quality of organ pipe sound, it is essential to evaluate its performance both qualitatively and quantitatively as well as have an aural assessment of its efects on the musical character of the instrument.

4.5.1 A Qualitative Evaluation

Figure 4.13 portrays the schematic block diagram of the method used for this evaluation

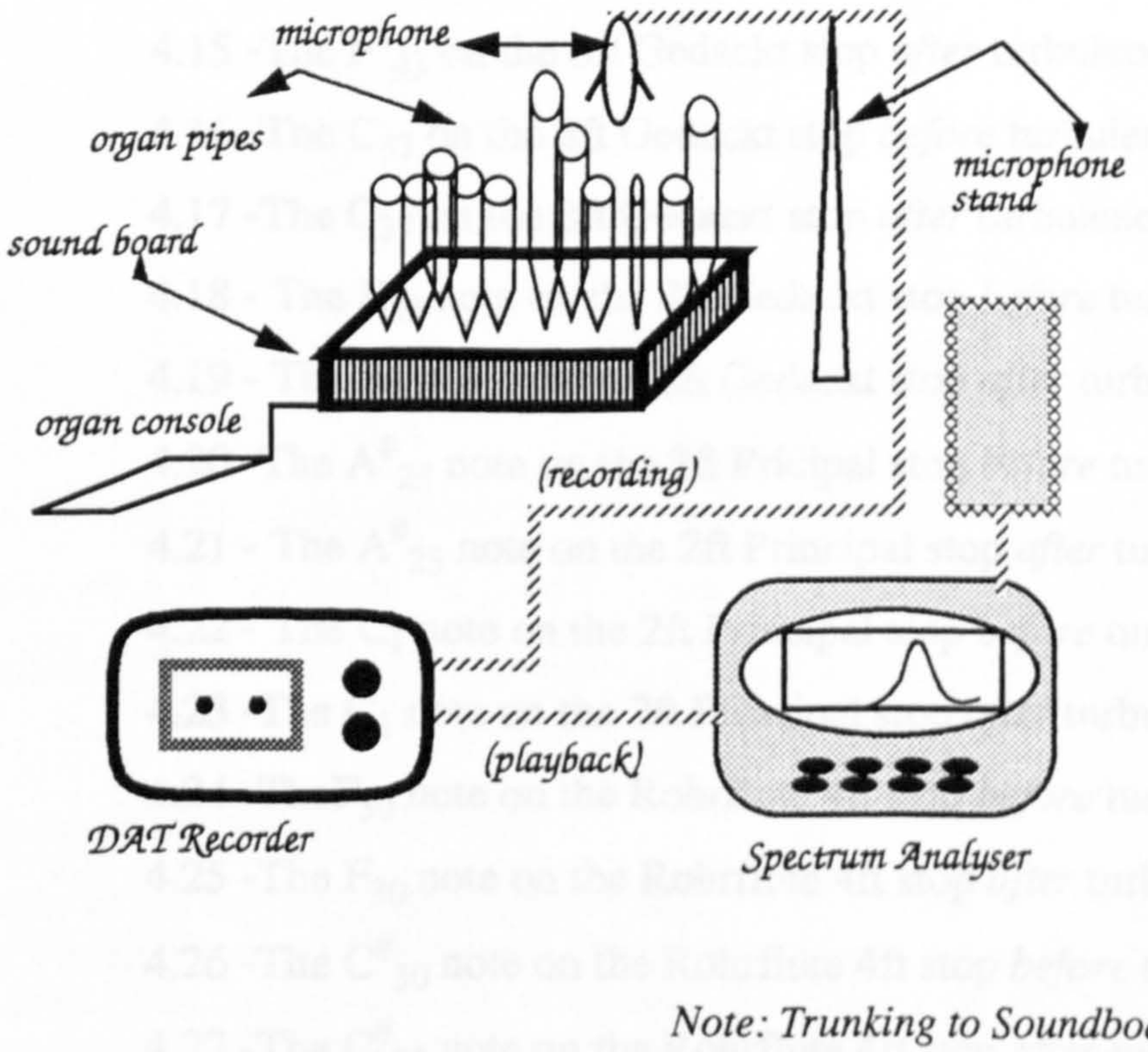

Fig. 4.13: Block Diagram of System used for Qualitative Evaluation of attenuator

This technique involves recording individual notes on certain stops on the organ where the problem of flutter and ripple thought to be induced by turbulence is most prominent. These recordings were done on HHb PQ92 digital audio tapes with the help of a CASIO DA-7, digital audio tape (DAT) recorder. The recordings were taken before and after the turbulence attenuator was installed in the organ wind trunk.

Samples taken included recordings of about three dozen notes on the Gedackt 8ft, the 4ft Rohrflöte and the 2ft Principal stops.

On play back, the output of the recorder was channelled into the spectrum analyser to evaluate the characteristics of fundamental of some of the pipes.

In figures 4.14-4.27 are spectrographs of some notes before and after the attenuator was installed on the St. Paul's organ.

Fig. 4.14- The $F^{\#}_{43}$ on the 8ft Gedackt stop *before* turbulence filtering

4.15 -The $F^{\#}_{43}$ on the 8ft Gedackt stop *after* turbulence filtering

4.16 -The C_{37} on the 8ft Gedackt stop *before* turbulence filtering

4.17 -The C_{37} on the 8ft Gedackt stop *after* turbulence filtering

4.18 - The E_{29} note on the 8ft Gedackt stop *before* turbulence filtering

4.19 - The E_{29} note on the 8ft Gedackt stop *after* turbulence filtering

4.20 -The $A^{\#}_{23}$ note on the 2ft Pricipal stop *before* turbulence filtering

4.21 - The $A^{\#}_{23}$ note on the 2ft Principal stop *after* turbulence filtering

4.22 - The C_1 note on the 2ft Principal stop *before* turbulence filtering

4.23 -The C_1 note on the 2ft Principal stop *after* turbulence filtering

4.24 -TheF_{30} note on the Rohrflute 4ft stop *before* turbulence filtering

4.25 -The F_{30} note on the Rohrflute 4ft stop *after* turbulence filtering

4.26 -The $C^{\#}_{30}$ note on the Rohrflute 4ft stop *before* turbulence filtering

4.27 -The $C^{\#}_{30}$ note on the Rohrflute 4ft stop *after* turbulence filtering

(The verical axis = magnitude; horizontal axis = frequency for figs. 4.14-4.27)

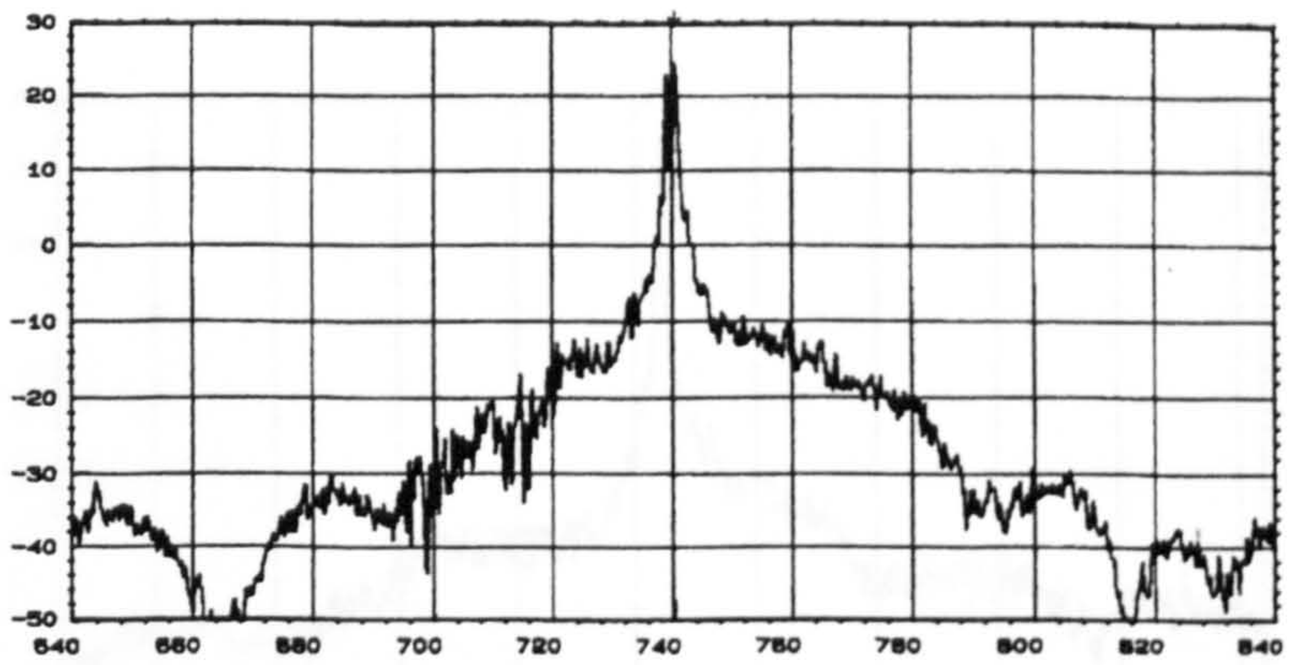

Fig. 4.14- The $F^{\#}_{43}$ on the 8ft Gedackt stop before turbulence filtering

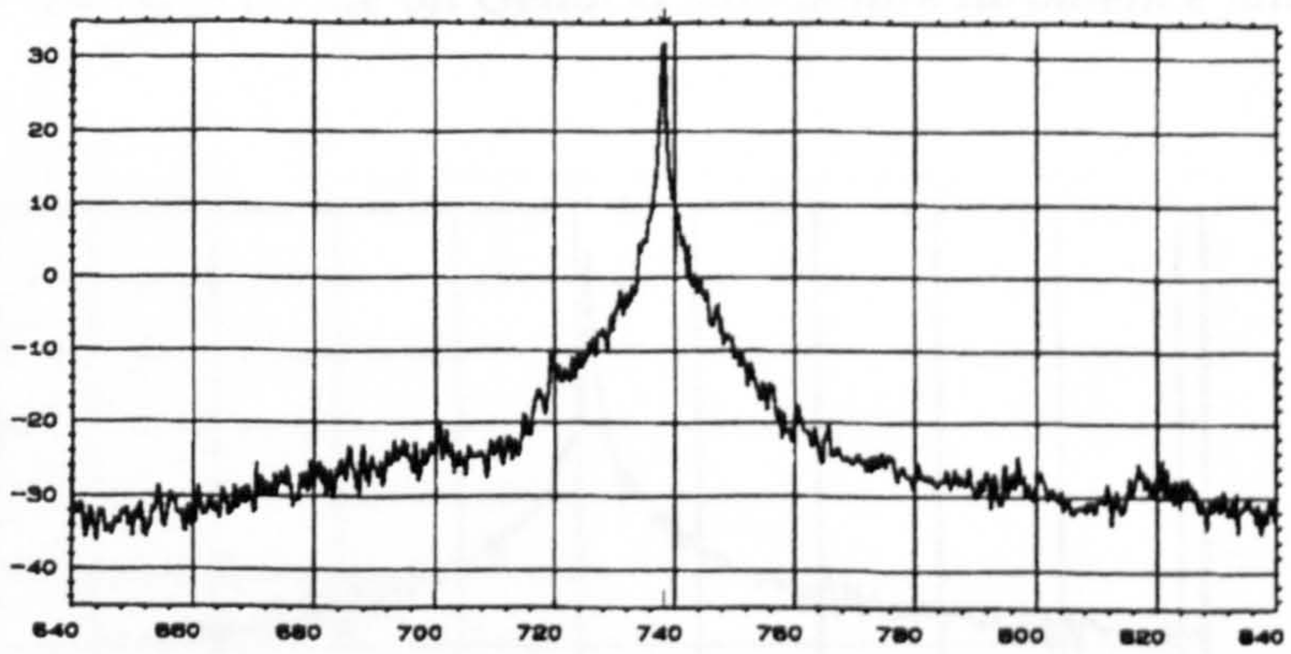

Fig. 4.15- The $F^{\#}_{43}$ on the 8ft Gedackt stop after turbulence filtering

Note how the note had a spectrum with bumps and troughs as well as two peaks (at 738 Hz & 742Hz with a diference of ~2dB beween them) before turbulence attenuation. After attenuation, the note is much smoother, i.e. it is less bumpy and has just one peak.

Some notes on figures 4.14 - 4.27

In some of the ensuing figures, serious attention should not be paid to the scales of the vertical axis. The figures should be regarded more as an illustration to aid the qualitative evaluation of the note. This is because the recordings were done on different days. In addition, the microphone position was not the same for every note or corresponding pairs of notes recorded with and without the turbulence attenuator.

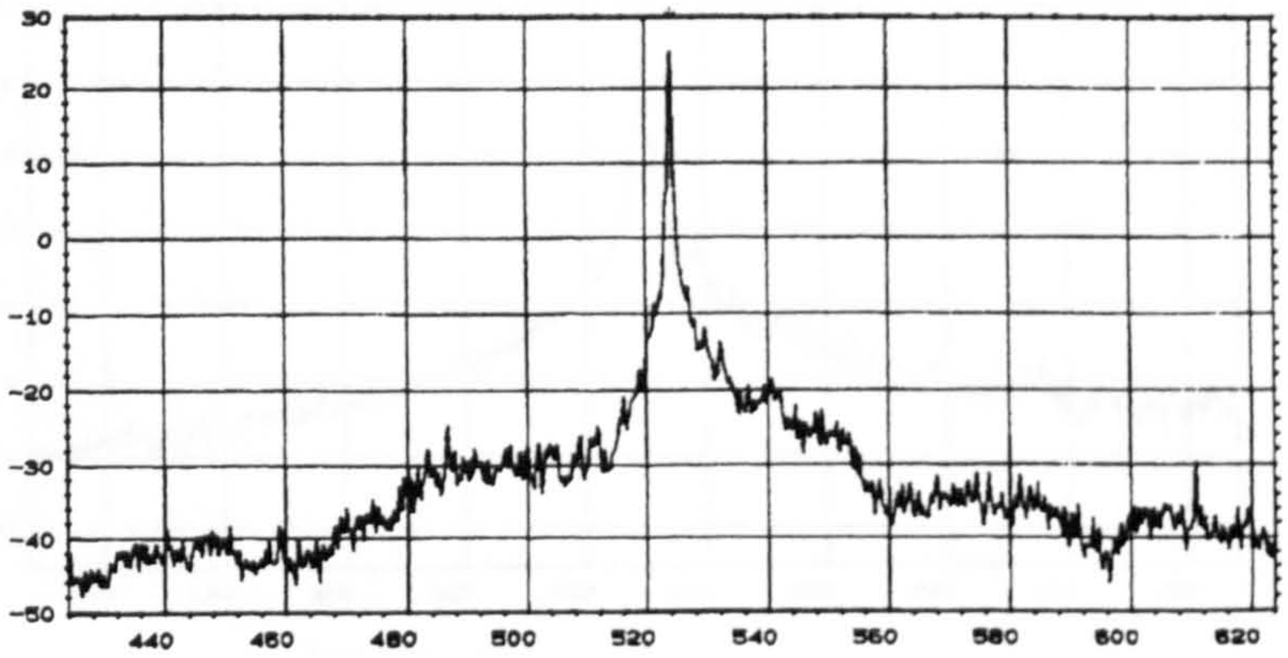

Fig. 4.16 -The C_{37} on the 8ft Gedackt stop before turbulence filtering

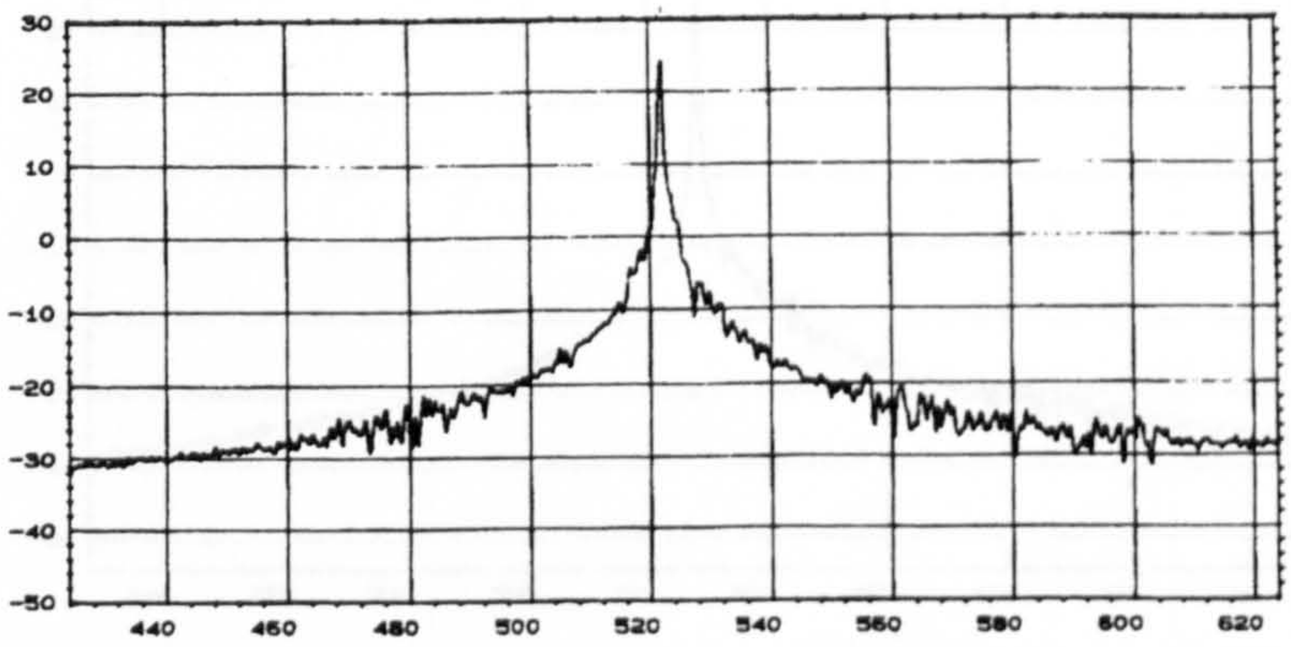

Fig. 4.17 -The C_{37} on the 8ft Gedackt stop after turbulence filtering

Note that the peak at 610Hz has been eliminated. A rough looking note before turbulence attenuation is now much smoother apart from the much attenuated bumps in the neighbourhood of 480Hz and 560Hz.

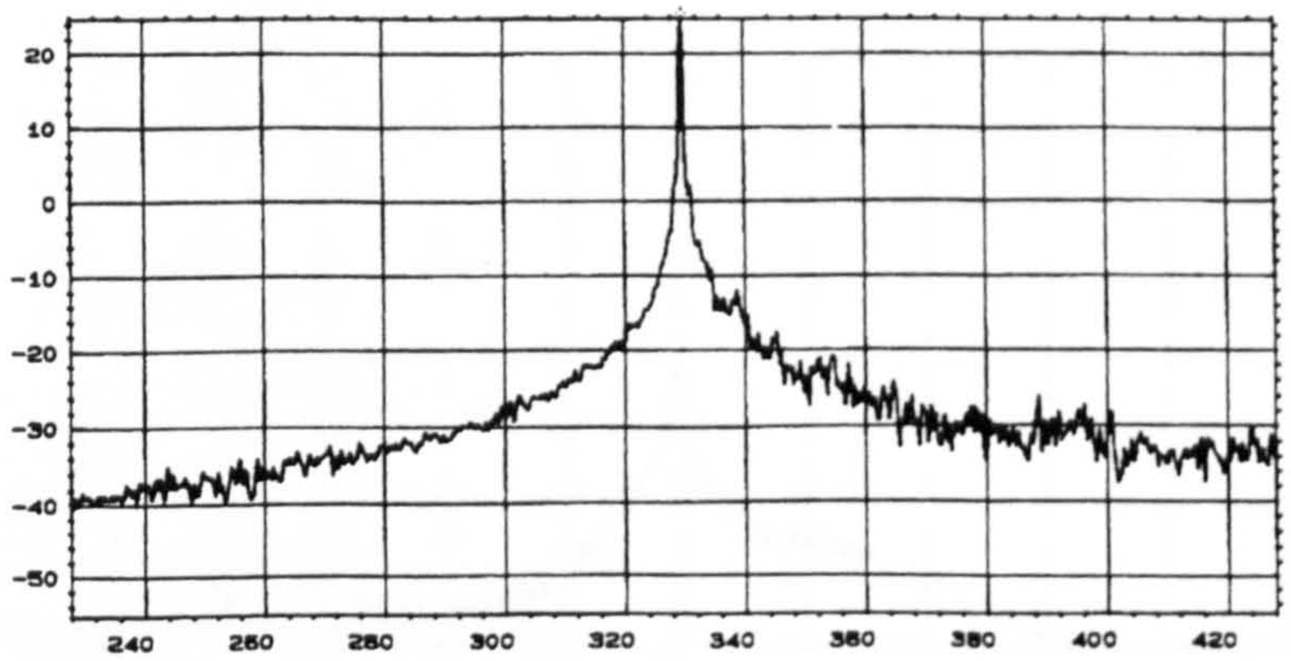

4.18 - The E_{29} note on the 8ft Gedackt stop before turbulence filtering

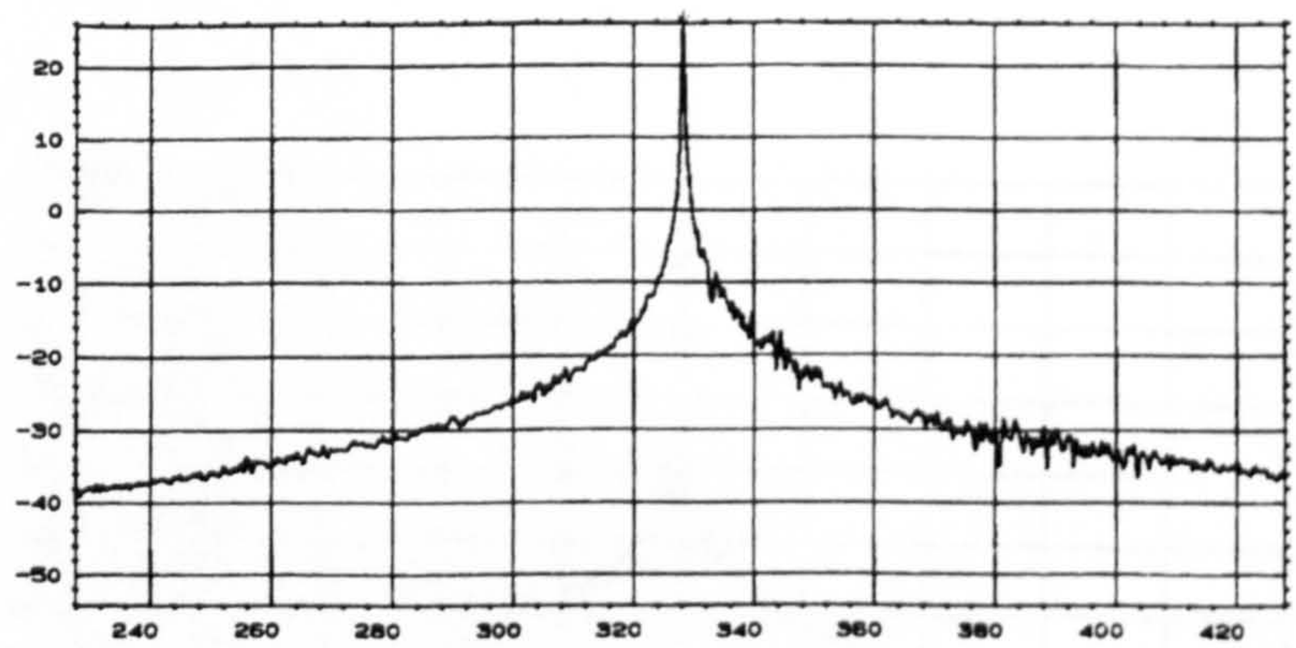

4.19 - The E_{29} note on the 8ft Gedackt stop after turbulence filtering

The bumps between 240Hz and 260Hz have been suppressed with turbulence attenuation. Bumps at 340Hz and beyond have been significantly attenuated.

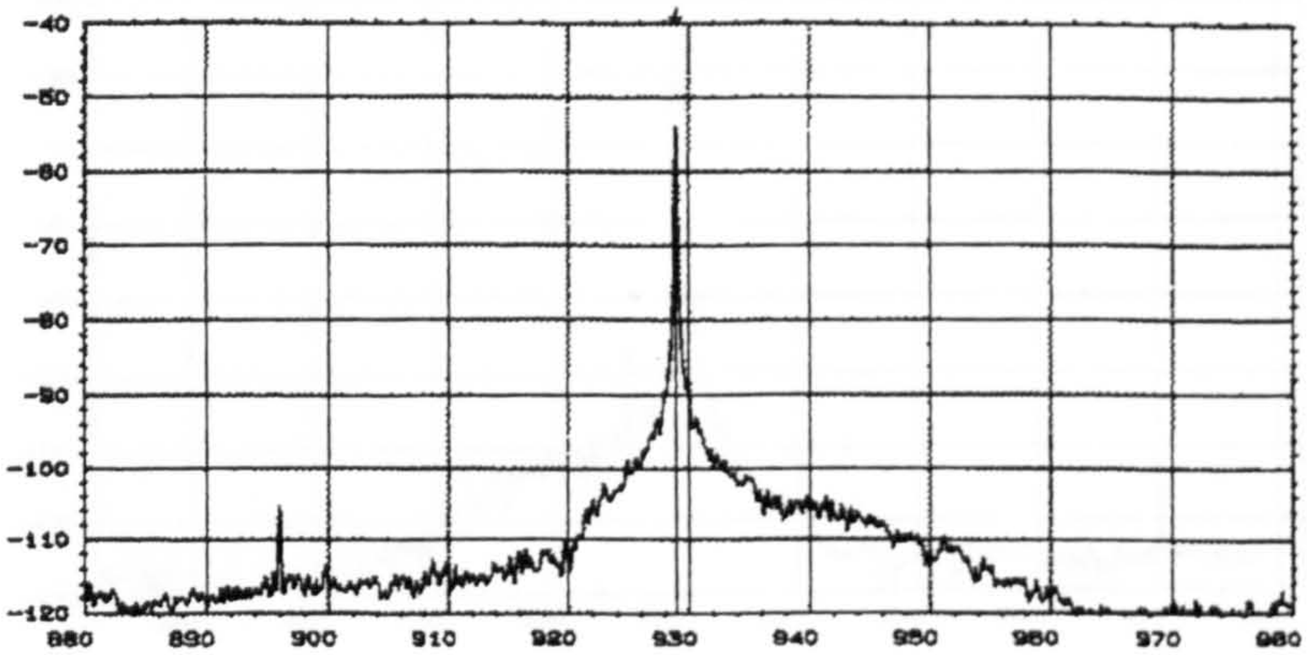

Fig 4.20 -The $A^{\#}_{23}$ note on the 2ft Principal stop before turbulence filtering

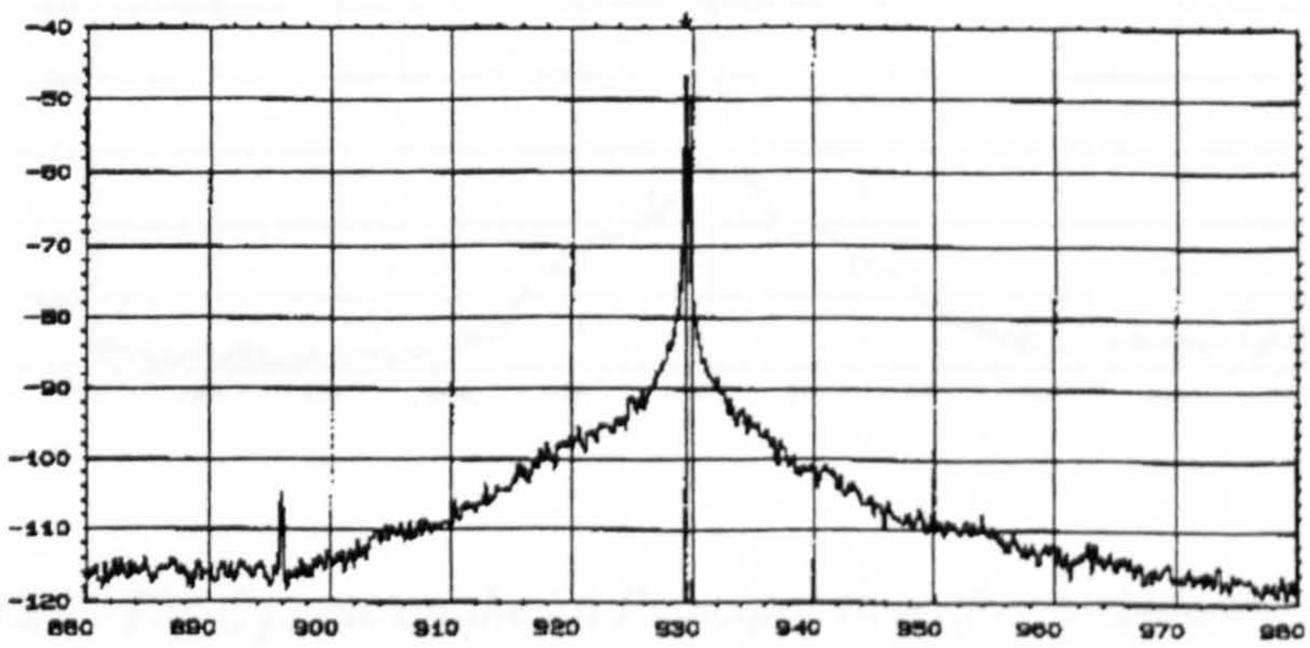

Fig. 4.21 -The $A^{\#}_{23}$ note on the 2ft Principal stop after turbulence filtering

The note has a much smoother spectrum with turbulence attenuation. The peak at near 900Hz is still prominent. The peak could be a component of some resonant effect in the soundboard or a component of the Blade Pass Frequency of the fan.

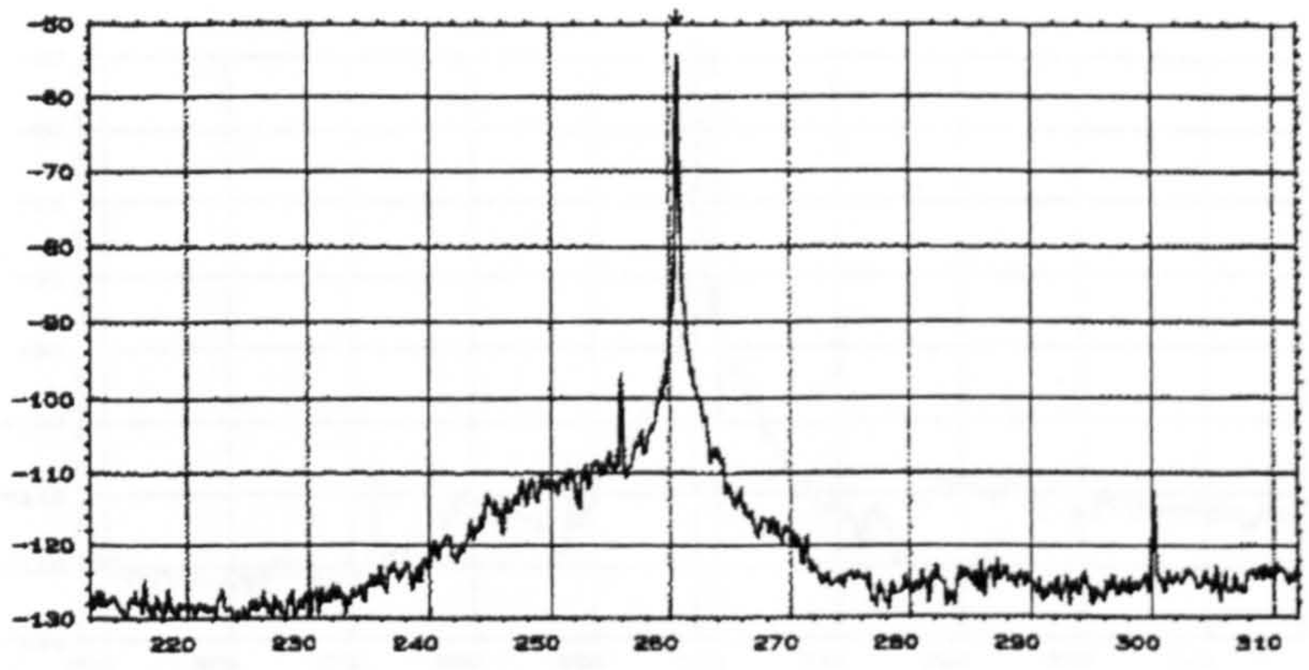

Fig. 4.22 - The C_1 note on the 2ft Principal stop before turbulence filtering

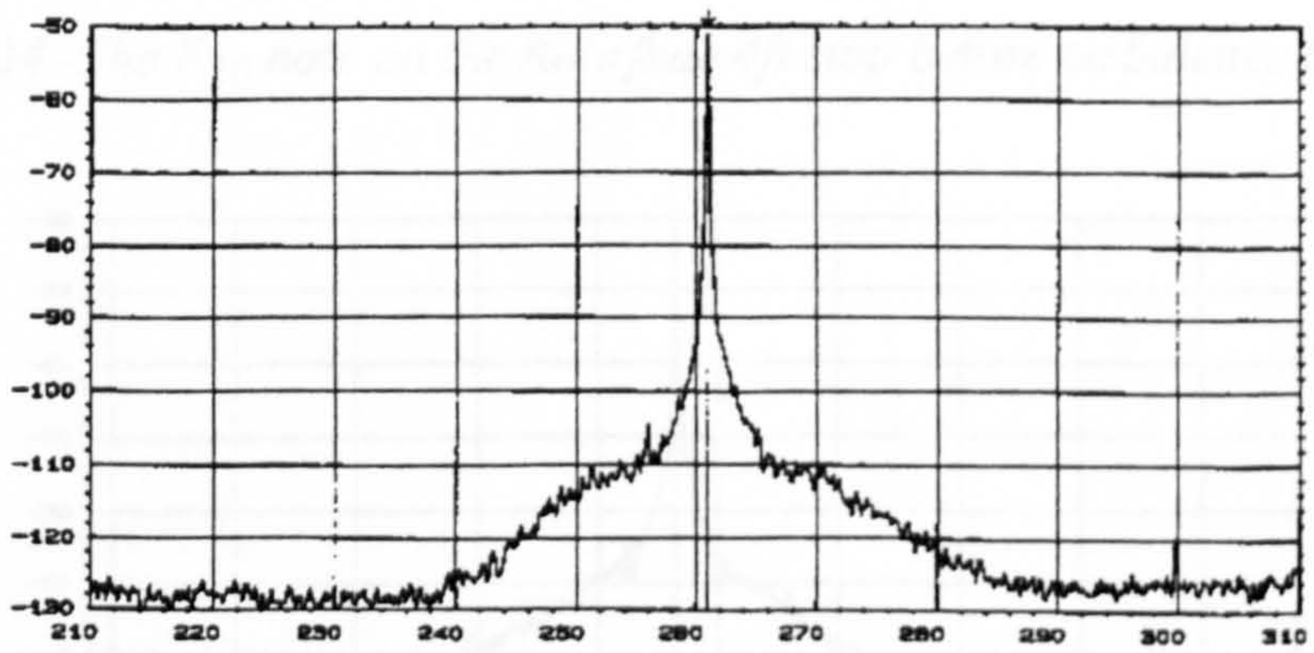

Fig. 4.23 - The C_1 note on the 2ft Principal stop after turbulence filtering

The ripples on the note have been attenuated with turbulence attenuation. The peaks at 256Hz and 300Hz have also been curtailed.

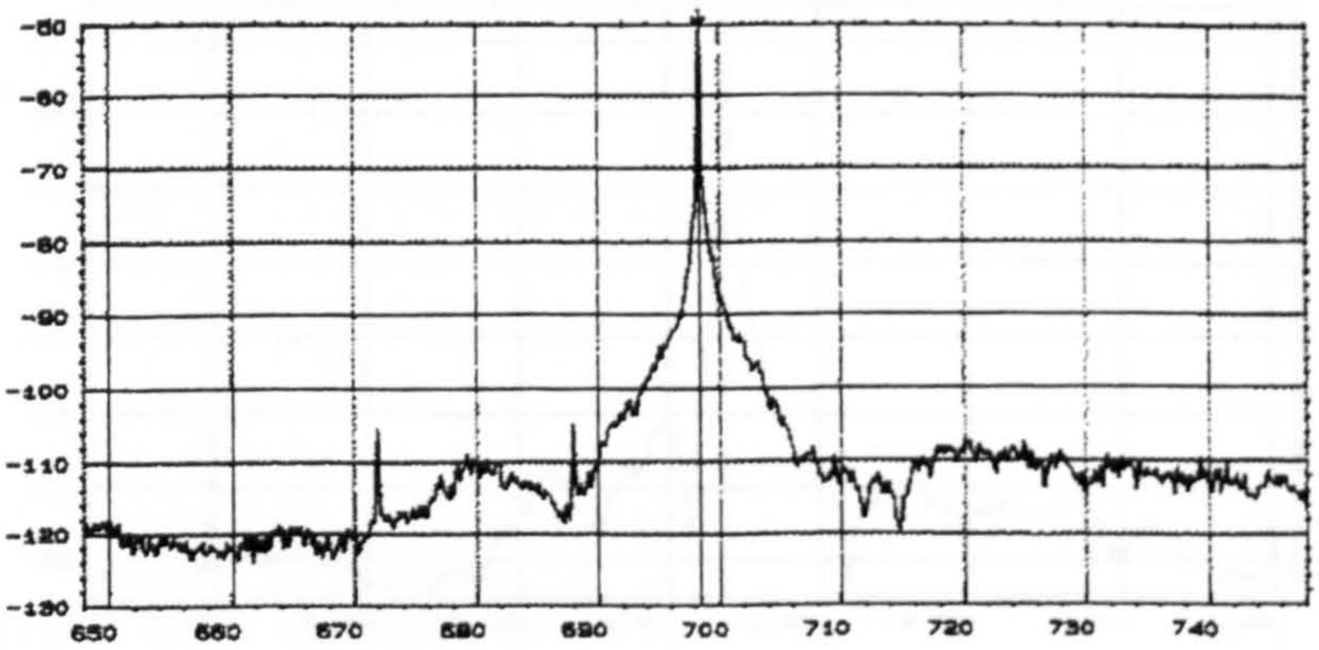

Fig. 4.24 -The F_{30} note on the Rohrflute 4ft stop before turbulence filtering

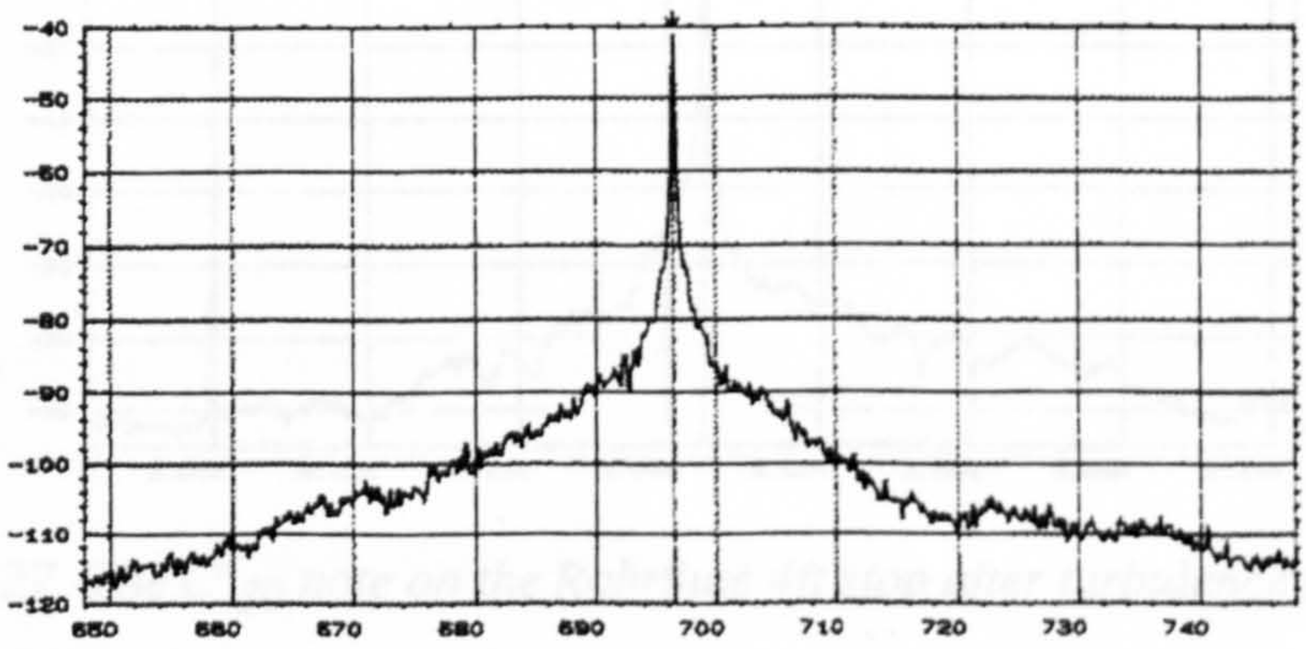

Fig. 4.25 -The F_{30} note on the Rohrflute 4ft stop after turbulence filtering

The peaks at 673Hz and 688Hz have been attenuated with turbulence attenuation. The rise to and fall from the peak is gradual. There is also a decrease in the bumpiness of the note.

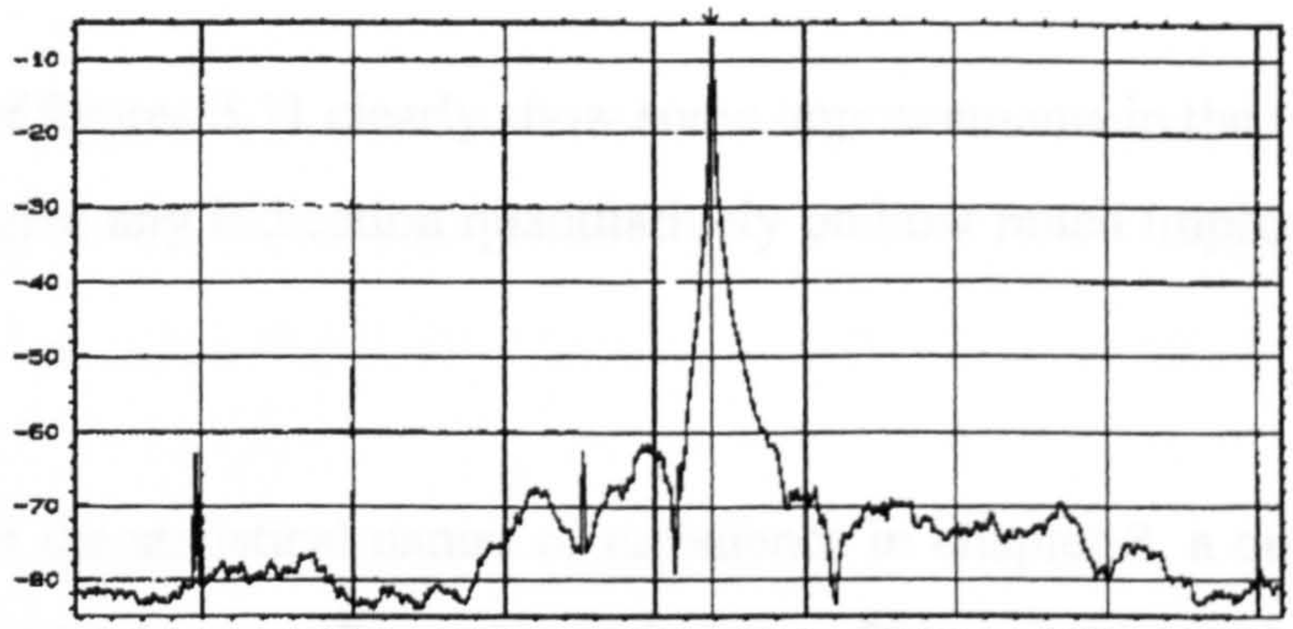

Fig. 4.26 -The $C^{\#}_{30}$ note on the Rohrflute 4ft stop before turbulence filtering

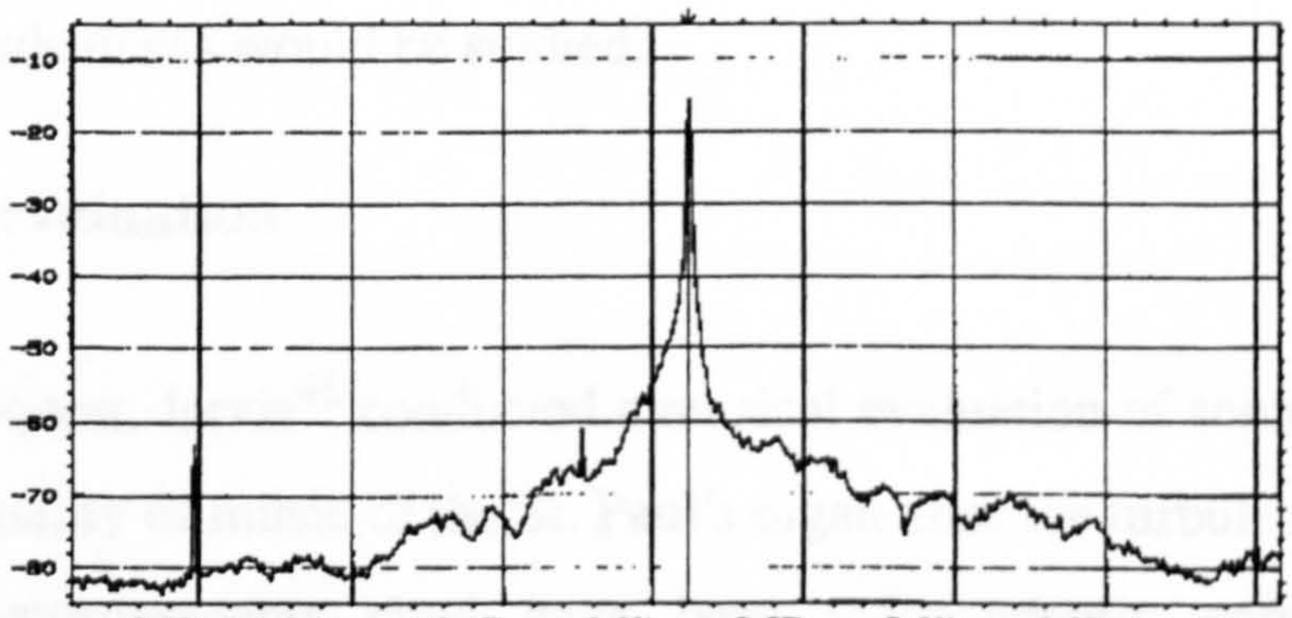

Fig. 4.27 -The $C^{\#}_{30}$ note on the Rohrflute 4ft stop after turbulence filtering

The peak at ~2.05kHz and 2.18kHz are still prominent, however, the spectrum of this note is much smoother

---

Overall, the plots reveal much reduction in the bumps of the leading and trailing edge of the fundamentals of the notes under examination. The overall shape of the fundamental is smoother. In Chapter five it will be shown that the shift in frequency is a characteristic that comes with the change in the turbulence condition of the wind supply.

Prior to turbulence attenuation, $F^{\#}_{43}$ spectrum has two peaks, the lower frequency peak has disappeared after the wind was subjected to turbulence attenuation.

4.5.2 A Quantitative Evaluation

While the plots of figures 3.11 clearly show some improvements in the sound quality, they do not however give any indication quantitatively on how much improvement have been achieved.

Having examined the statistical nature of turbulence in chapter 3, a quantification of the changes experienced by installing the turbulence filter could be done by means of statistical procedures.
Further discussion of this is delayed till chapter 5, where the effects on frequency, note symmetry and peakedness would be studied.

4.5.3 An aural evaluation

At the authors request, Jarvis[48] conducted a musical evaluation of some of the perceived changes in the quality of music of the St. Paul's organ after the turbulence attenuator was installed. The improvements cited have been independently corroborated by the manufacturers of the instrument, Wood of Huddersfield.

A decrease in the non-harmonic noise of the instrument as a whole was experienced. The pipe work of the 8 ft Gedackt stop, one of the stops on which some notes on the manual were recorded - has undergone "considerable improvement" as well as a steadier pitch. Some of the pipes still exhibit unsteadiness, however, this is more likely due to the non-harmonic noise generated by the pipework after the filter.

On other stops where the influence of the turbulence was thought not to be too significant, there has also been some notable improvements. Amongst these stops are the 16ft Gedackt Pommer, 4ft Spitzflöte, 8ft Principal (manual 2), the Cromhorne (manual 1), 2ft Flute (manual 3); the 16ft and 8ft Principal, 16ft Sub-bass and Reeds (all pedal). There has also

been considerable improvement to the 16ft and 8ft Trumpets (manual 2).

The 16ft Gedackt Pommer (manual 2) has lost its "acidity ... in the treble registers". It also blends in much better with the pipework in that division. The 4ft Spitzflote and the 8ft Principal (manual 2) speak much more clearly, as well as the Reeds, which have a "more penetrating tone."

The pedal stops have generally undergone an improvement in tonal quality. They now exhibit a greater depth and steadiness of tone.
The 8ft flute and the 2ft Blockflöte (manual 3) are less shrill: furthermore the pipework of these stops now have a much better blend.

In all, Jarvis[48] adds that there is a "pronounced degree of articulation from the instrument [along with a greater possibility] to control the speech of the pipes to a much greater degree of accuracy".
These improvements clearly augment the expressiveness of the St. Paul's Organ.

4.6 Use of Centrifugal Fan at off Optimum Design Condition as means of Minimizing Turbulence

A turbulence filter was also installed on the trunking system of an organ built by Harrison & Harrison (Durham -UK) destined for USA, while it was being erected at their workshop. A Centrifugal blower (1425 rpm, 1.125 kW -1.5hp- 12 paddle/radial blades) was used for supplying wind to the organ. It turned out that the filter did not produce any perceivable improvements. It was speculated that the machine maybe unexpectedly producing near laminar wind by feeling the wind flow emanating from it. Tests had to be conducted to confirm this.

The blower was tested in Huddersfield.

The flow from the blower was varied between ~0% and 100% output by blocking the outlet of a duct with orifice plates. The diameters of the orifices were not more than the duct diameter. The power consumption of the motor driving the blower was measured as the flow was varied. From these, the power (as well as head and efficiency) versus flow rate curves were plotted to determine the optimum operating point of the centrifugal blower. The curves are as in figure 4.28 and 4.29 below.

The blower was delivering wind into the organ destined for USA, to a pressure of 6.4mbar (ie 2.5inches H_2O). From the curves of figure 4.28 and 4.29, this corresponds to an efficiency of 26% and a power consumption of 914.5 Watts

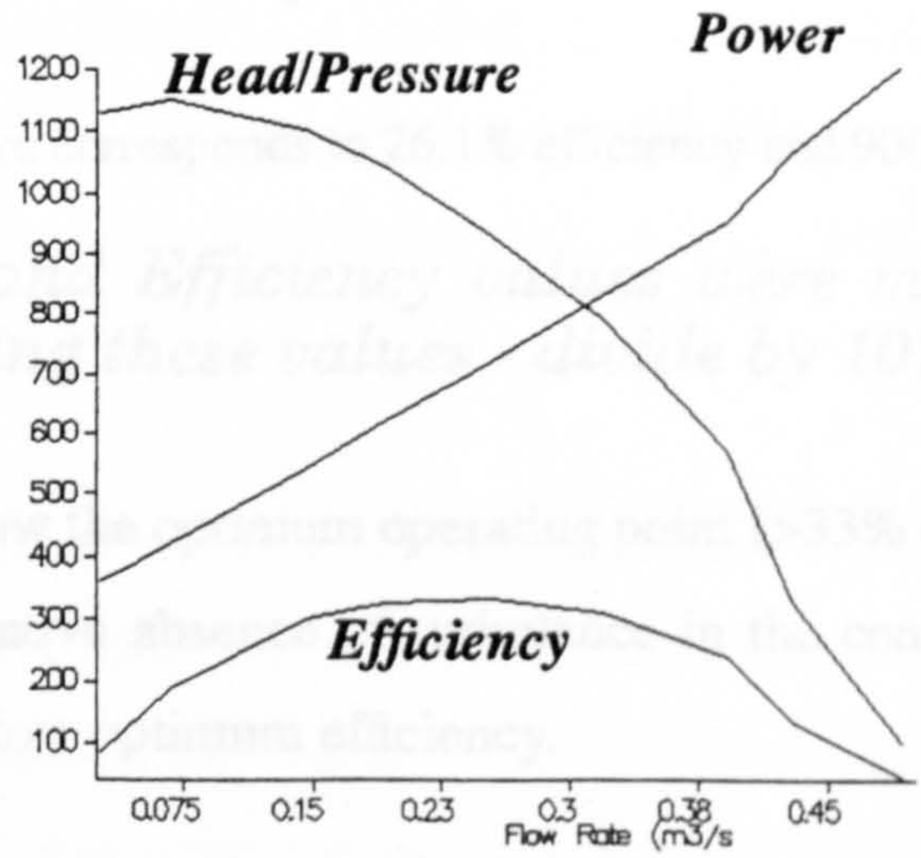

*Fig 4.28 Head, Power & Efficiency vs flow rate for Harrison Centrifugal Blower(**before turbulence filter installed***

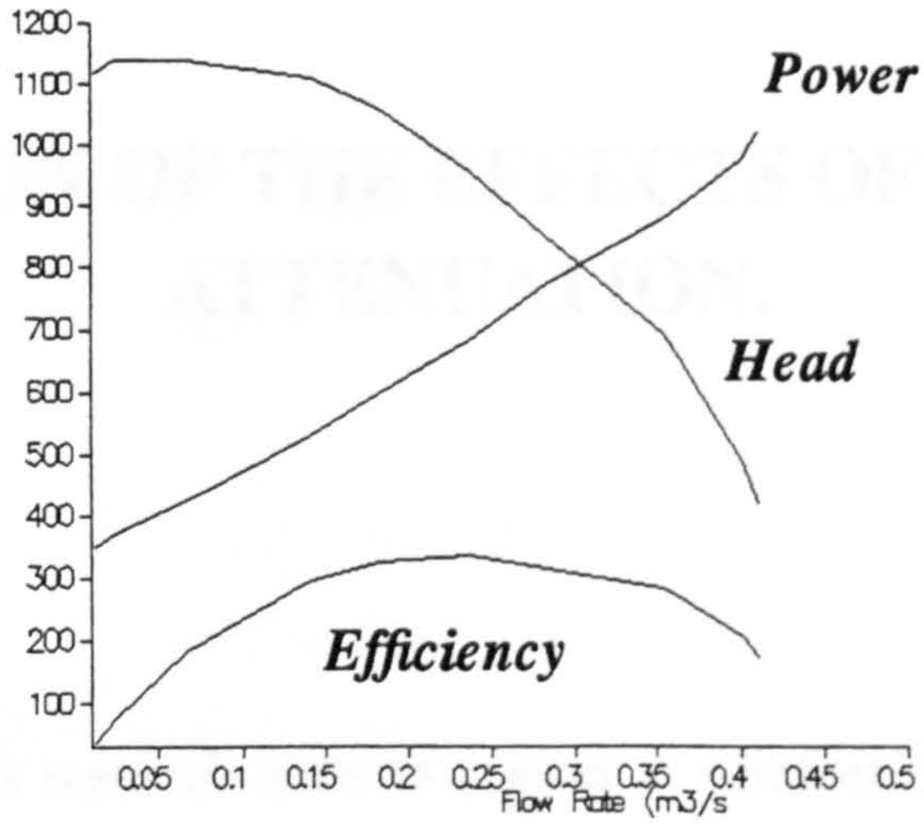

*Fig 4.29 Head, Power & Efficiency vs flow rate for Harrison Centrifugal Blower(**after turbulence filter installed**)*

[6.4mbar of pressure corresponds to 26.1% efficiency and 906.3Watts of power]

(Note: The Power and Efficiency values were multiplied by 10 for clarity - when reading these values - divide by 10)

These parameters are below the optimum operating point (>33% efficiency) of the blower. It is possible that the relative absence of turbulence in the centrifugal blower could be because it is operating below optimum efficiency.

CHAPTER 5

AN EVALUATION OF THE EFFECTS OF TURBULENCE ATTENUATION.

5.1 Introduction

One of the questions this research aims to answer is whether organ pipe sound changes with varying degrees of turbulence. Furthermore, whether these changes are aurally perceivable. To answer these questions some qualitative analysis was conducted with sound from the St. Pauls Organ (reported in section 5.4) and later from a laboratory test rig (reported in section 5.5). Remarks were solicited from individuals and members of an audience after they had listened to the pipes blown with filtered and unfiltered wind. It was noted that the pipes on the test rig were "noticeably clearer" with turbulence attenuation as will be discussed in section 5.3.

An experiment was conducted on a test rig that had 4 Principal pipes of various frequencies. Wind with five different mixtures of turbulent to laminar flow was pumped into the windchest (soundboard) holding the pipes. Over three dozen students were used as guinea pigs in a blind test to evaluate the sound produced. This experiment was conducted to establish whether varying the levels of turbulence of wind into the pipe is perceivable and whether there is a threshold of turbulence in the wind that is acceptable. In section 5.3.2, more details on this experiment and results will be given

Aural perception of changes in sound is largely subjective because the frequency response of the ear varies from person to person. It is essential therefore to seek to quantify the changes in the note as the flow condition changes. To achieve this, statistical principles

were used. The statistical concept used are derived from the concept of moments. The 3rd and 4th moments about a reference point were used to determine changes in skewness and peakedness/kurtosis of the note. The mathematical procedure used is discussed in appendix 7 while the results of the qualitative evaluation are outlined in section 5.5 for data from St. Paul's and the test rig.

Each pipe produces sound consisting of its fundamental and harmonics. When a pipe is said to have a frequency, f_p; f_p is the fundamental - therefore it is the fundamental that defines the frequency of a pipe not its harmonics, hence the quantitative evaluations carried out in the ensuing sections were with the fundamental only.

It was noted that changing the levels of the turbulence causes a frequency shift in the note. These observations are also outlined in this chapter (section 5.5.2 and 5.5.1 for data from St Paul's and the test rig respectively)

In the organ building trade, there is a strong perception that organs that use human operated blowers provide a superior wind supply relative to fans and other wind machinery in use. A quatitative analysis was conducted on notes recorded from an organ in a local church that has a dual blowing system, a centrifugal fan and a manually operated bellows. Some notes were recorded when the organ was fed wind from either blowing systems for a comparative analysis. The details of this analysis is also given in this chapter in section 5.7.

Before embarking on a discussion of the aural evaluation of data from St. Paul's and the lab test rig, an outline of the test rig used will be given.

5.2 Evaluation of data from test rig

A laboratory test rig was designed and built to evaluate the effects of different levels of turbulence on the quality of sound.

The aims of the experiments were:

-i- To numerically evaluate the effects of changing the level of turbulence,

-ii- To ascertain whether the effects of turbulence are aurally perceivable;

-iii- To find out whether there is a threshold of turbulence at which the effects of turbulence on the quality of organ pipe sound can be tolerated.

5.2.1 Test rig design.

Figure 5.1 (overleaf) is an illustration of the test rig used for this exercise

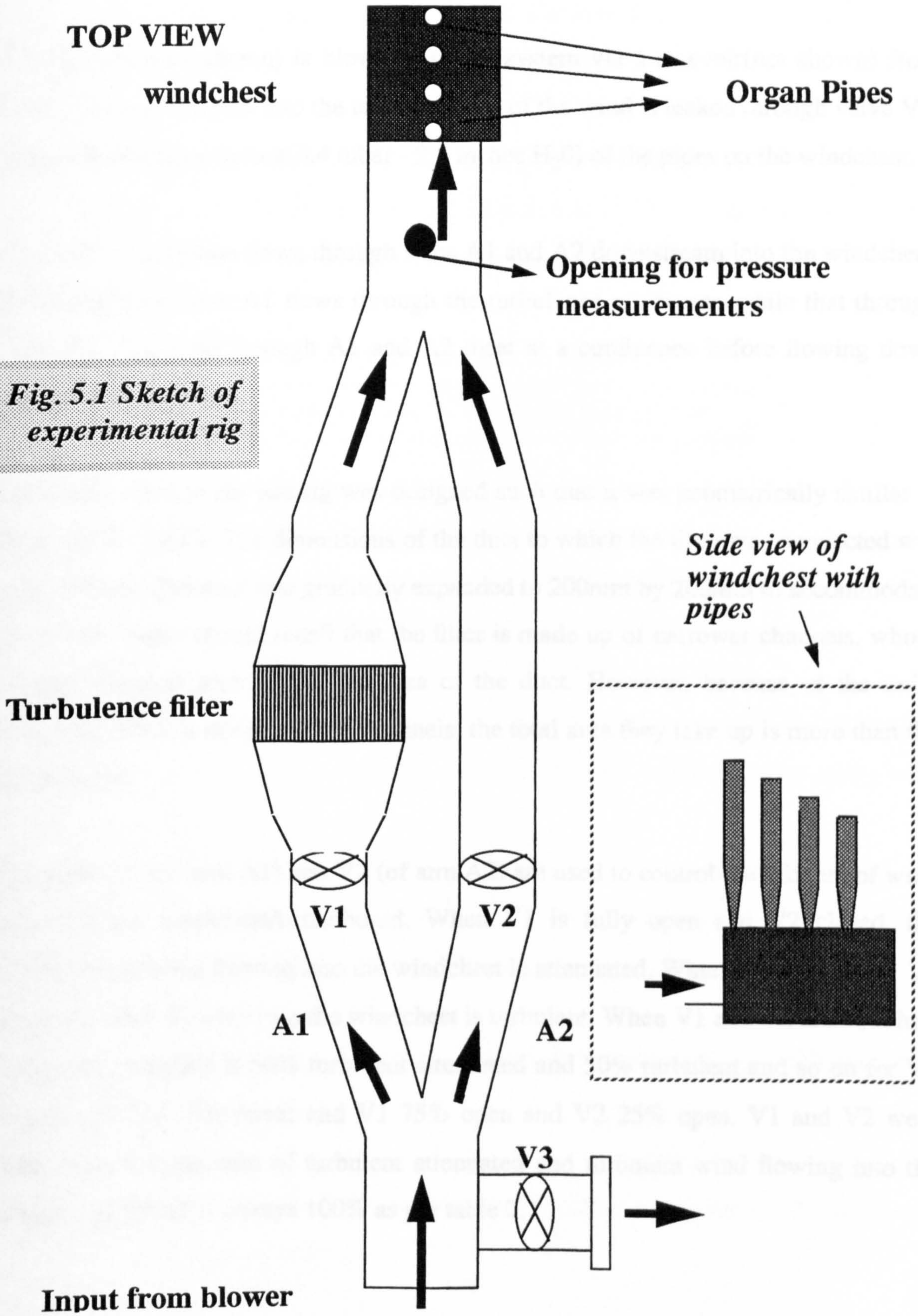

Fig. 5.1 Sketch of experimental rig

5.2.1.1 The test rig.

Wind from a fan(not shown) is blown in to the system via a resevoir(not shown) from where it flows downstream into the test rig. Some of the wind is leaked through valve V3, to provide the design pressure(6.4 mbar - 2.5 inches H_20) of the pipes on the windchest.

The wind into the system flows through arms A1 and A2 downstream into the windchest. Wind flowing down arm A1 flows through the turbulence attenuator, while that through A2 does not. The wind through A1 and A2 meet at a confluence before flowing down stream into the windchest.

The attenuator used in the test rig was designed such that it was geometrically similar to that built for St. Paul's. The dimensions of the duct to which the filter was connected was 80mm by 80mm. The duct was gradually expanded to 200mm by 200mm to accommodate the filter. The reader should recall that the filter is made up of narrower channels, whose total cross sectional area equals the area of the duct. However, because of the finite thickness of the walls of the narrow channels, the total area they take up is more than the area of the duct.

Orifice plates V1 (of arm A1) and V2 (of arm A2) are used to control the mixture of wind flowing into the windchest/soundboard. When V1 is fully open and V2 closed, the turbulence of the wind flowing into the windchest is attenuated. When V2 is open and V1 is closed, the wind flowing into the windchest is turbulent. When V1 and V2 are both half open, the wind mixture is 50% turbulent attenuated and 50% turbulent and so on for V1 25% open and V2 75% open; and V1 75% open and V2 25% open. V1 and V2 were operated such that the sum of turbulent attenuated and turbulent wind flowing into the windchest was (ideally) always 100% as per table 2.

The pipes, Pipe 1 to Pipe 4 sit on the windchest. Four switches open or close the inlet into the toe hole to each pipe. When switch one is open, air flows into the toe hole of Pipe 1 to produce sound. Pipes 2, 3 and 4 can be similarly switched on.

The switches were energized from a Farnell E30/2 power supply. The switches controlled a the solenoid magnet that closed and opened the pallet at the foot of the pipe. An opened pallet allowed wind to flow into the pipe and vice versa for the closed pallet.

Table 2: Flow Conditions of Test Rig

Percentage turbulent flow	Percentage laminar flow
100	0
75	25
50	50
25	75
0	100

The bifurcating Y junction before V1 and V2 and converging Y junction after, were designed such that their angle of separation was small enough to minimise boundary layer separation.

On the windchest were four flue pipes, with the following frequencies: Pipe 1, 260Hz; Pipe 2; 520Hz; Pipe 3, 1078 Hz and Pipe 4 2084 Hz

The windchest was built to the following internal dimensions: length 300mm, width 150mm, and height 150mm.

Each pipe was played under the five different flow conditions of table 2, above, and the sound recorded on a DAT recorder.

The wind into the system was provided by a DISCUS centrifugal blower, propelled by a Brook Crompton 250W motor, running at 2850 rpm; with an output pressure of ~560Pa(2.25 inches H_2O)

5.3 An aural assessment of the tones from test rig

5.3.1. An assessment via individual remarks

About a dozen students taking organ studies as their main option within the Music Department of the University were invited to listen to the four pipes on the windchest of the test rig under two flow conditions: 100% turbulence and 100% lamina flow. They were invited to write a brief report on what they heard for the different blowing conditions. Some of the remarks they made are given below.

-1- "There was a marked difference in the turbulence free pipe sounds in that it was a generally cleaner, more pure sound. However this was only really noticeable in the lower registers..."

-2- "A slight difference in sound can be detected by ear in lower frequency pipes."

-3- "With the high-pitched pipes it was not possible to hear an audible difference, though a slight difference was heard when the largest pipe was used. The filtered wind gave the pipe a smoother speech quality."

-4- "It was easy to detect the improvement of sound with filtered wind compared with turbulent wind, with the lower frequencies, but no change was detectable with the higher frequencies."

-5- "...the sound heard with the presence of the air filter was more pure, it was closer to the center of the particular pitch ... The difference in sound was noticeably clearer ..."

-6- "...without a filter, you are able to hear an unevenness of tone as the note wavers. This is more apparent in the lower registers. ...with a filter the notes are more stable."

-7- "..it was the two higher pitched pipes which sounded better on filtered air ... the lower pitched pipes produced a barely obvious difference."

-8- "..the experiment proved to me that there is a difference to sound quality with the use of filtered wind, but I think the difference is appreciated at lower pitches."

-9- ".. [the] lower sounding pipes were clearer with more 'bite' to the sound. Higher sounding [frequency] notes were not heard so much ..."

-10- "Even though the difference to me was slight on one note, I can imagine that on a large scale (full organ) the difference is quite considerable."

These remarks suggest that the changes in tone due to changing wind flow conditions are perceivable. The changes seem to be more perceivable for the lower registers (pitches).

5.3.2. An assessment via questionnaire

For each of the different flow conditions, each pipe was switched on to an audience of music students from the Department of Music of the University. The students were asked to give a subjective appreciation of the tone produced by the pipe. To assist the students in their response, each of them was given a questionnaire - reproduced in appendix 6. About 4o students took part in the exercise. Their responses are tabulated in table 3 overleaf, with corresponding bar charts in figure 5.2..

A clear pattern emerged from table 6 overleaf. The tone changes with changing levels of turbulence is aurally perceivable. However, there is no clear distinction as to which turbulence condition is the most preferred - which comes as no surprise as each person's ear has his/her own particular frequency response. As such, the judgement of each 'guinea pig' remains wholly subjective.

Consider row 6, containing results for 50% laminar flow. For pipe 1, none in the audience thought the note was poor. About 3% felt the note was poor: a similar percentage perceived the note as brilliant for this flow mixture. 51% perceived the note to be good, while 43% thought the note was better.

For Pipe 2, the story is different: 54% judged the note was poor, 3% thought the note was poor, while 35% judged it to be good. Only 8% judged the note to be better, while 35% thought the note was good.

Pipe 3 attracted responses dissimilar to those of pipes 1 and 2. About 38% of the audience felt the note was better with this wind mixture. 19% judged the note to be poor; a similar percentage perceived the note to be good. Under 25% of the audience judged that the note had become horrible.

	Pipe 1					Pipe 2					Pipe 3					Pipe 4				
(Lamina)	Audience Response(%)					Audience Response(%)					Audience Response(%)					Audience Response(%)				
Flow Condition	**(1 = Horrible, 2 = Poor, 3 = Okay, 4 = Good, 5 = Brilliant)**																			
	1	2	3	4	5	1	2	3	4	5	1	2	3	4	5	1	2	3	4	5
100	2.7	8.1	59.5	24.3	5.4	16.2	37.8	32.4	13.5	0	16.2	37.8	27.0	16.2	2.7	0.0	29.7	32.4	32.4	5.4
75	0	28.6	21.4	42.9	7.1	0	50.0	28.6	14.3	7.1	0	14.3	50	28.6	7.1	0.0	35.7	21.4	35.7	7.1
50	0	2.7	51.4	43.2	2.7	2.7	54.0	35.1	8.1	0	24.3	18.9	18.9	37.8	0	10.8	32.4	37.8	13.5	5.4
0	0	13.5	46.0	40.5	0	2.7	32.4	43.2	21.6	0	8.1	5.4	43.2	43.2	0	2.7	10.8	35.1	46.0	5.4

Table 5 Audience response to questions in questionaire of appendix 8

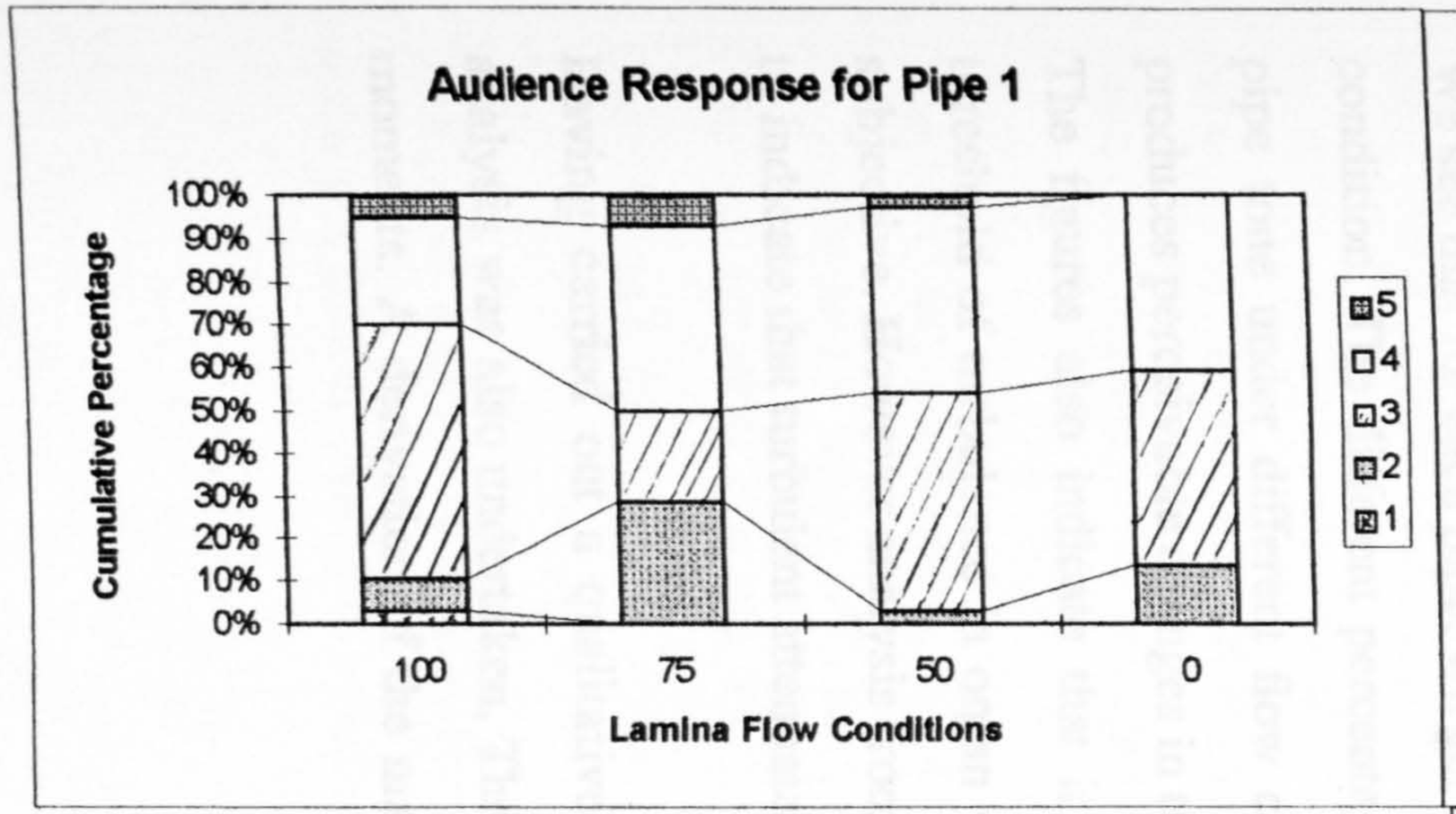

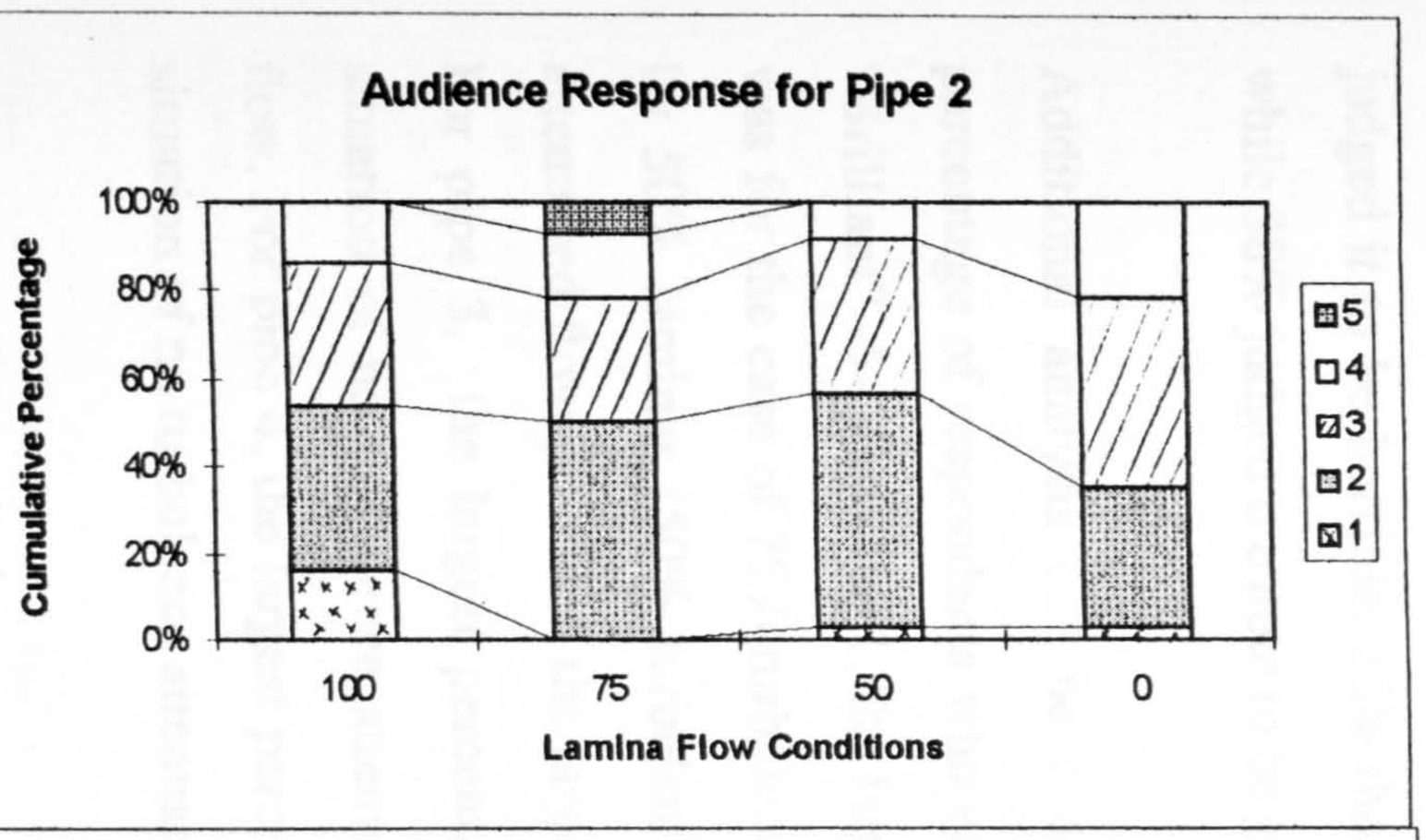

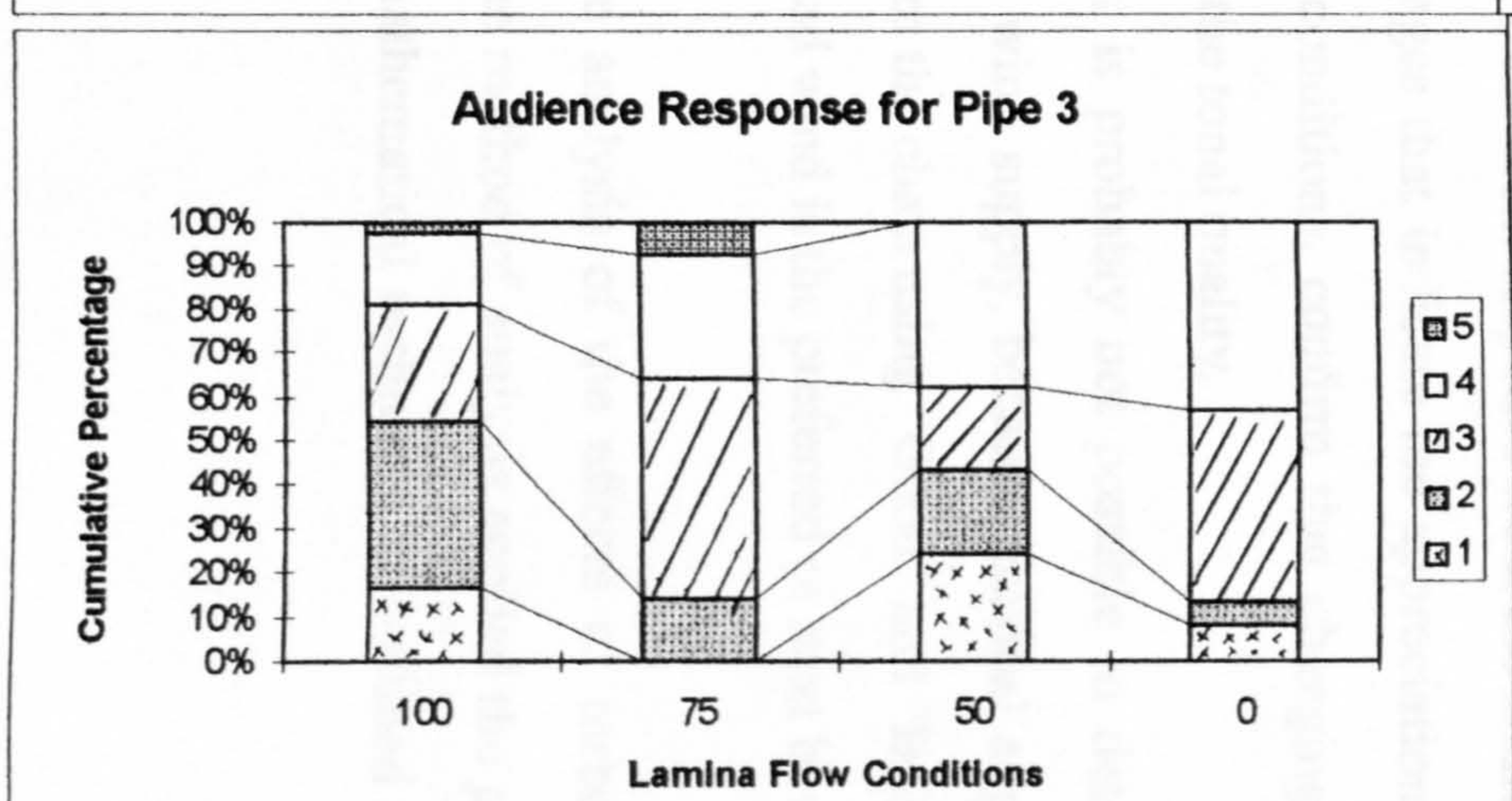

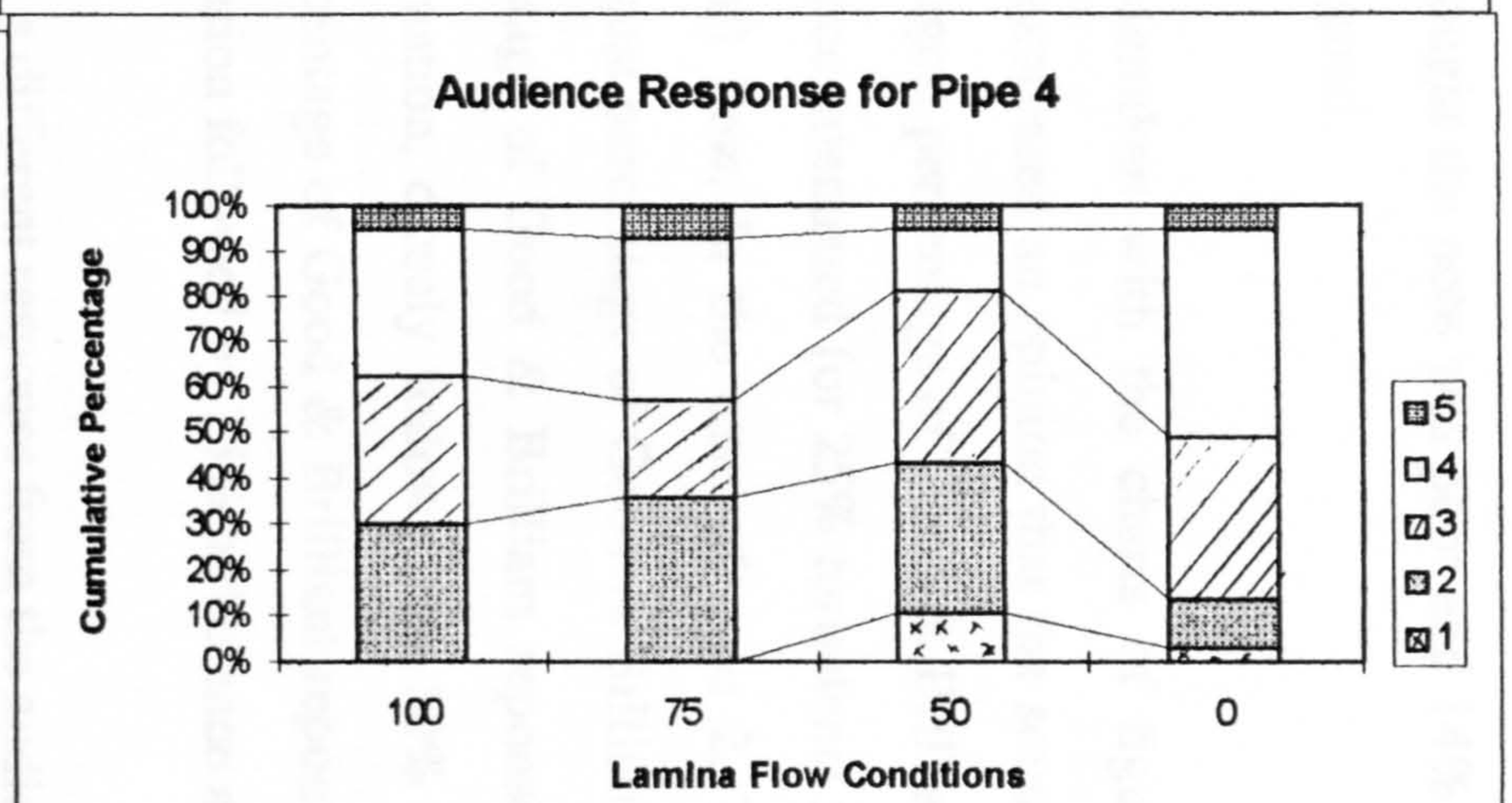

5 = Brilliant, 4 = Good, 3 = Okay, 2 = Bad, 1 = Horrible

Figure 5.2 Charts of audience response for different pipes

For pipe four: over 5% of the audience felt the note had become brilliant, while 11% judged it to be horrible. 32% thought the note was poor and 14% thought it was better, while 38% judged the note to be good.

Additional analysis can be undertaken with the charts of figure 5.2. Consider the percentage of respondents who expressed an opinion that the sound was "Good" - 4- or "Brilliant" -5-. For pipe 1, the largest percentage of Good & Brilliant reponses combined was for the case of 75% turbulence attenuated (or 25% turbulent) flow, closely followed by 50% laminar (50% turbulent) flow. In the case of pipe 2, 75% & 0% turbulent attenuated flow provided the largest percentage of Good & Brilliant reponses combined. For pipe 3, the largest percentage of Good & Brilliant reponses combined was the situation of no turbulence attenuation, closely followed by 50% turbulence attenuated flow. For pipe 4, the largest percentage of Good & Brilliant reponses combined was the situation of no turbulence attenauted flow.

We see that for each pipe, we get a different response from the audience for the same flow condition. The different percentages that indicate the appreciation of the audience of a pipe tone under different flow conditions, confirm that changing the turbulence level produces perceivable changes in the tonal quality.

The figures also indicate that it is probably not possible to determine an acceptable threshold of turbulence in organ wind supply, because musical appreciation is primarily subjective. However analysis from the chats using "Good" and "Brilliant" responses seem to indicate that turbulent attenuated wind is the preferred or next best option.

Having carried out a qualitative analysis of the effects of turbulence, a quantitative analysis was also undertaken. The method of analysis applied the principles of statistical moments. A derivation of the mathematical technique is outlined in appendix 7. In the

ensuing sections, the results from the calculations of data from St Paul's and the test rig are discussed.

5.4 An aural evaluation of St. Paul's Data

At the authors request, Jarvis,[48] conducted a musical evaluation of some of the perceived changes in the quality of music of the St. Paul's organ after the turbulence attenuator was installed. The improvements cited have been independently corroborated by the manufacturers of the instrument, Wood of Huddersfield.

A decrease in the non-harmonic noise of the instrument as a whole was experienced. The pipe work of the 8 ft Gedackt stop, one of the stops on which some notes on the manual were recorded - has undergone "considerable improvement" as well as a steadier pitch. Some of the pipes still exhibit unsteadiness, however, this is more likely due to the non-harmonic noise generated by the pipework after the filter.

On other stops where the influence of the turbulence was thought not to be too significant, there has also been some notable improvements. Amongst these stops are the 16ft Gedackt Pommer, 4ft Spitzflöte, 8ft Principal (manual 2), the Cromhorne (manual 1), 2ft Flute (manual 3); the 16ft and 8ft Principal, 16ft Sub-bass and Reeds (all pedal). There has also been considerable improvement to the 16ft and 8ft Trumpets (manual 2).

The 16ft Gedackt Pommer (manual 2) has lost its "acidity ... in the treble registers". It also blends in much better with the pipework in that division. The 4ft Spitzflote and the 8ft Principal (manual 2) speak much more clearly, as well as the Reeds, which have a "more penetrating tone."

The pedal stops have generally undergone an improvement in tonal quality. They now exhibit a greater depth and steadiness of tone.

The 8ft flute and the 2ft Blockflöte (manual 3) are less shrill: furthermore the pipework of these stops now have a much better blend.

It was also observed that there is a "pronounced increase in the degree of articulation from the instrument [along with a greater possibility] to control the speech of the pipes to a much greater degree of accuracy".[48] These improvements clearly augment the expressiveness of the St. Paul's Organ.

5.5 Quantitative Evaluation of Pipe Data

Data collected from both the test rig and St Paul's were quantified using the concept of statistical moments as outlined in appendix 7. The 3rd momemts which measured the change in skewness of the data and the 4th moment which gave a measure of the "peakedness" of the note were calculated. The results outlined in the rest of section 5.5 are from the test rig data and St. Paul's respectively.

5.5.1 Evaluation of moment of data from test rig

The recordings of the notes taken under different flow conditions were played back into the B&K spectrum analyser and their fundamentals sampled (as earlier described in appendix 7) for analysis.

The 3rd and 4th moments were computed using the statistical software package MINITAB. The flow chart of the programme used is as in appendix 8a. The moments calculated are given in the next two.

5.5.1.1 Third moments of test rig data

Table 4 below contains the 3rd moments of the different pipes under different flow

conditions.

Table 4: Data Table of Skewness with Increasing Laminar Flow[a]

Flow Condition(lamina) %	Pipe 1 (P1)	Pipe 2 (P2)	Pipe 3 (P3)	Pipe 4 (P4)
0	-0.4498	-0.4317	-0.2976	-0.23223
25	-0.4845	-0.4186	-0.3161	-0.32786
50	-0.5161	-0.4362	-0.2684	-0.34267
75	-0.4888	-0.4618	-0.343	-0.3591
100	-0.5045	-0.4388	-0.3168	-0.3123

a. Example of sampled data from test rig is presented in appendix 8 together with the dimensions of pipes 1-4

It is evident that all the third moments are negative, further indicating that the shape of the organ pipe tone generally has negative asymmetry (skewness).

The data of table 4 was plotted. The curves in figure 5.3 depicts the behaviour of the third moment with increasing laminar flow

PN = Pipe N

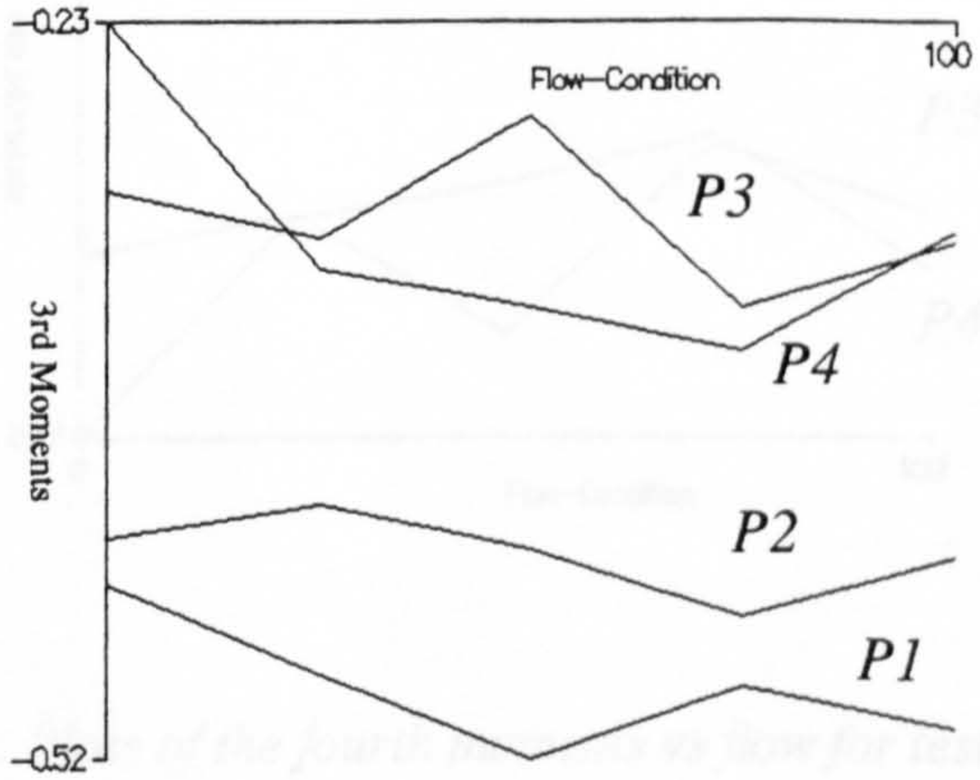

Fig 5.3 - Plots of skewness with increasing laminar flow

There is a pattern in the curves. The curves exhibit a non-monotonical increase in asymmetry of the shape of the pipe fundamental with increasing laminar flow.

5.5.1.2 Fourth moments of test rig data

Table 5 contains the fourth moments of the different pipes under different flow conditions.

Table 5: Fourth Moments for Different Flow Conditions

Flow Condition(lamina) %	Pipe One	Pipe Two	Pipe Three	Pipe Four
0	0.38276	0.36603	0.2382	0.16648
25	0.42306	0.34915	0.25558	0.25371
50	0.45863	0.36812	0.2069	0.26752
75	0.42487	0.39861	0.28373	0.28734
100	0.43878	0.41275	0.2557	0.23301

The data in table 5 was plotted to yield the family of curves in figure 5.4 below.

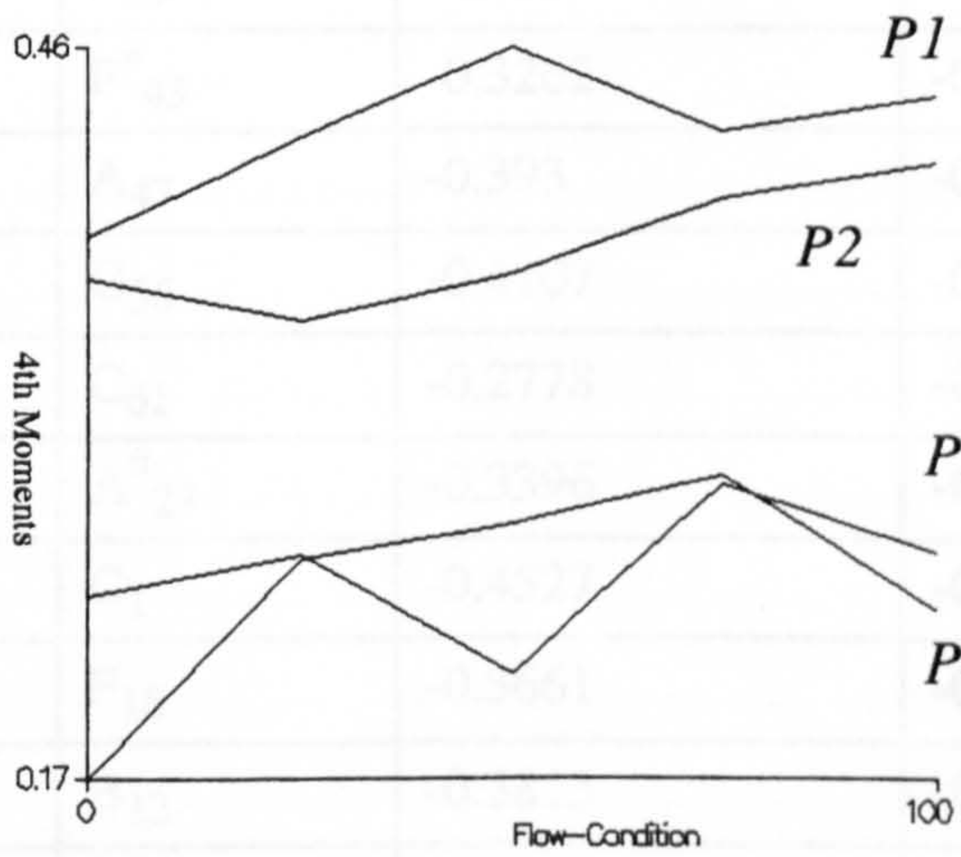

PN = Pipe N

Figure 5.4: Plots of the fourth moments vs flow for test rig data.

The curves bear some pattern. There is a non-monotonical increase in peakedness of the pipe fundamental with increasing laminar (decreasing turbulence) flow.

5.5.2 Evaluation of moments of data from St. Paul's

The statistical software package, MINITAB[61 70] was used to evaluate the moments.

5.5.2.1 Moments of St Paul's Data

The 3rd and 4th moments were computed using the statistical software package MINITAB. The flow chart of the programme used is as in appendix 8a. The moments calculated are given in tables 6 (3rd moments) 7 (4th moments) overleaf.

.

Table 6: Turbulence Effects on Note Symmetry, (St. Paul's)

Stop	Notes	3rd Moment before filtering	3rd Moment after filtering
Gedackt 8ft	E_{29}	-0.3321	**-0.4022**
Gedackt 8ft	$F^{\#}_{43}$	-0.3262	-0.3212
Gedackt 8ft	A_{47}	-0.393	-0.326
Gedackt 8ft	G_{56}	-0.4107	-0.2997
Gedackt 8ft	C_{61}	-0.2778	**-0.2925**
Principal 2ft	$A^{\#}_{23}$	-0.3396	**-0.4395**
Principal 2ft	C_1	-0.4527	**-0.5351**
Principal 2ft	F_{18}	-0.3661	**-0.3806**
Rohrflute 4ft	B_{12}	-0.3813	**-0.4211**
Rohrflute 4ft	$C^{\#}_{50}$	-0.2017	**-0.3547**
Rohrflute 4ft	F_{30}	-0.3724	**-0.4269**

It is clear that the 3rd moments of all the notes are negative, suggesting that the natural state of the note is one of negative skewness or negative asymmetry. Of the eleven notes analysed, eight have become more negatively asymmetrical (in bold) after turbulence

attenuation: suggesting that the lower the amount of turbulence in the flow, the more negative is the asymmetry within the note.

Turbulence tends to even things out. The tendency for a tone to become more symmetrical when generated by turbulent wind could be due to the "evening out" process.
For instance, if milk were poured into the centre of a still cup of tea, the tea principally stays dark, with a white central area: stirring the tea, i.e., introducing turbulence in the tea, spreads the milk evenly within the tea.
It is likely that turbulence in wind supplied to an organ, also evens out the tone - aspiring to give it symmetry about the centre frequency.

Table 7 below contains the calculations of the fourth moment.

Table 7: Turbulence Effects on Physical Sharpness (St. Paul's)

Stop	Notes	4th Moment before filtering	4th Moment after filtering
Gedackt 8ft	E_{29}	0.258	**0.3243**
Gedackt 8ft	$F^{\#}_{43}$	0.2596	0.2539
Gedackt 8ft	$A^{\#}_{47}$	0.3166	0.2499
Gedackt 8ft	G_{56}	0.3366	0.2319
Gedackt 8ft	C_{61}	0.2166	**0.2271**
Principal 2ft	$A^{\#}_{23}$	0.2549	**0.359**
Principal 2ft	C_{1}	0.3762	**0.468**
Principal 2ft	F_{18}	0.2891	**0.3036**
Rohrflute 4ft	B_{12}	0.3075	**0.3529**
Rohrflute 4ft	$C^{\#}_{50}$	0.1464	**0.3032**
Rohrflute 4ft	F_{30}	0.3044	**0.3553**

It is realised here that the 4th moments generally increase after turbulence attenuation - suggesting an increase in the peakedness of the note. Eight of the eleven notes studied

have peaked more with the turbulence attenuator in place. This can be associated with the improved brightness[48] and "more bite" [See remarks section 5.3.1] encountered.

5.6 Effects of changing flow conditions on frequency

It was also noted that changing the levels of turbulence resulted in a frequency shift in the note. These effects were observed both in data from St. Paul's and the test rig.

5.6.1 Frequency variations and Turbulence in St Paul's Organ

The frequency of the fundamentals of some of the pipe tones were determined using the B&K spectrum analyser. It was noticed that there were changes in the value of the frequency before and after the turbulence attenuation. These changes are illustrated in table 8 below.

Table 8: Frequency Shift With Change in Turbulence Condition

Stop	Note	Frequency before F_b(Hz)	Frequency after F_a (Hz)	Frequency change F_a-F_b (Hz) -(in %)
Rohrflute 4ft	B_{12}	246.625	246.125	**-0.5 (0.2%)**
Principal 2ft	C_1	260.75	261	+0.25 (0.1%)
Gedackt 8ft	E_{29}	329.75	328.5	**-1.25 (0.4%)**
Rohrflute 4ft	F_{30}	698.5	696.625	**-1.875 0(.3%)**
Gedackt 8ft	$F^{\#}_{43}$	740.625	738.25	**-2.375 (0.32 %)**
Principal 2ft	$A^{\#}_{23}$	929	929.5	+0.5 (0.05%)
Gedackt 8ft	$A^{\#}_{47}$	932.875	929.75	**-3.125 (0.34%)**
Rohrflute 4ft	$D^{\#}_{40}$	1244.375	1240.375	**-4 (0.32%)**
Principal 2ft	F_{18}	1388	1390.5	+2.5 (0.2%)
Gedackt 8ft	G_{56}	1571.375	1566	**-5.125 (0.33%)**
Gedackt 8ft	C_{61}	2096.625	2089.375	**-7.25 (0.35%)**
Rohrflute 4ft	$C^{\#}_{50}$	2219.25	2211.875	**-7.375 (0.33%)**

Table 8 shows a general decrease in the magnitude of the centre frequency: 75% of the notes have experienced a decrease. In musical terms, this is equivalent to a flattening of the note. The flatness observed in table 8, coincides with perceptions from aural evaluation[48].

It is observed that only the Principals have gone sharper while the flutes have become flatter. The principals, unlike the other pipes, were nicked. Their behaviour, though out of pattern with those of the other pipes, is a characteristic of nicked pipes as shall be discussed later in section 5.6.2.

It will seem that the frequency shifts increase with increasing pipe frequency, however as a percentage, the shifts are broadly the same, ≈ 0.3% shifts. The percentage change may look small, however, the changes are perceivable. Experiments conducted by Gueritey[39], has shown that a pressure drop of 10% in an organ system caused a frequency shift in the "D-major chord" of the St. Jean de Losne organ, in France, from 1064Hz to 1058Hz. A shift of 6Hz or 0.56%, which Gueritey described as "fully perceptible to the ear!"[39]

5.6.2 Frequency variations and Turbulence in Test Rig

Measurements of the centre frequency of the note, taken on the spectrum analyser showed some variation. The centre frequency was found to shift with changing flow conditions. Table 9 below contains the frequency shifts measured.

Table 9: Measured Frequency Shifts

Flow Condition (lamina) %	Pipe 1	Pipe 2	Pipe 3	Pipe 4
	Pipe Frequencies at Full Turbulence Flow			
	260.5 Hz	520.312 Hz	1078.812 Hz	2084.5 Hz
	Freq Shift (Hz)	Freq Shift (Hz)	Freq Shift (Hz)	Freq Shift (Hz)
0	0	0	0	0
25	0.062	-0.062	0.063	3.5
50	0.125	0	-0.125	4.5
75	0.125	0	0.25	1
100	0.187	0.125	0.5	6

From table 9, it is observed that there is an increase in frequency with increasing laminar flow condition. This frequency shift was normalised to enable the appreciation of the changes taking place.

The normalised value of the frequency shift, Δf, was obtained using equation 5.12 below:

$$\Delta f = \frac{F_p - F_{100T}}{F_{100T}} \qquad \text{.....5.12}$$

where F_p is the pipe frequency for a given flow condition, and F_{100T} is the pipe frequency, when the wind is unfiltered - 100% turbulence flow.

Ordinarily, a blower would have been used to supply air into the organ without a turbulence attenuator, hence it was appropriate to use the pipe frequency generated by unfiltered wind as a frame of reference.

Using equation 5.12, the data of table 10 below was computed from table 9. Table 10 therefore contains the normalised frequency shift experienced under different flow conditions.

Table 10: Normalised Frequency Shifts with Changing Flow Conditions

	Pipe 1	Pipe 2	Pipe 3	Pipe 4
Flow Condition(lamina) %	Δf (x 10^{-4})			
0	0	0	0	0
25	2.38	-1.192	0.584	16.79
50	4.798	0	-1.16	21.59
75	4.798	0	2.317	4.797
100	7.179	2.4	4.635	28.78

The normalised frequency shifts were plotted as in figure 5.5. The horizontal axis represents the change in laminar flow condition. The vertical axis represents the normalised value of the frequency change.

PN = Pipe N

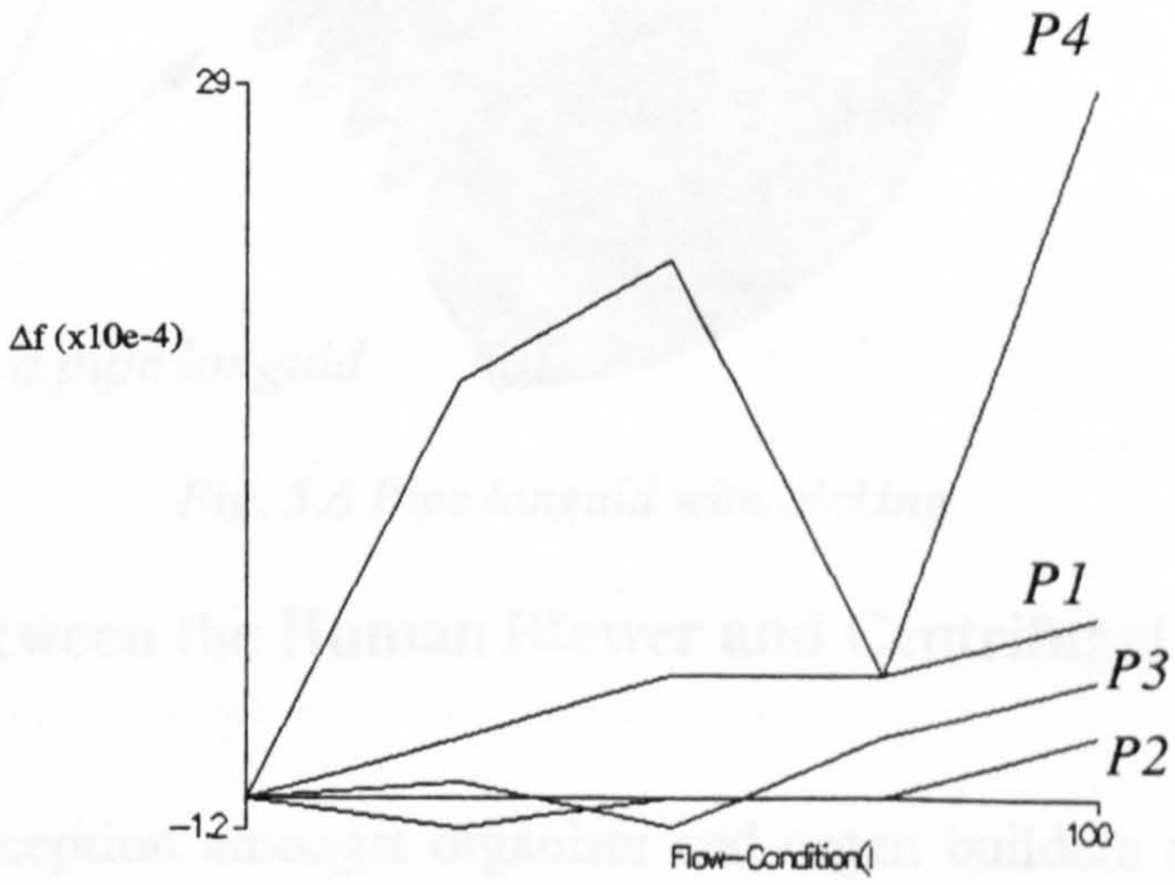

Fig. 5.5: Δf vs flow condition

The curves confirm that the pipe note has expressed a positive (upward) shift in frequency, with increasing laminar flow. The pipe note has grown sharper with increasing laminar (decreasing turbulent) flow.

It is also observed that the higher the pipe frequency, the greater the frequency shift.

This is unlike the observation experienced with the data from St. Paul's.

All the pipes on the test rig had **nicked** languids (cf. figure 5.6). Nicked pipes behave differently from non-nicked pipes. Fletcher and Rossing,[35] reported that nicking introduces "homogeneous turbulence" in the jet emanating from the windway. This turbulence, in the pipe mouth area, may be contributing to the sharpening of the note. If less turbulent wind flattens the note, it would be reasonable to assume that more turbulent wind would sharpen it.

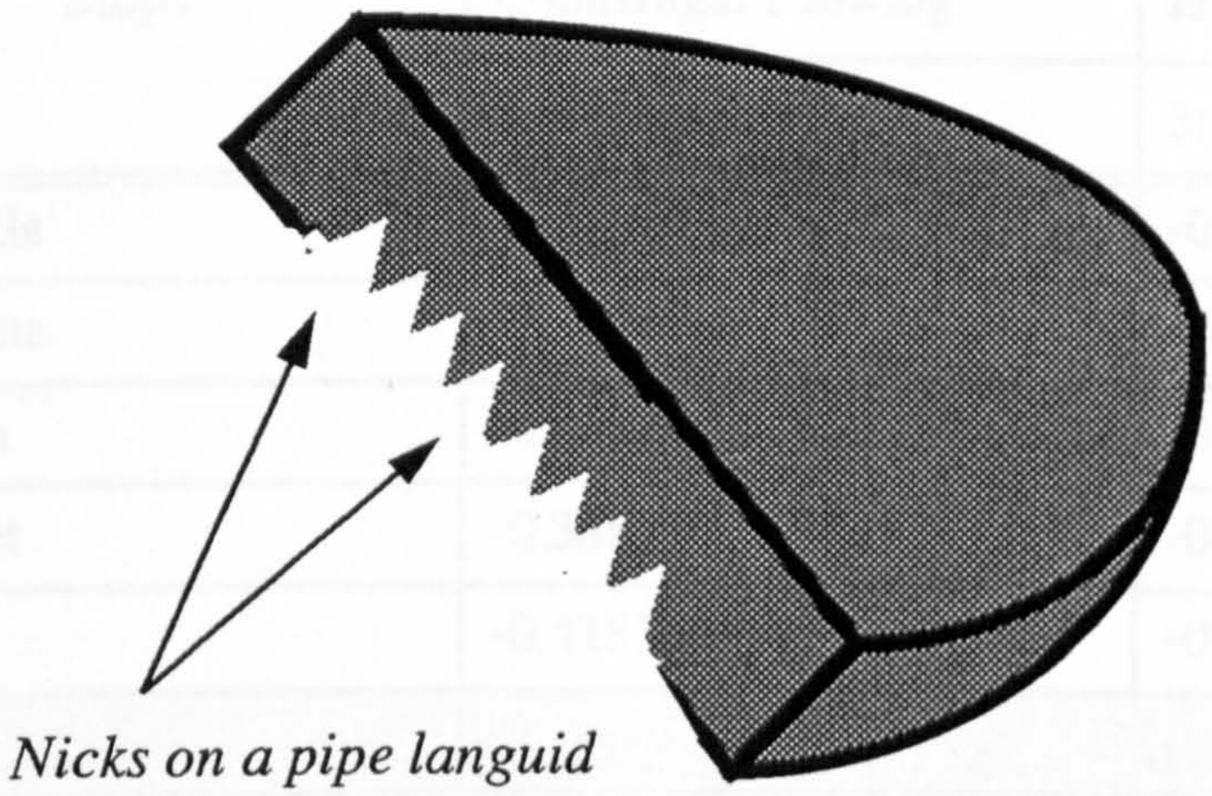

Fig. 5.6 Pipe languid with nicking

5.7 Comparison between the Human Blower and Centrifugal Blower.

There is a strong perception amongst organists and organ builders that organs that use human operated blowers provide a superior wind supply relative to fans and other wind machinery in use. To establish whether this is the case, it is useful to do a comparative

analysis on some notes played under both blowing systems.

Amongst the organs visited as part of this project was the organ of St. Thomas' Church, Thurstonland, West Yorkshire, UK. The organ here has two types of blowers, a hand operated blower and a centrifugal fan. During a trip to the Church, two notes of the organ; C_{25} and G_{32} were played on different stops and recorded. Recordings were made under both blowing situations: centrifugal blowing and hand blowing. The 3rd and 4th moments of five of the notes were evaluated for both types of blowing processes; the following results were obtained.

5.7.1 Third moments

Table 11: Third Moments Human vs Centrifugal Blowing

Stops	C_{25}	
	Centrifugal Blowing	Hand Blowing
	3rd Moment	3rd Moment
Clarabella	-0.373029	-0.455812
Clear flute	-0.353894	-0.447778
Bourdon	-0.469239	-0.473469
Flageolet	-0.386599	-0.386631
Oboe	-0.418355	-0.473616
	G_{32}	
Clarabella	-0.360975	-0.373340
Clear Flute	-0.393398	-0.399334
Bourdon	-0.422367	-0.291883
Flageolet	-0.343035	-0.312154
Oboe	-0.460199	-0.559633

It was also observed that the 3rd moments here are all negative.

Most of the third moments have become more negative with hand blowing. It has been reported that hand blowing generally produced less turbulent wind.[102] The increase in negative asymmetry, ties in with previous results for air flow that underwent turbulence attenuation.

5.7.2 Fourth moments

Table 12: 4th Moments - Human vs Centrifugal Blowing

	C_{25}	
	Centrifugal Blowing	Hand Blowing
Stops	4th Moment	4th Moment
Clarabella	0.297336	0.391654
Clear Flute	0.287781	0.381484
Bourdon	0.401227	0.407070
Flageolet	0.319795	0.320191
Oboe	0.350667	0.384380
	G_{32}	
Clarabella	0.287940	0.299676
Clear Flute	0.322797	0.329257
Bourdon	0.356184	0.224966
Flageolet	0.287144	0.248795
Oboe	0.395498	0.488303

The fourth moments have largely increased from centrifugal blowing to hand blowing. This increment ties in with previous results for air flow that underwent turbulence attenuation.

5.7.3 Frequency variations

The center frequency of the pipes analysed manifest a shift in frequency. The ensuing table depicts the frequency changes measured.

Table 13: Frequency Shifts from Human to Centrifugal Blowing

STOPS	C_{25} Frequency -Hz	C_{25} Frequency -Hz	G_{32} Frequency -Hz	G_{32} Frequency -Hz
	Centrifugal Blower	Hand Blower	Centrifugal Blower	Hand Blower
Clarabella	260.062	260.187	390.625	390.937
Clear Flute	130.062	130.187	781.250	781.875
Bourdon	520.812	520.812	194.875	194.937
Flageolet	1040.937	1041.5	1562.75	1564.625
Oboe	779.5	780.25	777.25	777.437

The fundamentals have shifted to the right (increased) with hand blowing - i.e. the pipe tones have become slightly sharper. Attention should be drawn to the fact that all the pipes on this organ [Thurstonland Organ] are nicked.

The results here mentioned follow a similar trend to the nicked pipes of the test rig.

The differences in tonal quality for pipes that have wind fed directly from a fan and that supplied via a turbulence attenuator are similar to the differences between fan wind and wind supplied by hand blowing via feeders. The turbulence filter will therefore enable a quality of wind to be fed to an organ similar to that produced by hand blown feeders, thus enabling organ builders to recreate the highly admired qualities of instruments pre-1900 in modern instruments.

CHAPTER 6

ON AN ELECTRICAL ANALOGOUS CIRCUIT OF THE ORGAN PIPE FOR TURBULENCE STUDIES

6.1 Electrical Analogues of Mechanical Elements.

Electrical analogues circuits have been used to study the production of sound in several tubular musical wind instruments by many researchers including:Yoshikawa & Saneyoshi[98], Coltman[11-15] , Nolle and Finch[69], Caddy and Pollard[9], Finch and Nolle[27] and Elder[22] . These instruments are made of several constituent parts. Morse[63] argues that when the constituent parts of these musical instruments are longer than the wavelength of the sound they produce, the instrument can be modelled in electrical terms as a transmission line. When the elements of the instrument are shorter relative to the sound wavelength it produces, the instrument can be modeled as an electrical circuit with lumped elements such as Resistance, Capacitance and Inductance. An explainanation as to how the lumped circuit components are determined will be given later.

In the model developed in this research the air supply portion and part of the generator have been reduced to a driving potential (or electromotive force) into the equivalent circuit. The resonator or resonance portion of the pipe is conceptually split into several interconnected entities: the mouth (M) ans input segment (I), oscillator (O) and oscillator-air interface(A).

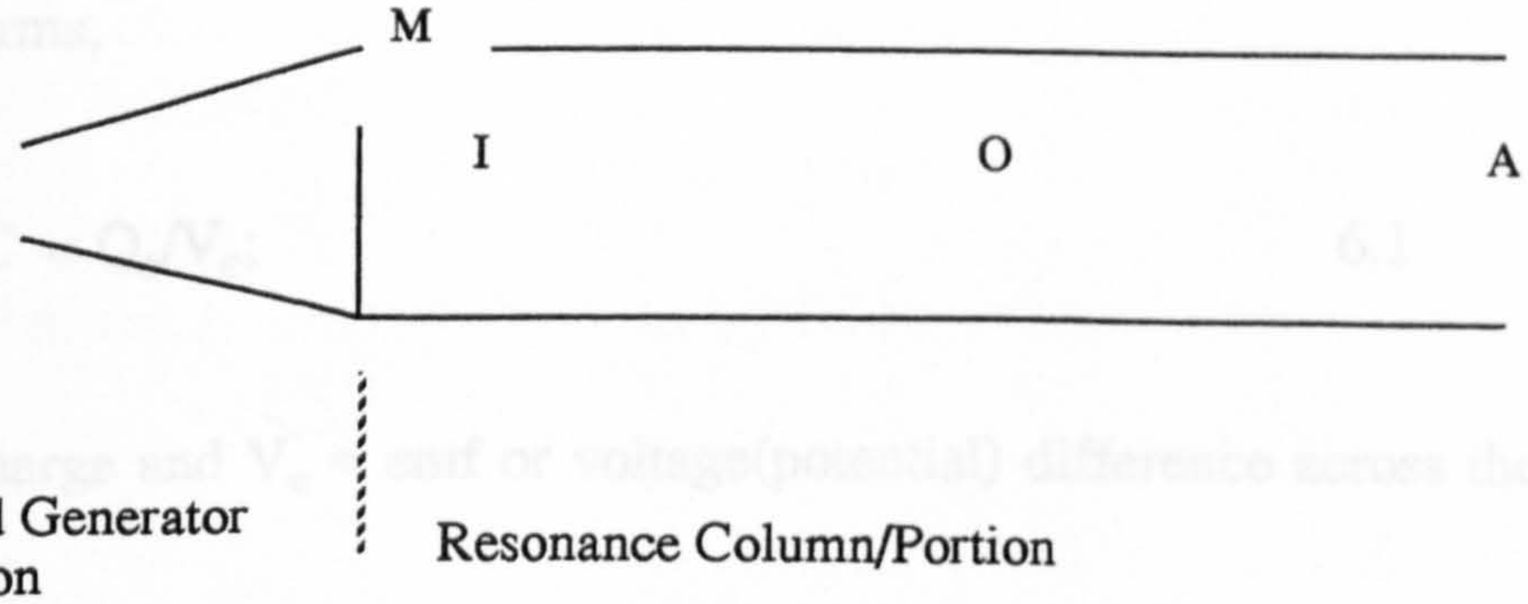

Figure 6.0: Basic Configuration of Pipe

6.1.1 Impedance

The acoustic impedance of sound vibrations is analogous to electrical impedance of an AC circuit since sound vibrations alternate like AC currents.[50 87]

The acoustic impedance is defined as the excess pressure divided by volume rate of flow in the direction of propagation.[32 50 63 87] Pressure is analogous to the electromotive force (emf) and the volume rate of flow is analogous to the electrical current.

The units of measurement of volume flow rate and pressure are customarily taken to be in cubic centimeters per second (cc/s) and in grams per centimeter per second squared ($gcm^{-1}s^{-2}$) respectively.

The equivalent electrical impedance is also given by the specific acoustic impedance divided by the cross sectional area of the pipe. The impedance is a complex quantity; the real part is the resistive component, while the imaginary part is the reactive component.

6.1.2 Capacitance

The capacitance is that characteristic which resists any change in applied pressure on an acoustic system.

In electrical terms,

$$\text{Capacitance, } C = Q_e/V_e; \qquad 6.1$$

where Q_e = charge and V_e = emf or voltage(potential) difference across the capacitance plates.

The electrical charge, Q_e is given by the equation.

$$Q_e = \int I dt \quad \text{.....6.2}$$

where I is the electrical current.

In acoustic terms, the charge will be the volume displacement, in a tank say. This follows from the knowledge that the volumetric flow rate is equivalent to the electrical current. The volume displacement is usually due to a change in pressure (or voltage difference).

A capacitance is usually represented by a "buffer volume",[87] which introduces a stiffness in a manner similar to a spring.

If the pressure changes from P to P + Δp, and the volume displacement from V to V + ΔV, then the acoustic capacitance, C will be given by;

$$C = \Delta V/\Delta p. \qquad 6.3$$

The bulk modulus of a given medium, K, is given by the expression:

K = stress/strain = pressure change/fractional change in volume

$$\text{i.e.} \qquad K = \Delta p/(\Delta V/V) \qquad 6.4$$

The velocity of sound, c, in a fluid is given by the equation;

$$c = (K/\rho)^{0.5}$$

where ρ = density of the fluid.

$$\Rightarrow c^2 = \Delta p/(\Delta V/V)\ (1/\rho)$$

$$= (V/C)\ 1/\rho$$

$$\Rightarrow C = V/\rho c^2 \qquad 6.5$$

If V is in cc, ρ in g/cc and c in cm/s; then the capacitance C_a will be in $cm^4s^2g^{-1}$.

6.1.3 Inductance

The electrical inductance(inertance) is equivalent to the mechanical inertance.[87] The inertance resists any change in volume current in a similar manner to the way that an inductance opposes electrical current flow.

Inertance effects are usually exhibited at constrictions.[63] At constrictions the air within is mass controlled.

If the total mass, m, of air in a constriction, were subjected to an excess pressure, Δp, then the fluid in the constriction will acquire some Kinetic Energy due to the velocity, X, of the fluid. The KE can be expressed as:

$$KE = 0.5\ mX^2$$

$$\therefore KE = 0.5m\left(\frac{dX}{dt}\right)^2 \qquad \text{.....6.6}$$

The volume displaced due to the excess pressure = $S_pX = \Delta V$

$$KE = \frac{0.5m}{S_p^2}\left(\frac{d}{dt}XS_p\right)^2 \quad \text{.....6.7a}$$

$$KE = 0.5\frac{m}{S_p^2}\left(\frac{d}{dt}\Delta V\right)^2 \quad \text{.....6.7b}$$

$$KE = 0.5M\left(\frac{d}{dt}\Delta V\right)^2 \quad \text{.....6.7c}$$

Where the inertance,[87] M, is equal to $m/(S_p)^2$. The inertance is analogous to the inductance.[63 87]

The mass can be determined from the density, ρ, using the expression;

$$m = \rho S_p L_p$$

substituting the above equation into the expression for inertance, we have an equivalent inductance, *L*, given below.

$$L = \rho S_p L_p / S_p^2$$

$$L = \rho L_p / S_p \qquad 6.8$$

L_p = pipe length

S_p = pipe cross sectional area

6.3 Development of Analogous Electric Circuit of Organ Pipes

The basic configuration of organ pipes is as in figure 6.1 below[1]. The pipe foot and languid can be represented as sound generator;[3] the area around the mouth as the feedback sector[98]

1. A detailed schematic of a organ pipe given earlier in chapter one is also repeated in appendix 10.

and the rest of the pipe as the resonantor column.

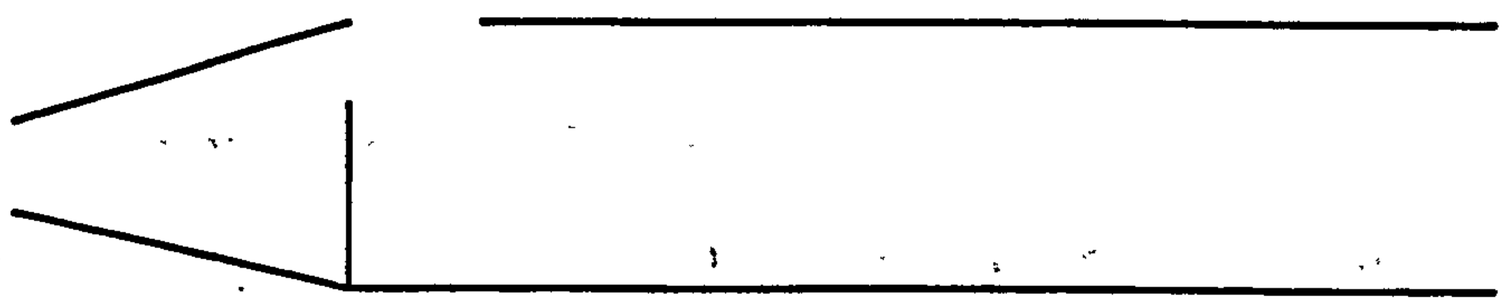

Fig 6.1: Basic Configuration of Organ Pipe

As a musical wind instrument, the organ pipe can be illustrated conceptually in the block diagram of figure 6.2; after Fletcher,[32 33] Mahu,[52] and MacIntyre.[58]

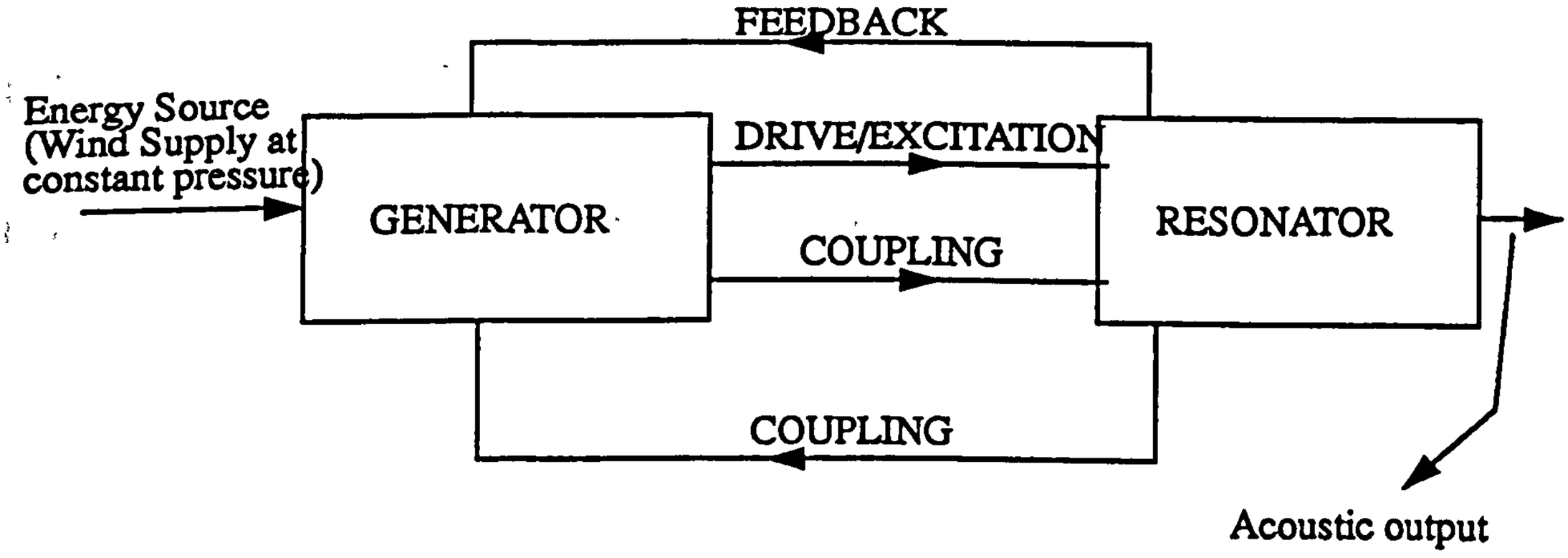

Fig 6.2: Block Diagram of Musical Wind Instrument

McIntyre[58] states that the generator is a non-linear element that is both coupled to and feeds into the resonator. The resonator is made up of passive linear elements. Their idealized model was developed as part of an investigation of the time domain description of oscillation of musical instruments.

Fletcher[32] also states that the resonator portion can be treated in principle as linear in behaviour, whereas the generator is non-linear. The non-linearity could be due to the coupling with the resonantor .

In analyzing the generator; which in fluid dynamic terms is the jet excitation mechanism of the sound in the pipe, Fletcher[32] concedes their theoretical and experimental analysis are limited to the laminar flow regime. In other words, the influence of turbulence has been ignored or excluded. The jets are turbulent. The effects of turbulence from the wind supply into this jet was not considered.

While the jet behaviour is not investigated in this work, understanding its impact on sound generation is relevant. Later, it will be shown that the input impedance experienced by the jet is useful in determining the electrical analogue of the input impedance to the electrical equivalent circuit.

6.2.1 The Pipe Input Impedance

For open pipes, Fletcher[32] shows that the input impedance, Z_{in}, is:

$$Z_{in} = nj\left(\frac{\rho c}{S_p}\right)\tan\left(K - jK'\right) \quad \text{.....6.9}$$

K = wave propagation number= ω/c; ω = angular frequency and c = speed of sound

K' = loss parameter of K; j is the square root of minus one.

K' is proportional to the square root of the angular frequency

In arriving equation 6.9, Fletcher[32] assumes free air propagation conditions and negligible energy loss at the open end (i.e. λ (wavelength) >> pipe circumference)

Yoshikawa and Saneyoshi[98] derived an expression for the input impedance, Z_{in}, of an open pipe as in equation 6.10 below.

$$Z_{in} = n\pi\left(\frac{\rho c}{S_p}\right)\left(\frac{1}{2Q_n} + j(\Omega_n - 1)\right) \ldots\ldots\ldots\ldots\ldots\ldots 6.10$$

S_p = pipe cross sectional area

Q_n = Quality factor of the nth resonant mode

$\Omega_n = f/f_o$; where f = pipe resonant frequency, n = modal number of f

and f_o = calculated fundamental of pipe.

In both equations 6.9 and 6.10, Z_{in} has a reactive and a resistive term.

Z_{in}(of eqn. 6.9) = Z_{in} (of eqn 6.10) if;

$$j\tan(K - jK^1) = \pi\left(\frac{1}{2Q_n} + j(\Omega_n - 1)\right) \ldots\ldots\ldots\ldots\ldots\ldots 6.11$$

Morse[63] gave the equation for the *specific* acoustic impedance at the driving end of an open pipe with an infinite flange, z_i, (i.e. the input specific acoustic impedance) as:

$$z_i = -j\rho c\left(\frac{\tan(2\pi\frac{L_e}{\lambda}) + j2\pi^2\left(\frac{a}{\lambda}\right)^2}{1 - j2\pi^2\left(\frac{a}{\lambda}\right)^2\tan(2\pi\frac{L_e}{\lambda})}\right) \ldots\ldots\ldots\ldots\ldots\ldots 6.12$$

for $\lambda > 8\pi a$

and

$$z_i = \left(\rho c - \frac{j\rho c^2}{\pi\omega a}e^{(j4\pi\frac{L_e}{\lambda})}\right) \ldots\ldots\ldots\ldots\ldots\ldots\ldots\ldots\ldots\ldots 6.13$$

for $\lambda < \pi a/3$

where L_e = acoustic (effective) length of the pipe = $L + 8a/3\pi$

If the pipe flange is infinitisimally small, L_e becomes $L + 0.6a$. The pipes under study were flangeless, assummed to have infinitisimally small flanges.

λ = the wavelength of the sound, a = pipe radius, c = speed of sound in air

and ρ = the density of air.

The pipe under study met the requirements stipulated for equation 6.12 (i.e. $\lambda > 8\pi a$), hence that equation was used.

For a pipe cross sectional area of, S_p, the analogous electrical input impedance, Z_{in} is given by the equation

$$Z_{in} = z_i/S_p$$

$$Z_{in} = -j\frac{\rho c}{S_p}\frac{\tan\left(\frac{2\pi L_e}{\lambda}\right) + j2\pi^2\left(\frac{a}{\lambda}\right)^2}{1 - j2\pi^2\left(\frac{a}{\lambda}\right)^2 \tan\left(\frac{2\pi L_e}{\lambda}\right)} \quad \text{.....6.14}$$

Z_{in} is made up of a real and an imaginary part, i.e. a resistance and a reactive component.

Fletcher's formula[32] for Z_{in} has the loss parameter K' which is proportional to $\omega^{0.5}$. The constant of proportionality has to be determined. Determining Z_{in} from Fletcher's formula is not straight forward.

Yoshikawa and Saneyoshi's[98] formula require prior knowledge, or experimental measurements of acoustic data from the test rig that would in turn be used to determine the pipe resonance quality factor. The input impedance can be wholly resistive if

$\Omega_n = 0$

Morse's formula[63] for Z_{in} looks complicated but is easier to compute. It relies mainly on geometric measurements of the pipe for its parameters. The Morse formula (equation 6.14) was used to evaluate Z_{in}.

Fletcher's (equation 6.9)[32], Yoshikawa and Saneyoshi's(equation 6.10)[98] and Morse's(equation 6.14)[63] equation for Z_{in} will yield the same result if

$$jn\tan(K-jK^1) = \pi n\left(\frac{1}{2Q_n}+j(\Omega_n-1)\right) = j\frac{\tan\left(\frac{2\pi L_e}{\lambda}\right)+j2\pi^2\left(\frac{a}{\lambda}\right)^2}{1-j2\pi^2\left(\frac{a}{\lambda}\right)^2\tan\left(\frac{2\pi L_e}{\lambda}\right)}$$

6.2.2 Pipe Mouth Impedance

In their investigation of the feedback excitation mechanism of organ pipe sound, Yoshikawa and Saneyoshi,[98] developed an equation for the acoustic mouth impedance, Z_m as in equation 6.15,

$$Z_m \approx j\left(\frac{\rho\omega_o}{S_{eff}}\right)(n\Omega_n)L_m \qquad \text{.....6.15}$$

where, S_{eff} = effective cross sectional area of mouth ($S_{eff} = (S_m S_p)^{0.5}$)

S_m = mouth area; S_p = cross sectional area of the pipe

L_m = length of pipe mouth; $\Omega_n = f/nf_o = \omega/n\omega_o$

f_o = calculated fundamental frequency of the pipe; i.e. $f_o = c/2L_e$

L_e = pipe acoustic length; c = speed of sound

n = modal number of the pipe excitation

Yoshikawa and Saneyoshi estimated L_m to be;

$$L_m = \frac{3d}{\left(1 + \frac{S_m}{S_p} + \left(\frac{S_m}{S_p}\right)^{0.5}\right)} \quad \text{.....6.16}$$

and $$S_{eff} = (S_m S_p)^{0.5} \quad 6.17$$

d = distance between the lip (jet nozzle of pipe) and edge

S_m = mouth area

S_p = cross sectional area of the pipe

$\Rightarrow$ if $S_p >> S_m$; $L_m \simeq 3d$

if $S_m \simeq S_p$; $L_m \sim d$

Yoshikawa and Saneyoshi's[98] estimations of L_m and S_{eff} were based on the assumption that the pipe mouth was equivalent to the circular truncated cone of height L_m, whose volume was equivalent to the mouth volume.

In their study of jet-resonator interaction in organ pipes, Fletcher and Rossing[35] derived an expression for the mouth impedance for pipes with resonant frequencies that are "not too high", Z_m, as

$$Z_m = j\frac{\rho\omega\Delta L}{S_p} \quad \text{.....6.18}$$

where ΔL = end correction of the open mouth.

From his analysis of the pipe as an electrical circuit, Morse[63] suggested that a hole in the wall of a cylindrical tube is analogous to a shunted resistance and inductance. Morse worked out the mouth inductance L_m and resistance, R_m as given below;

$$R_m \equiv \rho\omega^2/2\pi c = \rho\omega/\lambda \qquad 6.19a$$

$$L_m = 0.5\rho/a_m \qquad 6.19b$$

where the mouth impedance $Z_m = R_m + j\omega L_m$ 6.20

where a_m = mouth radius

ρ = density of air; λ = wavelength; c = speed of sound.

The Fletcher & Rossing[35] (equation 6.18) as well as the Yoshikawa and Saneyoshi[98] (equation 6.16) formulas for the mouth impedance are purely reactive. They probably assumed, though did not state, that the resistive component of the mouth impedance was negligible.

If the value of the inductance was to be deduced from either Fletcher & Rossing's[35] or Yoshikawa and Saneyoshi's[98] formula, then Z_m would be considered to be equivalent to the impedance, Z_L, of the inductor, L, where $Z_L = j\omega L$
such that , using Yoshikawa and Saneyoshi's formula (equation 6.15):

$$j\omega L = j\omega\rho(n\Omega)L_m(S_{eff})^{-1} \qquad 6.21$$

$$L = \rho(n\Omega)L_m(S_{eff})^{-1} \qquad 6.22$$

Using Fletcher & Rossing's formula (equation 6.18)[35]

$$j\omega L = j\omega\rho\Delta L(S_p)^{-1} \qquad 6.23$$

$$\Rightarrow \quad L = \rho\Delta L(S_p)^{-1} \qquad 6.24$$

If $\omega n\Omega \approx 1$; $S_p \approx S_{eff}$ and the length of Yoshikawa and Saneyoshi's[98] conceptual cone ≈ ΔL; then the Yoshikawa and Saneyoshi, & Fletcher and Rossing[35] formula would yield similar results for Z_m.

$\Delta L(S_p)^{-1}$ and $L_m(S_{eff})^{-1}$ have the limiting value of $1/(2a_m)$.

and $\omega(n\Omega) = 1$, then all three formulas should yield similar values for (inductance) L_m.

Morse's formula was used for consistency. The equation for the input impedance was based on the equation of the specific acoustic impedance of the pipe input as derived by Morse.

6.2.3 Pipe Resonator Impedance

The pipe resonant column can be considered to have a distributed inductance per unit length, $L_p = \rho/S_p$ per unit length; and a distributed capacitance per unit length; C'_p; given by

$$C'_p = S_p(\rho c^2)^{-1} \qquad 6.25$$

The analogous capacitance and impedance of the resonance column becomes

$$L_p = \rho L_e/S_p \qquad 6.26$$

and

$$C_p = V_p(\rho c^2)^{-1}; \qquad 6.27$$

where V_p = pipe volume (= S_pL_e).

The impedance due to the inductance (Z_L) and capacitance (Z_c) are given by the equations:

$$Z_L = j\omega\rho L_e/S_p$$

$$\text{and } Z_c = -j(\rho c^2)(\omega V_p)^{-1} \qquad 6.28$$

Morse[63] and Lighthill[50] have showed that the pipe resonant frequency f_r is related to C_p and L_p by the equation:

$$f_r = 1/2\pi(L_pC_p)^{0.5} \qquad 6.29$$

6.2.4 Pipe Termination Impedance

Morse[63] worked out the limiting values of the specific acoustic impedance at the open termination of an organ pipe with an infinite flange, z_o, as:

$$z_0 = \frac{\rho\omega^2a^2}{2c} - j\omega\left(\frac{8\rho a}{3\pi}\right) \qquad 6.30a$$

$$\textit{for } \lambda > 8\pi a$$

$$z_o = \rho c - \frac{j2\ \rho c^2}{\pi a\omega} \qquad 6.30b$$

$$\textit{for } \lambda < \pi a/3$$

The imaginary term in equation 6.30a is equivalent to a mass air of value $8\rho a/3\pi$ gcm^{-2} For flangeless pipes, this term reduces to $0.6\rho a$. Recalling that the analogous electrical impedance is obtained by dividing the specific acoustic impedance by the cross sectional area of the pipe, S_p, the equivalent electrical termination impedance, Z_T, for flangeless

pipes becomes:

$$Z_T = \frac{\rho\omega^2 a^2}{2cS_p} + \frac{0.6\omega\rho a}{jS_p} \quad \ldots\ldots 6.31$$

The reactive component of $Z_T \equiv$ Capacitance. The impedance, Z_T, of a capacitance, C_T, is given by the expression:

$$Z_C = \frac{1}{j\omega C_T} \quad \ldots\ldots 6.32$$

$$if \ldots Z_c = \frac{0.6\omega\rho a}{jS_p}$$

$$\Rightarrow C_T = \frac{S_p}{0.6\omega\rho a} \quad \ldots\ldots 6.33a$$

and

$$R = \frac{\rho\omega^2 a^2}{2cS_p} \quad \ldots\ldots 6.33b$$

6.5 Rules of Arrangement of Circuit Components

It was shown earlier that the resonance column of the pipe is made up of a distributed capacitance and inductance. The position of these two components in the circuits is determined using guidelines outlined by Stephen and Bates.[87] They give a set of guidelines for determining whether a specific circuit component should be placed in parallel or series relative to the rest of the circuit.

The rules they gave were:

(a) when a set of equivalent mechanical elements undergo the same displacement, they are to be connected in series,

(b) elements under the influence of the same force are to be connected in parallel,

(c) the stiffness between two consecutive elements in motion is equivalent to a shunt capacitance,

(d) a moving element attached to a fixed support is equivalent to a series capacitance.

6.4 Arrangement of Circuit Components of Electrical Equivalent Circuit

Let the mouth, input, pipe inductance, pipe capacitance and termination impedances be represented respectively by, Z_m, Z_{in}, Z_{Lp}, Z_{cp}, and Z_T.

It has been shown that a hole on the side of a tube, which is what the pipe mouth is, is equivalent to an inductance and resistance shunted across at the appropriate point.[63]

Coltman[11] applied this concept in his electrical analogy of a flute. His impedance was purely reactive. A legitimate assumption if the hole is very narrow relative to the tube perimeter .[63]

Following the arguments of Morse,[63] the pipe equivalent circuit can be perceived to be equivalent to a circuit similar to figure 6.3.

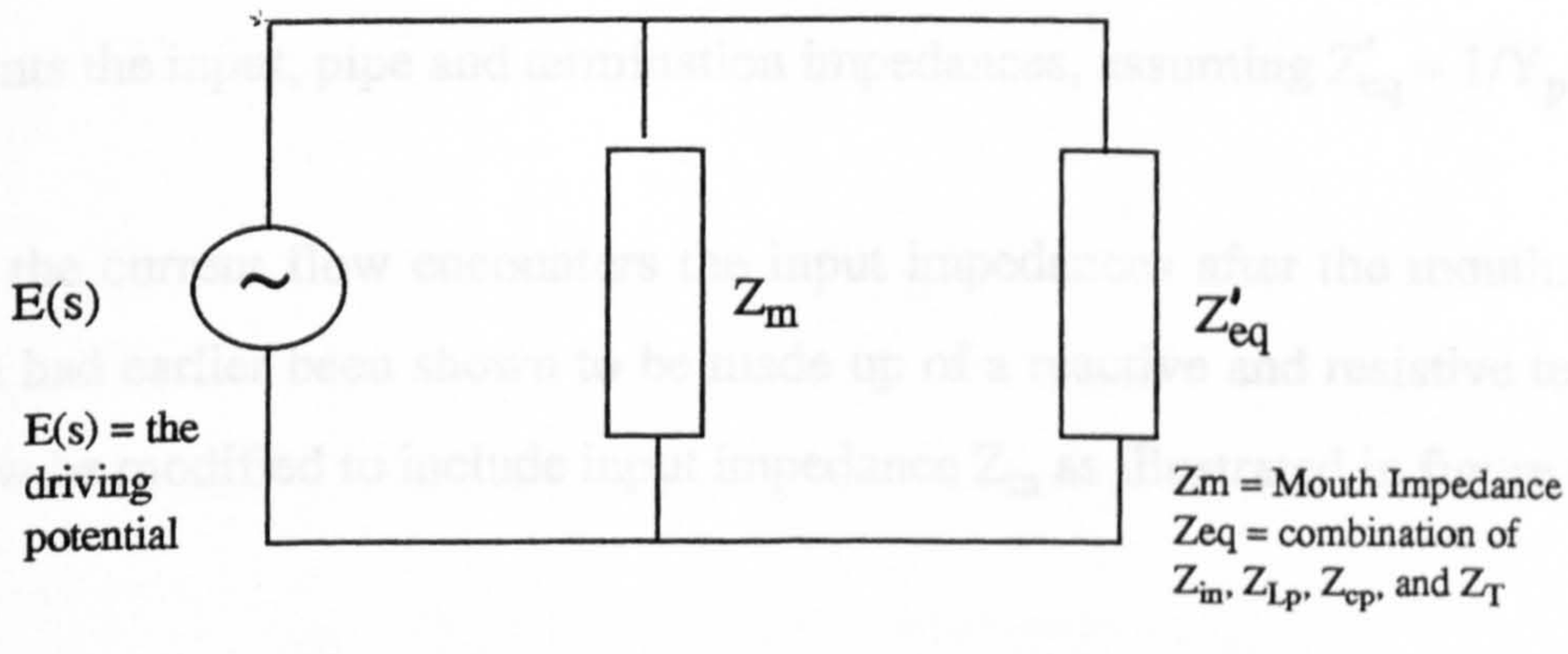

Fig 6.3. Pipe circuit model - development stage 1

The mouth impedance Z_m in parallel with the equivalent impedance, Z'_{eq}, of the combination of the input, pipe and termination impedances (Z_{in}, Z_{Lp}, Z_{cp} and Z_T).

As the full circuit is developed in the ensuing stages outlined below, the manner in which Z_{in}, (input impedance) Z_{Lp}, (reactance due to pipe inductance) Z_{cp} (reactance due to pipe capacitance) and Z_T (termination impedance) combine will be shown.

Z'_{eq} is taken as being in parallel rather than in series following Fletcher and Rossing's[35] electrical analogue of the regenerative excitation mechanism that describes jet excitation of organ pipe resonators. In it, they show the generator admittance, Y_g linked to the overall pipe admittance in a parallel combination as per figure 6.4. This scheme was adopted from Yoshikawa and Saneyoshi's[98] analysis - an analysis which produced fairly accurate results.

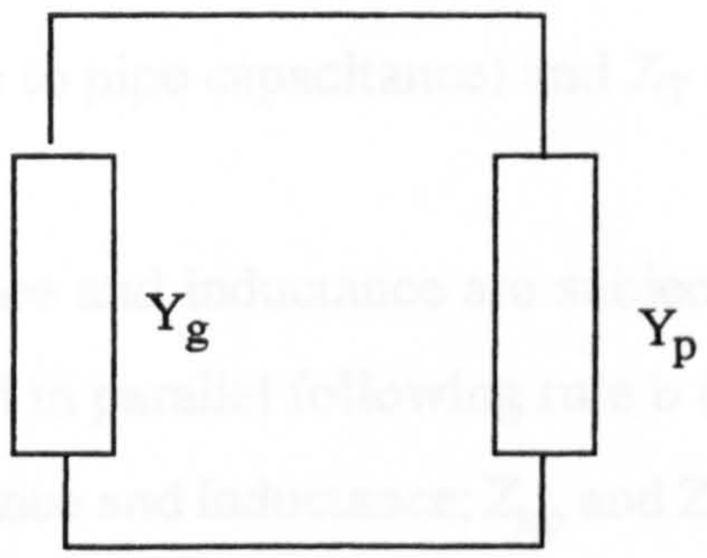

Fig. 6.4 Pipe circuit model - development stage 11

Y_p represents the input, pipe and termination impedances, assuming $Z'_{eq} = 1/Y_p$.

Logically, the current flow encounters the input impedances after the mouth. The input impedance had earlier been shown to be made up of a reactive and resistive term. Figure 6.3 can now be modified to include input impedance Z_{in} as illustrated in figure 6.5 below.

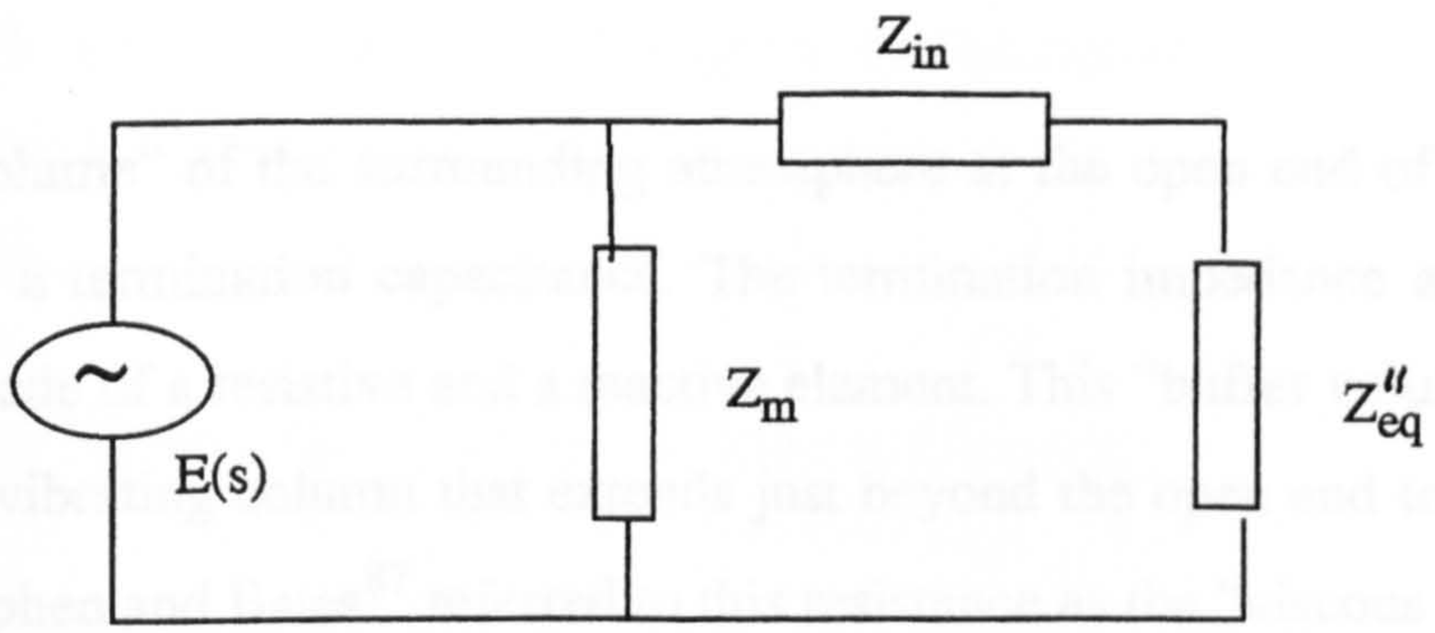

Fig. 6.5 Pipe circuit model - development stage III

Z_m = mouth impedance and Z_{in} = input impedance

Z''_{eq} now comprises the pipe and termination impedances: Z_{Lp}, (reactance due to pipe inductance) Z_{cp} (reactance due to pipe capacitance) and Z_T (termination impedance) .

The pipe distributed capacitance and inductance are subjected to the same pressure force and can therefore be connected in parallel following rule b (section 6.5). Expanding figure 6.5 to include the pipe capacitance and inductance; Z_{cp} and Z_{Lp} respectively, we have figure 6.6 below.

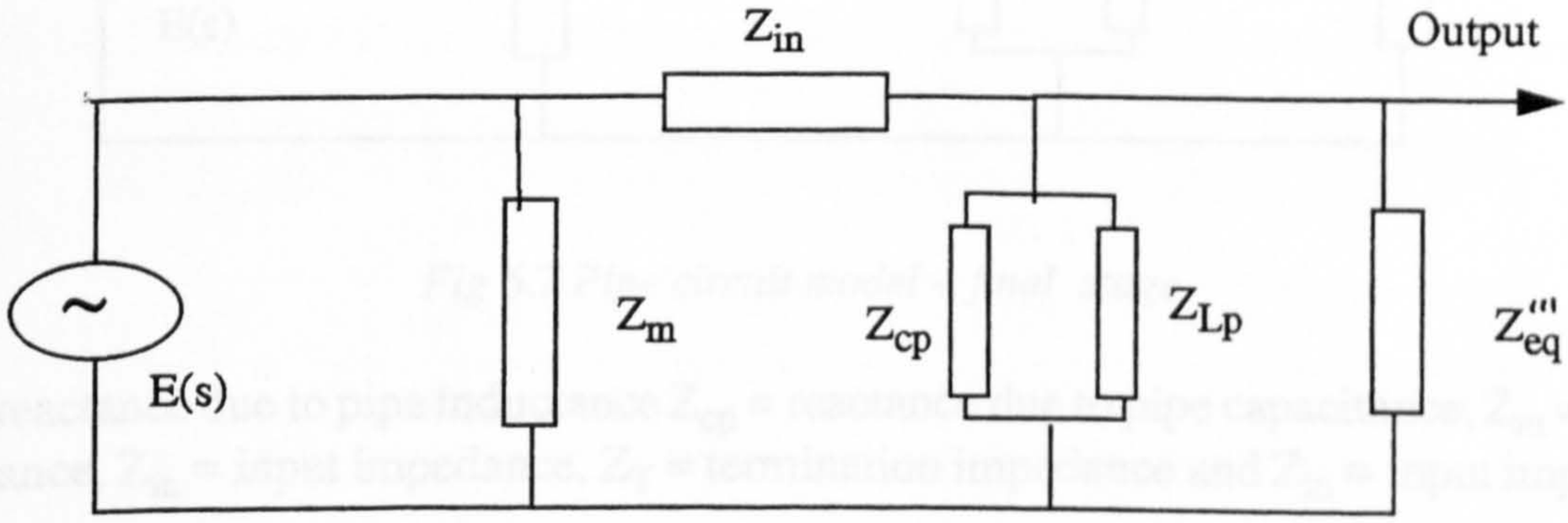

Fig. 6.6 Pipe circuit model - development stage IV

Z_{Lp} = reactance due to pipe inductance Z_{cp} = reactance due to pipe capacitance, Z_m = mouth impedance and Z_{in} = input impedance - Z'''_{eq} = equivalent circuit impedance of remaining components.

This leaves just the positioning of the termination impedance Z_T.

The "buffer volume" of the surrounding atmosphere at the open end of the pipe can be constructed as a termination capacitance. The termination impedance at the outlet was shown to be made of a resistive and a reactive element. This "buffer volume" subjects the motion of the vibrating column that extends just beyond the open end to some frictional resistance. Stephen and Bates[87] referred to this resistance as the "viscous resistance". The buffer volume in the viscinity of the pipe mouth is subjected to the displacement of the vibrating air column. Following the rules outlined by Stephen and Bates[87] the elements that make up Z_T (= $R_T + 1/(j\omega C_T)$: termination resistance and Capcitance respectively) can be connected in series and then introduced as a shunt impedance in place of Z'''_{eq} as depicted in Fig 6.7 below

.

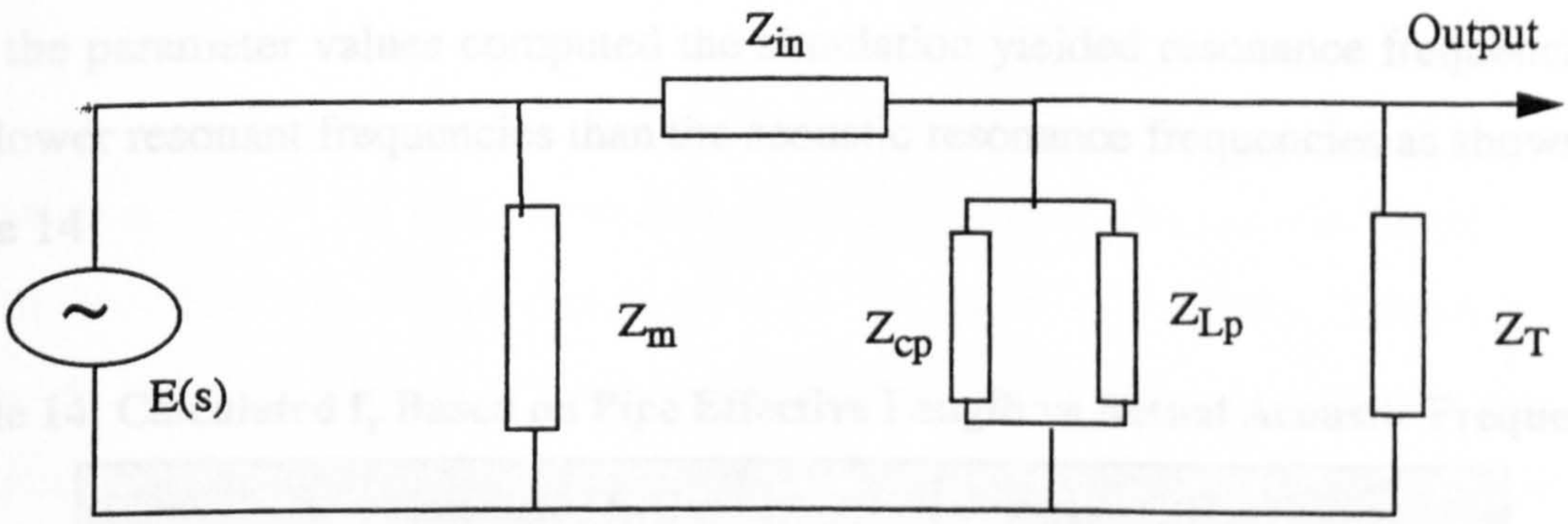

Fig 6.7 Pipe circuit model - final stage

Z_{Lp} = reactance due to pipe inductance Z_{cp} = reactance due to pipe capacitance, Z_m = mouth impedance, Z_{in} = input impedance, Z_T = termination impedance and Z_{in} = input impedance

6.5 Calculation of Circuit Impedances

The equations for the different circuit elements were used to evaluate the resistances, capacitances and inductances of the different circuit elements. Equation 6.14 was used in evaluating Z_{in}, Z_m was determined using equation 6.20, Z_{Lp} and Z_{cp} were determined using

equations 6.26 and 6.27 respectively, while equation 6.33 was used to calculate R_T and C_T. The component values were calculated using the mathematical package Maple™ Version 2.[100] (Maple is a software used to perform symbolic or numerical mathematical calculations). The program flow chart is given in appendix 10.

6.6 Computer Simulation of Pipe Analogous Circuits

The values of the circuit components were used to simulate the circuit using the circuit simulation package HSPICE.[47] The circuit was designed on the ECAD package Powerview[1], where from a wire listing of the circuit was automatically generated for HSPICE simulation.

6.6.1 Circuit Simulation Results

Using the parameter values computed the simulation yielded resonance frequencies with much lower resonant frequencies than the acoustic resonance frequencies as shown below in table 14

Table 14: Calculated f_r Based on Pipe Effective Length vs Actual Acoustic Frequencies

Pipe	Calculated f_r(Hz)	Acoustic f_r(Hz)
1	93.89	260.5
2	193.22	520.3
3	397.62	1078.8
4	784.28	2085.5

The results of the calculations yielded inaccurate frequencies, as such an ECAD simulations was not undertaken, for these set of component values.

---

1. Powerview is an electronic CAD package for designing circuits in preparation for HSPICE simulation.

In figure 6.7 (repeated below for clarity) it was indicated that the driving mechanism not only excites the resonance column of the pipe. There is coupling between the generator and the resonance column as well as feedback.

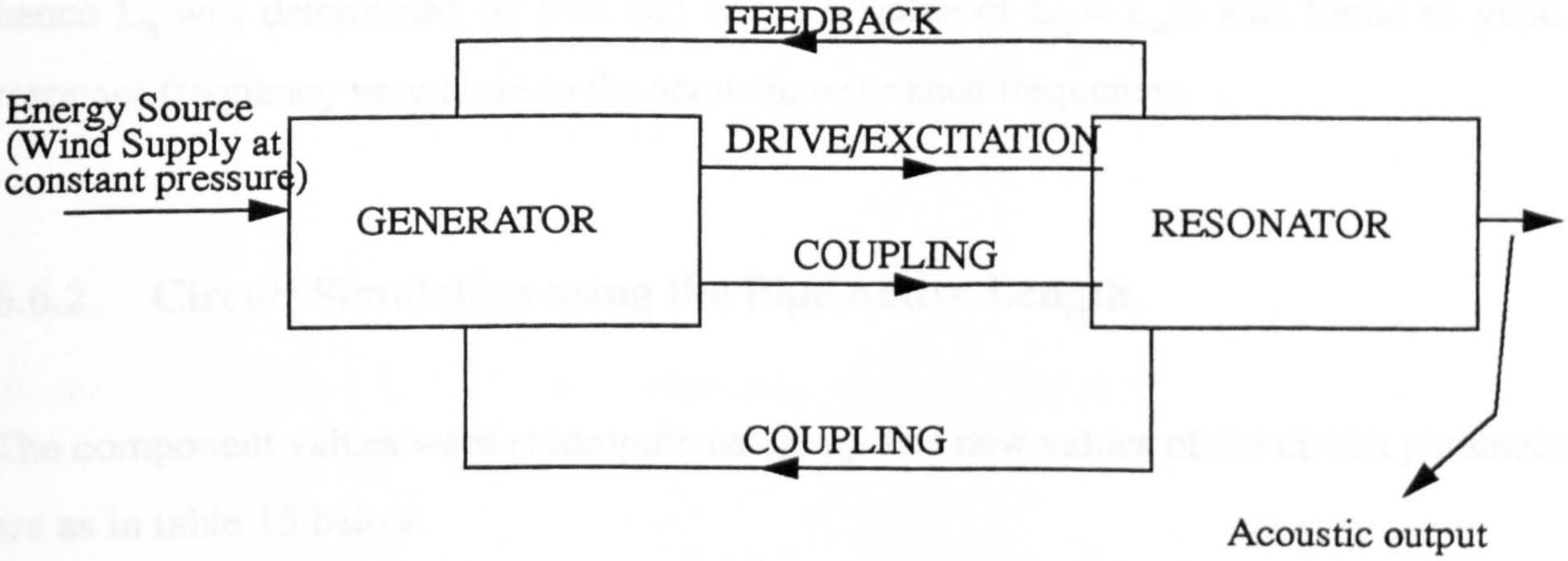

Fig 6.7 Block Diagram of Pipe Resonator

The mouth area and the pipe input both have inductance elements. If there is coupling between these two segments, it can be inferred that there will be some "coupling" between the passive elements. This would mean there is some coupling between the mouth and input inductance. The coupling gives rise to a mutual inductance, M_L which is proportional to the square root of the product of the input and mouth inductance; i.e.

$$M_L \propto (L_{in}L_m)^{0.5}.$$

L_{in} depends on the pipe length, from equation 6.17.

$\Rightarrow$ L_m also depends on pipe length and of course, M_L.

It can thus be argued that the whole pipe length does not fully participate in the resonance process. Resonance could only be taking place within a certain active length of the pipe, L_a. The sound generated propagates within the entire pipe, with the portion that constitutes the

active length, L_a serving as the radiation source. L_a would therefore be only a fraction of L_e, the acoustic length of the pipe.

The pipe resonator capacitance and inductance values (equations 6.25 and 6.34) were recomputed substituting L_a in place of L_e. The amount of coupling is not exactly known, hence L_a was determined by trial and error. A value of $L_a \cong L_e/3$ was found to yield a resonant frequency very close to the acoustic resonance frequency.

6.6.2. Circuit Simulation using the Pipe Active Length.

The component values were recompute using L_a. The new values of the circuit parameters are as in table 15 below.

Table 15: Circuit Component Values

Component	Pipe 1	Pipe 2	Pipe 3	Pipe 4
R_m (Ω)	38.8	155.16	667.8	2493.3
L_m (mH)	0.729	1.24	1.97	3.13
R_{in}(Ω)	0.3	0.618	0.732	0.958
L_{in} (mH)	99.6	7.59	.36	2.1
C_p(μF)	246.9	53.6	8.11	1.21
L_p (mH)	1.421	1.6	2.54	4.42
R_T(Ω)	0.015	0.06	0.3	1
C_T(μF)	2693.4	14.88	19.2	2.78
f_r (Hz)	268.7	543.8	1109.2	2177.7

The circuit simulation produced the resonance curves given in figures 6.16 - 6.19. The resonant frequencies are very similar to theoretically calculated values as well as those obtained from acoustic experiments as shown in table 16 below

Table 16: Calculated Simulated and Acoustic Resonant Frequencies of Pipe

Pipe	Calculated f_r(Hz)	Simulated f_r (Hz)	Acousitc f_r (Hz)
1	268.7	269.153	260.5
2	543.8	529.645	520.312
3	1109.2	1064.14	1078.812
4	2177.7	2114.26	2084.5

Note: For figures 6.8 - 6.11, the horizontal axis is on a log scale

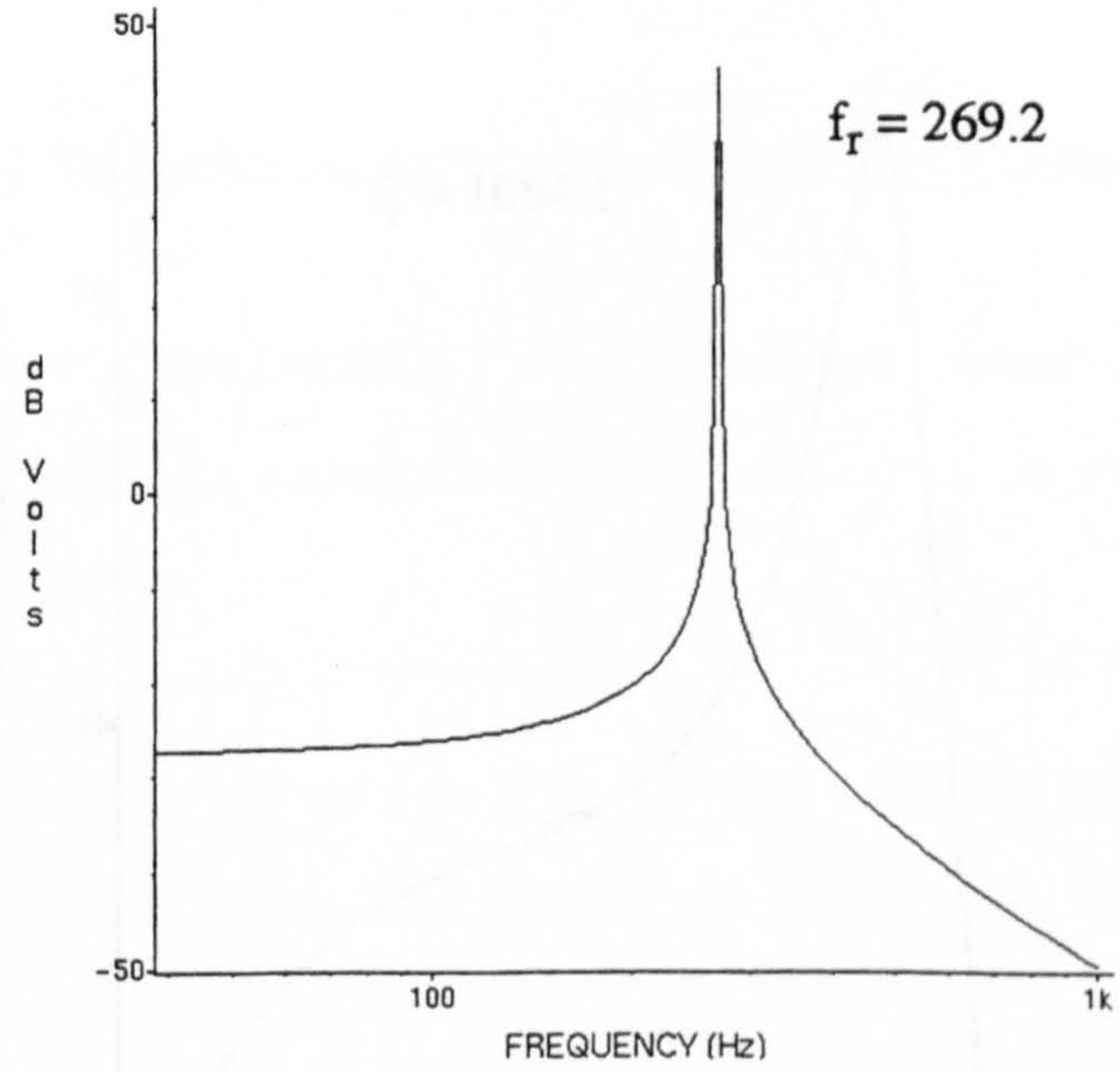

Fig 6.8 Response of HSPICE simulation of the equivalent circuit of pipe 1

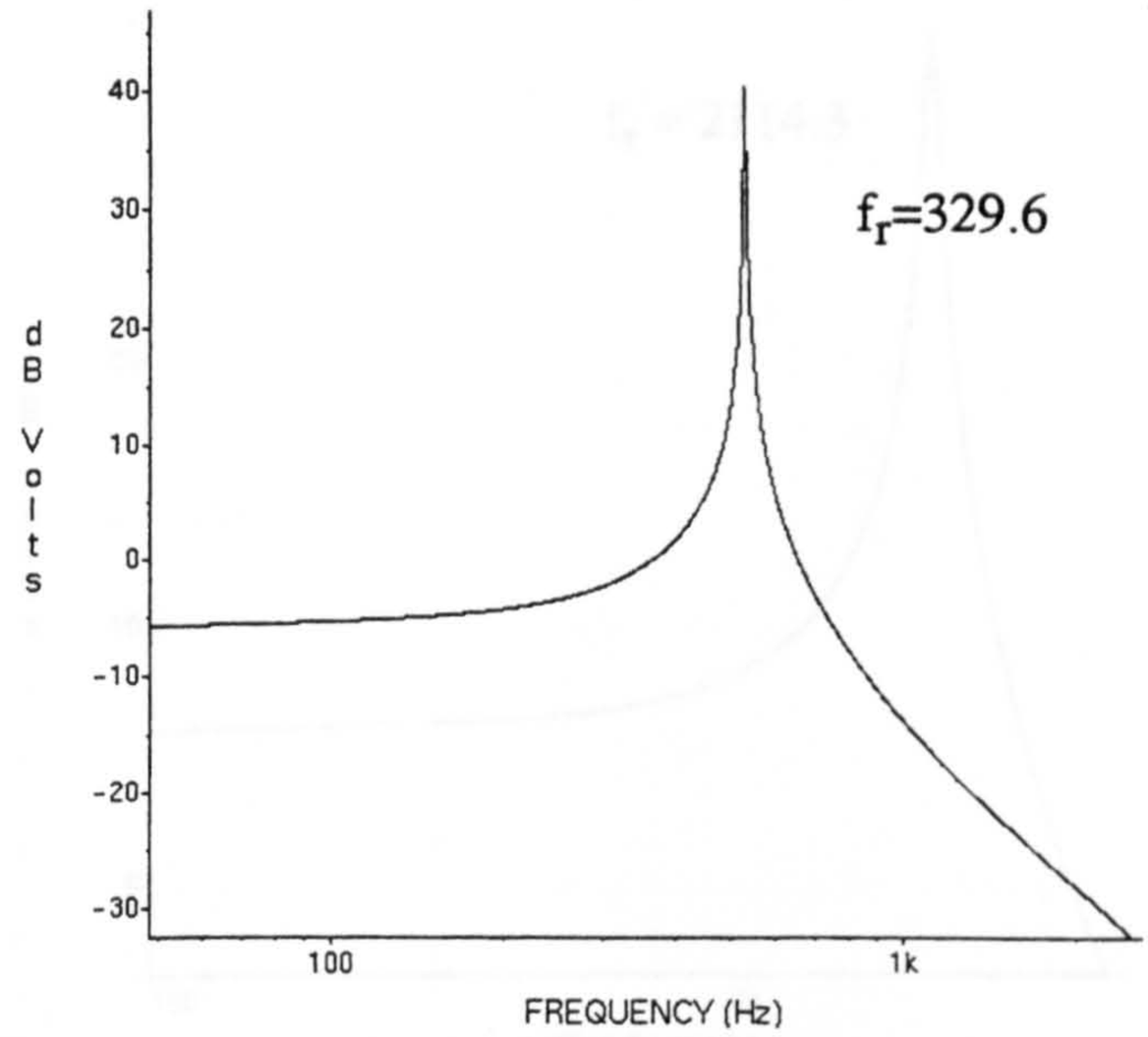

Fig 6.9 Response of HSPICE simulation of the equivalent circuit of pipe 2

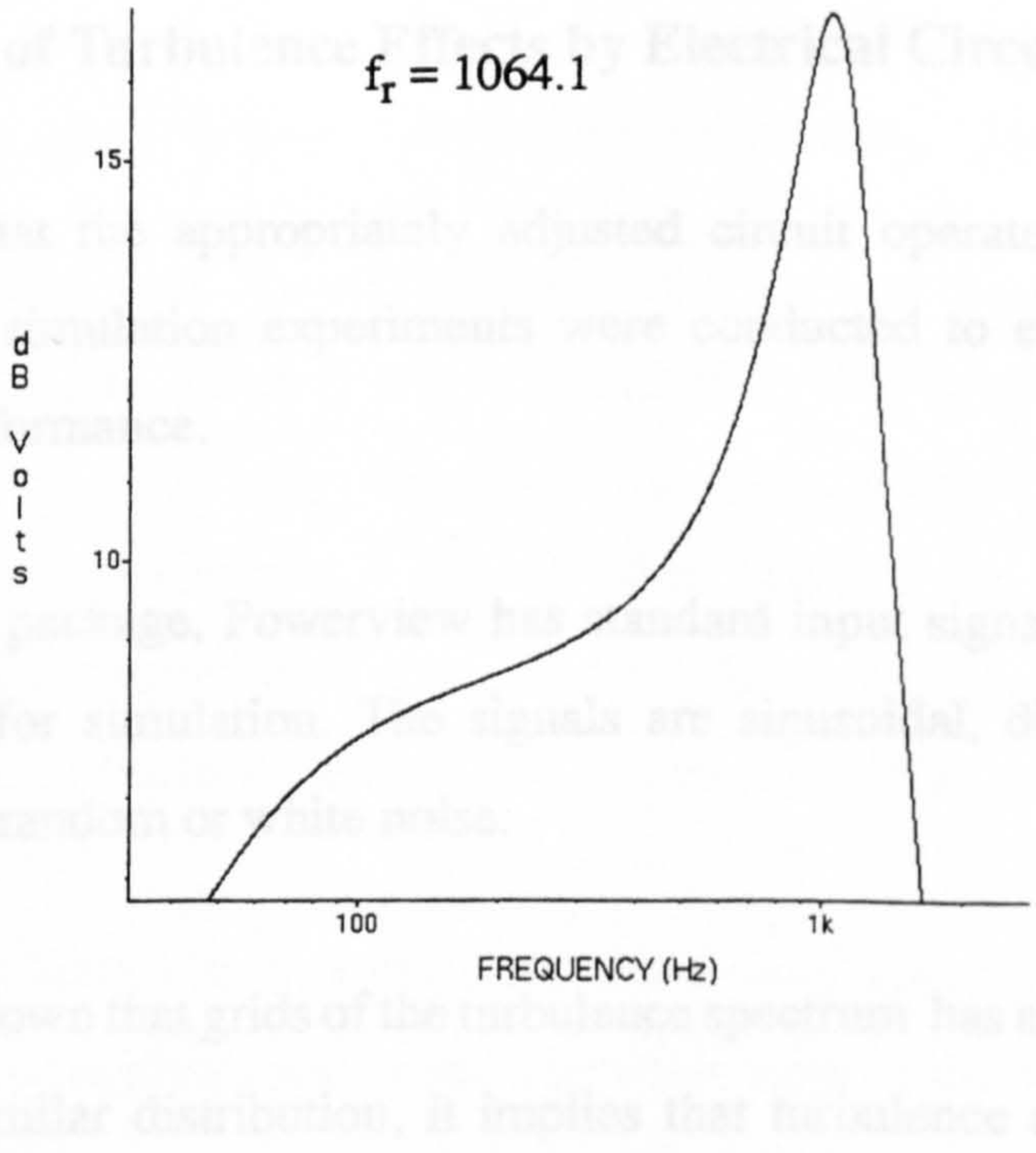

Fig 6.10 Response of HSPICE simulation of the equivalent circuit of pipe 3

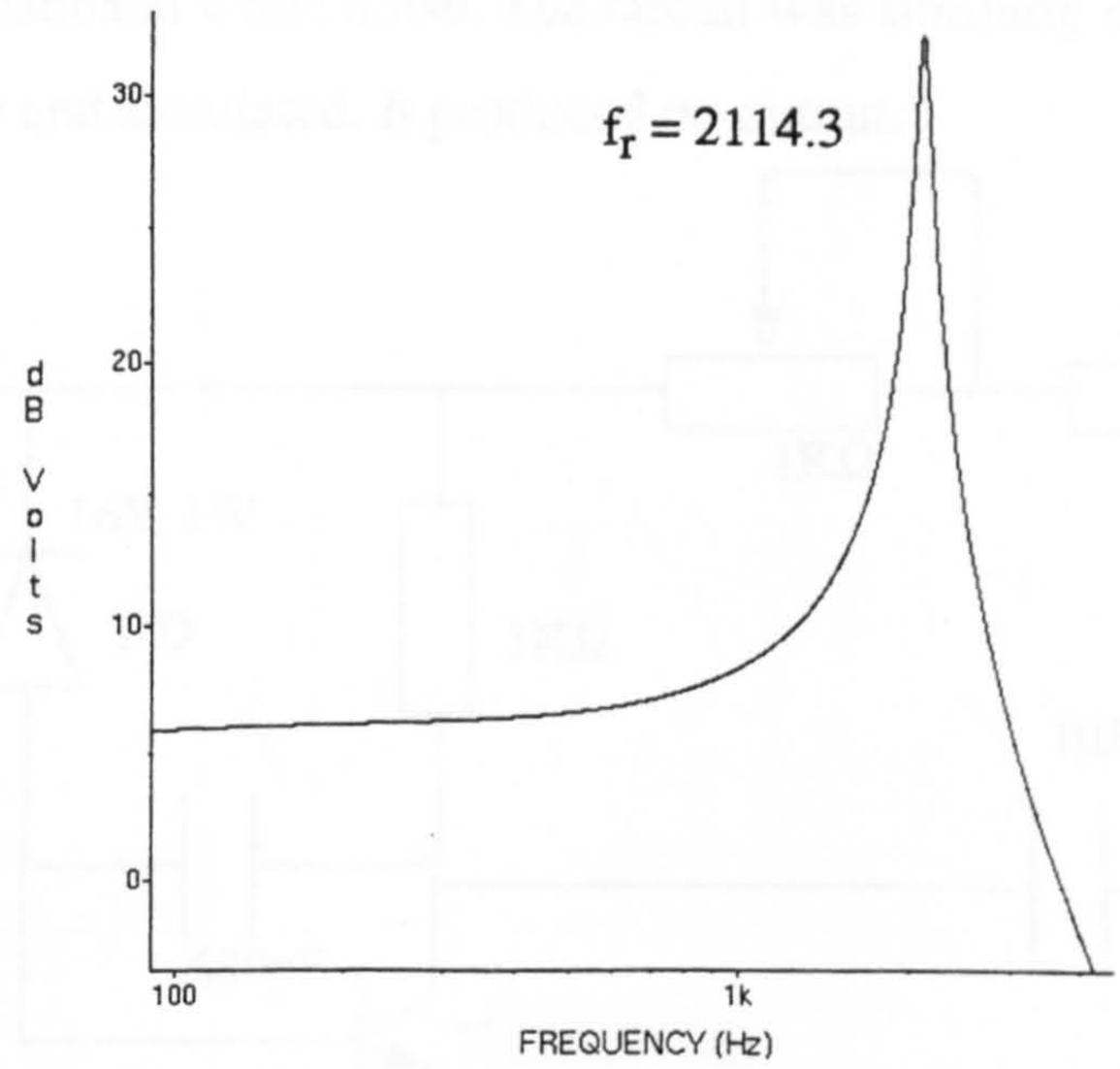

Fig 6.11 Response of HSPICE simulation of the equivalent circuit of pipe 4

6.6.3 The Study of Turbulence Effects by Electrical Circuit Simulation.

After establishing that the appropriately adjusted circuit operates at the approximate resonant frequency, simulation experiments were conducted to evaluate the effects of turbulence on its performance.

The electronic CAD package, Powerview has standard input signals that can be used as input into a circuit for simulation. The signals are sinusoidal, digital and exponential functions. None was random or white noise.

In chapter 3, it was shown that grids of the turbulence spectrum has a Guassian distribution. Since noise has a similar distribution, it implies that turbulence could be simulated as broadband noise.

A noise generator circuit, as per figure 6.12 [101] was designed, built on a vero board and

found to produce broadband white noise. The circuit was similarly designed on the ECAD package, Powerview and simulated. It produced no output.

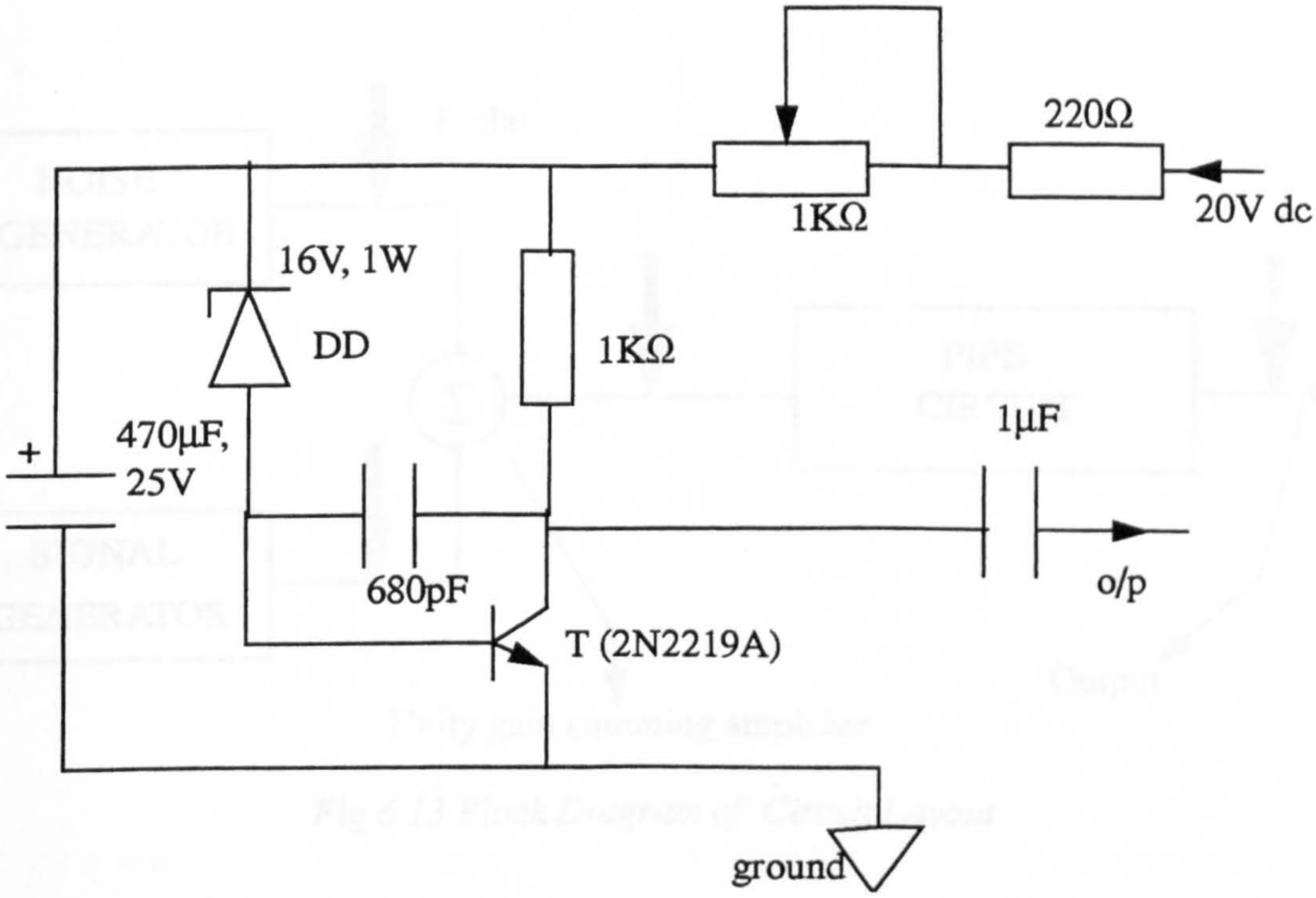

Fig 6.12: Circuit of Noise Generator

The noise generator circuit of figure 6.12 produces noise thanks to the break down noise generated by the diode, DD, which is in turn amplified by the transistor amplifier, T. While break down materializes physically, the simulation package could not deliver this effect, hence the there was no noise output. It turns out that HSPICE can only produce output to a circuit if the circuit is excited by a specific input. The noise generator has no input. As stated before, it relies on the break down noise of the diode DD.

The noise generator circuit was connected through a unity gain summing circuit that had two inputs into the pipe equivalent circuits. The other input to the summing circuit was an a.c. signal that swept through a range of frequencies. It is capable of sweeping through frequencies ranging from 1Hz to several mega Hertz. The a.c. sweep was programmed to sweep from a range of 1Hz to 10KHz as the frequency response is not expected to provide any additional information beyond 10KHz.

Figure 6.13 gives a block diagram of the circuit arrangement.

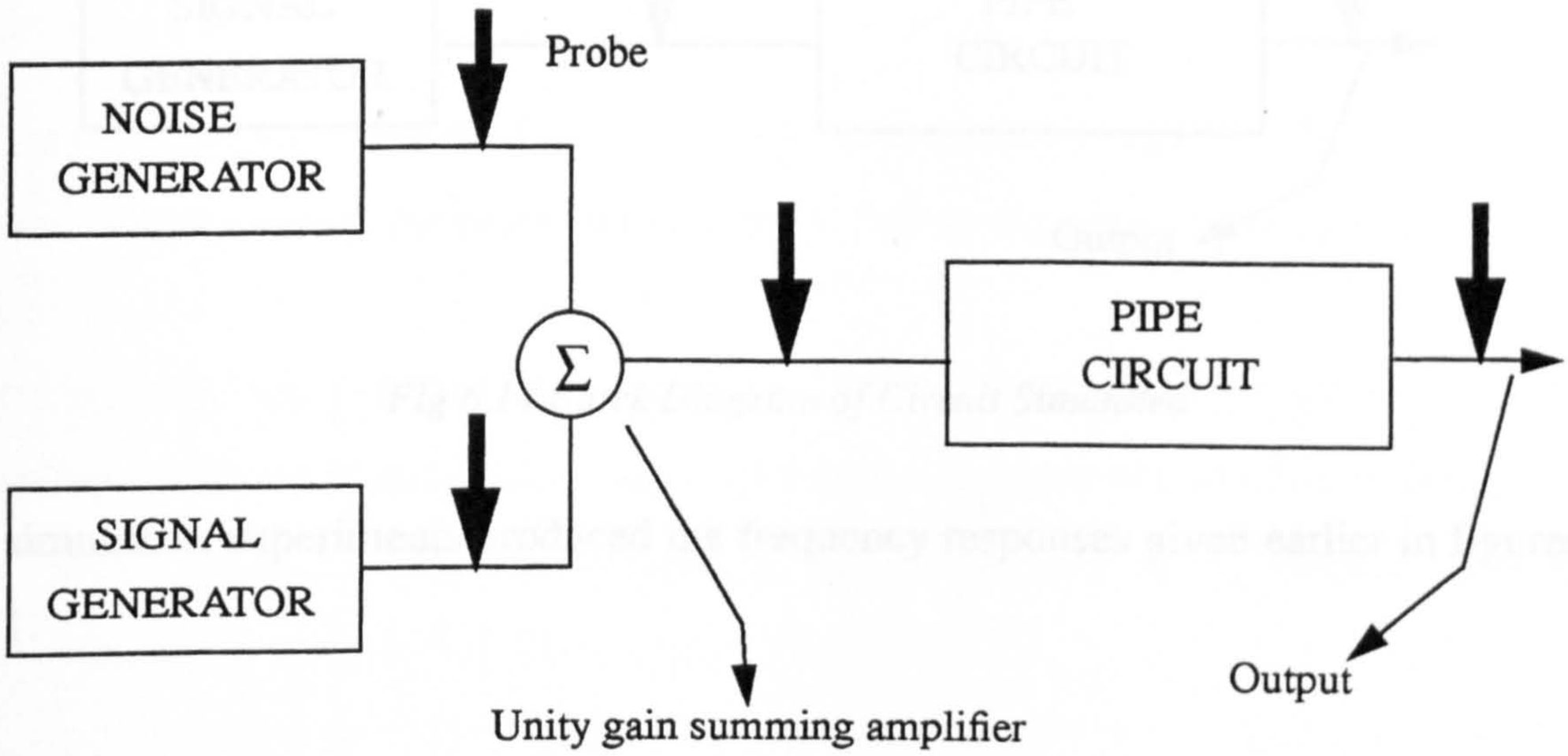

Fig 6.13 Block Diagram of Circuit Layout

When it was realised that the noise generator could not deliver noise during the ECAD simulation, Gaussian noise was numerically simulated and inserted as a signal input into the programme routine of the wire listing automatically generated by Powerview for HSPICE simulation. The set of random numbers that simulated the Gaussian distribution (noise) were generated using MINTAB™.[61] Even then, HSPICE could not handle the computation and the excercise was discontinued. An example of a modified program listing as described above is in appendix 12).

As the noise circuit was not producing the expected result, it was left out of the simulation and the system as per the block diagram of figure 6.14 was used.

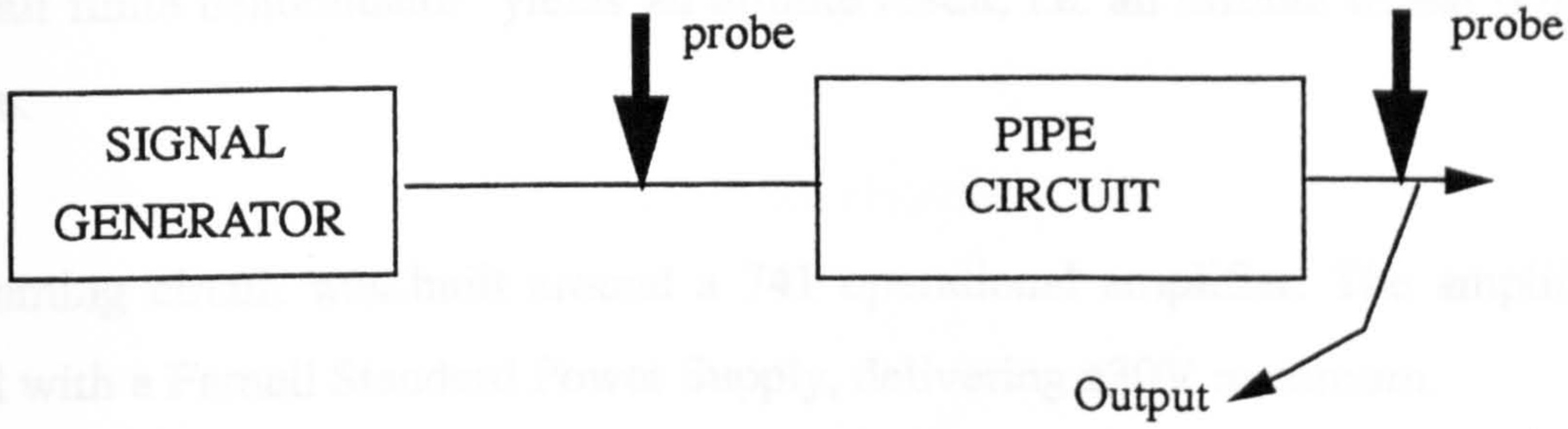

Fig 6.14 Block Diagram of Circuit Simulated

The simulation experiments produced the frequency responses given earlier in figures 6.8 - 6.11.

As the noise generator could not be relied on to provide a computer simulation of turbulence, it was necessary to carry out a hardware implementation of the system.

6.6.4. Evaluating Pipe Analogous Circuits by Experiment.

Each of the pipe circuits was constructed. A noise generator and function generator supplied a signal, into the circuits via a unity gain summing amplifier.

The function generator used was a FG600 Function Generator by Feedback. An HP HO1-3722A Noise Generator by Hewlett Packard was used to provide the noise. The noise generator has a maximum output amplitude of 3.16 V rms. The control panel was tuned to deliver broadband white noise. The sequence length of the shift registers in the noise generator was set to infinite. The clock period was set to 50KHz. The Hewlett Packard noise generator provides analogue and digital noise outputs. The analogue output is obtained by converting the pseudo random digital noise output. Horowitz and Hill[45] have shown that if the sequence length of a pseudo random bit sequence is infinite, the digital noise will require an infinitely large amount of time to repeat itself. The repeat time being

the (sequence length)/(clock frequency). The numerator is infinite; dividing the numerator by a small finite denominator yields an infinite result, i.e. an infinite repeat time of the sequence.

The summing circuit was built around a 741 operational amplifier. The amplifier was powered with a Farnell Standard Power Supply, delivering ±30V maximum.

On the acoustic test rig, the flow into the wind chest was arranged such that different proportions of filtered (laminar) wind and turbulent wind flowed downstream into the wind chest. Valves were used to deliver wind in the proportions as per table 5 (chapter 5) repeated below in table 17 for clarity.

Table 17: Flow Conditions

Percentage turbulent flow	Percentage laminar flow
100	0
75	25
50	50
25	75
0	100

The flow combinations of the above table had to be mimicked electrically. The volumetric flow current, Q, is analogous to the electrical current.

$$Q = \boldsymbol{U} S_d \qquad 6.34$$

Where S_d = duct cross sectional area. $\boldsymbol{U}$ implicitly will be directly proportional to the analogous electric current.

Hinze[41] showed that the instantaneous velocity of flow;

$$U = U + u \qquad 6.35$$

where U is the mean flow velocity and u the fluctuation about the mean. Hinze further defines the turbulence intensity as;

$$u'/U, \qquad 6.36$$

where u' is the root mean square value of u.

U can be taken to represent the sinusoidal electrical current emanating from the function generator and the current from the noise generator to represent the turbulent fluctuations about the mean flow, u'. Then

$$u'/U x 100\% \qquad 6.37$$

would be a percentage of turbulence flowing into the system.

A Blackstar 3210 true rms multimeter was used to measure the output currents of the noise and signal generators.

The current output for the different control knob position of both the signal and noise generators are as in table 18 below.

Table 18: Current Output of Signal and Noise Generators

Signal Generator		Noise Generator	
Control Knob Position	Output current (mA rms)	Control Knob Position	Output current (mA rms)
0	0	-	-
1	0.428	0.1	0.32
2	0.947	0.2	0.91
3	1.46	0.3	1.29
4	2.27	0.4	1.81
5	2.86	0.5	2.17
6	3.42	0.6	2.65
7	3.95	0.7	3.12
8	4.6	0.8	3.51
9	5.18	0.9	3.96
10	5.81	1	4.42

From the above table, the turbulence/laminar conditions are worked out using equation 6.37 are given in table 19.

Table 19: Electrical Equivalence of Flow Conditions

Turbulence Flow %	Laminar flow %	Signal Current (mA)	Noise Current (mA)	Noise/Signal %
0	100	3.95	0	0
25	75	5.18	1.29	24.9
50	50	4.6	2.17	47.17
75	25	5.81	3.51	76.1
100	0	0.16	4.42	100

These settings were used to simulate the appropriate turbulence/laminar flow conditions into the circuit.

The function generator, unlike that used for the computer simulation, does not automatically sweep through a range of frequencies, it could only be set to one frequency at a time.

While the noise generator was switched off, the function generator was panned till the resonant frequency of the circuit was reached - as observed on an oscilloscope. The noise generator output was then set accordingly and then switched on. The output was spectrally analyzed on the B & K spectrum analyser and the spectrum printed on an HP plotter. The circuit outputs for the different combinations of noise and sinusoidal inputs (representing the different combinations of turbulent and laminar flow) are given in figures 6.15 - 6.34

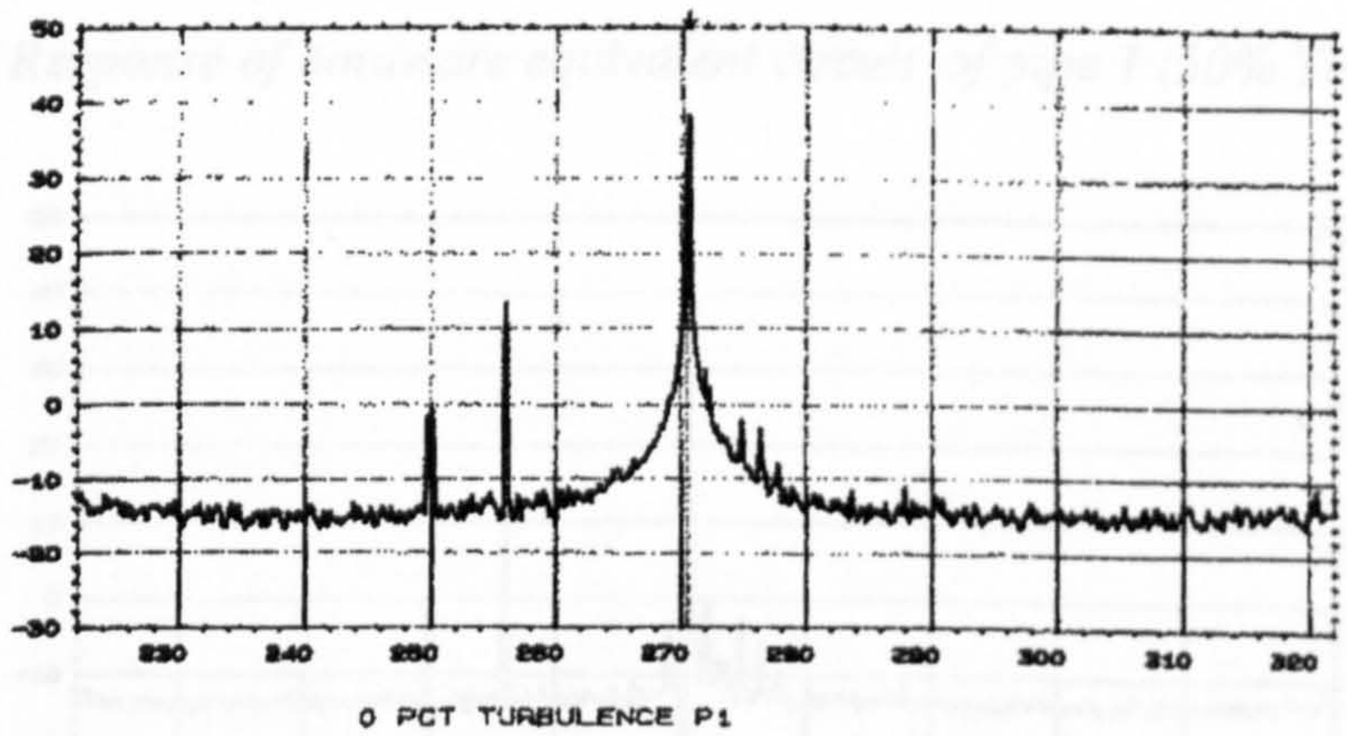

Fig 6.15 Response of hardware equivalent circuit of pipe 1 (0% Turbulence)

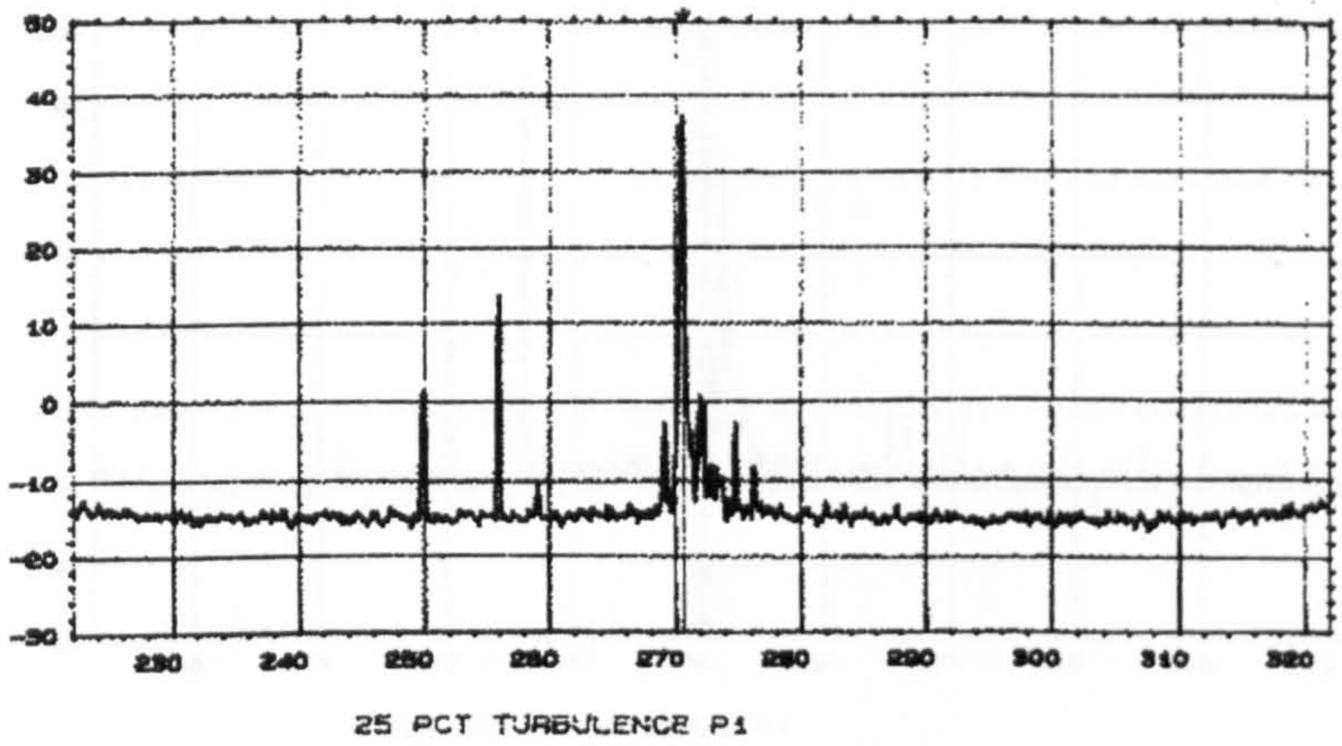

Fig 6.16 Response of hardware equivalent circuit of pipe 1 (25% Turbulence)

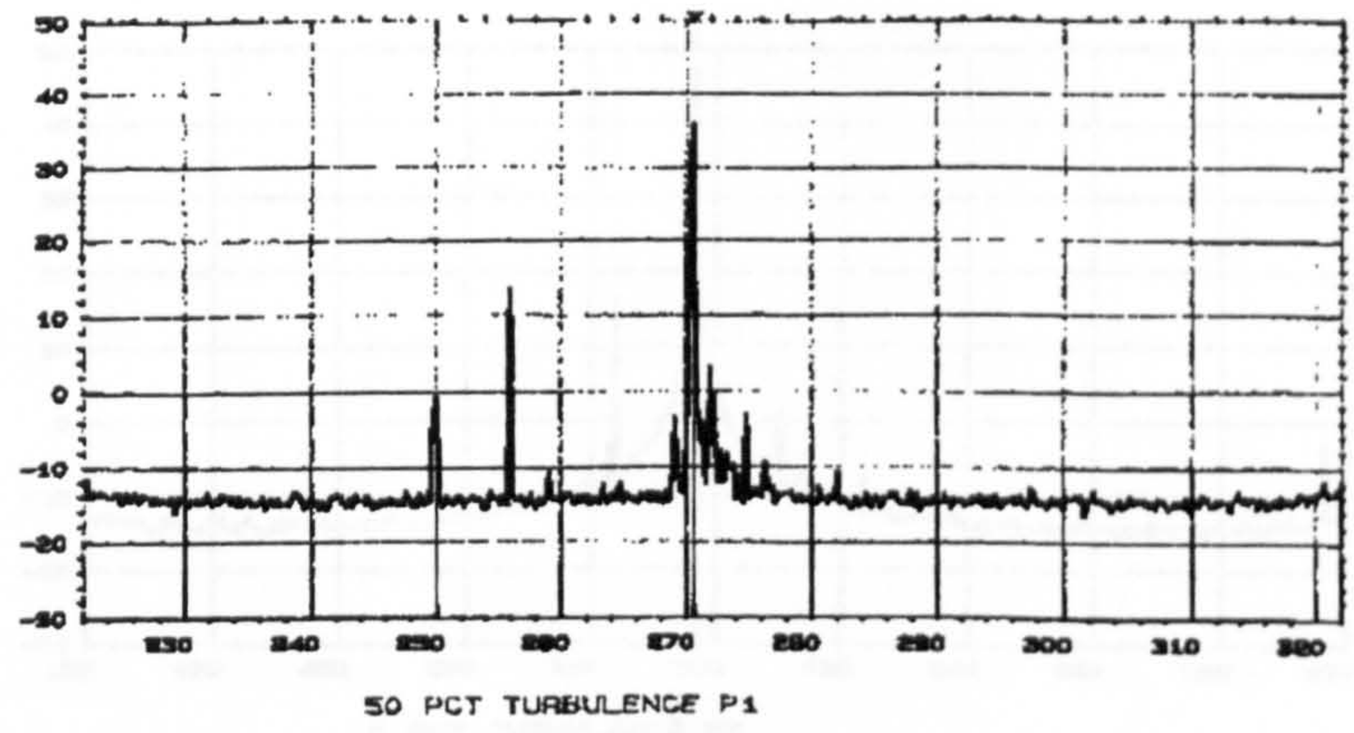

Fig 6.17 Response of hardware equivalent circuit of pipe 1 (50% Turbulence)

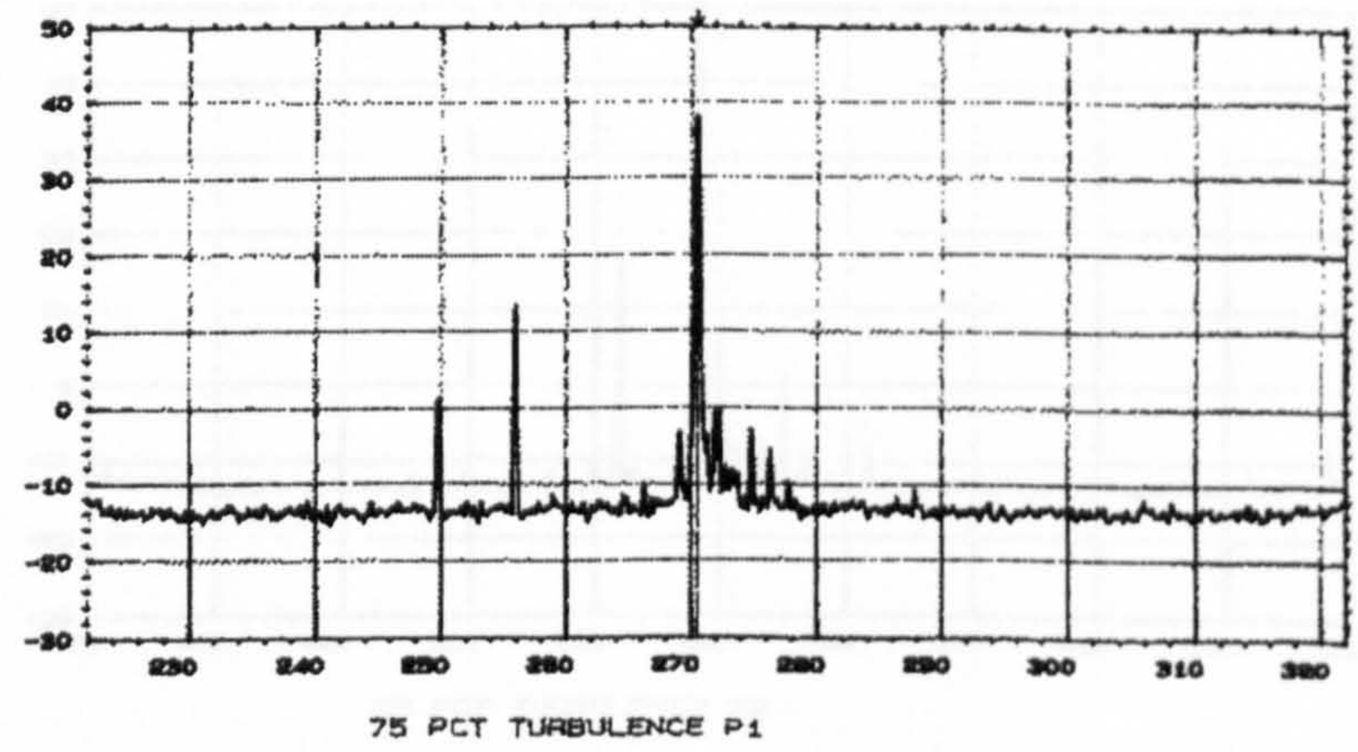

Fig 6.18 Response of hardware equivalent circuit of pipe 1 (75% Turbulence)

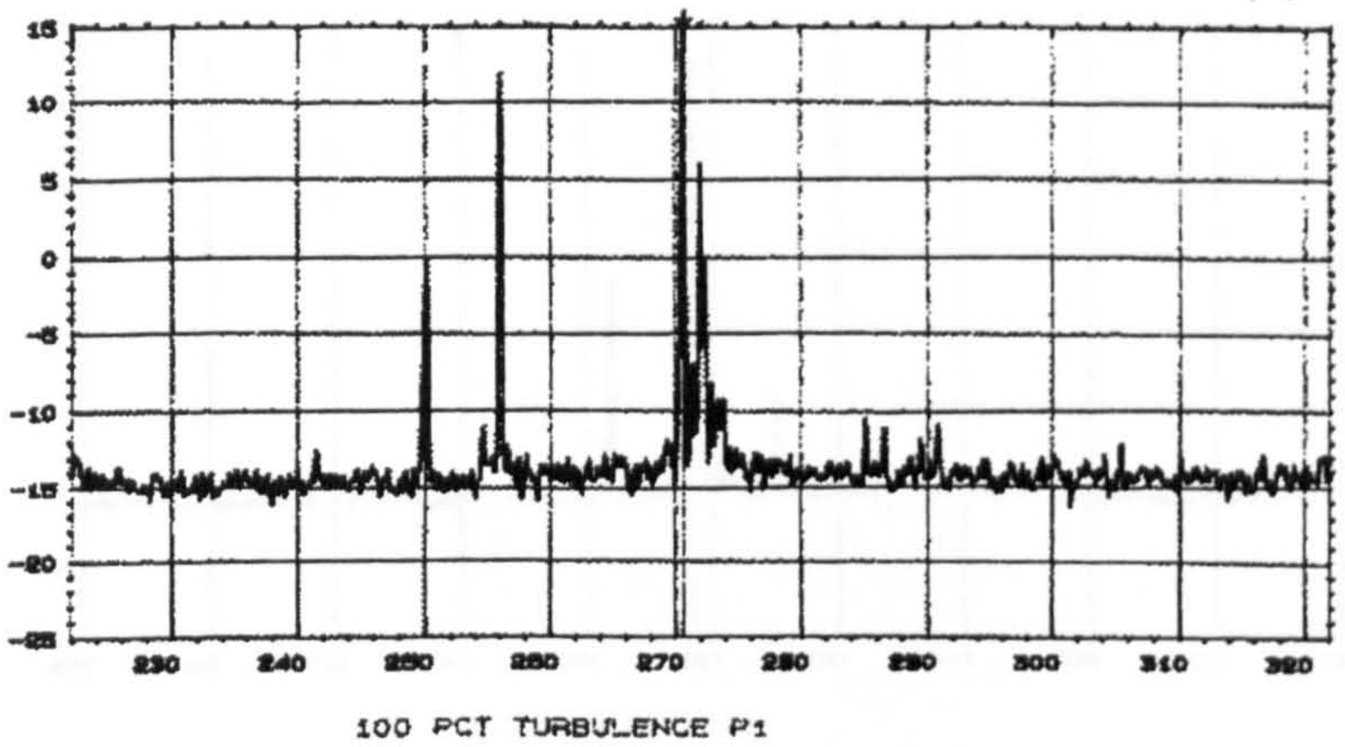

Fig 6.19 Response of hardware equivalent circuit of pipe 1 (100% Turbulence)

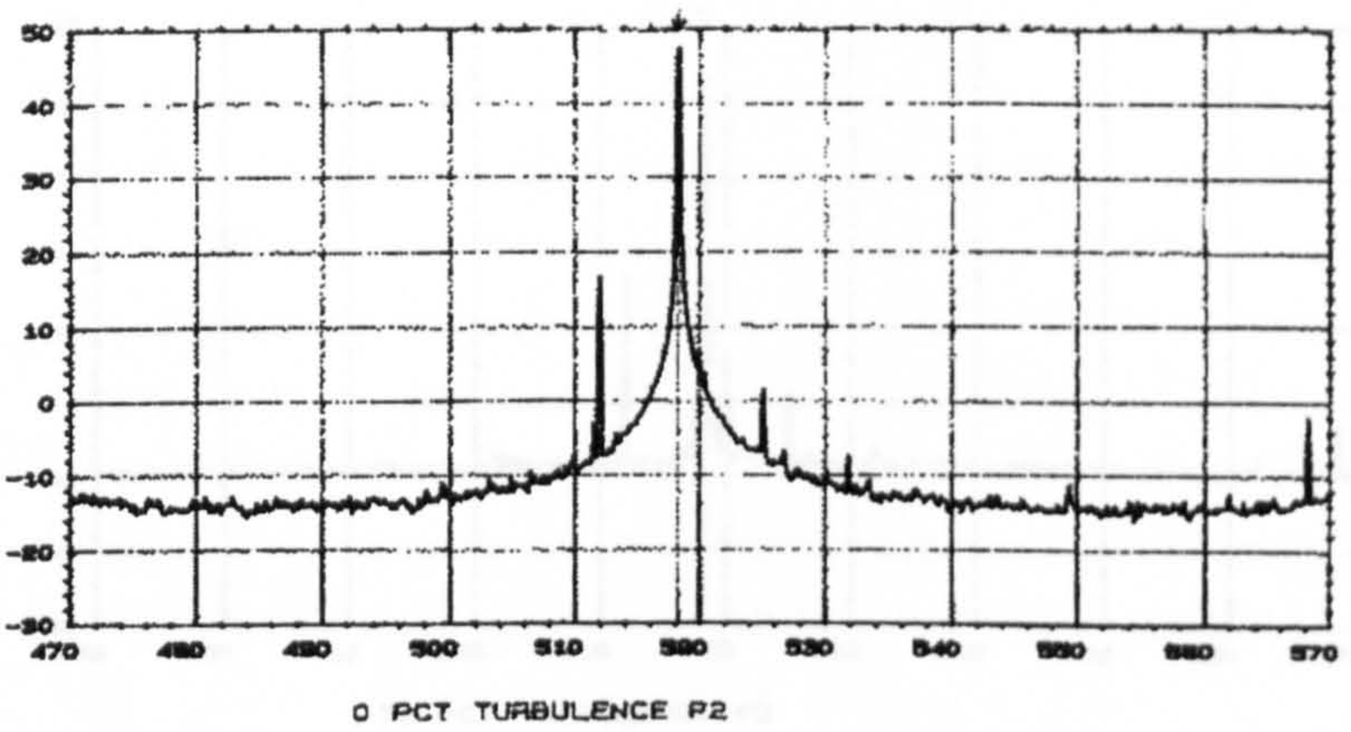

Fig 6.20 Response of hardware equivalent circuit of pipe 2 (0% Turbulence)

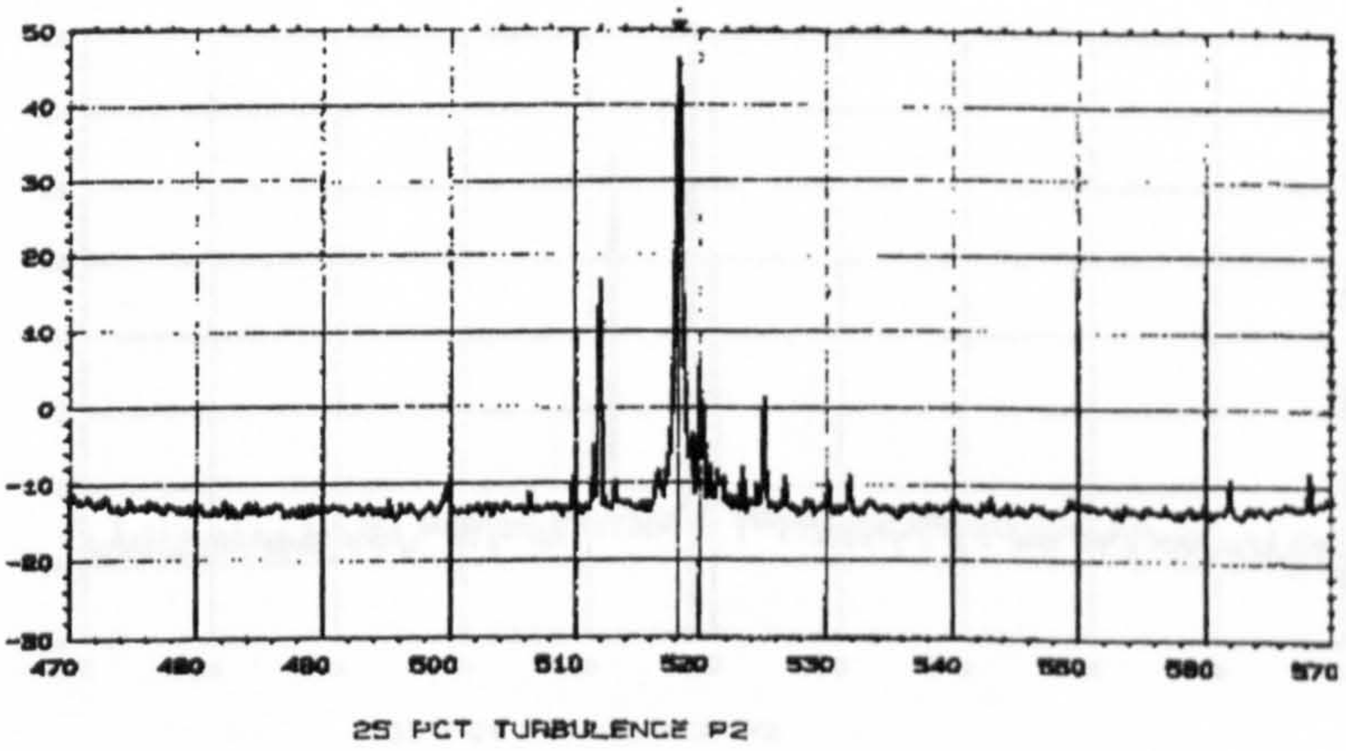

Fig 6.21 Response of hardware equivalent circuit of pipe 2 (25% Turbulence)

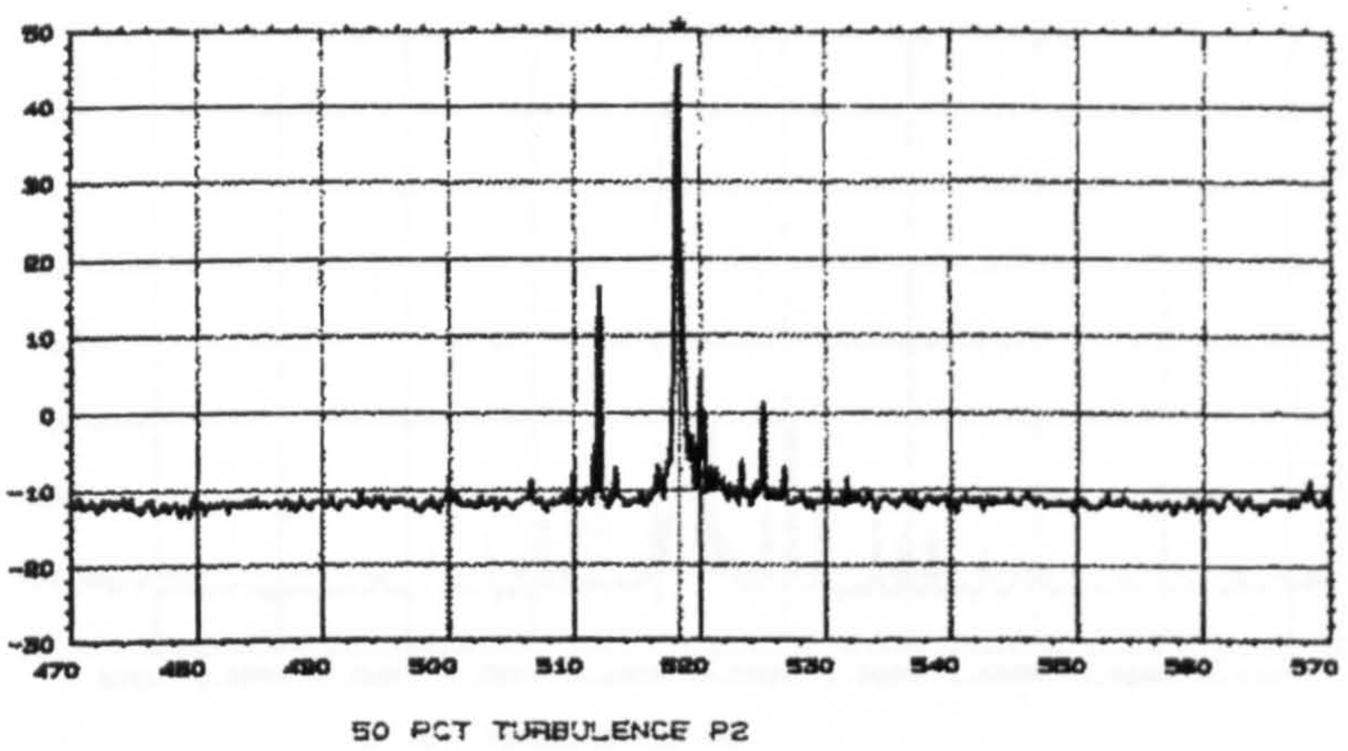

Fig 6.22 Response of hardware equivalent circuit of pipe 2 (50% Turbulence)

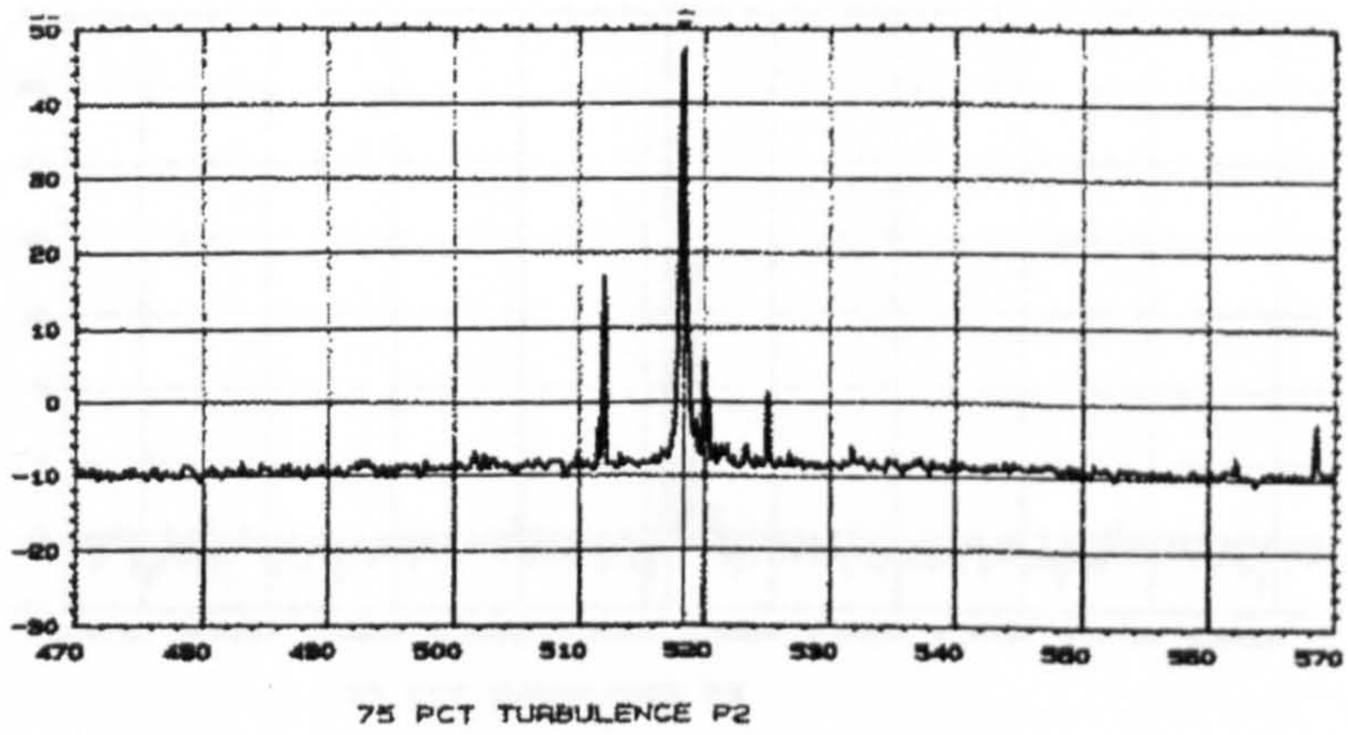

Fig 6.23 Response of hardware equivalent circuit of pipe 2 (75% Turbulence)

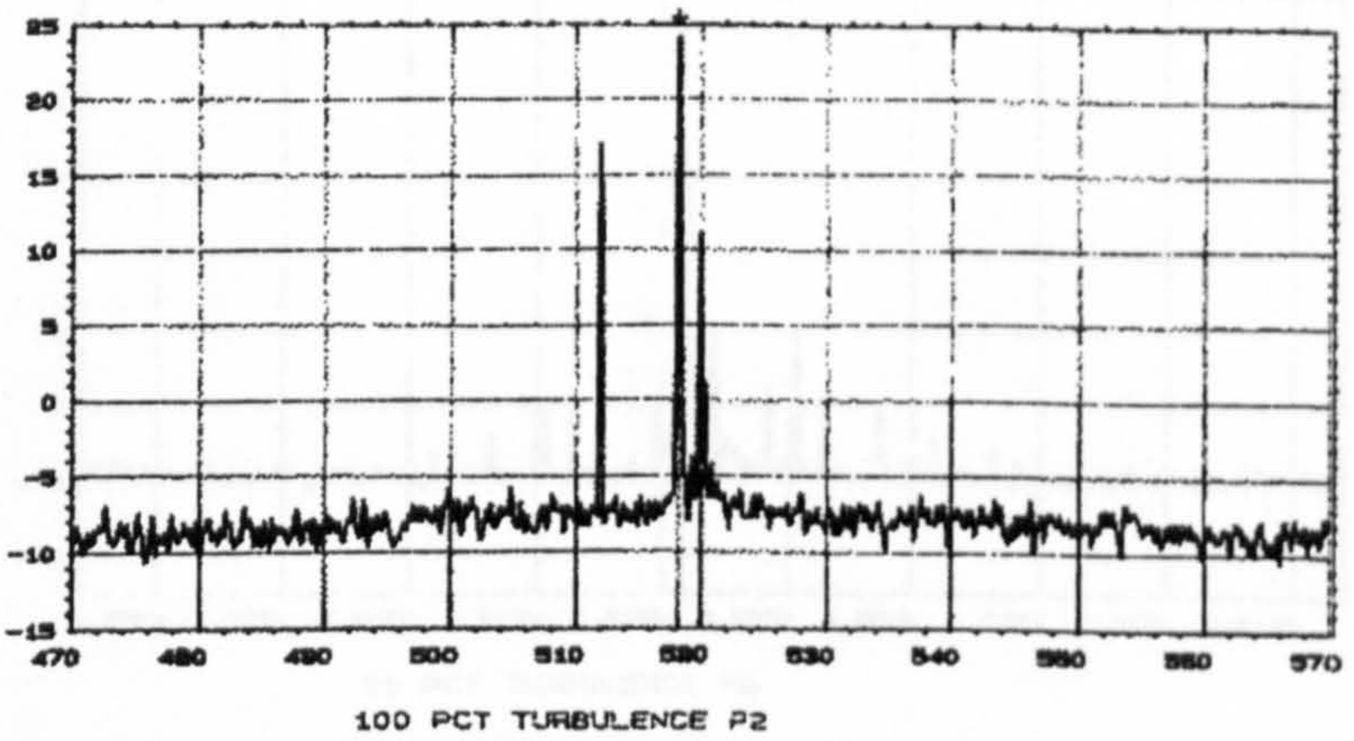

Fig 6.24 Response of hardware equivalent circuit of pipe 2 (100% Turbulence)

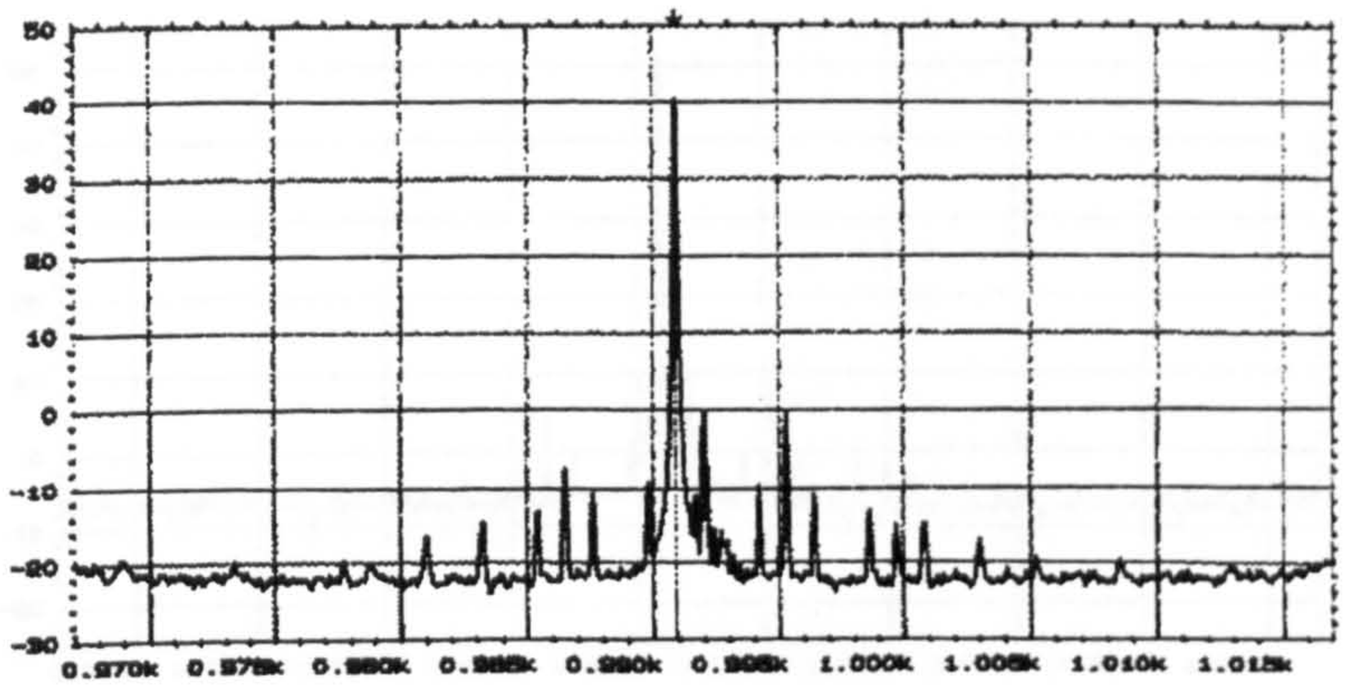

Fig 6.25 Response of hardware equivalent circuit of pipe 3 (0% Turbulence)

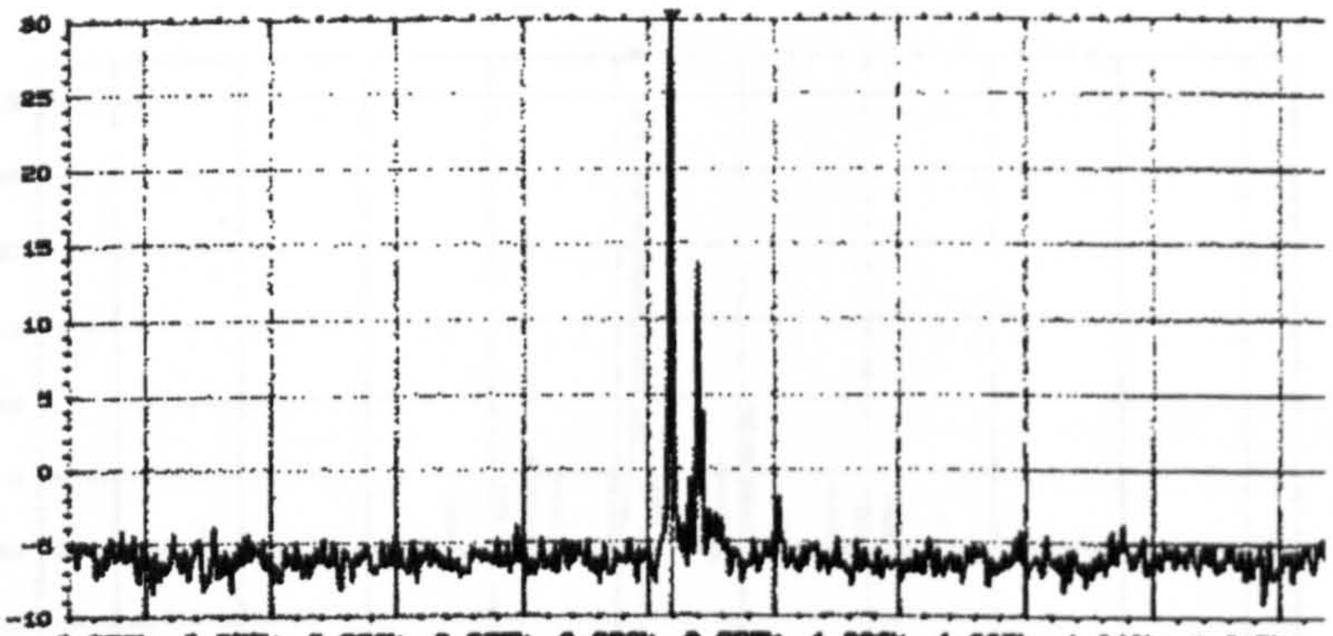

Fig 6.26 Response of hardware equivalent circuit of pipe 3 (25% Turbulence)

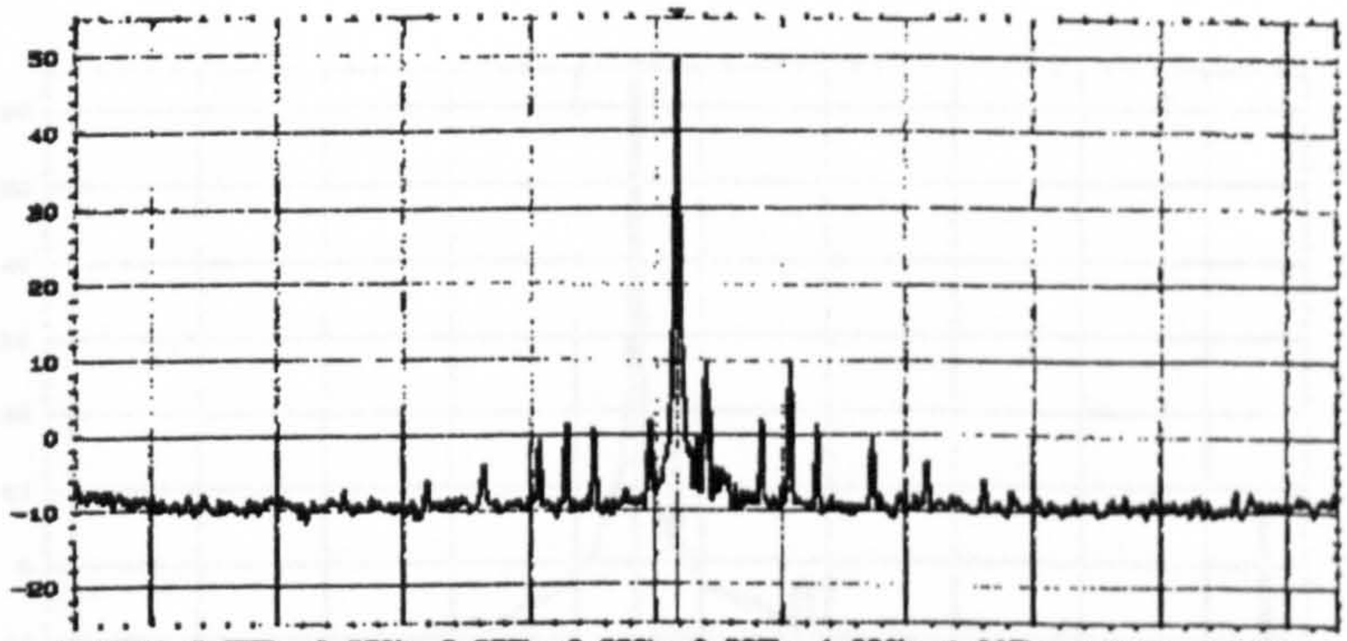

Fig 6.27 Response of hardware equivalent circuit of pipe 3 (50% Turbulence)

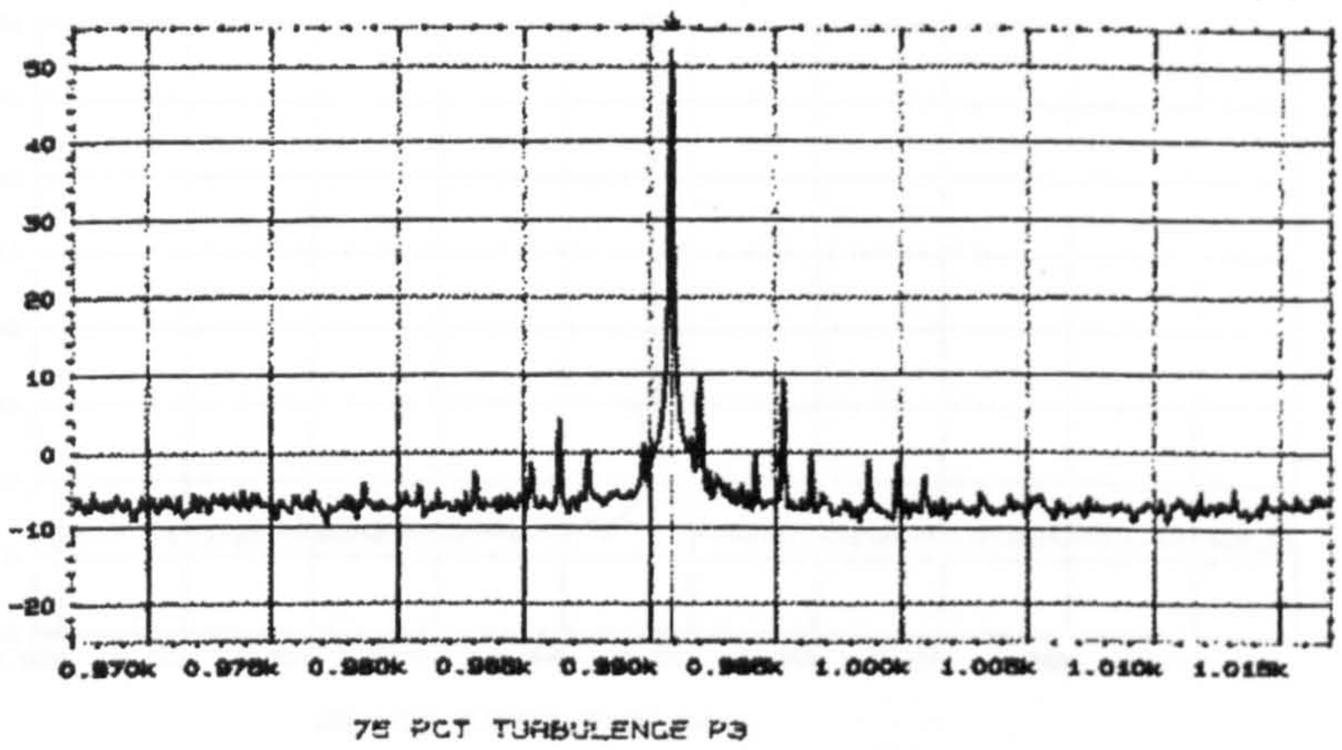

Fig 6.28 Response of hardware equivalent circuit of pipe 3 (75% Turbulence)

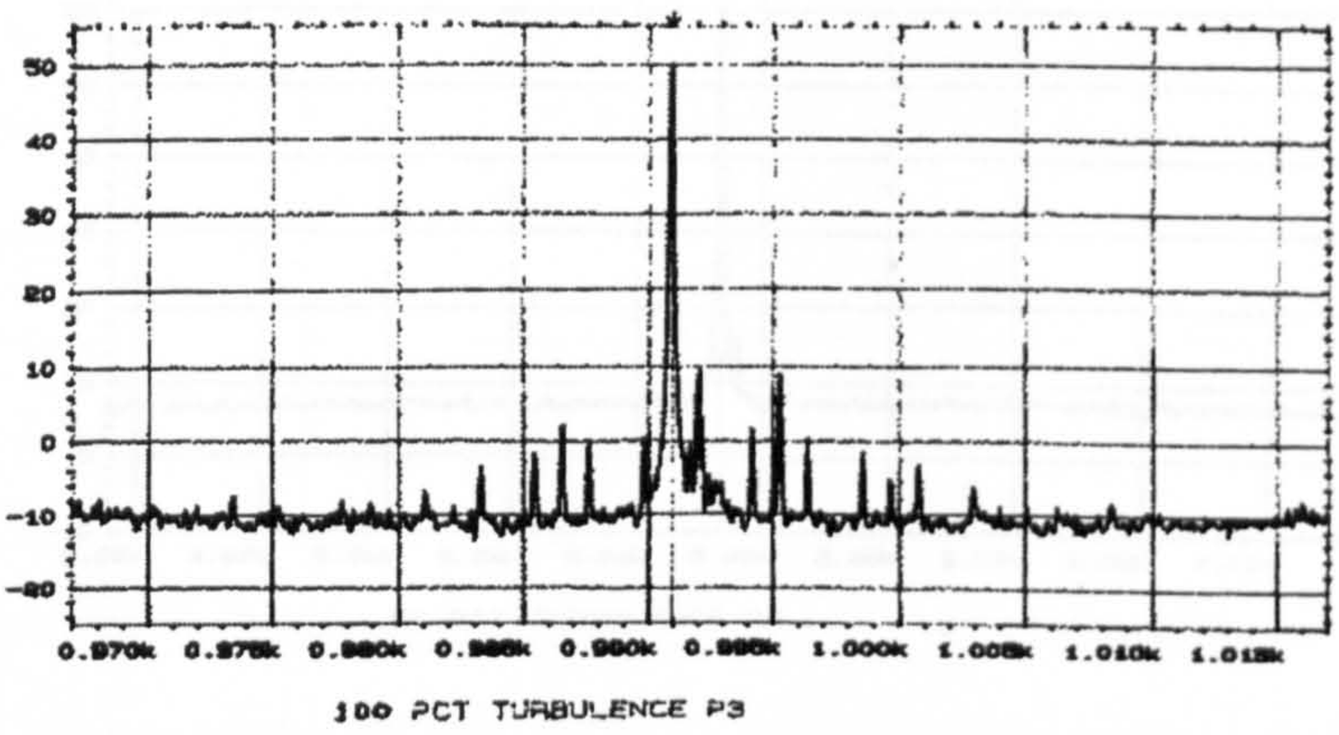

Fig 6.29 Response of hardware equivalent circuit of pipe 3 (100% Turbulence)

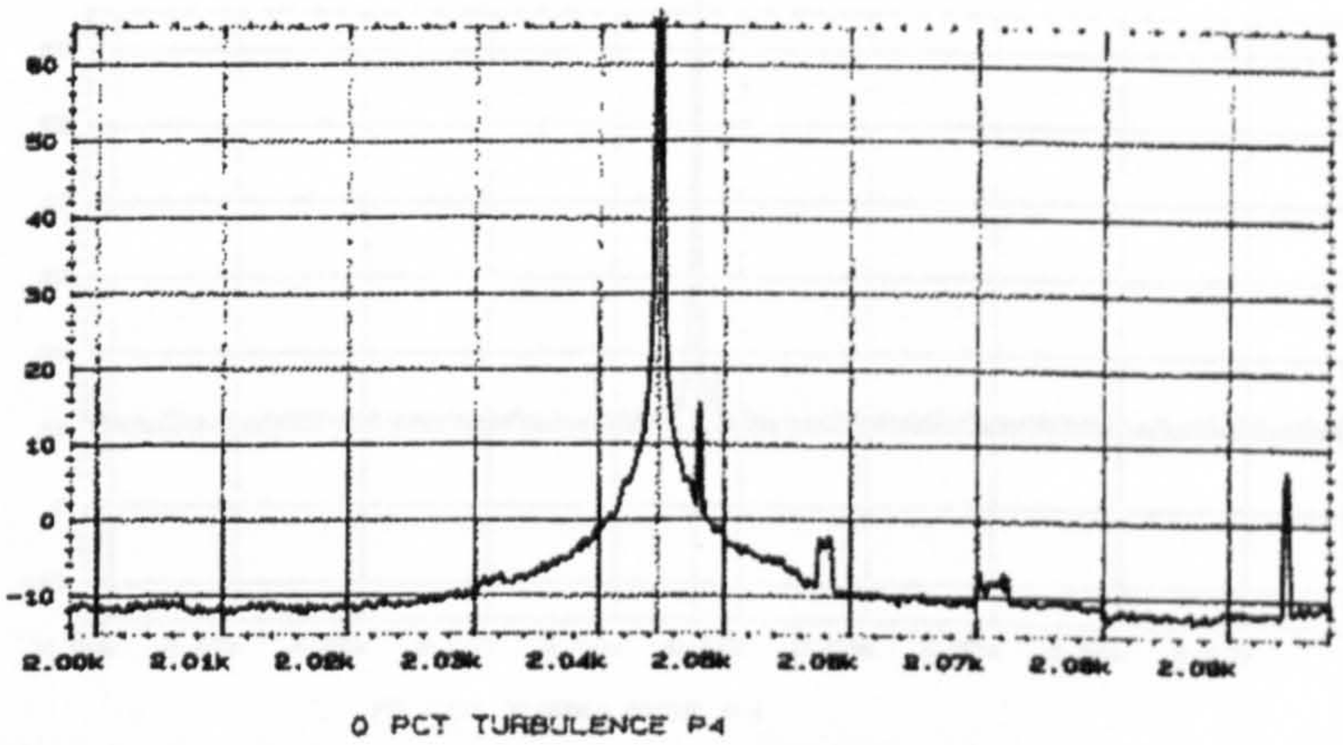

Fig 6.30 Response of hardware equivalent circuit of pipe 4 (0% Turbulence)

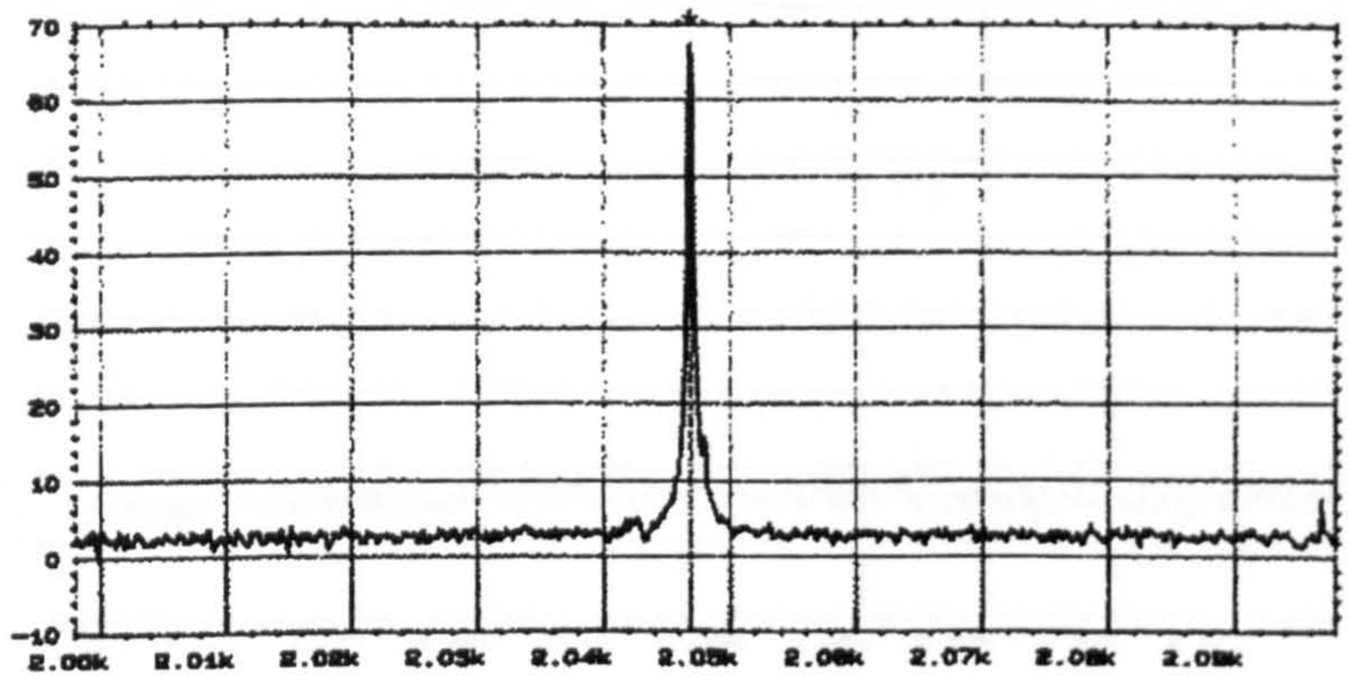

Fig 6.31 Response of hardware equivalent circuit of pipe 4 (25% Turbulence)

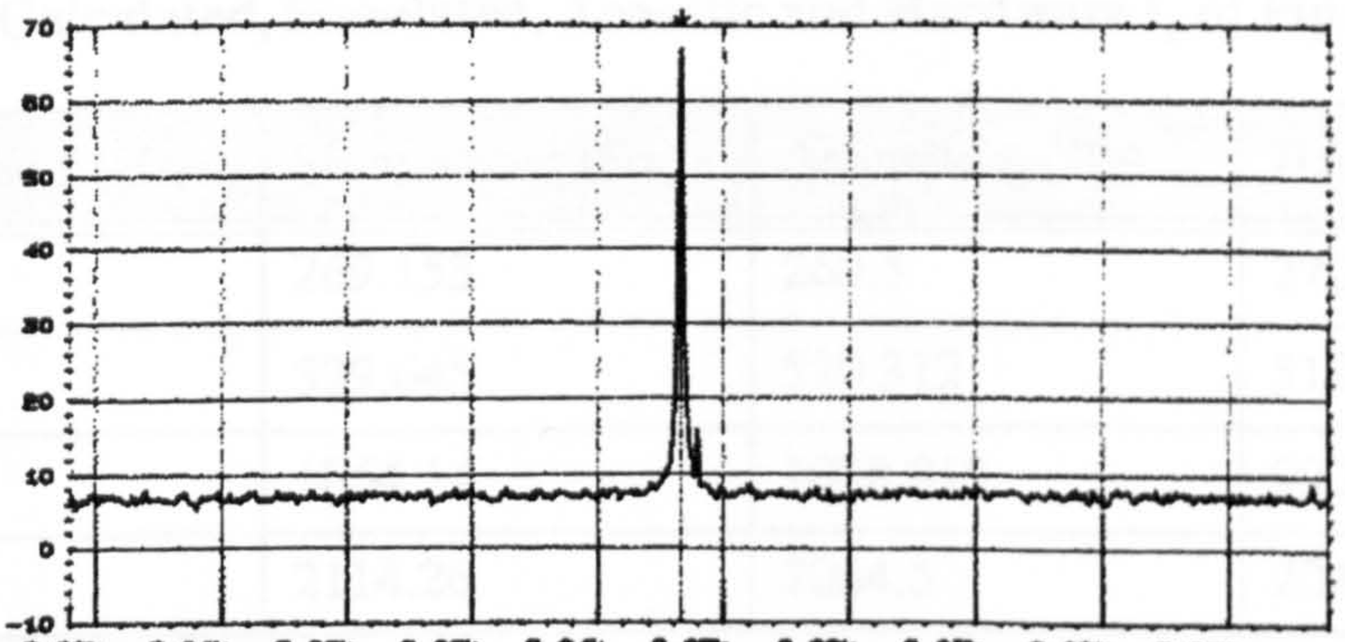

Fig 6.32 Response of hardware equivalent circuit of pipe 4 (50% Turbulence)

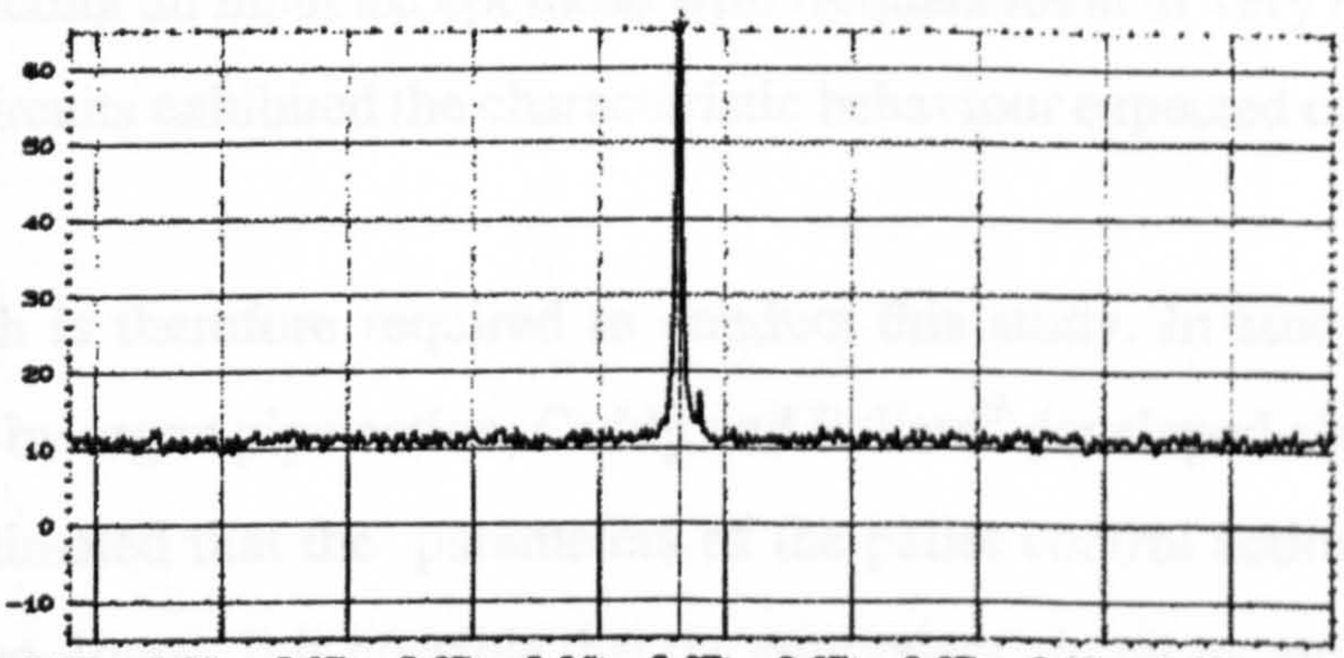

Fig 6.33 Response of hardware equivalent circuit of pipe 4 (75% Turbulence)

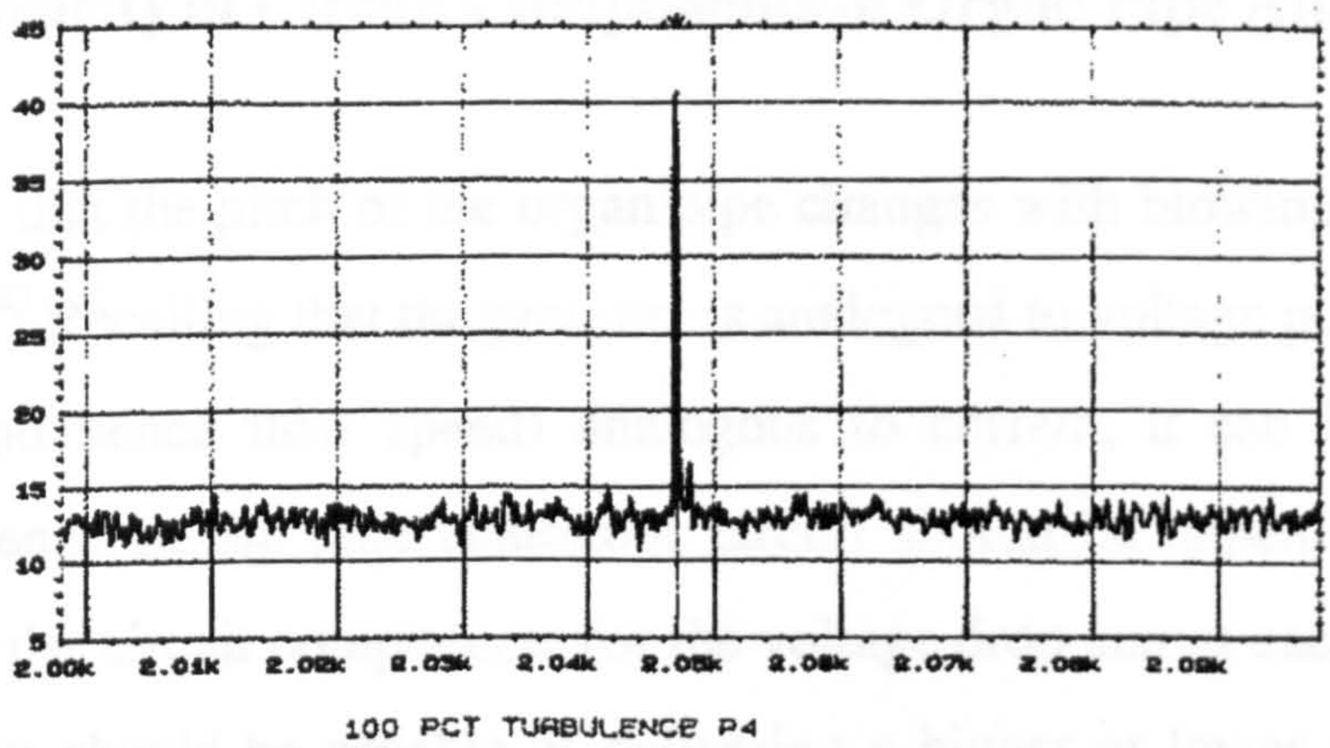

Fig 6.34 Response of hardware equivalent circuit of pipe 4 (100% Turbulence)

Table 20: Calculated, Simulated, Acoustic and Hardware f_r of Pipe Circuits

Pipe	Calculated f_r(Hz)	Simulated f_r (Hz)	Acousitc f_r (Hz)	Hardware f_r (Hz)
1	268.7	269.153	260.5	270.625
2	543.8	529.645	520.312	518.250
3	1109.2	1064.14	1078.812	990.875
4	2177.7	2114.26	2084.5	2044.625

It is observed that the output curve does not change significantly for the different input combinations. A closer examination of the pipe analogous circuits indicates that they are principally passive resonant circuits. At resonance, such circuits behave like narrow band pass filters, neglecting all input except those with frequencies at or very near the resonance point. The pipe circuits exhibited the characteristic behaviour expected of resonant circuits.

Another approach is therefore required to conduct this study. In studying the transient sounds produced by organ pipe action, Caddy and Pollard[9] developed electrical equivalent circuits. They intimated that the parameters of the pallet control action electrical circuit analogue were non- linear. It is possible that the equivalent circuit parameters of the circuit analogue of the pipe also exhibit non-linear characteristics.

6.6.5 Non-linearity of Circuit Components of Organ Pipe Analogous Circuits.

It is well known that the pitch of the organ pipe changes with blowing pressure and flow speed.[12 32 39 40 60] Recalling that the pressure is analogous to voltage potential and volume flow current (and hence flow speed) analogous to current, it can be argued that the resonance frequency of the pipe analogous circuit should be dependent on the current flowing through the circuit components (or the voltage drop across each component). The circuit parameters should be capable of delivering a higher or lower resonant frequency with changing current. This suggests that the circuit parameters should be a function of the current flowing into the circuit. It could be either the function of current or voltages since one is dependent on the other.

Lets re-examine the equivalent pipe circuit developed earlier and illustrated below in figure 6.35.

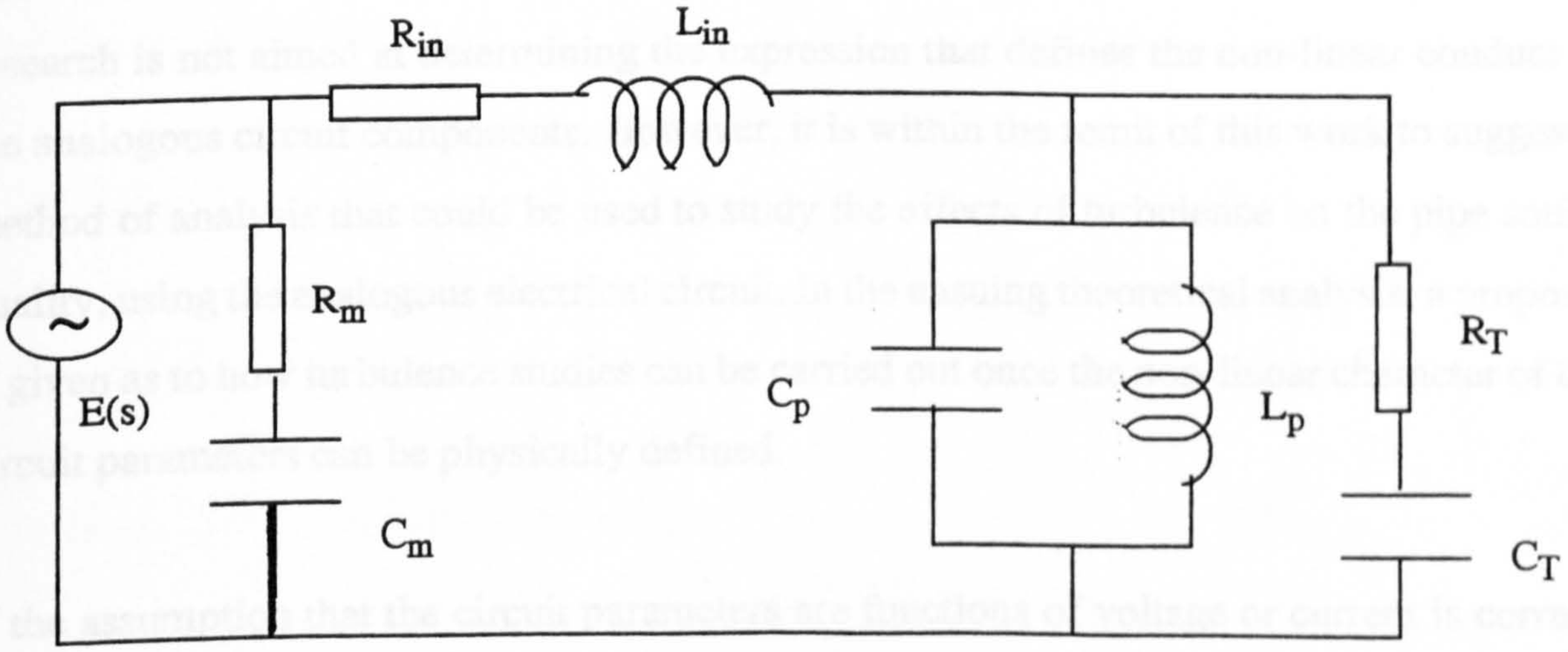

Fig 6.35 :Electrical Equivalent Circuit of Organ Flue Pipe

R_m Mouth resistance; C_m Mouth capacitance; R_{in} Input resistance; L_{in} Input inductance; C_p Pipe capacitance; L_p Pipe inducatance; R_T Termination resistance and C_T Termination capacitance - E(s) is the driving potential

The components can be reduced into impedance blocks such that figure 6.35 can be

redrawn in the manner depicted in figure 6.36.

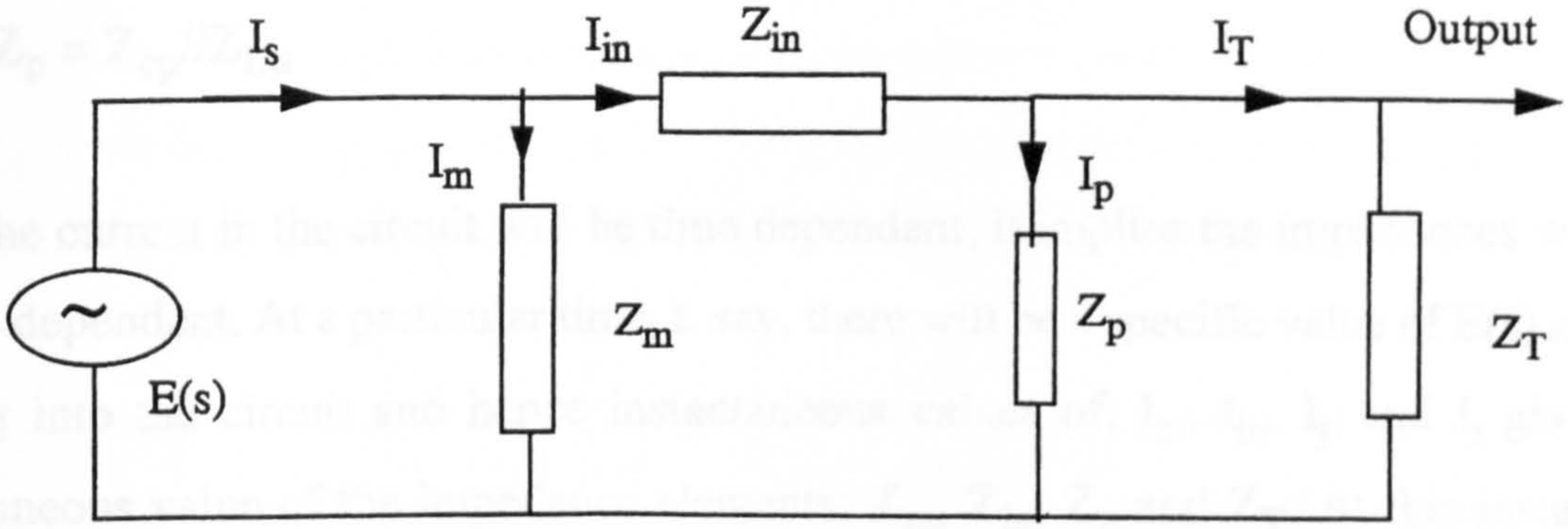

Fig 6.36: Electrical Equivalent Circuit of Organ Pipe in Impedance Blocks

Z_p = reactance due to pipe inductance & capacitance, Z_m = mouth impedance, Z_T = termination impedance and Z_{in} = input impedance - I_s source current, I_{in} pipe input current, I_m mouth current

The exact non-linear behaviour of the different components is not known. The thrust of this research is not aimed at determining the expression that defines the non-linear conduct of the analogous circuit components. However, it is within the remit of this work to suggest a method of analysis that could be used to study the effects of turbulence on the pipe sound quality, using the analogous electrical circuit. In the ensuing theoretical analysis, a proposal is given as to how turbulence studies can be carried out once the non-linear character of the circuit parameters can be physically defined.

If the assumption that the circuit parameters are functions of voltage or current is correct, then the impedances can be expressed as follows:

$$\mathbf{Z_{in} = Z_{in}(I_{in})}$$
$$\mathbf{Z_m = Z_m(I_m)}$$
$$\mathbf{Z_p = Z_p(I_p)}$$

$$Z_t = Z_t(I_t) \qquad 6.38$$

where $Z_p = Z_{cp}//Z_{Lp}$

Since the current in the circuit will be time dependent, it implies the impedances will also be time dependent. At a particular time, t, say, there will be a specific value of E(s) and I(s) flowing into the circuit and hence instantaneous values of, I_m, I_{in}, I_p and I_t giving an instantaneous value of the impedance elements: Z_m, Z_{in}, Z_p and Z_T. At this instant, the overall equivalent impedance, $Z_{eq}(t)$ of the circuit can be computed using the expression:

$$Z_{eq} = (Z_p//Z_t + Z_i)//Z_m \qquad 6.39$$

For any two dummy variables, A & B expressed in the form A//B, it implies:

$$A//B = (1/A + 1/B)^{-1}; \qquad 6.40$$

From the current divider rule;

$$I_{in} = I_s Z_m/(Z_i + Z_m) \qquad 6.41$$

$$I_t = I_i Z_p/(Z_p + Z_T) \qquad 6.42$$

$$I_t = \{Z_p/(Z_p + Z_T)\}\{Z_m/(Z_m + Z_i)\}I_s \qquad 6.43$$

$$E(s) = I_m/Z_m \qquad 6.44$$

Using equations 6.51-6.54, an expression for the system function can be worked out. The system function at a particular instant, t, following Papoulis[71] is given by the expression:

$$I_t/E(s) = I_s/I_m\{Z_p/(Z_p + Z_T)\}\{1/(Z_m + Z_i)\} = h(t) \qquad 6.45$$

The magnitude of h(t) can then be plotted against time, to give the time domain response. The frequency domain response (spectral characterisitic) of the equivalent circuit(s) can be determined by taking the Fourier transform of the time domain response.

If the current into the circuit is a combination of the noise and sinusoidal currents, then the spectral response mentioned above would be the frequency response of the pipe equivalent circuit. By combining different ratios of noise and signal, different flow conditions can be simulated and different frequency response curves obtained that would provide some information on the effects of turbulence on the pipe sound quality.

CHAPTER 7

OTHER APPLICATIONS AND PROPOSALS FOR FURTHER RESEARCH

Some of the developments from this research could be applied in other areas of aero acoustics. Further developments can be added to what has been achieved. The ensuing discussion advances suggestions as to how the foregoing can be attained.

7.1 Other Applications of this Research

The findings of this research are likely to find applications beyond the realms of musical organs.

Research carried out in USA, France, Holland, Germany, Hungary UK and Australia in the different domains of aero-acoustics have borrowed from the hypothesis advanced from investigations into the flow acoustic interaction in organ pipes.

7.1.1 Resonance Effects in Moving Vehicles

In USA Elder[24] has applied some of the theories developed from the studies of the jet drive mechanism of organ pipes[11 18 22] to the understanding of cavity resonance generated by jets in moving vessels in research conducted for the US Navy. Some of his findings involved modelling the jet drive mechanism as an electrical analogous circuits. Perhaps some of the developments in chapter 6, dealing with the electrical analogue of an organ pipe could find application in the research they are conducting.

7.1.2 Studying Pulsations in Gas Plants

Research conducted in Holland has made use of the aero-acoustics mechanism in organ pipes to understand pulsations at T-junctions, closed side branches, stilling chambers and compressor stations at the gas plants of Nederlandse Gasunie (NG). Peters[72 73] also conducted experiments to evaluate flow induced pulsations at safety relief valves which can cause fracture. The research for NG were conducted for flow that had low Mach numbers with high Reynolds numbers. The research was geared mainly to eliminate the resonance, unlike in the organ pipe situation where it is desirable.

As customers to the gas plant switch on and off their gas appliances, the volumetric flow rate of gas through the pipelines will change, changing the Reynolds number of the flow and hence turbulence flow condition. How would these variations affect the pulsations at the compression stations, stilling chambers, valves and junctions? The analysis of the effects of changing levels of turbulence on pipe sound could be adapted for such a study.

Some investigations were carried out to understand the effects of changing flow speeds on the pressure fluctuations. Braggeman,[8] showed there was a shift in pulsation frequency with changing speed. In organ pipes increasing the flow rate of wind into the pipes produces sound of higher pitch. Braggeman's work may need to be extended to take into consideration the effects of various levels of turbulence, at constant flow speeds on these pulsations as well the nature of the deleterious effects they cause.

If gas pipe lines are modeled as electrical circuits (perhaps using transmission line theory) and subsequently analysed, more light could be shed on the nature of the pulsations. The electrical analysis could also provide an alternative method for analysing the problem, theoretically and by simulation.

7.1.3 Other Applications in Organs

In some organs bass pipes are stood off the sound board and wind supply is tubed to them via a small flexible hose, usually less than 3 cm in diameter. In chapter 4, it was shown that one of the methods for suppressing turbulence was by using a helically coiled wind trunk. If the turbulence of the wind into the sound board was attenuated, then channelling wind via a helically wound hose into the organ pipe foothole will suppress any further generation of turbulence in the transit of the air to the pipe.

7.2 Proposals for Further Research

In the development of electrical analogous circuits of the organ pipe, this study did not look into the feedback mechanism around the mouth of the pipe. The analogue of coupling between the mouth and input as well as the pipe outlet and surrounding atmosphere were not incorporated within the circuit. The initial objective was to get an approximate linear model. On achieving this it was realised that a more accurate model of the circuit would require non-linear electrical components. More work will have to be done to develop a non-linear analogue circuit of the pipe. When this has been achieved, introducing the phenomenon of feedback and coupling encountered in acoustic systems will shed even more light on the behaviour of the organ pipe.

It is possible that organ wind trunks, sound boards and the key chamber can be modelled as electrical circuits, it may not be long before an electrical model of the entire system is developed.

Such techniques could be adapted to model gas pipelines, stilling chambers and compressor stations. In chapter 6, a suggestion is given as to how a non-linear electrical equivalent circuit of the organ pipe, when worked out, could be analysed. It maybe less time consuming, and perhaps even cheaper, to simulate the performance of a pipe via its electrical analogue than by aero-acoustic experiments or Finite Element Analysis.

CHAPTER 8

CONCLUSIONS

This research began by surveying the development of organ blowing mechanisms from human operated blowers through to centrifugal blowers, giving their advantages and disadvantages. Several trips were undertaken to over a dozen different sites to look at the blowing mechanisms used to supply wind to the organs and also observe the sound quality produced.

In order to understand the effects of turbulence on organ sound, the nature of turbulence itself had to be understood. Investigations showed that turbulence had similar statistical characteristics to broad band noise.

Investigating the effects of turbulence on pipe sound quality required the turbulence levels to be varied to see how varying it affects pipe sound. Different techniques for suppressing and or attenuating turbulence were examined. Amongst those considered were: channel enlargement, spanwise axis rotation of the flow channel, helically coiled pipes as well as flow stratification. Of all these techniques only that of flow stratification could attenuate turbulence in flows with Reynolds numbers (Re) exceeding 20000. In organ blowing situations, Reynolds numbers greater than 50000 are usually encountered.

A turbulence attenuator designed for St. Paul's Hall, University of Huddersfield was built and tested and found to have a cut off frequency of 3.8 KHz. The organ pipe sound with and without the turbulence filter installed was evaluated aurally, qualitatively and quantitatively.

❒ Turbulence effects can be represented qualitatively using spectrographs

It was noted there was a shift in resonance frequencies. Ripples in the leading and trailing edges of the spectrum of the different fundamentals were much reduced after turbulence attenuation. Two resonant peaks observed in the $F^{\#}_{43}$ 8 ft Gedackt resolves to one after the pipe was supplied with turbulence attenuated wind.

❒ Turbulence effects are significant and percievable

An aural evaluation of the turbulence attenuator (St. Paul's) also indicates there were significant improvements in the tonal quality of the pipes. Some registers lost their acidity, others had a better blend, while others had a more penetrating tone. Additional experiments on a laboratory test rig corroborated the aural perceptions observed in St. Paul's. It has been established that changing the levels of turbulence of wind flowing into organ pipes, perceivably influences the pipe sound quality. This inference was drawn from an aural evaluation of the sound from pipes on the laboratory test rig blown with wind with a variety of turbulence levels, by a number of music students. With less turbulence the pipes on the test rig were found to produce "more pure ... and clearer sound" which had more "bite". In addition, the notes were considered more stable and smoother. Most of these improvements where thought to be experienced largely with the lower registers.

❒ Turbulence effects can be quantified using the concept of moments

A mathematical technique was developed to quantify the changes in pipe sound with changing effects of turbulence. The concept of statistical moments was used to achieve this. The spectrum of the fundamentals of the different pipes on the test rig were normalized and the third and fourth moments about the fundamental evaluated.

It was found that the spectrum of the pipe fundamentals all have a negative symmetry (i.e. were skewed to the left). The skewness was accentuated with increasing laminar flow. The fourth moment, which measured the "peakedness" of the pipe fundamental, was found to

increase with increasing laminar flow of wind into the organ.

❒ Turbulence causes frequency shifts in the pitch

It was further observed that decreasing turbulence intensity produces a frequency shifted to the right (got sharper) or to the left (got flatter) depending on whether the pipes were nicked or not, respectively. Frequency shifts of about 0.3% were observed. These shifts are perceivable. This behaviour maybe explained only after a detailed analysis of the effects of fluid flow and pressure have on the acoustic propagation of the the whole system.

❒ Organ pipes can be modelled as electrical circuits for turbulence studies

Several other researchers have conducted their studies into the sound generation mechanism of organ pipes by using electrical analogous circuits. They used circuit analogues for studying the effects of pressure fluctuations within the key chamber, feedback mechanism at the pipe mouth, the jet drive mechanism of the pipe resonator and initial transients that occur when the pipe foot hole is first opened. A technique for modeling the pipe circuit as an electrical circuit for turbulence studies was also undertaken.

A circuit model of the flue organ pipe similar to those used on the experimental test rig was developed. The components of the electrical equivalent circuit were calculated from appropriate equations. These equations contain physical properties of air. They are also dependent on the geometric dimensions of the pipe. An electrical simulation of the circuit on HSPICE gave resonant frequencies well below expected/measured values.

The aero-acoustics of organ pipes involves coupling between the pipe mouth and pipe inlet as well as the outlet and atmosphere. The coupling, it was argued, gives rise to a mutual inductance between the pipe mouth and pipe resonant column. The mutual inductance is also dependent on the pipe length. It is inferred that the whole pipe length may not fully be participating in the resonant process. Resonance is most likely taking place within a certain active length, L_a, which is less than the geometric of the pipe, L_e. The sound generated

propagates within the entire geometric length of the pipe, however, only the active length is the radiation source. Through trial and error, an $L_a = L_e/3$ was found to give circuit component values that yielded resonant frequencies closer to the experimental values.

Electronic CAD (ECAD) simulation studies on the pipe circuits for turbulence were successfully carried out to evaluate the resonance frequencies of the circuits. However this technique could not be fully realised because the CAD package, HSPICE, available could not simulate a noise circuit to represent turbulence. Modifications to the wirelisting program generated by the drawing package, POWERVIEW for HSPICE simulation, to include numerical values of noise (turbulence) could not be compiled because the package could not handle tasks of such complexity.

Hardwired circuits of the pipes were built and tested. Various magnitudes of noise signal simulating turbulence and a sinusoid signal voltages tuned to the pipe resonant frequency, were applied to the circuit. The circuits are found to exhibit resonance effects at frequencies similar to those obtained by computer simulation and experimental test rig. However no major changes in spectral characteristics were observed with changing levels of turbulence (noise). The analogous electrical circuits of the different pipes are principally passive resonance circuits. At resonance, such circuits usually behave like narrow band pass filters, transmitting only frequencies at or very near the vicinity of the resonant point. The pipe circuits are most likely to have been exhibiting a similar behaviour. It is likely that a non-linear circuit model of the pipe may exhibit a behaviour similar to the behaviour of the observed organ pipe.

The detailed analysis of a circuit with non-linear components is beyond the scope of this work, however, it appears that such a study may be useful for simulating the effects of turbulence in a general case, including the organ pipe and wind delivery system.

APPENDICES

APPENDIX 1

Some notes on the St Paul's organ

The stop list, details of wind pressures plus some information on the console as well as pipe scaling are outlined below.

Stop List

The stops on the 3 manuals and pedal are as outlined in table 1 below

Table 21: Pipe stops for St Paul's

Manual I	Manual II	Manual III	Pedal
Tremulant	Tremulant	Tremulant	Tremulant
Cromhorne (8)	Trompete (8)	Trompete (8)	Schalmei (4)
Cymbel III ($\frac{1}{2}$)	Trompete (16)	Basson (16)	Trompete (8)
Sesquialtera II ($2\frac{2}{3}$)	Scharf IV (1)	Scharf IV (1)	Posaune (16)
Octave (1)	Mixture IV-VI	Tierce ($1\frac{3}{5}$)	Mixture VI ($2\frac{2}{3}$)
Quinte ($1\frac{1}{3}$)	Gemshorn (2)	Waldflute (2)	Nachthorn (2)
Principal (2)	Spitzflute (4)	Nazard ($2\frac{2}{3}$)	Octave (4)
Rohrflute (4)	Octave (4)	Koppelflute (4)	Rohr Gedackt (8)
Praestant (4)	Rohrflute (8)	Principal (4)	Octave (8)
Gedackt (8)	Principal (8)	Holz Gedackt (8)	Subbass (16)
III - I [a]	Gedacktpommer (16)	Spitzgamba (8)	Principal (16)
Cymbelstern[b]	III - II[a]	Celeste tc (8)	III - Pedal[c]
	I - II[a]		II - Pedal[c]
	II & Pedal Combs.[d]		I - Pedal[c]
	III on Pedal pistons[d]		
	I on Pedal pistons[d]		

a. III-I: III-II: I-II are manual couplers (i.e. when down, manual III plays on manual 1 etc.)
b. A series of small bells hit by hammer
c. III-P: II-P: I-P are manual to pedal couplers (i.e. when drawn, the bottom 32 notes of manual III are coupled to the pedals etc. 1
d. These stops offer methods of controlling the computer based registration system fitted to the organ

Wind Pressure

The design pressure for the manuals and pedals are as follows:
Manual I, 53 mmH_2O; Manual II, 60mmH_2O; Manula III, 63mmH_2O and Pedal, 70mmH_2O

Pipe Scales

The pipe diameter (in mm) for the stops used in the experiment are as given in table 2 below:

Table 22: Some Pipe Scales for St Paul's

Stop	Pitch (ft)	C_1	C_{13}	C_{25}	C_{37}	C_{49}	C_{61}
Gedackt	8	102	65	42	27	17	$G^{\#}_{57}$ gemshorn[a]
Rohrflute	4	70	44	27	16	$G^{\#}_{45}$ gemshorn	-
Principal	2	44	25	15	9	5.6	4

a. Stopped pipes can not be made above G_{56} at 8ft pitch, the corresponsing pipe at 4 ft pitch, $G^{\#}_{57}$ gemshorn is used. A similar rule applies for the C_{49}, Rohrflute

The author was informed by the organ builders that the pipes were scaled using the Rensch System. The a_{22} (4 ft Principal) was set to 440 Hz. This settiing is usally determined by the organ builder on the basis of the specification supplied by the person/organisation commissioning the organ.

The organ builders also indicated that the diameter of the flue pipes, except flutes, were halved not on every octave but on the 17th note. The flutes were halved on the 16th note.

Details of the scales of the other pipes are available in: *The Concert Organ of St Pauls*, Nov 1977; published by the University of Huddersfield

The Organ Console

The organ console is made up of 3 manuals (equivalent to the Keyboard - played by hand), the pedals (equivalent to a keyboard operated with feet) and the stops. Each manual has 61 notes. The notes are the same for each manual. The three manuals are: manual I (choir organ); manual II (great organ) and manula III (swell). The method of indicating notes is as follows:

Manuals:- Compass, $C_1\ C^{\#}_2\ D_3\ D^{\#}_4\ E_5\ F_6\ F^{\#}_7\ G_8\ G^{\#}_9\ A_{10}\ A^{\#}_{11}\ B_{12}\ C_{13}\ ..C_{25}\ ..C_{37}\ ...\ C_{49}\ ...\ C_{61}$
C_1 is bottom C (bass), C_{25} (middle C) and C_{61} top C (treble)

Pedals:- Compass, $C_1\ C^{\#}_2\ D_3\ D^{\#}_4\ E_5\ F_6\ F^{\#}_7\ G_8\ G^{\#}_9\ A_{10}\ A^{\#}_{11}\ B_{12}\ C_{13}\ ...C_{25}\ ...$ G32
C_1 is bottom C_{13} (bass) and G_{32} top G (treble)
Pitches are indicated by stop and note e.g. 4 ft Principal A_{22} is tuned to 440Hz

APPENDIX 2

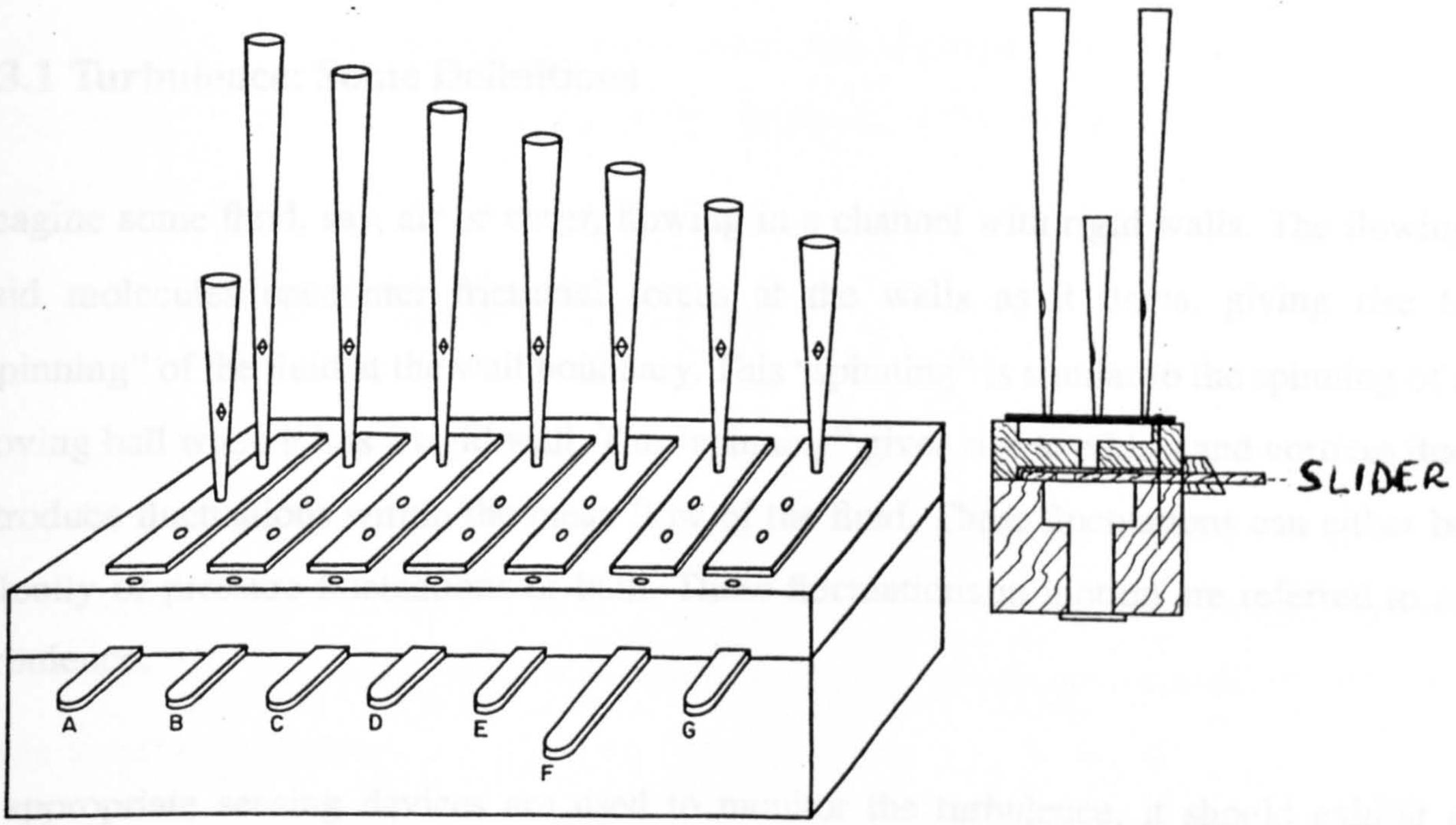

Figure a1: Overall view of sound board

A - G are sliders.
Each slider is marked with a letter appropriate to its position on scale.
When the a stop is pulled it pulls a slider(s). Each slider has holes in it which when the slider is pulled, is aligned with the toe hole of the pipe and allows wind into the pipe foot.
(More details on the soundboard can be found in *The Organ*, by J. Perrot, Oxford University Press, 1971, ch12)

APPENDIX 3

A3 A Theoretical Overview of Turbulence

A3.1 Turbulence: Some Definitions

Imagine some fluid, say, air or water, flowing in a channel with rigid walls. The flowing fluid molecules encounter frictional forces at the walls as it flows, giving rise to "spinning" of the fluid at the wall boundary. This "spinning" is similar to the spinning of a moving ball when it hits a rigid wall. The "spinning" gives rise to eddies and vortices that introduce fluctuations within the mean flow of the fluid. These fluctuations can either be velocity or pressure fluctuations or both. These fluctuations in motion are referred to as turbulence.

If appropriate sensing devices are used to monitor the turbulence, it should exhibit a random amplitude and spread across a broad frequency band.

Bradshaw,[7] has a more complex definition of turbulence. He defines it as: *A three dimensional time-dependent motion in which vortex stretching causes velocity fluctuations to spread to all wavelengths between a minimum determined by viscous forces and a maximum determined by the boundary conditions of the flow. [This is the] state of flow in all fluid motion except those with low Reynolds numbers."*

Defining turbulence in terms of "wavelengths" or wavenumber is a misnomer as this implies that turbulence has a velocity of propagation and can accommodate the sort of analysis that would be used in electromagnetic waves, acoustic waves etc. It is more sensible to consider turbulence fluctuations to be spread across different frequencies within the spectral band of turbulence under study.

Hinze[41] argues that the fundamental characteristics of turbulence in fluids is "irregular motion". These irregular motions are random in space and time;[83] i.e. for a given point in the flow, the instantaneous values of the turbulence motions are not predictable, rendering it difficult to define the function of turbulence motion. Accepting Hinze's arguments to be valid, these fluctuations, could be better understood by using some principles of probability and statistics.

A3.2 The Statistical Nature of Turbulence

The statistical analysis of turbulence, borrows from amongst several, the works of Hinze,[41] Bradshaw,[7] Bendat and Piersol[6] and the Russian Physicists Smol'yakov and Tkachenko.[83] Correlation techniques shall be used in the spectral analysis of the turbulence. The turbulence signal emanating from a turbulence sensor, shall be analysed using spectral techniques.

Measurements on the turbulent nature of the airflow were taken using a hot wire anemometer and spectrum analyser.

A3.2.1 Assumptions made on the statistical nature of turbulence

The measurements taken were analysed exploiting some assumptions based on concepts in Statistics and Probability, namely:

1 That the turbulence signal from the transducer, is a continuous random variable. That is; in the observation of the turbulence signal in the time domain, over a definite or indefinite interval (impractical), the signal continuously has an unpredictable (or indeterminate) value.[83]

2 In the experiments conducted for this work, turbulence measurements were made on the assumption that the flow was homogenous[1]. Smol'yakov and Tkachenko[83]

argue that flow is homogenious along streamlines parallel to the duct wall if the duct has a constant cross-section and is "long enough". The long rectangular ducts used in our experiments ensured these conditions were met. As far as practicable, flow measurements were taken at distances of 20 times the hydraulic (equivalent) diameter, D_e, of the duct down stream.

Where D_e is given by the equation;[21]

$$D_e = (4 \times \text{Area})/\text{Perimeter} \qquad 3.1$$

3 It is further assumed that the turbulence fluctuations are statistically stationary (see illustration of figures a1 & a2). This assumption is only valid if the one dimensional probability density function of the turbulence signal is time independent.

---

1. A note on homogenous fluid flow:

If a plane perpendicular to the duct wall and the flow of a fluid in a duct is taken, and turbulence monitiored at different points within the plane, and it is observed that the turbulence situation is different at each point, then the flow exhibits spatial inhomogenity. In other flow situations, the turbulence at the same point in the plane may vary with time: this varation yields a time inhomgenous situation.

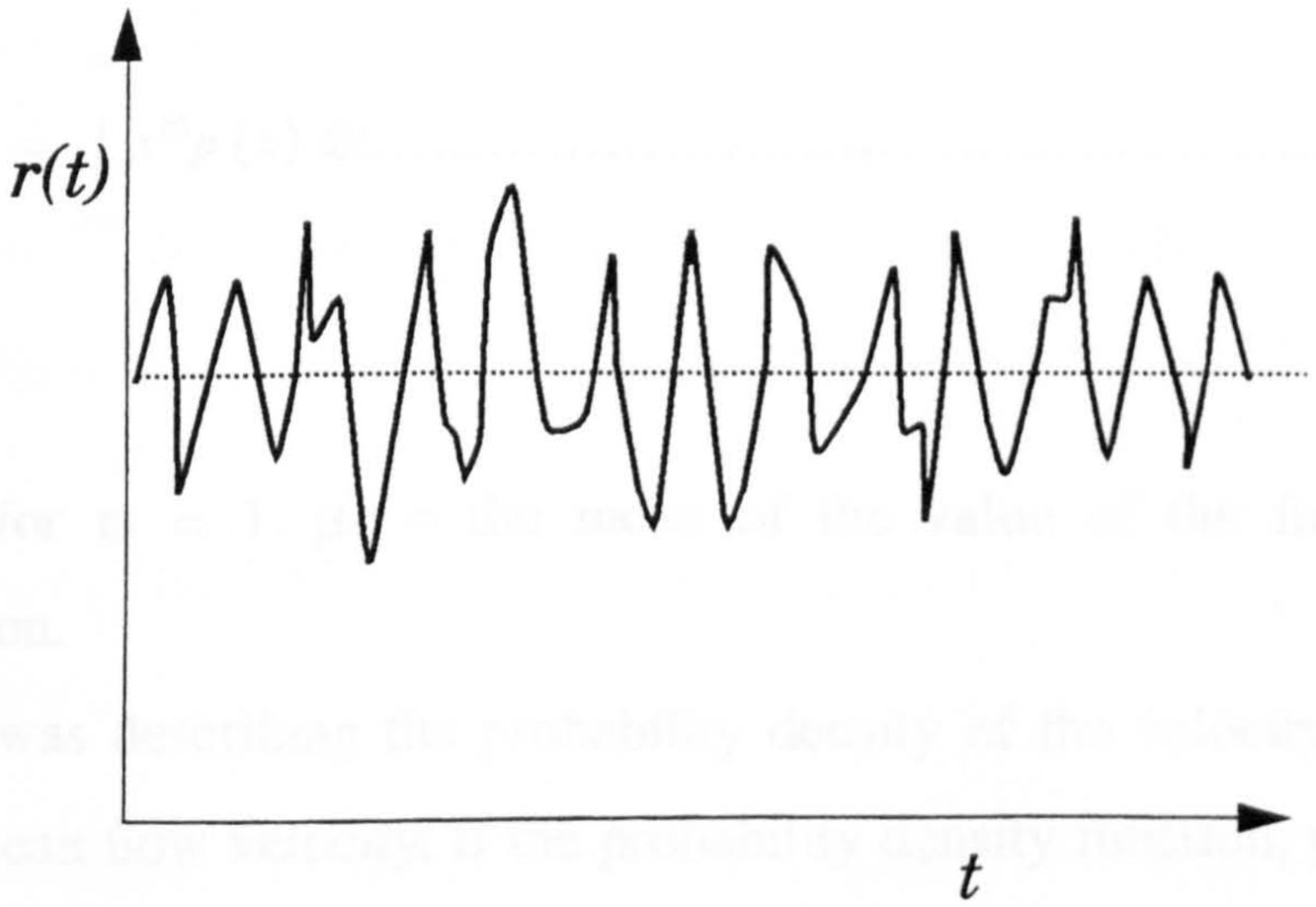

Fig a2 An example of a statistical stationary random signal r(t)

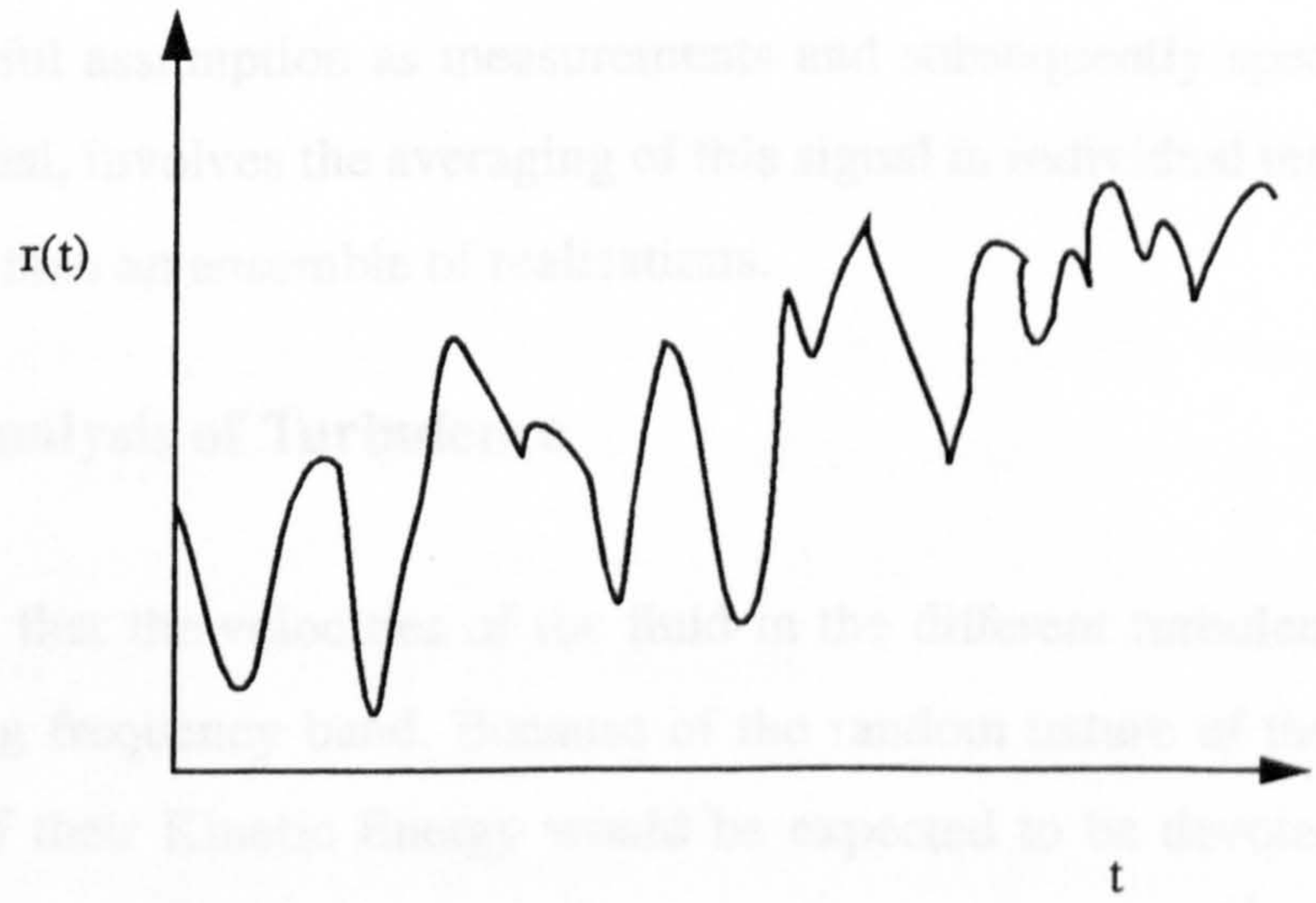

Fig a3 An illustration of a non-stationary random signal $r^1(t)$

The moment, μ_m, of a continous signal [x(t)] is prescribed by the equation:

$$\mu_m = \int_{-\infty}^{\infty} x^m p(x)\, dx \quad \text{.....3.2}$$

such that for m = 1, μ_1 = the mean of the value of the flow characteristic under consideration.

So if p(x) was describing the probability density of the velocity fluctuations, μ_1 would yield the mean flow velocity. If the probability density function, p(x), is not constant, the moment of the signal will not be constant.

4 If in addition to the homogenous and the statistically stationary property, the time and ensemble average of the turbulence fluctuations are assumed to be identical, then the turbulence signal can be described as ergodic.

This is a very useful assumption as measurements and subsequently spectral analysis of the turbulence signal, involves the averaging of this signal in individual realisations over a time period rather than an ensemble of realisations.

A3.3 Spectral Analysis of Turbulence

It can be assumed that the velocities of the fluid in the different turbulent motions have their corresponding frequency band. Because of the random nature of these motions, an average amount of their Kinetic Energy would be expected to be devoted to some very small but finite individual frequency band over a range of frequencies.[41]

It would be unrealistic to say that this energy is concentrated on discrete frequencies because this would imply that turbulence exhibits wave characteristics; a phenomenon earlier discounted.

The spreading or distribution of this average energies over the different frequencies yields

the Energy Spectral Density (also called, the Power Spectral Density or Energy Spectrum or Spectral Density)

The purpose of studying the spectrum of turbulence of the air supplied to organs, is to elucidate the acoustic effects of turbulence rather than its fluid dynamic character.

The spectrum of the turbulence signal was obtained using the B&K dual channel spectrum analyser (model 2340).

A3.3.1 Principles of Correlation Techniques in the Spectral Analysis of Turbulence

The superposition of the vortices and various eddies within the flowing fluid generally induce (turbulence) random motions about the mean flow velocity such that the instantaneous value of the velocity could be written as:

$$U = \overline{U} + u \quad \text{.....3.3}$$

where; $\overline{U}$ = average velocity and u velocity of random fluctuation, with the time average of random fluctuations, $\overline{u}$, = 0 and the average of the absolute value of the turbulence fluctuations, $|\overline{u}|$ = measure of the aggression of the fluctuation:[41] (these should not be confused with u' ($= \sqrt{\overline{u}^2}$), the intensity of turbulence).

If two temporal history records of the turbulence signal are taken from two sensors S_x and S_y providing signals X(t) and Y(t) say, then the procedure for determining the dependence of Y(t) on X(t) or vice versa, for continuous ergodic data, following Bendat and Piersol[6] is via the cross covariance function, C_{yx}, between the signals of S_x and S_y as given in equation 3.4 below.

$$C_{yx}(\tau) = E[\{Y(t) - \mu_y\}\{X(t+\tau) - \mu_x\}] \quad \text{.....3.4}$$

E[] = Expectation of []; μ_x and μ_y = mean values of X(t) and Y(t) respectively

τ = spatial distance in the time domain between sensors.

Following appendix 3B:

$$C_{yx}(\tau) = \lim_{T\to\infty}\frac{1}{T}\int_0^T (\{Y(t) - \mu_y\})\{X(t+\tau) - \mu_x\})\,dt \quad \text{.....3.5}$$

$$\text{.....} = R_{yx}(\tau) + \mu_y\mu_x \quad \text{.....3.6}$$

where;

$$R_{yx} = \lim_{T\to\infty}\frac{1}{T}\int_0^T (Y(t)X(t+\tau))\,d\tau \quad \text{.....3.7}$$

$R_{yx}(\tau)$ = crosscorrelation between Y(t) and X(t)

Using Fourier transform techniques, the cross power spectral density of the continuous and ergodic time history records of the signals Y(t) and X(t) can be determined.[7 41 65 83] This is realised by taking the Fourier Transform of the cross correlation function of these records in the manner prescribed by equation 3.8 below,

$$S_{yx}(f) = \int_{-\infty}^{\infty} R_{yx}(\tau)\, e^{-j2\pi f\tau} d\tau \quad \text{.....3.8}$$

$S_{yx}(f)$ = Cross power spectral density function.

If Y(t) = X(t) i.e. the signals are from the same source then equation 3.8 transforms into:

$$S_{yy}(f) = \int_{-\infty}^{\infty} R_{yy}(\tau)\, e^{-j2\pi f\tau} d\tau \quad \text{.....3.9}$$

Since $R_{yy}(\tau)$ is an even function;

i.e. $R_{yy}(-\tau) = R_{yy}(\tau) \Rightarrow$ $S_{yy}(f)$ is also an even function.

In this situation, $S_{yy}(f) \equiv$ Auto power spectral density function or Autospectrum.

In practice, signal analysis is mainly concerned with the positive frequencies, hence if this practical understanding were applied to the equation 3.9; only evaluations from zero to ∞ would be considered which after a few arithmetic manipulations would yield the one-sided auto power spectral density function, $G_{yy}(f)$, where;

$$G_{yy}(f) = 2S_{yy}(f) = 2\int_{-\infty}^{\infty} R_{yy}(\tau)\, e^{-j2\pi f\tau} d\tau \quad \text{.....} \forall (f \geq 0) \text{ .....3.10}$$

$$= 0 \qquad \forall\, (f < 0)$$

i.e.

$$G_{yy}(f) = 2S_{yy}(f) = 2\int_{-\infty}^{\infty} R_{yy}(\tau)\, \{\cos(2\pi f\tau) + j\sin(2\pi f\tau)\}\, d\tau \quad \text{.....3.11}$$

$$\forall\, f \geq 0$$

$$= 0 \quad \forall\, f < 0$$

Knowing that $R_{yy}(\tau) = R_{yy}(-\tau)$ it implies that the one-sided autospectrum can be extracted from the real part of the Fourier transform in equation 3.11, such that:

$$G_{yy}(f) = 4\int_{0}^{\infty} R_{yy}(\tau)\cos(2\pi f\tau)\, d\tau \quad \text{.....3.12}$$

that is: the one-sided power spectral density function (or one-sided autospectrum, when S_y

$= S_x$) of the turbulence signal emanating from the turbulence sensor can be obtained by taking the real component of the positive frequencies of the Fourier transform of the cross correlation (or autocorrelation) of the signal.

Given the random nature of the turbulence fluctuations, its time domain signal is expected to be similar to broadband noise. The autospectrum should reveal the frequency span of the turbulence signal.

The size of the eddies inducing the turbulence depends on the duct size and the character of the vortices; the latter resulting in a decrease in the size of the eddies with increase in wind speed.[41] These in turn are expected to influence the frequency span of the turbulence signal.

APPENDIX 3B

A-3.4 Derivation of the Covariance for two Random Continuous Data

Given a random variable, Y(t), with μ_y and σ_y^2 as its mean and variance respectively and with a probability density p(y): if (like a turbulence signal) the random variable, Y, is a Continuous function f(Y) $\forall$ real Y, then the *mathematical expectation* of f(Y) is given by the equation:

$$E[f(Y)] = \int_{-\infty}^{\infty} f(Y)\,p(y)\,dy \qquad \ldots\ldots a1$$

Let $f(Y) = Y^m \; \forall \; m \in \{I^+ > 0\}$; equation a1 will become

$$E[(Y^m)] = \mu_{y,m} = \int_{-\infty}^{\infty} Y^m p(y)\,dy \qquad \ldots\ldots a2$$

$E(Y^m)$ is known as the m^{th} moment of f(Y)

when m = 0; (i.e. 0 th moment) $\mu_{y,0} = 1$

m = 1; (i.e. 1st moment) $\mu_{y,1} = \mu_y$

m = 2; (i.e. 2nd moment) $\mu_{y,2} = \Psi^2$ (the mean sq. value of y(t))

If f(Y) is substituted by $(Y-\mu_y)^n$ instead, then;

$$E[(Y-\mu_y)^n] = \int_{-\infty}^{\infty} (Y-\mu_y)^n p(y)\,dy \qquad \ldots\ldots a3$$

$E[(Y-\mu_y)^n]$ is known as the nth central moment of f(Y)

[Note: when n=2; eqn. a3 yields, σ, the variance i.e. the 2nd central moment]

If f(Y) is continuous and ergodic data in the time domain, and captured over a time frame, T,

then the 2nd central moment from equation a3 can be re-written as:

$$E\left[(y(t)-\mu_y)^2\right] = \lim_{T\to\infty}\frac{1}{T}\int_0^T (y(t)-\mu_y)^2 dt \quad \ldots\ldots a4$$

Consider two ergodic and continuous data y(t) and x(t) with a time delay of, τ, between them. If in addition we wish to determine the linear relationship between them, this can be obtained by evaluating the cross covariance, $C_{yx}(\tau)$, of these datum via equation a5 below:

$$C_{yx}(\tau) = E[\{y(t) - \mu_y\}\{x(t+\tau) - \mu_x\}] \quad \ldots\ldots a5$$

substituting eqn. a5 into eqn. a4, yields eqn. a6, below

$$C_{yx}(\tau) = \lim_{T\to\infty}\frac{1}{T}\int_0^T \{y(t)-\mu_y\}\ \{x(t+\tau)-\mu_x\}\, dt \quad \ldots\ldots a6$$

$$= \lim_{T\to\infty}\frac{1}{T}\int_0^T y(t)\,x(t+\tau)\,dt - \lim_{T\to\infty}\frac{1}{T}\int_0^T \mu_y y(t)\,dt - \lim_{T\to\infty}\frac{1}{T}\int_0^T \mu_x x(t+\tau)\,dt + \lim_{T\to\infty}\frac{1}{T}\int_0^T \mu_y\mu_x dt$$

$$\text{I} \qquad \text{II} \qquad \text{III} \qquad \text{IV} \quad \ldots a7$$

Expression: $\text{I} \equiv R_{yx}(\tau)$

II = III = 0: y(t) & x(t+τ) are Continuous random variables, while μ is constant; the time average of such variables always yield zero.[6]

$$\text{IV} = \lim_{T\to\infty}\frac{1}{T}\left[\mu_y\mu_x t\right]_0^T = \mu_y\mu_x$$

$$\Rightarrow \quad C_{yx} = R_{yx} + \mu_y\mu_x$$

APPENDIX 4

A-4 Calculations for the Turbulence Suppressor Built for St. Paul's

Given that honeycomb dimensions of suppressor are: (ID) 2.4 mm x 3.5 mm and an OD of 2.8 mm x 3.7 mm, the blockage ratio of the honeycomb, β, = (3.5x2.4)/(3.7x2.8) = 0.8108.

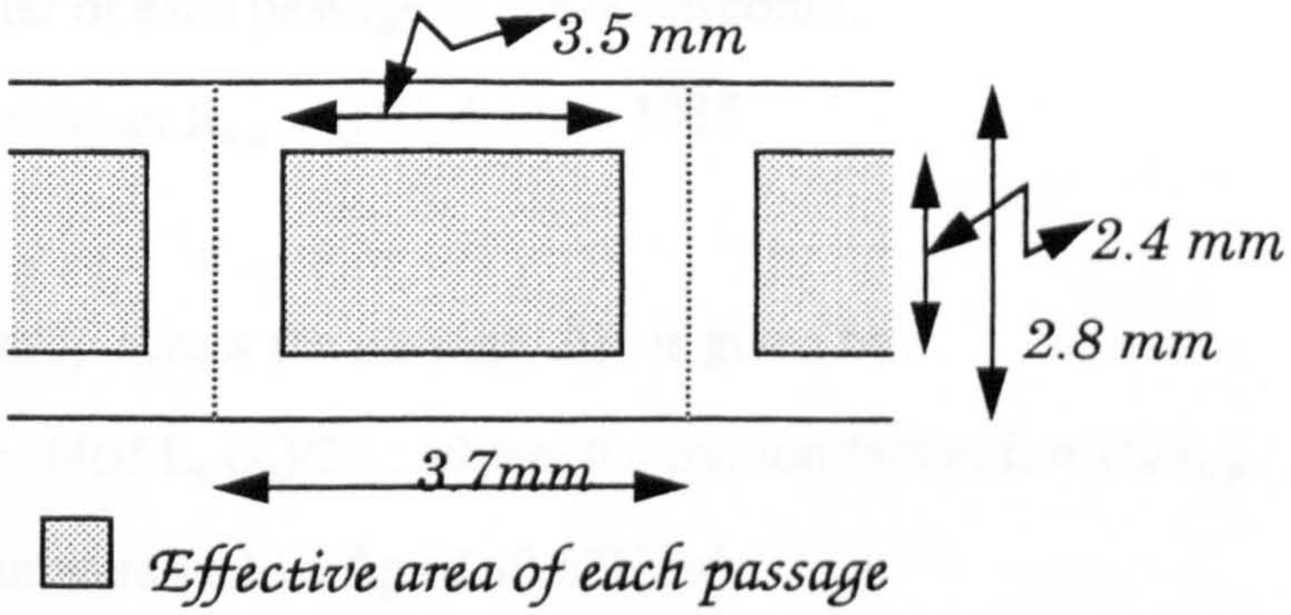

Fig. a 4; Dissection of Suppressor Passage.

Determination of R_e before honeycomb passage:

Given duct dimensions (of St. Paul's) of 419 mm by 146 mm;

and maximum flow rate, Q, of centrifugal blower of 1200 cubic ft./min. (i.e. = 0.5663 m^3/s)

$\Rightarrow$ Mean flow velocity, U, of Q/A (= 9.258 m/s) and a Hydraulic Diameter;

$D_e = 4A/P$ of 0.2165; where P = perimeter of duct and A = Area of duct.

Assuming viscosity, μ, and density of air, ρ, to be 1.8 x 10^{-5} Ns/m^2 and 1.2 Kg/m^3 respectively, **R_e {= $(UD_e\rho)/\mu$} evaluates to 133723** (>> 2300, the laminar to turbulent transition R_e)

Determination of $R_{e,p}$ within honeycomb passage

Dimensions of honeycomb = 100 mm x 419 mm x 292 mm.

Effective area of honeycomb, A_e, = β (419x292) mm^2 = 0.0992 m^2.

Mean velocity through passage $U_p = Q/A_e = 5.7087$ m/s

Passage hydraulic diameter, d_e, = $4A_e/P_p$ = 2.85 mm;

where P_p = Perimeter of each passage of the honeycomb.

These parameters yield an $\mathbf{R_{e,p} = (\rho U_p d_e)/\mu = 1085}$

Now, the pressure drop across the passage, Δp, is given by:

$$\Delta p = (4\rho f L_\omega U_p)/2d_e; \text{ where, the friction factor, } f, = 16/R_{e,p},$$

The foregoing parameters yield a Δp of 40.62N/m^2

APPENDIX 5

A-5 Procedure for Checking the Frequecy Response of the Constant Temperature Anemometer(CTA)

The frequency response of the HWA is determined using the experimental set up of figure a-2. A 1 KHz sqaure wave from a signal generator is fed into the bridge input. The output of the CTA is displayed on an oscilloscope. The output should be similar to the simulated trace of figure a-3.

If the Pulse has a width, τ, (for hot films), then the frequency response, $f = \tau^{-1}$

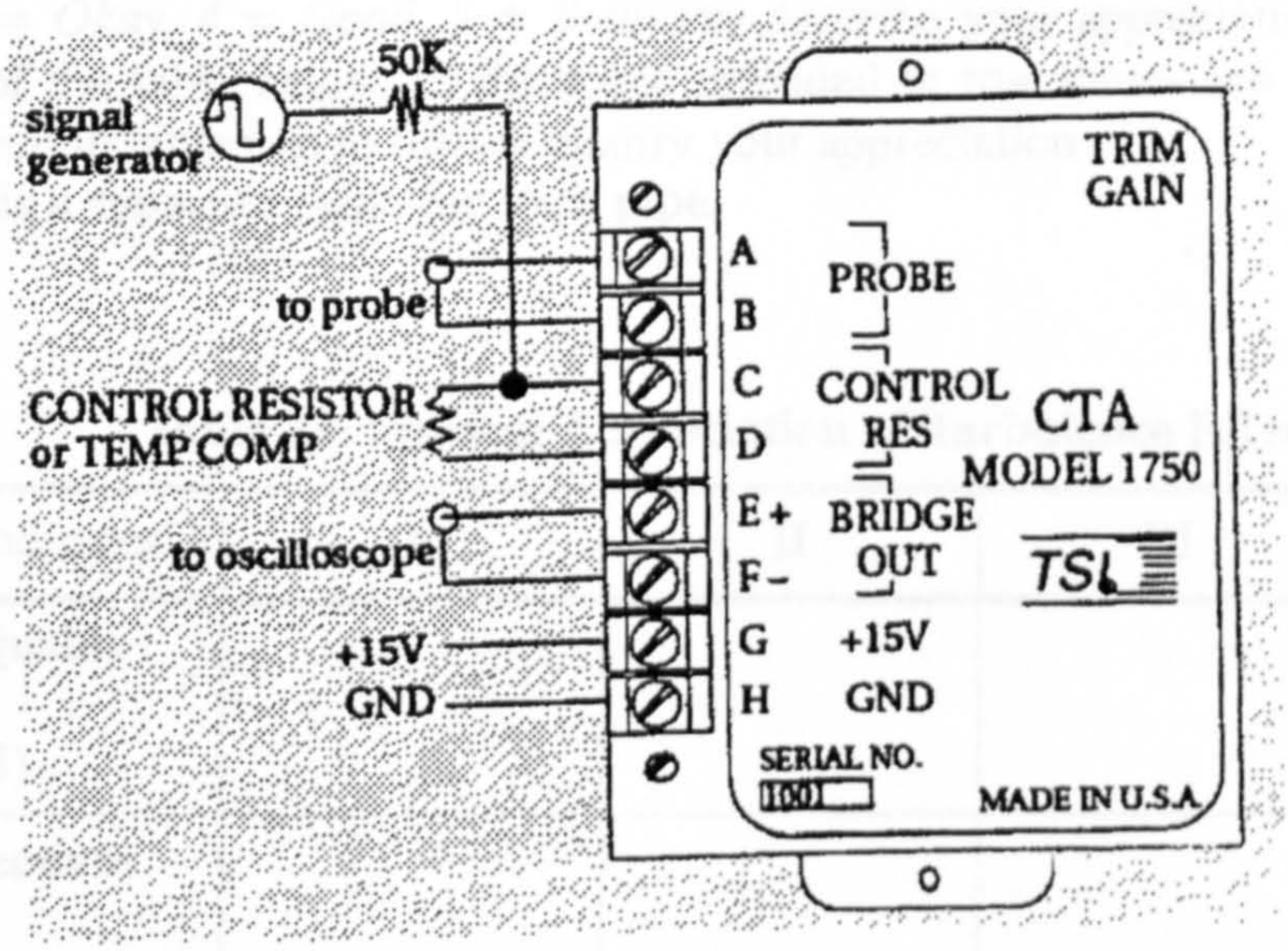

Fig. a5: Setup for measuring CTA frequency response (Scanned from TSI Manual[92])

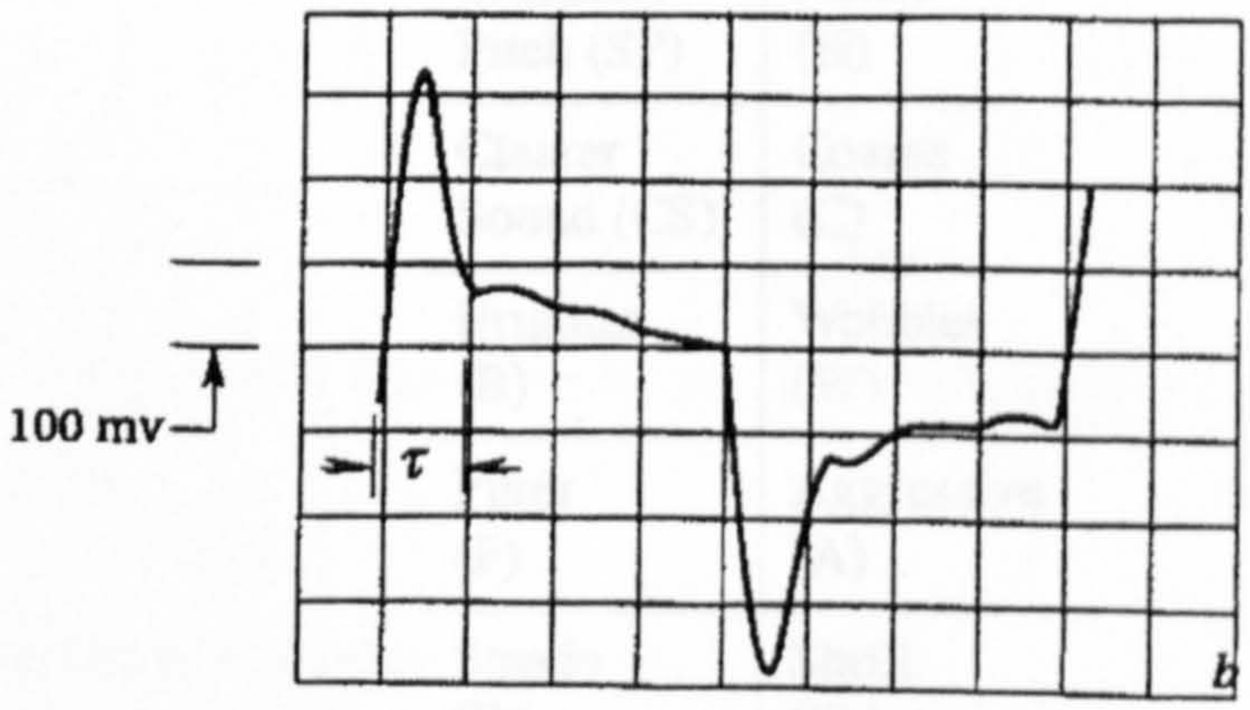

Fig a6: Output trace for probe frequency response test (Scanned from TSI Manual[92])

APPENDIX 6

A-6 Questionaire on Research on the Effects of Turbulence on Organ Pipe Sound.

Year .....

Instrument(s) Studied (i).....(ii).....

GROUP:.....

FOUR pipes will be played under FOUR different conditions. On a Scale of 1 to 5 *(1 = Horrible, 2 = Poor, 3 = Okay, 4 = Good, 5 = Brilliant)* describe your appreciation of each note in the second row of the table below. In the space provided in row three- use words from the list of adjectives given in table two to further qualify your appreciation.
Note: There is a separate table for each pipe.

Pipe 1

Table 23: Musical Appreciation of Turbulence Effects

Flow Conditions	I	II	III	IV
Describe Quality of Sound (Using 1-5)				
Using Adjectives in Table 2				

Table 24: List of Adjectives

Smoother Pitch (SP)	Harsh (H)
Clearer Sound (CS)	Coarse (C)
Brighter (B)	Wobbles (W)
Purer (P)	Aggressive (A)
Steady (St)	Shrill (Sh)

APPENDIX 7

A7.2 On (statistical) moments

A measure of the spread about the mean can be calculated in terms of the 2nd, 3rd and 4th moments. The 2nd moment is the variance of the data. The 3rd moment provides information on the degree of asymmetry relative to the mean. The 4th moment is a measure of the amount of peakedness or physical sharpness of the distribution relative to the mean.

A7.2.1 On the fourth moment

Figure a7.1 is an illustration of curve shapes that describe the variation in the 4th moments. A very flat distribution is platykurtic, a rounded peak is described as mesokurtic, while a sharp peak, leptokurtic

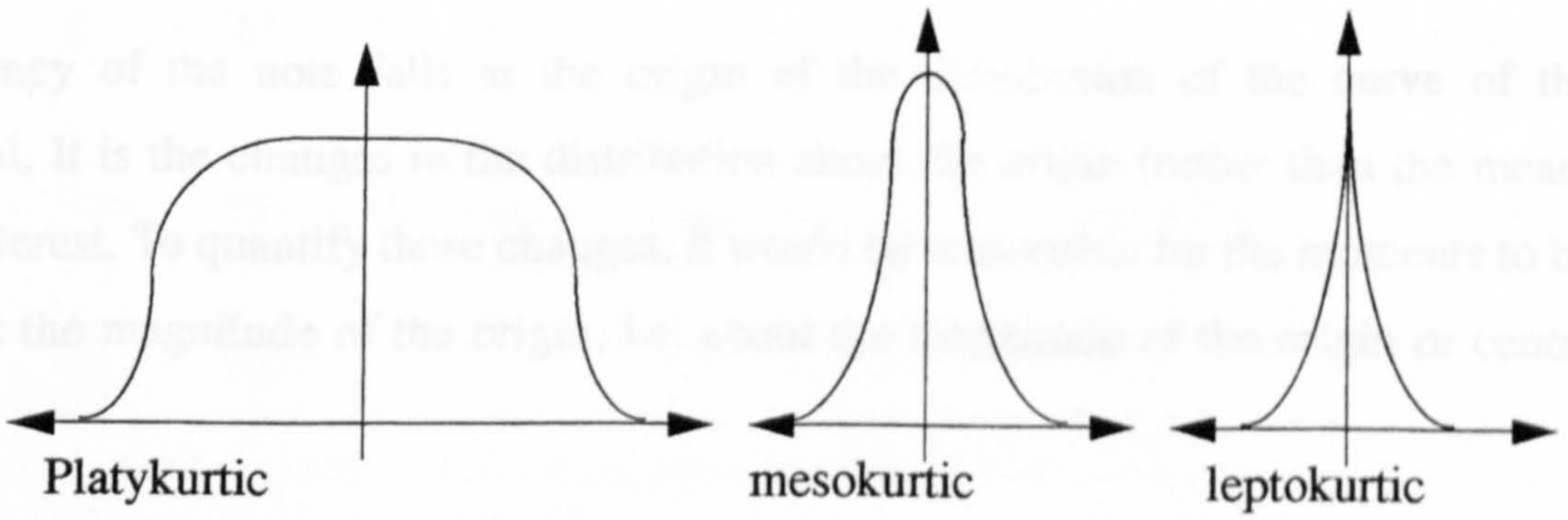

Figure a7.1 Curve shapes for different types of 4th moments.

A7.2.2 On the third moment

When the distribution is not skewed, the 3rd moment is zero.

A distribution can be skewed to the right or left. Skewness to the right (or positive skewness) implies the distribution tails more to the right than left and vice versa for skewness to the left (or negative skewness).

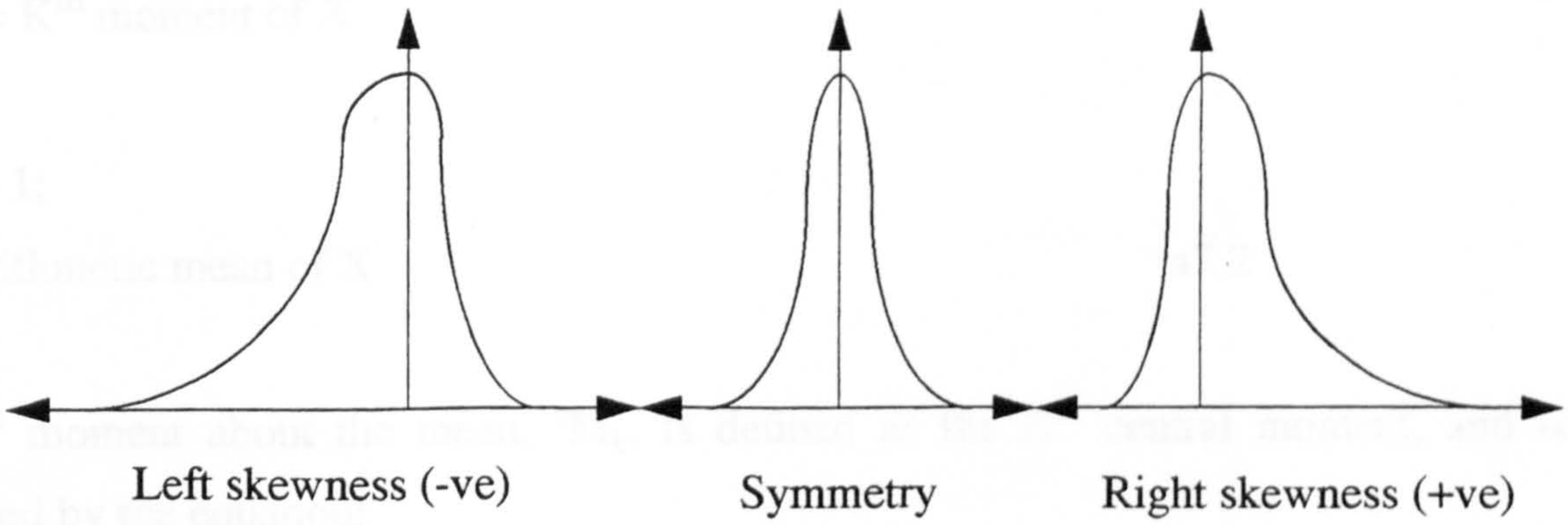

Fig.a7.2 Distributions illustrating types of 3rd moments

When moments relative to the mean are evaluated they are generally referred to as central moments.

The frequency of the note falls at the origin of the distribution of the curve of the fundamental. It is the changes in the distribution about the origin (rather than the mean) that is of interest. To quantify these changes, it would be reasonable for the moments to be taken about the magnitude of the origin, i.e. about the magnitude of the origin or centre frequency.

A7.3 Numerical analysis of pipe fundamentals.

If a variable, X, has N different values; such that $X = X_n$, $\forall$ n = 1, 2, 3 .... N, the K^{th} moment of the variable, X, is given by equation a7.1 below:

$$\overline{X^k} = \frac{\left(\sum_{n=1}^{N} (X_n^k)\right)}{N} \qquad \text{.....a7.1}$$

i.e. $X^k = K^{th}$ moment of X

For K = 1;

$\overline{X}^1$ = Arithmetic mean of X a7.2

The K^{th} moment about the mean, ${}^1M_k$, is defined as the K^{th} central moment, and is prescribed by the equation:

$$ {}^1M_k = \frac{\sum_{n=1}^{N} (X_n - \overline{X})^k}{N} \qquad \text{.....a7.3}$$

When K = 2, ${}^1M_2$ = second central moment or variance about the mean.

K = 3, ${}^1M_3$ = 3rd central moment or degree of asymmetry relative to the mean.

K = 4, ${}^1M_4$ = 4th central moment or degree of peakedness relative to the mean.

If the moments are computed about the magnitude of the origin, ψ say, such that

$$M_k = \frac{\sum_{n=1}^{N} (X_n - \psi)^k}{N} \qquad \text{.....a7.4}$$

M_k becomes the k^{th} moment about ψ.

If X_n and ψ are not dimensionless, the dimensionless form of M_3 and M_4 would have to be determined in a manner given in equations a7.5 and a7.6, to yield, the moment coefficient of skewness, M_{cs}, and the moment coefficient of kurtosis, M_{ck}, respectively; where:

$$M_{cs} = \frac{M_3}{M_2^{1.5}} \quad \text{.....a7.5}$$

$$M_{ck} = \frac{M_4}{M_2^2} \quad \text{.....a7.6}$$

If the shape(distribution) of the fundamental changes about the centre frequency is to be studied, then, it would be proper to take moments about the centre frequency -in other words, compute M_k (equation a7.4).

A7.4 Application of principles of moments to evaluation of experimental data

Notes that were to be analysed were played back into the spectrum analyser, and their power spectral density taken. The fundamental was zoomed into at ±50Hz about the central frequency. The cursor of the spectrum analyser was used to sample the readings of the magnitude of the curve at frequencies ±10Hz about the fundamental.

The change in the data within ±1Hz of the centre frequency was more drastic, hence samples within this range were taken in steps of 0.125Hz or 0.0625Hz; then 0.25Hz, 0.5Hz, later progressing to steps of 1Hz on either side of the centre frequency. An example

of the sampled data, with the precise points of measurement for the different notes analysed is presented in appendix 8.

The peak magnitude of the fundamental varied from note to note. This varied for the same note under different blowing conditions. Though the microphone was held in the same position under laboratory conditions, all the measurements were not conducted on the same day.

In circumstances where the recordings where taken inside the organ of St. Paul's, it was difficult to maintain the position of the microphone as recordings where done on different days - in addition, the microphone position had to be adjusted frequently to obtain a high recording level on the DAT recorder.

In order to ascertain some level of uniformity in the data before analysis, the sampled spectrum was normalised. The illustration below describes the approach used.

Assume a note had a central (fundamental) frequency, f_c Hz, say, and the shape given in the example of figure a7.3 below.

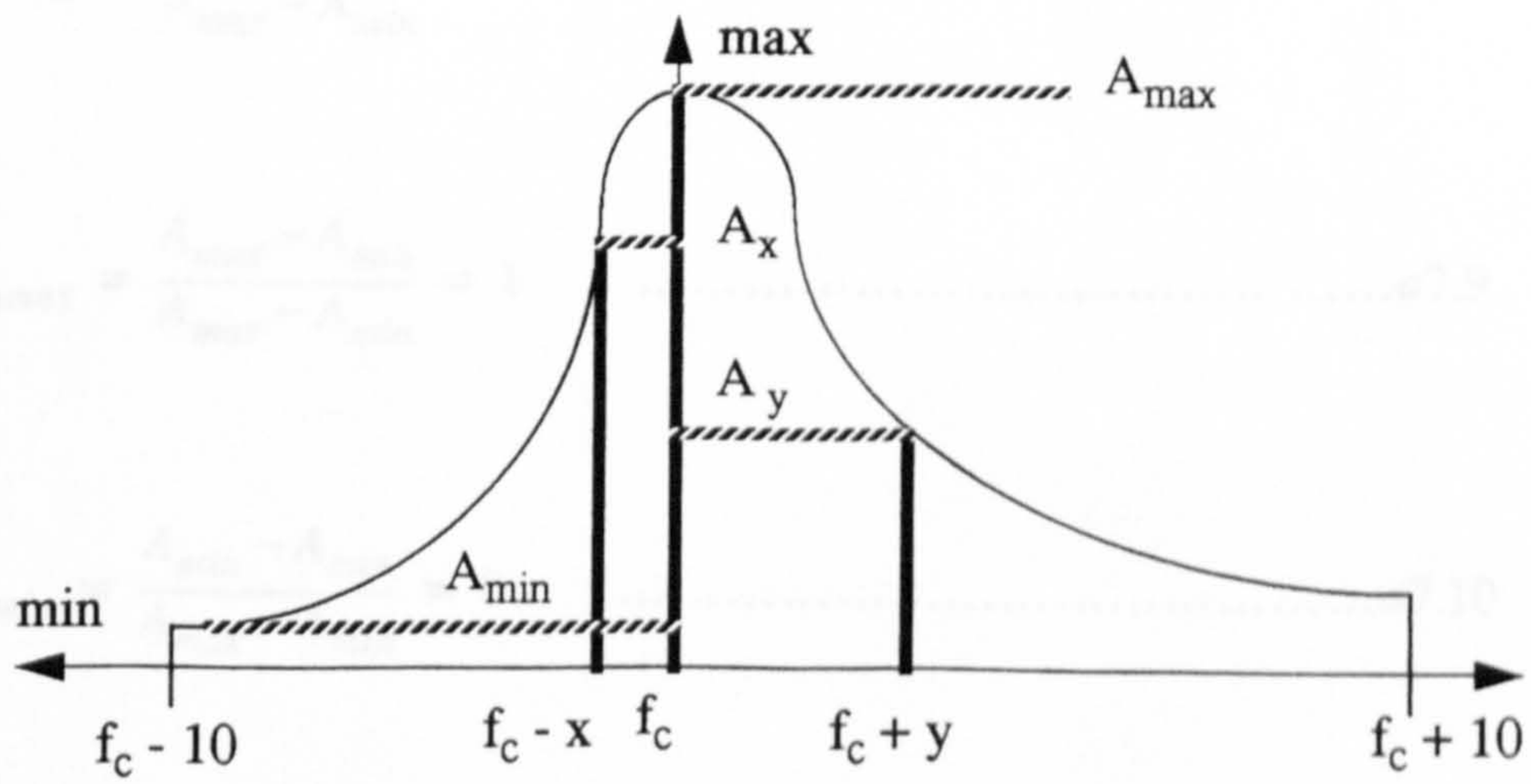

Fig a7.3 Sampling of frequency data for analysis

The cursor was moved say to f_c - x Hz and its amplitude, A_x was read, through to f_c-10 Hz. Similarly the amplitude of f_c Hz, A_{max}; f_c + y Hz, A_y; etc. were taken till the frequency range, $f_c \pm 10$ Hz was covered.

A_{max} varied for different notes. To get the same frame of reference for comparison, the data was normalised; such that $A_{max} = 1$ and $A_{min} = 0$ for all the data evaluated.
To transform a data point A_p, to its normalised value A_{np}, the following expression was used.

$$A_{np} = \frac{A_p - A_{min}}{A_{max} - A_{min}} \quad \text{.....a7.7}$$

Examples

$$A_{nx} = \frac{A_x - A_{min}}{A_{max} - A_{min}} \quad \text{.....a7.8}$$

$$A_{nmax} = \frac{A_{max} - A_{min}}{A_{max} - A_{min}} = 1 \quad \text{.....a7.9}$$

$$A_{nmin} = \frac{A_{min} - A_{min}}{A_{max} - A_{min}} = 0 \quad \text{.....a7.10}$$

$\Longrightarrow A_{nj}\ \forall\ j$ are now dimensionless entities.

It was earlier discussed that the moments are to be taken about the centre frequency, f_c. Since the magnitude of f_c for the normalised curve is one for all notes, it implies the k^{th} moment about the magnitude of f_c would be equivalent to the k^{th} moment about unity; from equation a7.5. This transforms equation a7.4 to equation a7.11 below

$$M_k = \frac{\left(\sum_{n=1}^{N} (X_n - 1)^k\right)}{N} \quad \text{.....a7.11}$$

As such, when k = 4, it can be reasonably assumed that we have a measure of the physical sharpness of the fundamental. For k = 3, equation a7.11 computes the skewness of the data.

A comparative examination of M_4 and M_3 about the fundamental frequency under different turbulence conditions would therefore provide some information on how turbulence affects the shape of the notes and therefore tonal quality.

APPENDIX 8a

A-8a Flow chart of MINITAB programme used to calculate moments

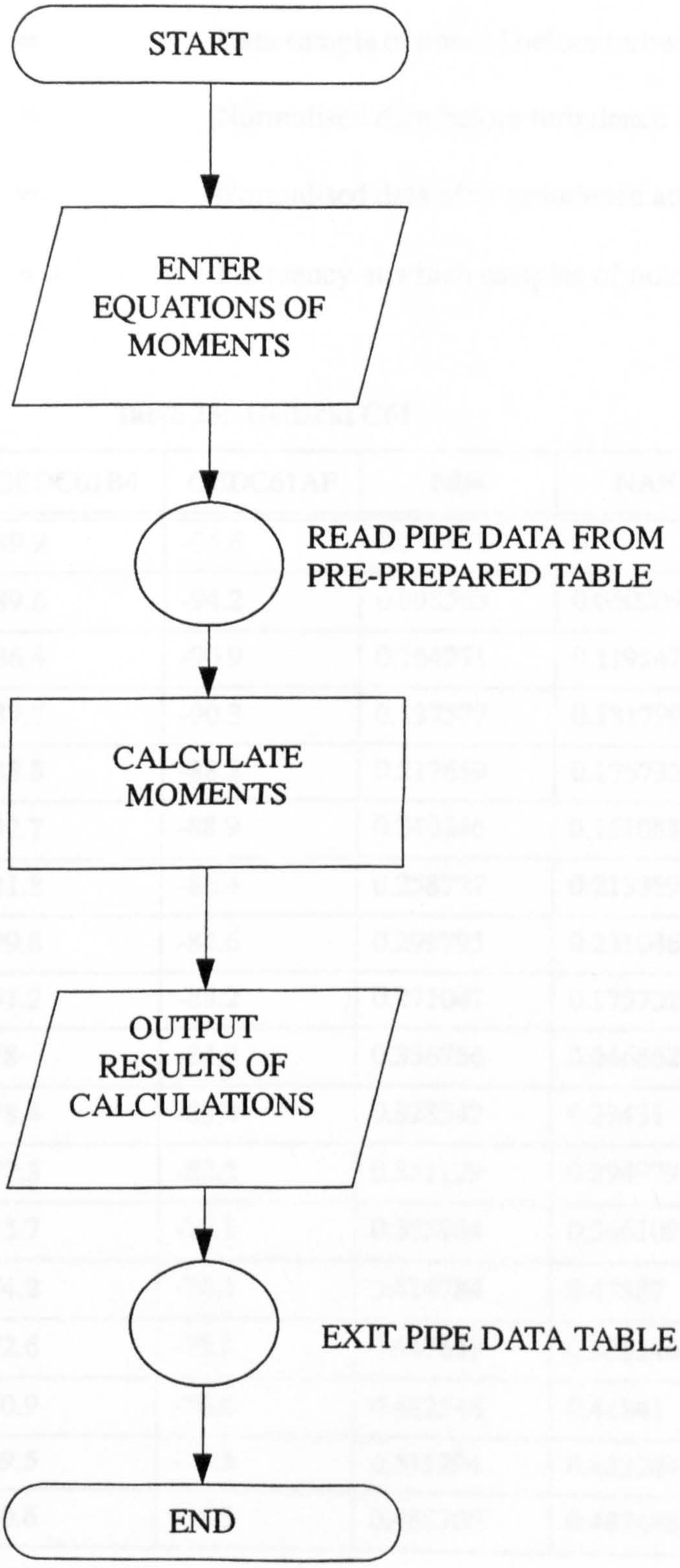

APPENDIX 8b

A-8b Sampled Data from St Paul's (an example)

Generally: [ ]B4 = Data sample of note [ ] before turbulence attenuation.

NB4 = Normalised data before turbulence attenuation

NAFT = Normalised data after turbulence attenuation

FREQ[*note*] = Frequency at which samples of note were taken

Table 25: Gedackt C61

FREQC61	GEDC61B4	GEDC61AF	NB4	NAFT
-10	-89.9	-96.6	0.092402	0
-9	-89.6	-94.2	0.098563	0.050209
-8	-86.4	-90.9	0.164271	0.119247
-7	-87.7	-90.3	0.137577	0.131799
-6.5	-83.8	-88.2	0.217659	0.175732
-6	-82.7	-88.9	0.240246	0.161088
-5.5	-81.8	-86.4	0.258727	0.213389
-5	-79.8	-84.6	0.299795	0.251046
-4.5	-81.2	-88.2	0.271047	0.175732
-4	-78	-84.8	0.336756	0.246862
-3.5	-78.4	-85.4	0.328542	0.23431
-3	-77.3	-82.5	0.351129	0.294979
-2.5	-75.7	-79.1	0.383984	0.366109
-2.25	-74.2	-76.1	0.414784	0.42887
-2	-72.6	-75.8	0.447639	0.435146
-1.875	-70.9	-76.6	0.482546	0.41841
-1.75	-69.5	-73.5	0.511294	0.483264
-1.5	-70.6	-73.3	0.488706	0.487448

Table 25: Gedackt C61

FREQC61	GEDC61B4	GEDC61AF	NB4	NAFT
-1.375	-69.1	-72.3	0.519507	0.508368
-1.25	-67.7	-70.2	0.548255	0.552301
-1.125	-67.5	-70.7	0.552361	0.541841
-1	-64.8	-69.9	0.607803	0.558577
-0.875	-64.2	-69.2	0.620123	0.573222
-0.75	-63.1	-67.3	0.642711	0.612971
-0.625	-59.3	-64.3	0.720739	0.675732
-0.5	-58.3	-62	0.741273	0.723849
-0.375	-55.1	-60.3	0.806982	0.759414
-0.25	-50	-55.4	0.911704	0.861925
-0.125	-46.7	-50	0.979466	0.974895
0	-45.7	-48.8	1	1
0.125	-45.9	-51.1	0.995893	0.951883
0.25	-48.3	-56.5	0.946612	0.838912
0.375	-54.9	-61.1	0.811088	0.742678
0.5	-58.1	-62.4	0.74538	0.715481
0.625	-58.2	-65.9	0.743326	0.642259
0.75	-61.5	-68.2	0.675565	0.594142
0.875	-64.3	-69.6	0.61807	0.564854
1	-66.5	-71.2	0.572895	0.531381
1.125	-67.3	-72	0.556468	0.514644
1.25	-68.1	-73.8	0.540041	0.476987
1.375	-69.6	-73.4	0.50924	0.485356
1.5	-71.2	-74.3	0.476386	0.466527
1.75	-74.3	-75.7	0.412731	0.437239
1.875	-75.5	-76.1	0.38809	0.42887
2	-74.6	-75.3	0.406571	0.445607
2.25	-75.4	-78.3	0.390144	0.382845

Table 25: Gedackt C61

FREQC61	GEDC61B4	GEDC61AF	NB4	NAFT
2.5	-77.7	-79.6	0.342916	0.355649
3	-77.7	-83.7	0.342916	0.269875
3.5	-80.8	-84.3	0.279261	0.257322
4	-82.2	-83.8	0.250513	0.267782
4.5	-83.9	-87	0.215606	0.200837
5	-85.6	-85.9	0.180698	0.223849
5.5	-86.2	-87.4	0.168378	0.192469
6	-87	-88.6	0.151951	0.167364
6.5	-88.9	-89.5	0.112936	0.148536
7	-89.3	-88.5	0.104723	0.169456
8	-91.1	-91.2	0.067762	0.112971
9	-93.4	-90.9	0.020534	0.119247
10	-94.4	-92.4	0	0.087866

APPENDIX 9

A-9 Example of Test Rig Sampled Data

Table 26: Pipe 1 Data

FREQ	L0T1	L2T7	L5T5	L7T2	L1T0
-10	-53.4	-54.1	-53.6	-54.7	-54.3
-9	-52.7	-54.1	-53	-54	-54.3
-8	-53.6	-56.7	-53.1	-53.5	-54.3
-7	-52.9	-53.8	-52.8	-54	-52.3
-6	-52.8	-51.6	-53.1	-55.4	-51.9
-5	-51.3	-51.4	-48.3	-52.5	-52.6
-4	-48.8	-49.4	-51.6	-49.4	-52.4
-3	-47.7	-50.9	-50.3	-48.9	-52.4
-2	-45.7	-44.2	-44	-45.1	-46.2
-1.5	-43.2	-41.5	-43.7	-41.5	-42.8
-1.375	-39.8	-39.9	-42	-42.5	-42.1
-1.25	-40.2	-38.1	-38.7	-39.3	-40.4
-1.125	-37.7	-39.1	-38.6	-36.5	-39.6
-1	-35.9	-39.3	-37.4	-36.7	-38
-0.875	-34.8	-37.3	-34.5	-36.2	-37
-0.75	-33.4	-33.3	-33.1	-32.7	-34.5
-0.625	-30.1	-32.4	-30.6	-33.3	-33.9
-0.5	-28.1	-27.7	-27.4	-29	-28.7
-0.375	-24.1	-23.7	-25.9	-27.1	-28.6
-0.25	-18.8	-19.9	-20.1	-20.7	-23.1
-0.187	-13.9	-13.9	-15.6	-17.1	-18.5
-0.125	-2.8	-7.3	-10.1	-10.9	-10.2
-0.062	3.3	1.8	-0.6	2	2.3
0	3.5	4	4	4.2	3.8

Table 26: Pipe 1 Data

FREQ	L0T1	L2T7	L5T5	L7T2	L1T0
0.062	-3.5	-1.3	1.2	-4.7	-5.9
0.125	-13.1	-10.8	-9.4	-16.3	-17.7
0.187	-18.5	-19.3	-19.1	-19	-22.9
0.25	-22.9	-23.3	-22.8	-22.3	-23.8
0.375	-27	-24.9	-24.4	-29.3	-32
0.5	-30.6	-31.8	-30.5	-31.1	-31.1
0.625	-31.4	-32	-30	-33.4	-34.1
0.75	-34.1	-32.1	-33.3	-34.8	-38.5
0.875	-35.1	-36.3	-32.4	-36.9	-38.8
1	-37.5	-38.6	-37	-37.9	-39.8
1.125	-37.9	-38.5	-39.8	-37.4	-41.3
1.25	-41	-38.5	-38.9	-43.1	-40.5
1.375	-41	-39.5	-43.6	-44.2	-43
1.5	-42	-41.1	-45.1	-42.5	-42.9
2	-45.6	-45	-45.1	-44.3	-45.9
3	-46.3	-49.6	-49.8	-48.8	-51.9
4	-51.9	-50.2	-50.6	-50.1	-54
5	-49.7	-53.9	-51.8	-50.6	-53.5
6	-54.2	-53.5	-53	-55.1	-51.6
7	-53.2	-53	-53.5	-56.5	-53.2
8	-55.1	-53	-55.6	-54.6	-52.8
9	-52.7	-56	-51.8	-54.2	-52.9
10	-50.8	-54	-53.2	-54	-54.9

APPENDIX 10

A-10 Flow Chart of Maple Program used to determine pipe circuit parameters.

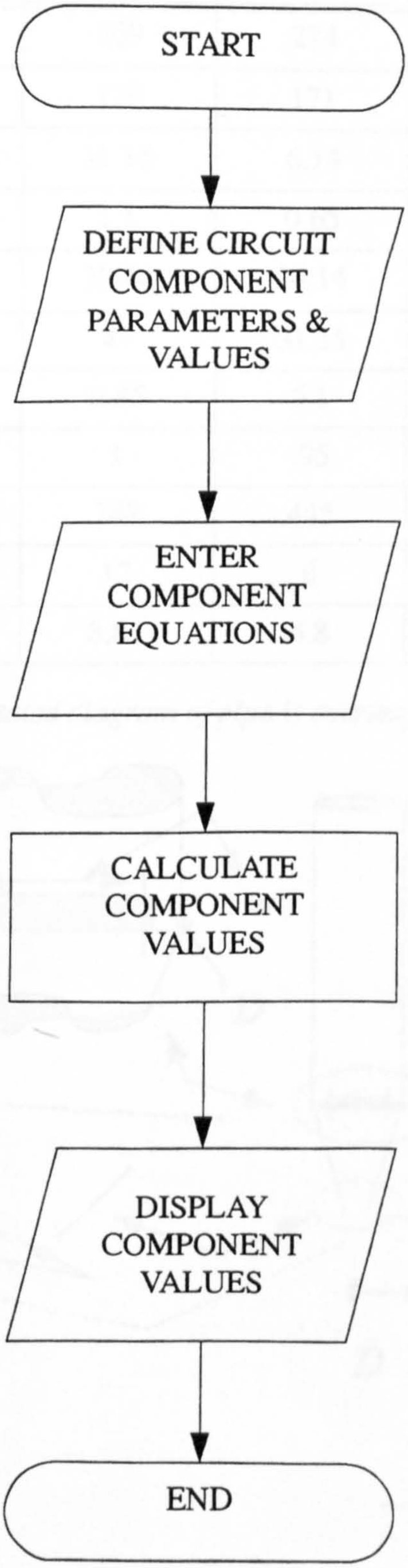

APPENDIX 11

A11.1 Pipe Outline and Dimensions used in calculations

Dimension (mm)	Pipe 1	Pipe 2	Pipe 3	Pipe 4
H	569	274	132.5	67
h	179	171	149.3	154.8
D	11.16	6.14	4.2	2.6
d	1.1	0.65	0.65	0.4
w	32.44	24.14	11.15	7.5
R	47	31.15	17.31	9.36
r	6.85	5.1	3.6	2.6
t	1	.95	.5	.5
h + H	748	445	281.8	221.8
l	12	6	2	1.5
D'	8.85	4.8	3.5	1.9

A11.2 Pipe segments *(annotated diagram of pipe is overleaf)*

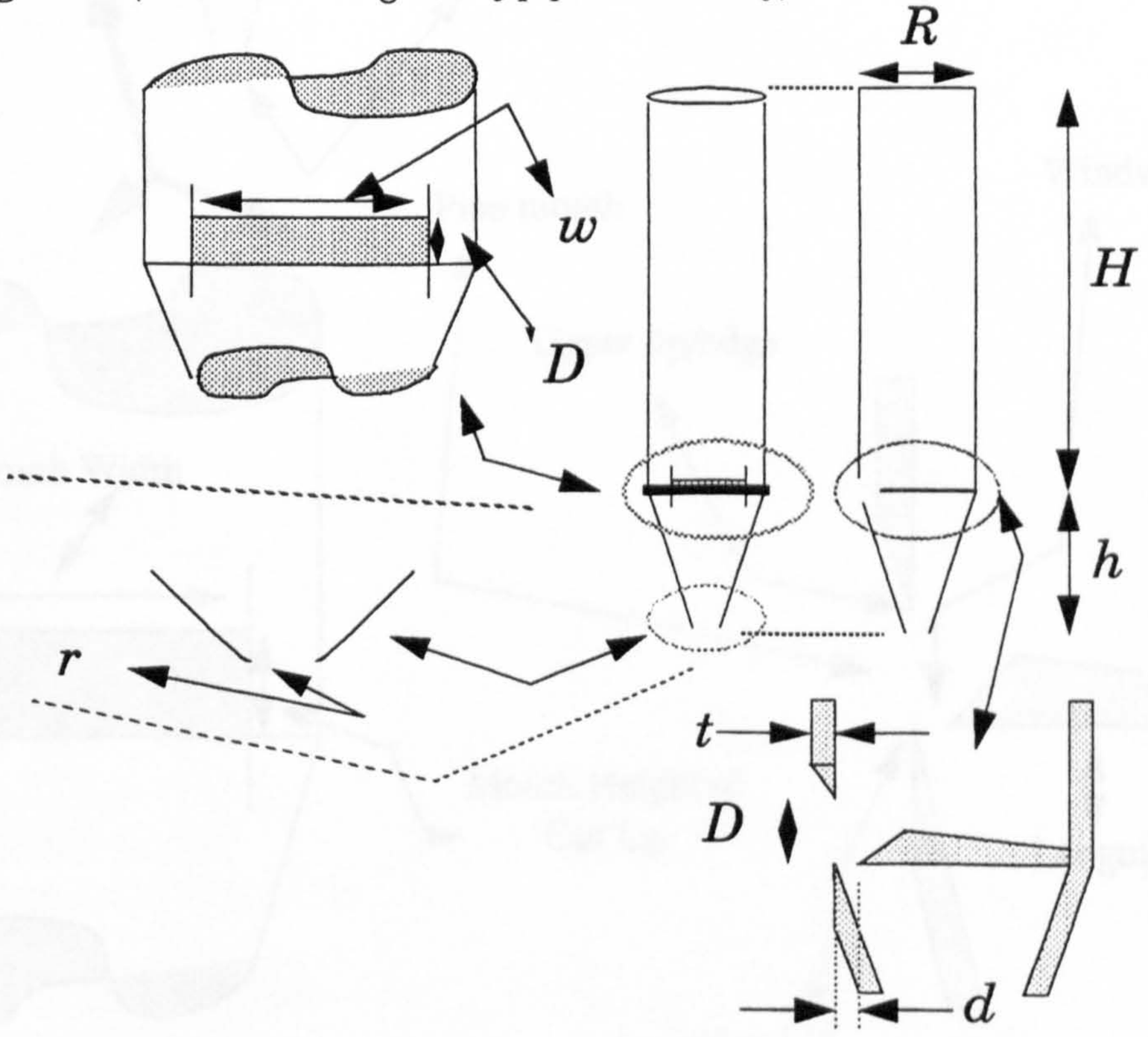

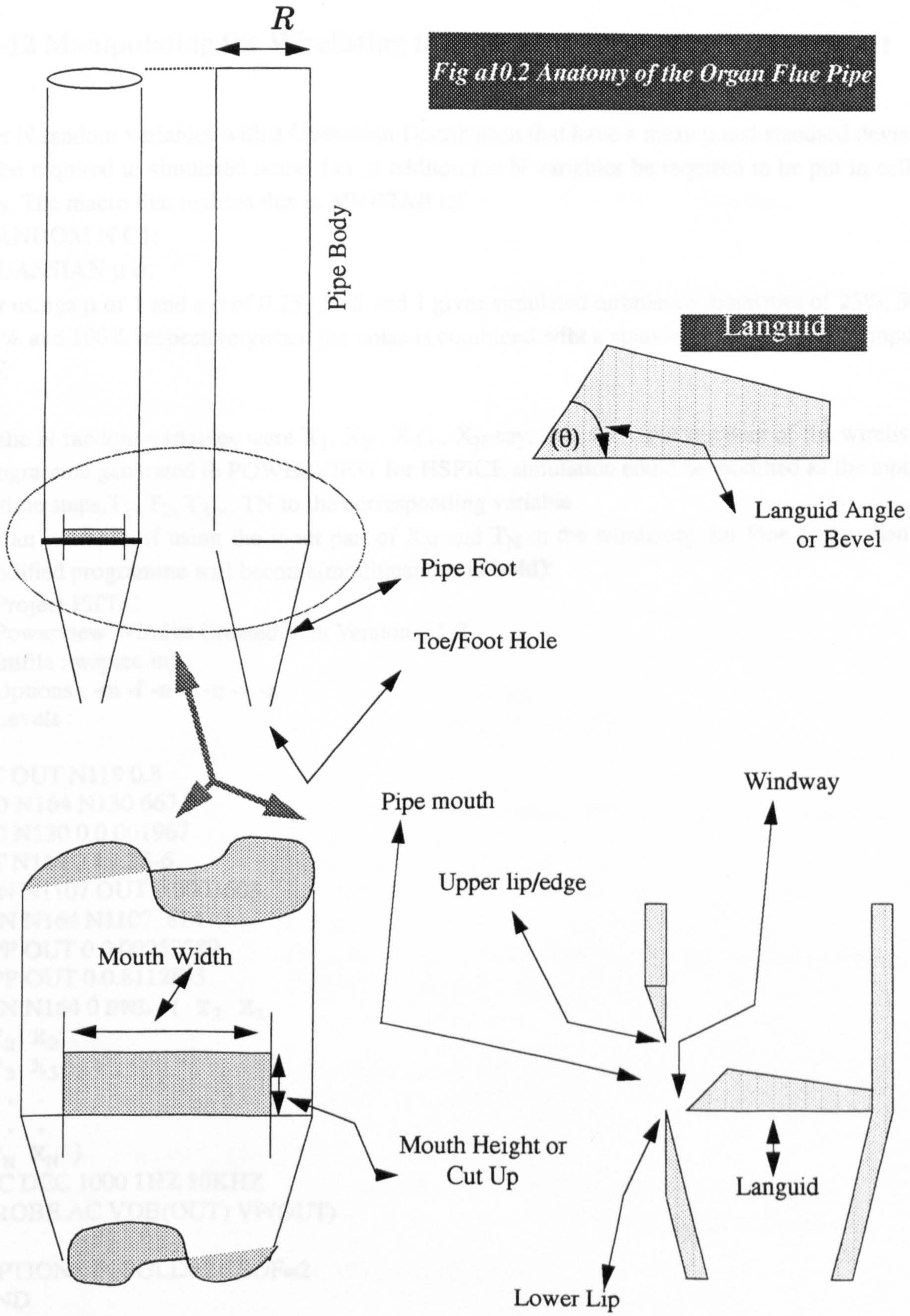

Fig a10.2 Anatomy of the Organ Flue Pipe

APPENDIX 12

A-12 Manipulating the Wirelisting to Introduce a Turbulence(noise) input

Let N random variables with a Guasdsian Distribution that have a mean μ and standard deviation σ be required to simulated noise. Let in additon the N variables be required to be put in cell C1 say. The macro that realises this in MINITAB is:

RANDOM N C1;
GUASSIAN μ σ.

By usinga μ of 1 and a σ of 0.25, .5 75 and 1 gives simulated turbulence intensities of 25%, 50%, 75% and 100% respectivelywhen the noise is combined wiht a sinusiodal signal (μ) with input of 1V.

If the N random variables were X_1, X_2 , X_3 ... X_N say, then the input segment of the wirelisting programme generated ib POWERVIEW for HSPICE simulation could be modified as the input in N time steps,T_1, T_2, T_3 ... TN to the corresponding variable.
As an example, if using the input pait of X_N and T_N in the wirelisting for Pipe 1 say, then the modified programme will become(modifications in **bold**):

```
* Project PIPEC
* Powerview Wirelist Created with Version 5.1.2
* Inifile : wspice.ini
* Options : -m -f -n -z -q -v -x
* Levels :

RT OUT N119 0.3
RO N164 N130 667.8
LO N130 0 0.001967
CT N119 0 19.2E-6
LIN N1107 OUT 0.0003603
RIN N164 N1107 .814
LPP OUT 0 0.00253789
CPP OUT 0 0.8112E-5
VIN N164 0 PWL ( T1 X1
+T2 X2
+T3 X3
+ . .
+ . .
+TN XN )
.AC DEC 1000 1HZ 10KHZ
.PROBE AC VDB(OUT) VP(OUT)

.OPTIONS INGOLD=2 CSDF=2
.END
```

REFERENCES

Acronyms:

JASA:- J. Acoustical Society of America
JASJpn- J. Acoustical Society of Japan
JFM:- J. Fluid Mechanics
JSV:- J. Sound & Vibration
ASME:- American Society of Mechanical Engineers.

1 Agullo J, Barjau A, & Martinez J
Alternatives to the impulse response to describe the acoustical behaviour of conical ducts.
JASA 1988 84(5) 1606-1612

2 Andersen Poul-Gerhard
Organ building and design
George Allen & Unwin Ltd., 1976, ch5

3 Angster J & Miklos A
New developments on the understanding of the buildup of organ sounds.
13th Int. Congress on Acoustics, Yugoslavia 1989, 99-102

4 Audsley G A
The art of organ building vol II
Dover Publications, 1965, ch. XLV

5 Benade A. H.
Relation of air column resonances to sound spectra produced by wind instruments.
JASA 1966 40(1) 247-249

6 Bendat J S & Piersol A C
Engineering applications of correlation and spectral analysis.
John Wiley 1980 Ch 1-3.

7 Bradshaw A P
An introduction to turbulence and its measurements.
Pergamon Press, 1971

8 Bruggeman J C, Hirscberg A et al
Self Sustained aeroacoustics pulsations in gas transport systems: experimental study of the influence of closed side branches.
JSV, 1991, 150(3) 371-393

9 Caddy R S & Pollard H F
Transient sounds in organ pipes
ACUSTICA 1957 v7 277-280

10 Cargill A M
Low-frequency sound radiation and generation due to the interaction of unsteady flow with a pipe jet.
JFM 1982 v121 59-105

11 Coltman J W
Sounding mechanism of the flute & organ pipe
JASA 1968 44(4) 983-992

12 Coltman J W
Sound radiation from the mouth of an organ pipe
JASA 1969 46(2) II 477-??

13 Coltman J W
Jet drive mechanisms in edge tones and organ pipes.
JASA 1976 60(3) 725-733

14 Coltman J W
Momentum transfer in jet excitation of flute-like instruments
JASA 1981 69(4) 1164-1168

15 Coltman J W
Time domain simulation of the flute
JASA 1992 92(1) 69-73

16 Coltman J W
Private Communication, 1993

17 Coughlin R F & Driscoll F F
Operational amplifiers and linear integrated circuits
Prentice Hall 1991 4th ed. ch 6.

18 Cremer, von L & Ising H
Die selbsterregten schwingungen von orgelpfeifen (The self-excited vibrations of organ pipes)
ACUSTICA 1968 19 143-153

19 Diehl, G M
Machinery Acoustics
John Wiley & Sons, 1973

20 Disselhorst JHM & Wijngaarden L Van
Flow in the exit of open pipes during acoustic resonance
JFM 1980 99(2) 293-319

21 Douglas JF, Gasiorek JM & Swaffield JA
Fluid Mechanics
1985, Pitman Pub. Ltd., Part I - III

22 Elder S A
On the mechanism of sound production in organ pipes.
JASA 1973 54(6) 1554-1564

23 Elder S A
Private Communication, 1993

24 Elvin L
Organ blowing: its history and development.
Laurence Elvin Pub., 1971

25 Fabre, B. & Castellengo, M.
Representation de l'evolution du timbre des instruments de musique en fonction de la tessiture: application a l'orgue.
13th International Conference on Acoustics, Yugoslavia, 1989

26 Fabre, B; Hirscberg et al
Jet drive and edgetone in flue organ pipes.
Submitted to JASA, 1993

27 Finch, T.L. & Nolle A. W.
Pressure wave reflections in an organ note channel
JASA, 1986, 79(5) 1584-1591

28 Fletcher H, Blackham E D & Christensen DA
Quality of organ tones
JASA, 1963 vol 35(3), 314-325

29 Fletcher, N. H.
Nonlinear interactions in organ flue pipes.
JASA 1974, vol 56(2), 645-652

30 Fletcher, N. H.
Jet-drive mechanism in organ pipes
JASA, 1976, 60(2) 481-483

31 Fletcher, N. H.
Mode locking in nonlinearly excited inharmonic musical oscillators.
JASA, 1978, 64(6), 1566-1569

32 Fletcher, N. H.
Air flow and sound generation in musical wind instruments.
Annual Rev. Fluid Mech. 1979, v11, 123-146

33 Fletcher, N. H.
Nonlinear theory of musical wind instruments.
Applied Acoustics, 1990, v30, 85-115

34 Fletcher, N. H.
Private Communication, 1993

35 Fletcher, N. H. & Rossing T. D.
The physics of musical instruments.
Springer-Verlag 1991 {Ch16- Flutes & flue organ pipes, 17, Pipe Organs, 7, Sound radiation}

36 Fletcher, N. H.& Thwaites S
Wave propagation on an acoustically perturbed jet.
ACUSTICA 1979, v42 323-334

37 Glegg, S.
Fan Noise
Ch 19 of: *Noise & Vibration* (Eds. White RG & Walker JG)
Ellis Horwood Pubs. 1982

38 Guelich, JF & Bolleter U
Pressure pulsations in centrifugal pumps.
(Trans ASME) J. Vib. & Acoustics, 1992, v114, 272-279

39 Gueritey P M
Reflexions et observations sur les souffleries
ISO Year Book, 1992, 64-91

40 Helmholz, Herman L.F.
On the sensations of tone as a physiological basis for the theory of music
Longmans, Green & Co, 1885, Ch v - Sectn. 5-6, 88-102

41 Hinze, J O
Turbulence
McGraw Hill 1975, ch 1 & 2

42 Hirscberg A et al
A quasi-stationary model of air flow in the reed channel of single reed woodwind instruments.
ACUSTICA,1990, v70, 146-154

43 Hirscberg A.
Some fluid dynamic aspects of speech
Bulletin de la communication parlee, 1992, v2, 7-30

44 Hopkins E.J. & Rinbault E. T.
The organ: its history and construction
Frits Knuf, Holland, 1965

45 Horowitz and Hill
The Art of Electronics
Cambridge University Press, 1993, ch 9.

46 Howe M.S.
On the absorption of sound by turbulence and other hydrodynamic flows.
IMA J. App. Maths., 1984, 32, 187-209

47 HSPICE
HSPICE User's Manual H9001
Meta-Software, 1990

48 Jarvis E K
Private Communication 1992

49 Kergomard, J.
Tone hole external interactions in woodwinds musical instruments.
13th Int. Congress. on Acoustics, Yugoslavia, 1989, 53-56

50 Lighthill, James
Waves in Fluids
Camb. Univ. Press., 1979 (Ch-1)

51 Magnusson, S.
Die klaaglichen auswirkugen von balgphatenschwingungen
(The tonal effects of bellow reverberation)
ISO Info. 1974, 827-830

52 Mahu, W.E.A Peters, M.C.A.M. et al
Attack transient of a flue organ pipe.
2nd Dutch conference on mechanics; Rolduc, Netherlands, 1992.

53 Mahu, WEA
Unsteady Free Jets
T.U. Eindhoven, Fac. Tech. Nat., Report No R-1204-A, 1993

54 Manlapaz R.L. & Churchill S.W.
Fully developed laminar flow in a helically coiled tube of finite pitch.
Chem. Eng. Comm., 1980, v7 57-78

55 Martinez J & Agullo J
Conical bores, Part I, reflection functions associated with discontinuities.
JASA, 1988, 84(5) 1613-1620

56 Martinez J & Agullo J
Conical bores, Part II, multiconvolution.
JASA, 1988, 84(5), 1620-1627

57 McBride, W.E., et al
Scattering of sound by atmospheric turbulence: predictions in a refractive shadow zone.
JASA, 1992, 91(3), 1336-1340

58 McIntyre M.E, Schumacher, R.T. & Woodhouse J.
On the oscillations of musical instruments.
JASA, 1983, 74(5), 1325-1345.

59 Mebold H P
Uberlegungen zum orgelwind; der offene wind (considerations about the organ wind supply - the open wind)
ISO Info, 1989, v3o, 11-24

60 Mercer, DMA
The voicing of organ flue pipes
JASA, 1951, 23(1) 45-54

61 Minitab Inc.
Minitab Reference Manual, release 8, PC version.
Minitab Inc, 1991

62 Morrison, R
Hi-tech digital organ hit all the right notes
"The Times" (UK), Feb 4, 1995 No. 65182

63 Morse P.M.
Vibration and sound
McGraw Hill, 1948, Ch 6- Sd Prop in tubes, Ch 7, sound transmission through ducts, ch 2, coupled oscillations.

64 Narasimha, R & Sreenivasan K R
Relaminarisation of fluid flows.
Advances in Applied Mechanics, 1979, v9, 221-309

65 National Physical Lab.
Turbulence measurements with hot wire anemometers.
Notes on applied sciences, #33

66 Nelson, P.R., Halliwell, N.A. & Doak, P.E.
Fluid dynamics of flow excited resonance, Part I
JSV, 1981, 78(1), 15-38

67 Nelson, P.R., Halliwell, N.A. & Doak, P.E.
Fluid dynamics of flow excited resonance, Part II: flow acoustic interaction.
JSV, 1983, 91(3), 375-402

68 Nisenfeld, A.E.
Centrifugal compressors.
ISA Monograph Series, 1982, #3: Ch-1 & 3

69 Nolle A.W. & Finch, A.L.
Starting transients of flue organ pipes in relation to pressure rise time.
JASA, 1992, 91(4), Part 1, 2190-2202

70 Norman H & Norman HJ
The organ today
Barrie & Rockliff Pub., 1967

71 Papoulis A
Circuits and Systems, a modern approach
Holt, Rinehart & Winston 1980, Ch5

72 Peters, MCAM et al
Damping and reflection coefficient measurements for an open pipe at low Mach and low Helmholtz numbers.
Technical Univ. of Eindhoven, April 1993

73 Peters, MCAM
Aeroacoustic sources in internal flows.
Technical Univ. of Eindhoven, Ph.D. Thesis, 1993

74 Powell, Alan
Some aspects of aeroacoustics from Rayleigh until today.
J. Vibrations & Acoustics, 1990, 112, 145-159.

75 Praet, W. et al.
Organ dictionary
CEOS v.z.w. Zwijndrecht, Belgium, 1989

76 Rienstra, S.W.
A small Strouhal number analysis for acoustic wave-jet flow-pipe interaction.
JSV, 1983, 86(4) 539-556

77 van Rooij G.J.
Pressure waves in the pressure supply system of an organ pipe.
T.U. Eindhoven, Faculteit Tech. Nat., Report No. R-1162-5

78 Rosenhouse, G
Acoustic wave propagation in bent thin walled wave guides.
JSV, 1970, 67(4) 469-486

79 Ryan, B, Joiner, BL & Ryan, TA
Minitab Handbook
Duxbury Press, 1985

80 Scumacher, R.T.
Self-sustained oscillations of organ flue pipes: an integral equation solution.
ACUSTICA, 1978, 39, 225-238.

81 Spiegel, M.R.
Theory and problems of statistics.
McGraw Hill, 1972, Ch3-5

82 Sound Research Labs.
Noise control in industry.
E & FN Spon, 1991, Ch20 - on air moving systems.

83 Smol'yakov A V & Tkachenko V M
The Measurement of turbulent fluctuations.
Springer-verlag, 1983 ch 1 & 2.

84 Sreenivasan K R
Laminarescent, relaminarizing and retransitional flows.
Acta Mechanica, 1982, 44, 1-48

85 Sreenivasan K R &Strykowski P J
Stabilization effects in flow through helically coiled pipes.
Expts. in Fluids, 1983, 1, 31-36.

86 van Steenbergen, A
Endcorrections and resonance frequencies of the flue organ-pipe.
TU Eindhoven, Fac. der Tech. Nat., 1990, Report # R-1046-S

87 Stephens RWB & Bate AE
Acoustics and vibrational physics
Edward Arnols Pubs. Ltd., 1966, ch17:

88 Sumner, W L
The organ: its evolution, principles of construction and use.
McDonald & Co Pub. Ltd., 1975, Ch XI, 355-362.

89 Tarbell, J M & Samuels M R
Momentum and heat transfer in helical coils.
Chem. Eng. Journal, 1973, 5, 117-127

90 Thwaites S & Fletcher N H
Wave propagation on turbulent jets.
ACUSTICA, 1980, 45, 175-179

91 Thwaites S & Fletcher N H
Acoustic admittance of organ pipe jets.
JASA, 1983, 74(2), 400-408.

92 TSI
TSI Instruction Manual
CTA Model 1750, April 1988

93 Verge, M P, Fabre B et al
Jet formation and jet velocity fluctuations in a flue organ pipe.
Submitted to JASA, 1993

94 Visser P A
Understanding organ wind.
ISO Year Book, 1991, 39-59

95 Viswanath P R, Narasimha R & Prabhu A
Visualization of relaminarizing flows.
J. Indian Inst. of Science, 1978, 159-165

96 Wagner, G D
The problem of organ wind from an organist view point.
ISO Info, 1989, 30, 24-30

97 Wonnacolt T H & Wonnacolt R J
Introductory Statistics
John Wiley, 1969, Ch2 & 9.

98 Yoshikawa S & Saneyosh J
Feedback excitation mechanism in organ pipes.
JASJpn, 1980, E1(3) 175-191

99 Impeller configuration of the blower was designed by Prof H V Rao, and constructed by P J Norman both of the School of Engineering, University of Huddersfield

100 Maple V Release 2 is a scientific computer programming package designed in Canada.
The ref. text used was: *First Leaves: A Tutorial Introduction to Maple V*, by Char B W et al; Springer-Verlag, 1992

101 _____ Wireless World, May 1978, p70

102 Collins, Peter Peter Collins Organ Builders, Melton Mowbray, Leicestershire, UK. Independent observation.

103 Davies, P.O.A.L
Flow-acoustic coupling in ducts
JSV, 1981, 77(2), 191-209

104 Ramakrishnan, R & Davies P.O.A.L.
Sound generation by flow-acoustic coupling
In *Mechanics of Sound Generation in Flows*,
E-A Muller, Editor; Springer-Verlag, 1979,62-68.